MODELLING THE INTERACTIONS BETWEEN PANCREATIC TUMOUR CELLS AND CANCER-ASSOCIATED FIBROBLASTS: ENHANCING MODELS FOR DRUG DEVELOPMENT

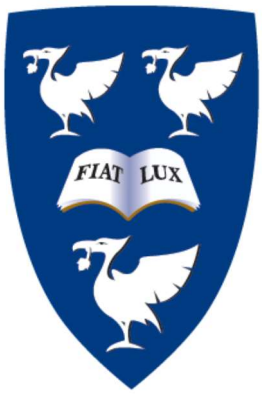

Sarah Brumskill
Department of Molecular and Clinical Cancer Medicine
Institute of Translational Medicine
University of Liverpool

Thesis submitted in accordance with the requirements of the University of Liverpool for the degree of Doctor in Philosophy

October 2017

Declaration

This dissertation is the result of my own work and includes nothing that is the outcome of work done in collaboration, except where specifically indicated in the text. It has not been previously submitted, in part or whole, to any university for any degree or other qualification.

Abstract

Pancreatic ductal adenocarcinoma (PDAC) is characterised by a complex tumour supportive microenvironment including a dense fibrotic stroma (Farrow et al., 2008). Embryonic signalling pathways such as the Hedgehog (Hh) and Wnt pathway are involved in the interactions between cancer-associated fibroblasts (CAFs) and pancreatic tumour cells as well as maintenance of the tumour supportive microenvironment (Bailey et al., 2008, Zhang et al., 2013). Prognosis for PDAC remains poor (global 5 year survival rate of less than 10% (Siegel et al., 2015)) owing, in part, to limited therapy options available and resistance to current therapies. The tumour microenvironment has been implicated in chemotherapy resistance (Dauer et al., 2017, Hessmann et al., 2017) which has led to a need for drug screening techniques which include elements of the tumour microenvironment. I therefore sought to develop a co-culture model incorporating CAFs and epithelial cells that would better represent the tumour microenvironment. This model would enable the study of embryonic signalling pathways and how these may be exploited in the treatment of PDAC. Mixed 3D cultures of CAFs and cancer cell lines showed a morphology close to that of a tumour with the presence of CAFs dispersed throughout the spheroid. The Hh pathway was found to be upregulated in CAFs in 2D co-cultures of CAFs and PDAC cancer cell lines. The Wnt pathway was found to be upregulated in PANC1 cells in a 2D co-culture of CAFs and PANC1 cells. This demonstrated that the embryonic signalling pathways (Hh and Wnt) are involved in the cross talk between CAFs and PDAC tumour cells. 2D, co-culture of CAFs with PANC1 cells reduced sensitivity to gemcitabine, dependent upon the number of CAFs when compared to the monoculture of the PANC1 cells. Furthermore, when SUIT2 and BXPC3 cell lines were cultured in a 3D model, the presence of CAFs significantly reduced the efficacy of gemcitabine effectively conferring resistance. Together these results demonstrate a complex interaction between CAFs and PDAC tumour cells in an *in vitro* model that is similar to the *in vivo* microenvironment. In addition the presence of CAFs within 2D and 3D co-culture models has a considerable impact on pancreatic cancer cell resistance to gemcitabine and thus better reflects the clinical response. The difference in gemcitabine sensitivity between mono- and co-culture together with the more physiologically relevant morphology in the co-cultured spheroids, highlights the importance of *in vitro* drug screening techniques which better represent the tumour microenvironment in order to more accurately predict a compound's clinical efficacy.

Acknowledgements

First and foremost I would like to thank my supervisors, Professor Eithne Costello, Dr Bill Greenhalf, Dr Peter Calcraft and Dr Caroline Philips. Their guidance and patience has been invaluable. I would also like to thank Professor Fiona Campbell for always making time to assist me.

I am also grateful to everyone in the pancreas research group especially Dr Lawrence Barrera-Briceno for all the work we have done together and the laughs we had doing it, I have thoroughly enjoyed working as part of this group.

I would like to thank my colleagues from Redx Pharma especially Dr Shona Harmon, Dr Jessica Edwards and Dr Rachel Stovold who have always been willing to answer my questions and provide motivation when required.

Special thanks to the NIHR Pancreas Biomedical Research Unit and Redx Pharma for funding this project.

Finally, I would like to thank Amy Cousins whose friendship has supported me throughout this project.

Table of Contents

1. Introduction

1.1. Cancer

1.1.1. Incidence

'Cancer' is the term given to a large number of heterogeneous diseases which result from uncontrolled cell proliferation in various organs of the body (Hanahan and Weinberg, 2000, Hanahan and Weinberg, 2011). To date, more than 200 different types of cancer have been defined with each having a unique pathology and treatment approach. Cancer was responsible for the death of 8.2 million people worldwide in 2012 and in 2013, 352,000 new cases of cancer were diagnosed in the UK alone (CRUK, 2016). There are many factors which can increase the risk of developing cancer: age, genetics and lifestyle choices such as smoking, diet, stress and alcohol consumption (McGuire, 2016).

1.1.2. Molecular mechanisms

Twenty-five years of research has resulted in a large volume of information which has exposed cancer as a disease resulting from multiple changes in the genome. Cancer is a genetic disease as it is a consequence of mutations in genes which are involved with normal cellular processes such as DNA repair, division and apoptosis. These genetic changes have been categorised into two groups: a dominant form which are collectively known as oncogenes, or the recessive form known as tumour suppressor genes. Mutations in oncogenes generally result in gain of function whereas any mutation in a tumour suppressor gene are loss of function (Bishop, 1991). In 2000, Douglas Hanahan and Robert Weinberg revolutionised the way in which we regard the development of a malignant phenotype from normal cells. They theorised that in order for a cell to be considered malignant it must have undergone six changes in its biology (Hanahan and Weinberg, 2000). Firstly the cell must be self-sufficient and no longer require the necessary growth signals from the host. In healthy tissue growth signals are carefully regulated; cells enter the cell-cycle in a manner which ensures

maintenance of a certain number of cells thereby ensuring the stability of tissue architecture allowing the tissues to operate effectively. In cancer cells these signals become deregulated and this deregulation occur in a variety of ways: they can secrete ligands which can effect proliferation in an autocrine manner, they can signal to other cells within the tumour microenvironment to influence proliferative signals, and they can express higher than normal levels of various receptors and become extremely sensitive to normal signals. Secondly, the cancer cells will be immune to antigrowth signals which are well-regulated pathways, controlled by tumour suppressor genes. One example of a tumour suppressor gene is the retinoblastoma (*RB)* gene. In adult tissues the role of *RB* is the regulation of apoptosis, acting as a G_1 checkpoint and it is involved in the maintenance of chromosomal stability. Loss of function mutations in this gene have been found to result in retinoblastoma; it can increase risk for osteosarcoma. Human papillomavirus is believed to inactivate *RB* resulting in cervical carcinoma and squamous cell carcinoma in the head and neck (Burkhart and Sage, 2008). Cancer cells are able to evade apoptosis by avoiding the regulations in place for control of tissue homeostasis. One example of this is the neurofibromatosis type 2 (*NF2*) gene and its product Merlin which is a cytoskeletal protein acting at the cell membrane to organise adherin junction stabilisation which co-ordinates contact inhibition between cells (Curto et al., 2007). In addition, it regulates epidermal growth factor (EGFR) by sequestering it in a membrane compartment and, loss of NF2 has been found to be linked to various cancers (Curto et al., 2007). This indicates an important role for contact mediated cell growth inhibition which is lost in various cancer cells. Furthermore, cancer cells must have the ability to undergo unlimited replications. In the lifespan of a normal cell, it is only able to go through a limited number of cycles before passing into senescence. In a malignant cell this process is dysregulated which is believed to be due to telomere alterations (Raynaud et al., 2010). In the same way that tissues require a rich blood supply to deliver oxygen and nutrients a tumour also needs vasculature to sustain growth. Many factors can impact

angiogenesis; one example is the regulation of vascular endothelial growth factor-A (VEGF-A) which has been found to be upregulated by oncogenic signalling (Ferrara, 2010). It has long been established that as a tumour progresses the likelihood of local invasion to healthy tissues and metastases increases (Yokota, 2000, Arvelo et al., 2016). In PDAC, early precursor cells have been found in circulation in mice (Rhim et al., 2012) suggesting that metastases in PDAC is an early event in tumour progression. The term metastasis was first used by French gynaecologist Joseph-Claude Recamier in 1829 to describe the spread of cancer throughout the body (Récamier, 1829). Metastasis is a critical clinical challenge which is difficult to predict and has a serious impact on the patient. In 1889, Stephen Paget investigated the interactions between the host and tumour, specifically how this relationship impacted the likelihood of metastasis and which organs would be involved (Paget, 1889). This work led to the “seed and soil” hypothesis which stated that in order for a tumour to successfully metastasise the circulating tumour cell or “seed” had to find an environment which was rich enough to support growth “soil.” This theory contradicted the current theory of the time which proposed that tumour cells were simply being obstructed and becoming stuck within the circulation system therefore metastases was dependant by mechanical factors (Virchow, 1989). Over 100 years since its conception the “seed” and “soil” hypothesis has been the subject of many studies and it is now accepted that the “seed” refers to progenitor cells or cancer stem cells and “soil” refers to a metastatic niche (Langley and Fidler, 2011, Plaks et al., 2015). In order for metastases to form, the tumour must undergo the following steps: progenitor cells must break off from the primary tumour and enter circulation both hematologic and lymphatic. These cells must survive conditions within circulation before resting in a capillary bed and, in a similar manner to the way a primary tumour will invade surrounding tissues, the progenitor cells will infiltrate tissues and proliferate. Once the progenitor cells are proliferating vascularisation forms and the metastases is established. (Talmadge and Fidler, 2010). The ability for cancers to metastasise

completes the acquired traits that Hanahan and Weinberg postulated were required for a tumour to be considered malignant (Figure 1.1.). This reductionist view of cancer as a mass of homogenous tumour cells has since been expanded to include a tumour promoting microenvironment.

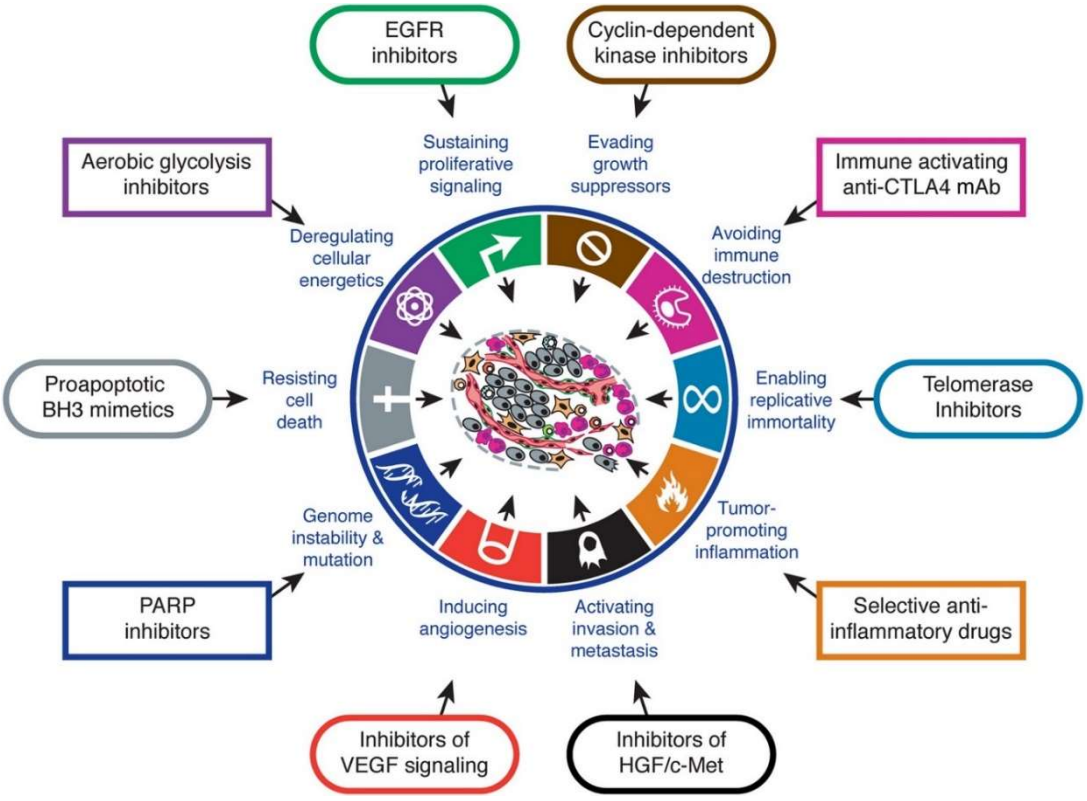

Figure 1.1. Therapeutic targeting of the hallmarks of cancer
Image obtained from Douglas Hanahan and Robert A. Weinberg's review article "Hallmarks of Cancer: The Next Generation" published in cell in 2011. (Hanahan and Weinberg, 2011) Copyright License from Elsevier.

In 2011 it was established that four additional factors influenced cancer progression and they referred to these additional characteristics as "emerging hallmarks" (Hanahan and Weinberg, 2011)(Figure 1.1.). One of which is the capacity cancer cells have to reprogram their ability to metabolise nutrients in a way that supports continued cell growth. The first time this metabolic switch was observed was in the 1930's during the investigations by Otto Warburg. He discovered that even in aerobic conditions cancer cells tend to undergo a metabolic switch which became known as the "Warburg effect", wherein they metabolise glucose using glycolysis (Warburg,

1931, Warburg, 1956). Glycolysis is considerably less efficient than mitochondrial oxidative phosphorylation, therefore they need to compensate for this deficit in ATP production per glucose molecule.

1.2. The pancreas

The pancreas is an organ that has both exocrine and endocrine functions, it is located posterior to the bottom half of the stomach. The head of the pancreas is the widest part and is located in the right side of the abdomen in close proximity to the duodenum. The neck is between the head and the body of the pancreas, the body is the middle section of the gland, the superior mesenteric artery and vein run behind the body. The tail is the thin tip of the pancreas which sits in the left side of the abdomen which is located next to the spleen. The vast majority of the pancreas (approximately 95%) is made up of pancreatic acinar cells and surrounding pancreatic ducts. Less than 5% of pancreatic cells are groups of endocrine cells which are referred to as islets of Langerhans (Figure 1.2.).

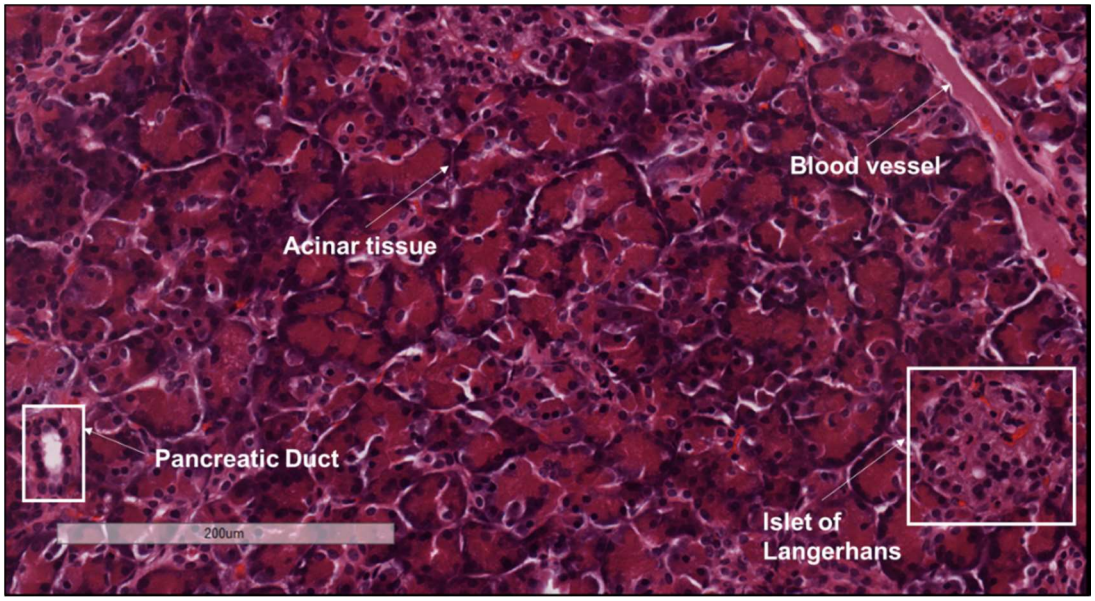

Figure 1.2. Hemotoxylin and Eosin (H&E) image showing the microstructures of the normal pancreas.

1.2.1. The exocrine function of the pancreas

The exocrine function of the pancreas is carried out by pancreatic acinar cells which secrete digestive enzymes into pancreatic ducts. The smaller pancreatic ducts increase in size until they form the main pancreatic duct. The acinar cells are pyramidal in shape and are filled with eosinophillic zymogen granules. These cells are arranged in “nests” with a central lumen. The function of these cells is the synthesis, storage and secretion of digestive enzymes, which become activated once they reach the duodenum.

1.2.2. The endocrine function of the pancreas

The islets of Langerhans are responsible for the endocrine function of the pancreas, they secrete the hormones insulin, glucagon, somatostatin and pancreatic polypeptide. There are four cell types which make up the islets of Langerhans: α-cells, β-cells, δ-cells and γ-cells. α-cells make up around 20% of the islets, and their primary purpose is to produce glucagon (Quesada et al., 2008). Glucagon is involved in the regulation of blood glucose levels and is released when blood glucose levels are low. It has three mechanisms of action: firstly, it causes the liver to convert its glycogen stores back into glucose in a process referred to as glycogenolysis; secondly, it stimulates the uptake of amino acids from blood by the liver in order to produce glucose, this is known as gluconeogenesis; finally, it causes the breakdown of triglycerides into fatty acids and glycerol, this process is known as lipolysis. The combination of these processes result in an increase in blood glucose levels. 75% of the islets of Langerhans are β-cells which are responsible for the secretion of insulin (Hellerstrom, 1984). Insulin is secreted in response to an increased blood glucose level. The most important function of insulin is to cause the uptake of glucose from blood. 4% of islets are made up of δ-cells which secrete somatostatin, which is an inhibitor of insulin and glucagon secretion. The final cell type which make up the islets are the PP or γ-cell which secrete pancreatic polypeptide hormone which is believed

to effect appetite in addition to regulating the exocrine and endocrine functions of the pancreas. The islets of Langerhans secrete their hormones directly into the blood stream.

1.3. Pancreatic cancer

1.3.1. Incidence and risk factors

Pancreatic cancer is the seventh most common cause of cancer-related mortality worldwide with approximately 330,000 deaths in 2012 accounting for 4% of total cancer related deaths. The pancreatic cancer mortality rate appears to be highest in North America however this could be an artefact of the ability to accurately collect data in the developing world. The incidence of pancreatic cancer is 12th worldwide with a mortality to incidence rate of 98% (Ferlay et al., 2015). Pancreatic ductal adenocarcinoma (PDAC) is the most common form of the malignancy accounting for more than 95% of cases (Becker et al., 2014). PDAC forms from the cells lining pancreatic ducts and is an exocrine tumour, most commonly found in the head of the pancreas (Hruban and Fukushima, 2007). Incidences of pancreatic cancer increase with age with the majority of cases appearing in the population in the 65-75 year age group. Median survival rate for metastatic pancreatic cancer is 3-5 months and in cases of locally advanced disease 6-10 months. Unfortunately due to the difficulties in diagnosis most cases are advanced upon diagnosis (Kaur et al., 2012, Oberstein and Olive, 2013). In the UK pancreatic cancer is the 11th most common form of cancer and in 2014 9,600 new cases were diagnosed which is approximately 26 per day. Over the past 10 years incidence of pancreatic cancer has increased by 10% and this is only predicted to increase. However it has been suggested that the apparent increase in incidence of pancreatic cancer could be due to more cases actually being identified as pancreatic cancer as advancements in diagnostics have developed (Kaur et al., 2012). Unfortunately this disease has a very poor prognosis with only a very small proportion of people diagnosed surviving with the disease for greater than

10 years which has not changed since the 1970's. Less than 3% of individuals diagnosed will survive for 5 years or more; 20% of patients diagnosed will only survive for 1 year or more (CRUK, 2016). All of the cancer statistics reviewed above highlight the need for advances in tools to diagnose early disease and more sophisticated personalised treatment options. There are various risk factors which have been linked to the development of pancreatic cancer; age is a critical factor for the development of pancreatic cancer as only 5-10% of new cases occur in patients below 50 years of age. The median age for development of pancreatic cancer in the USA is 72 years which indicates that this is a disease which will continue to pose a risk as the aging population increases (Raimondi et al., 2009). It has been demonstrated that there is strong correlation between smoking and the development of pancreatic cancer and it has been estimated that smoking is responsible for up to 25% of pancreatic cancer cases despite the fact that this is the most preventable risk factor (Iodice et al., 2008). It has long been suggested that there is a link between alcohol and pancreatic cancer, however clear data around this risk factor is lacking due to a number of confounding variables. A recent meta-analysis of dose of alcohol versus pancreatic cancer indicates that high levels of alcohol intake leads to an increased risk of developing pancreatic cancer (Wang et al., 2016b). There is an indirect role for alcohol consumption, over 40g per day increases an individual's risk of developing both acute and chronic pancreatitis (Samokhvalov et al., 2015) which in turn increases a patients risk of developing pancreatic cancer. Pancreatitis is a result of inflammation of the pancreas caused by the early activation and release of digestive enzymes. Chronic pancreatitis and hereditary pancreatitis have both been shown to dramatically increase a patient's risk of developing pancreatic cancer (Lowenfels et al., 1993, Lowenfels et al., 1997). Many investigations have been undertaken to determine a role of obesity in the development of pancreatic cancer (Reeves et al., 2007, Patel et al., 2005) however, the precise mechanism of association has yet to be defined. Nevertheless, there appears to be a link between body mass index (BMI) and risk of

pancreatic cancer (Bracci, 2012). Diabetes is associated with increased risk, commonly type 2 (Hassan et al., 2007), specifically long term sufferers who have had diabetes for over 10 years (Huxley et al., 2005). A sudden and unexpected diabetes diagnosis can also be a symptom of pancreatic cancer and occurs in more than half of pancreatic cancer patients (Chari et al., 2008).

1.3.2. Biology

The most common form of pancreatic cancer is PDAC which develops from non-invasive precursor lesions (PanIN) to an invasive cancer (Yachida et al., 2010). This tumour is a fibrotic white/yellow coloured mass invading neighbouring tissue which normally exhibits signs of fibrosis, atrophy and dilated ducts. All pancreatic lesions are classified based on the tumour node metastases (TNM) classification of malignant tumours staging system. This system takes into account the size of the primary tumour, lymph node status and the presence of distant metastases. Due to the lack of a screening test for pancreatic cancer, most patients are diagnosed already having distant metastases. Evidence suggests that if pancreatic cancer was detected at an earlier stage this would significantly increase the 5-year survival rate of patients (Chari et al., 2015).

1.3.3. Genome instability

1.3.3.1. KRAS

KRAS encodes a GTPase which is approximately 21 kDa in size; it cycles between two forms: a GTP bound active form, and the inactive GDP-bound form. This cycling between inactive and active forms is mediated via guanine nucleoside exchange factors (GEFs) which are involved in the transition from GDP to GTP. Inactivation of KRAS protein is achieved through GTPase activating proteins (GAPs) which hydrolyse GTP. If the interaction which is required for the correct functioning of KRAS and GAPs is damaged in any way, constitutive activation of KRAS occurs. This leads to the constant stimulation of many downstream signalling pathways such as

RAF/MEK/ERK, PI3K/PDK1/AKT and MAPK (Eser et al., 2014). These pathways are involved in many of the processes which have been highlighted as important in the development of cancer as they are responsible for proliferation, apoptosis and metabolic reprogramming as well as other key functions which determine cell fate (Eser et al., 2014). Mutations in the *KRAS* oncogene are prevalent in PDAC and are found in greater than 80% of cases (Biankin et al., 2012, Waddell et al., 2015, Witkiewicz et al., 2015). The importance of mutations in this gene as an initiating event for PDAC are clear from the ability of *KRAS* to drive genetically engineered mouse models (GEMMs), which progress through the disease stages from early PanIN to an advanced state (Perez-Mancera et al., 2012). It is also one of the earliest genetic mutations to occur and has been found in the earliest instances of PanIN 1A lesions (Kanda et al., 2012).

1.3.3.2. TP53

Up to 75% of PDAC cases have an inactivating mutation in the tumour suppressor tumour protein (*TP53*) gene which encodes the p53 protein which is essential for the normal functioning of the cell cycle (Liu and Kulesz-Martin, 2000). In a healthy cell p53 has a role in the regulation of the G1-S cell cycle checkpoint and is involved in the induction of apoptosis in response to damaged DNA. A loss of function mutation in this gene allows cells to continue to divide and survive even in the presence of damaged DNA which eventually leads to the accumulation of genetic mutations (Vogelstein and Kinzler, 2004).

1.3.3.3. DPC4/SMAD4

Loss of function mutations in *Deleted in pancreatic carcinoma* (*DPC4/SMAD4*) are present in approximately 55% of pancreatic cancers. SMAD4 is a member of the transforming growth factor-β (TGF-β) signalling pathway. Activation of TGF-β signalling results in the nuclear localisation of SMAD2/3 in complex with SMAD4. The TGF-β signalling pathway controls cell fate by regulating the expression of specific

target genes, therefore mutations which prevent the inhibition of cell growth by TGF-β confers a growth advantage on transformed cells (Siegel and Massague, 2003). Loss of SMAD4 expression is observed from PanIN-3 lesions and onwards in tumorigenesis (Wilentz et al., 2000).

1.3.3.4. CDKN2A

Loss of function mutations in Cyclin-dependant kinase inhibitor 2A (CDKN2A) are prevalent in over 50% of PDAC cases. It encodes two proteins, p16 and p14 which are both tumour suppressor proteins (Waddell et al., 2015, Barrett et al., 2017, Cicenas et al., 2017). p16 prevents phosphorylation of the retinoblastoma protein, which eventually results in inhibition of the E2F transcription factor which stops cells from progressing through the G_1 cell cycle checkpoint. p14 is also involved in the regulation of cell growth as it stabilises p53. p53 once activated can arrest cyclin dependant kinases at G_1 and G_2 checkpoints which can trigger apoptosis (McWilliams et al., 2011). p16- and p14-related cell growth arrest is highly involved in the prevention of transformation from normal to neoplastic cells (Barrett et al., 2017).

1.3.4. The PDAC tumour microenvironment

One definition of the tumour microenvironment is the non-transformed components found in the immediate vicinity of a tumour which include stroma, vasculature and immune cells (Madar et al., 2013). PDAC is a unique type of solid tumour due to the dense desmoplastic reaction which is characteristic of this cancer, the desmoplastic reaction is composed of activated CAFs which deposit excessive amounts of extracellular matrix proteins The correlation between fibrosis and poorer outcomes has been reported (Nakatsura et al., 1997, Watanabe et al., 2003), specifically the relationship between fibrosis and metastases to the liver, bone or lung (Distant metastases). The tumour microenvironment is an important source of support for tumour cells; it contains cancer-associated fibroblasts (CAFs) including pancreatic stellate cells (PSCs) a subpopulation of CAFs, extracellular matrix proteins (ECM)

such as collagen and fibronectin and immune cells which all contribute to the chemo-resistance of this aggressive tumour (Figure 1.3.).

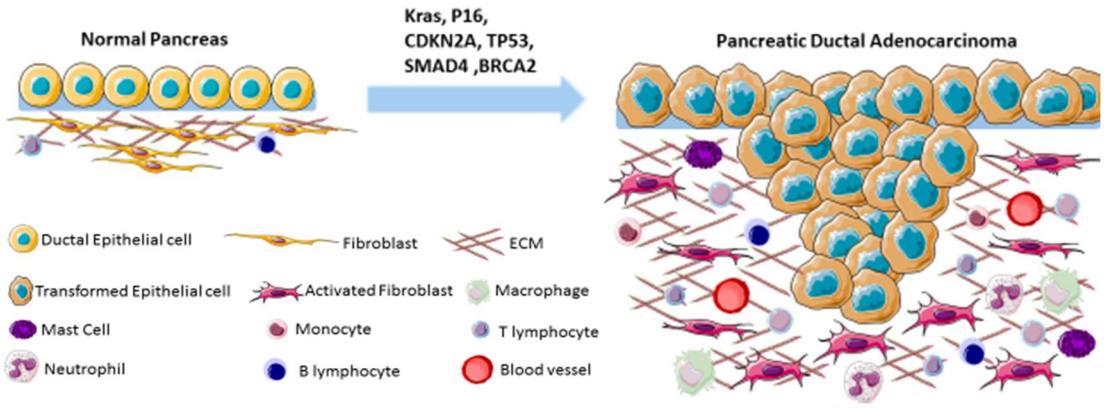

Figure 1.3.

Components of the Pancreatic Tumour Microenvironment

In an uninjured exocrine pancreas pancreatic ducts are lined by epithelial cells, quiescent fibroblasts with very few immune cells such as T and B lymphocytes and a very limited extra cellular matrix. In a PDAC cancer cells invade surrounding tissues and a large desmoplastic reaction is observed. The progression of tumorigenesis leads to the activation of CAFs which in turn leads to an increase in deposition of extra cellular matrix proteins. Immune cells infiltrate the stroma and can become part of the cancer supporting microenvironment. Angiogenesis increases due to the increased need to nutrients and oxygen to support the tumour.

1.3.4.1. Cancer-associated fibroblasts

The first description of fibroblasts was late in the 19th century (Virchow, 1989); they are not vascular, epithelial or immune cell derived but an elongated cell type found embedded within connective tissue (Kalluri and Zeisberg, 2006). Fibroblasts are responsible for maintaining the homeostasis of ECM. They produce many of the elements of ECM such as collagen (Type I, III and V) and fibronectin in addition to matrix metalloproteinases (MMPs) which have a role in the degradation of ECM proteins. In a damaged organ they have an important function in wound repair as they provide a scaffold for other cells types to infiltrate (Tomasek et al., 2002). Due to their role in the turnover of ECM they play an important role in scarring and tissue fibrosis. In an area of fibrosis or at the site of a healing wound, fibroblasts secrete higher levels of ECM and are found to be in an "activated" phenotype (Kendall and Feghali-

Bostwick, 2014). CAFs are derived from different parental cells which include PSCs, pancreatic fibroblasts and bone marrow derived cells (Hinz et al., 2007, Erkan et al., 2012a). PSCs are believed to be the most prevalent source of CAFs in the PDAC tumour microenvironment. PSCs were first identified in 1998 as star shaped cells which characteristically stored fat droplets and were rich in vitamin A; they were reminiscent of hepatic stellate cells (Apte et al., 1998, Bachem et al., 1998). Pancreatic injury results in a switch from quiescent PSC to myofibroblast with alpha smooth muscle actin (αSMA) expression, increased ECM secretion and loss of lipid droplets (Omary et al., 2007). The embryonic YAP-Hippo pathway was identified as a pathway involved in stem cell renewal and tissue regeneration (Cordenonsi et al., 2011, Cai et al., 2010, Papaspyropoulos et al., 2018). This pathway has been found to be upregulated in the PDAC tumour microenvironment specifically in the stroma and is believed to be involved in the proliferation and activation of CAFs (Morvaridi et al., 2015). There is a theory that epithelial cells could also be a possible source for CAFs when they undergo Epithelial-to-Mesenchymal transition (EMT) (Iwano et al., 2002).

1.3.4.2. Extracellular matrix

The PDAC tumour microenvironment contains an abundance of ECM, collagen, fibronectin, proteoglycans and hyaluronic acid. The presence of a large amount of ECM is believed to contribute to resistance to chemotherapy as it distorts the architecture of the pancreas, compressing capillaries and lymphatic vessels which leads to a reduced level of drug actually reaching tumour cells (Wehr et al., 2011, Mahadevan and Von Hoff, 2007).

1.3.4.3. Immune cells

Inflammatory cells are present in the PDAC tumour microenvironment and are believed to support the progression of PDAC. Inflammation of the pancreas in the form of chronic pancreatitis is a significant risk factor for PDAC (Lowenfels et al.,

1993). The infiltrating immune cells present in the PDAC tumour microenvironment have been found to be immunosuppressive in nature such as regulatory T-cells and myeloid derived suppressor cells (MDSCs) with very few cytotoxic T lymphocytes present (CTLs) (Clark et al., 2007).

1.3.4.4. Blood vessels

The PDAC tumour microenvironment is very poorly vascularised which results in a hypoxic microenvironment; this is believed to contribute to its resistance to chemotherapy (Provenzano and Hingorani, 2013). Despite this, *in vitro* tumour cells have been shown to secrete vascular endothelial growth factor (VEGF) and fibroblast growth factor (FGF) (Koong et al., 2000, Erkan et al., 2009). Higher levels of VEGF in patients correlates with increased vascular density and a worse prognosis in patients (Carr and Fernandez-Zapico, 2016). Depleting the blood supply has not had much success in the clinic but remains an attractive target on the basis that if it is possible to deplete the blood supply further it could cause hypoxic necrosis within the tumour (Cook et al., 2012).

1.3.4.5. Nerves

In a healthy pancreas there is an extensive nerve supply which contains ganglia, myelinated and unmyelinated nerve cells. Peri-neural invasion of the tumour correlates with worse survival in patients after resection of the tumour which is mediated by CXCR1 (Shen, 2010, Marchesi et al., 2008). The reason for this effect on prognosis is not clear, though it has been suggested that it could be due to the degree of differentiation of the tumour (Bapat et al., 2011). The nerves present in the PDAC tumour microenvironment appear to be large and denser than in the normal pancreas, but their impact on tumour progression is not well understood. The presence of these nerves in the PDAC tumour microenvironment is believed to contribute to patient morbidity through their role in facilitating chronic pain (Bapat et al., 2011).

1.3.5. Chemotherapeutic treatment of PDAC

Currently, only 15-20% of patients are diagnosed with disease that is eligible for surgical resection. A stage I PDAC tumour is present within the pancreas and does not have any blood vessel/lymph node involvement or distant metastases (Cid-Arregui and Juarez, 2015). Unfortunately approximately 65% of patients have a tumour recurrence due to the presence of micro-metastases. Stage II PDAC involves local invasion of the tissue surrounding the pancreas such as the duodenum or bile ducts, but does not extend to lymph nodes or metastases (Cid-Arregui and Juarez, 2015). Only stage I and II PDAC tumours are eligible for surgery. The majority of patients present with locally advanced or metastatic disease and are therefore not eligible for surgery (Neoptolemos et al., 2003).

1.3.5.1. Gemcitabine

Gemcitabine has been the standard of care for patients with PDAC for the last 20 years (Burris et al., 1997). It increased the survival rate in patients treated with Fluorouracil (5-FU) the standard of care at that time from 2% to 18% in patients treated with Gemcitabine; it also had reduced disease related symptoms such as pain, Karnofsky performance status (KPS) and weight (Burris et al., 1997). The uptake of Gemcitabine depends on transporters primarily the human equilibrative nucleoside transporter-1 (hENT-1), which has been found to be overexpressed on pancreatic cancer cells (Damaraju et al., 2003, Fujita et al., 2010). Once it is within the cells, Gemcitabine is phosphorylated by deoxycytidine (dCK) to the monophosphate form of the molecule followed by its conversion to difluorodeoxycitidine (dFdCTP) which is the active metabolite responsible for the cytotoxic effects of Gemcitabine as it is a substrate for DNA and RNA polymerases (Huang et al., 1991).

Unfortunately, not all patients respond to Gemcitabine due to mechanisms of chemotherapy resistance (Andersson et al., 2009). There are a variety of reasons a

patient may not respond to treatment with Gemcitabine. One study used transcriptional analysis of genes to determine the hENT-1 expression in patients, patients who were found to have high levels of hENT-1 responded significantly better to treatment with Gemcitabine (Giovannetti et al., 2006). Deficiencies in dCK have also been found to be associated with resistance to Gemcitabine (Kroep et al., 2002). High Mobility Group AT-Hook 1 (HMGA1) has been implicated in Gemcitabine resistance and has been found to be upregulated in PDAC patients (Liau and Whang, 2008). It is involved in chemotherapy resistance through an Akt-dependant mechanism which is believed to have an impact on resistance to apoptosis (Liau et al., 2006). One other major factor in the resistance to chemotherapy is the PDAC tumour microenvironment which has a very low vascular density which impedes the delivery of chemotherapeutic agents (McCarroll et al., 2014).

1.3.5.2. FOLFIRINOX

FOLFIRINOX is a combination of oxaliplatin, irionotecan, fluorouracil and leucovorin; it showed a modest increase on patient survival compared to Gemcitabine alone. However the adverse effects associated with this treatment were increased compared to patients in the Gemcitabine only control group (Schober et al., 2015).

1.3.5.3. Nab-Paclitaxel

Albumin bound paclitaxel (Nab-paclitaxel) in combination with Gemcitabine increased the 1 and 2 year survival rates of patients compared with Gemcitabine alone (Von Hoff et al., 2013). This synergy was related to the increased drug delivery due to the presence of the albumin (Frese et al., 2012). Secreted protein, acidic and rich in cysteine (SPARC) which is present in abundance in the PDAC tumour microenvironment binds albumin and sequesters nab-paclitaxel leading to an increase in its concentration in the tumour (Frese et al., 2012).

Unfortunately the current strategies to treat PDAC have not had a significant impact on the 5-year survival rate of patients compared to other gastrointestinal tumours

(Siegel et al., 2015), which highlights the need for the development of targeted therapies to treat PDAC.

1.4. The Embryonic signalling pathways in PDAC

1.4.1. The Hedgehog signalling pathway

1.4.1.1. Hedgehog ligands

The Hedgehog (Hh) family of signalling molecules are a highly conserved family of ligands with many roles within developing embryos. In adult organisms they have a diverse range of functions from controlling cell fate, maintaining stem cell populations, tissue repair and cellular differentiation (Michel et al., 2012, Matsumoto et al., 2016, Chen et al., 2016). Christiane Nusslein-Volhard and Eric Wieschaus first identified the *Hedgehog* gene during their investigations into the genes involved in the development and patterning of *Drosophila Melanogaster* (Nusslein-Volhard and Wieschaus, 1980). They won the Nobel Prize in Physiology or medicine for this work which gave new insight into the molecular mechanisms of early development in multicellular organisms. The Drosophila *Hh* gene was identified in the early 1990's by three groups (Lee et al., 1992, Mohler and Vani, 1992, Tabata et al., 1992). In 1993 three murine homologs of the Hh gene had been identified they were named *Sonic hh, Indian hh, and Desert hh (Shh, ihh, dhh) (*Echelard et al., 1993). These genes were discovered to be incredibly well conserved between mouse and human (Marigo et al., 1995).

1.4.1.2. Hedgehog post-translational modifications

In order to become functionally active ligands, the Hh precursor proteins (Shh) must undergo various post translational modifications. Hh proteins are produced as 45kDa proteins which are autocatalytically cleaved to form a 19kDa NH_2 fragment with all the signalling capacity and a 26kDa COOH- fragment which is responsible for the cleavage and has a role as a cholesterol transferase, which is the first lipid modification that the N-terminal fragment undergoes (Porter et al., 1996). The second lipid modification is the addition of a palmitic acid group, which is catalysed by the O-

acetyltransferase skinny hedgehog (Figure 1.4.). The combination of these modifications make it a poorly soluble molecule, however they allow its association with cell membranes which are rich in sterols (Chen et al., 2004). Shh ligands can signal as monomers short range (~40μm), but during development their role in limb patterning in vertebrates for example requires long range signalling (up to 300μm). In order for long range signalling to be possible the ligands must have undergone the lipid modifications described above as this it allows the formation of the large multimeric complexes that are required for this type of signalling (Koleva et al., 2015).

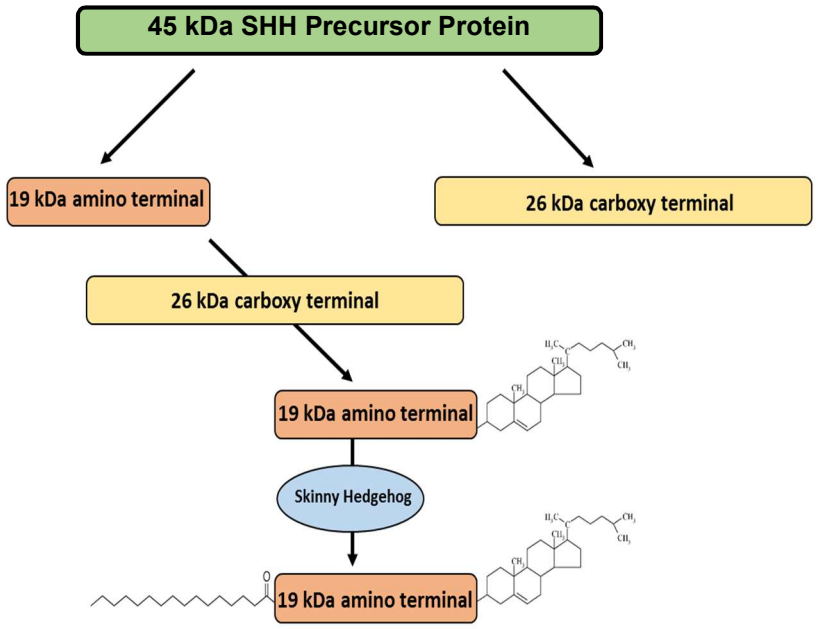

Figure 1.4. Post translational modifications of Shh

The 45kDa precursor protein is processed into a 26kDa and 19kDa terminal. The 19kDa is responsible for the signalling whereas the 26kDa carboxy terminal catalyses the addition of a cholesterol molecule to the amino terminus. In addition to a cholesterol molecule the amino terminal is further modified by the addition of a palmitic acid, this reaction is catalysed by Skinny Hedgehog. The cholesterol modification is also important for the secretion of Hh ligands from Hh producing cells, the cholesterol binds directly to the membrane transporter Dispatched which facilitates the secretion of ligands from cells.

1.4.1.3. The pathway

The first Hh receptor discovered was Patched (PTCH1) a 12-pass transmembrane protein with 2 extracellular loops which are responsible for the binding of Shh. PTCH1 has three co-receptors GAS1, CDON and BOC which are necessary for its signalling (Beachy et al., 2010). When Shh binds PTCH1 it releases its repression of

Smoothened (SMO) a 7-pass transmembrane protein. SMO is a G-protein coupled receptor (GPCR) which, once it is repression is relieved, translocates to the cell membrane via the primary cilia. SMO is the mediator of Hh signalling which triggers a downstream signalling cascade resulting in the dissociation of GLI proteins from kinesin-family protein, Kif7 and SUFU (Figure 1.5.). In the absence of a Shh ligand GLI proteins are still present in the cilia, however they are bound by SUFU and Kif7 which results in one of two possible outcomes: the phosphorylation of GLI by PKA, GSK3β and CK1 which causes it to be processed into its transcriptional repressor form GLI3; or GLI protein is targeted for degradation which is mediated by E3 ubiquitin ligase (Briscoe and Therond, 2013). The binding of Shh causes a disruption of the equilibrium between the activator (GLI1, GLI2) or the repressor forms (GLI3) of the GLI proteins.

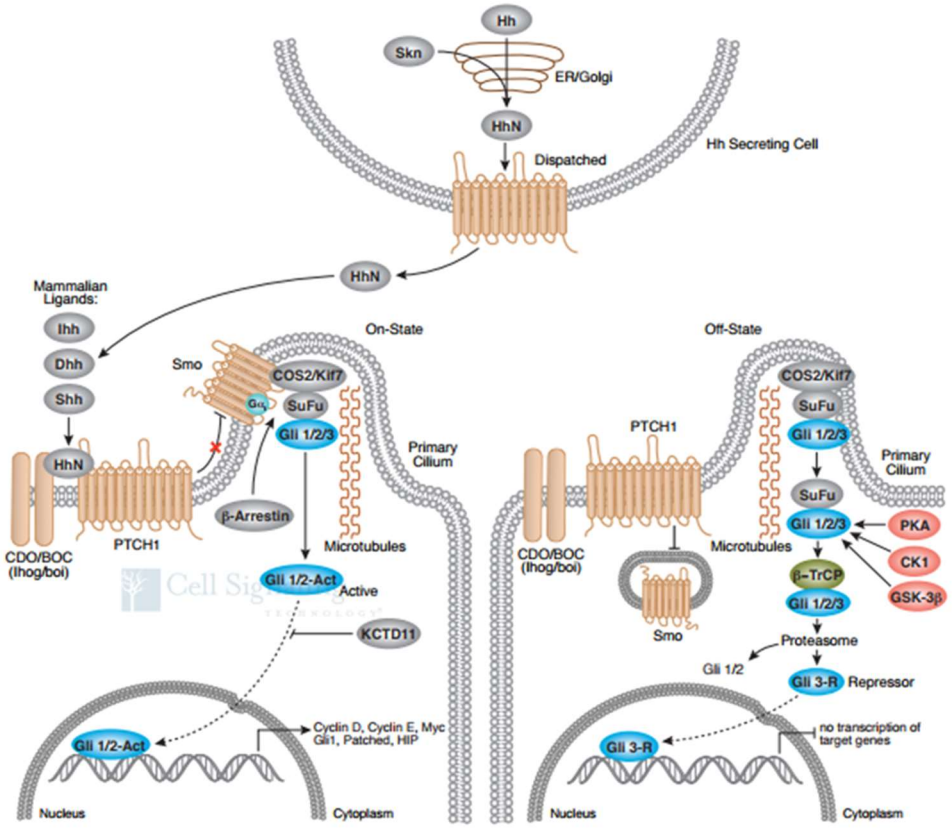

Figure 1.5. The hedgehog signalling pathway

Canonical Hedgehog signalling in the presence and absence of Shh ligand. Shh binding to Ptc results in a downstream signalling cascade which concludes in the activation of GLI1/2 and transcription of Hh target genes. HhN refers to Hh ligands (amino-terminal) which have undergone post translational modifications. Illustration reproduced courtesy of Cell Signalling Technology, Inc (www.cellsignal.com).

1.4.1.4. The GLI transcription factors

There appears to be an evolutionary division between *Drosophila* and vertebrate Hh signalling as vertebrate Hh signalling activation and repression requires the primary cilia of a cell (Goetz et al., 2009). Genetic screening has identified a plethora of cilia-related proteins which, when mutated are responsible for a variety of human diseases which have been termed ciliopathies. They have similar to symptoms to diseases resulting from defective Hh signalling (Bangs and Anderson, 2017). In the absence of Shh ligand PTCH1 is located at the base of primary cilia, but SMO and GLI proteins are absent they translocate through the cilia in the presence of Shh. There are three proteins (PKA, GSK3β and CKI) which are involved in GLI protein processing and they are located in the primary cilia. Upon Shh binding to PTCH1 there are changes which occur in the primary cilia, PTCH1 moves out of the cilia and SMO accumulates within it. In the absence of Hh signalling SUFU negatively regulates the pathway by sequestering the GLI1 proteins in the primary cilia, which begins the process by which they are degraded (Briscoe and Therond, 2013). Shh binding to PTCH1 results in an accumulation of GLI2 in the primary cilia, which overcomes Hh pathway repression by GLI3, GLI1/GLI2 are translocated to the nucleus and activates Hh target genes (Figure 1.5.) (Rimkus et al., 2016, van den Brink, 2007). Changes in the expression of Hh pathway components PTCH1, SMO and GLI1 are most commonly used to identify changes in Hh pathway activity (Lauth et al., 2007, Huang et al., 2006, Onishi et al., 2011).

1.4.1.5. The hedgehog signalling pathway in development

In order to yield a biological response, the Hh pathway maintains a balance between the activator (GLI1, GLI2) and repressor forms (GLI3) of the GLI transcription factors. During development Shh is expressed throughout the midline tissues specifically the notochord and floor plate which control left-right and dorso-ventral patterning of the embryo (Sampath et al., 1997, Pagan-Westphal and Tabin, 1998, Schilling et al., 1999, Watanabe and Nakamura, 2000). Shh is also expressed in the limb buds during development and is responsible for the patterning of the development of the distal limbs (Riddle et al., 1993, Johnson et al., 1994). In the later stages of development Shh also has a role in the development of epithelial tissues (Chuong et al., 2000). dhh expression is found mainly in the ovaries and testis and is involved in the maintenance of sertoli and granulosa cells (Bitgood et al., 1996, Wijgerde et al., 2005). ihh is expressed in a variety tissues including the endoderm, gut and bones (Dyer et al., 2001, van den Brink, 2007, Vortkamp et al., 1996). One unique characteristic of Hh signalling is its ability to exert a biological effect over long distances; in mammals this is approximately 300μm (Zhu and Scott, 2004) compared to short range signalling which is 40μm (approximately 10 cells). The gradient of Hh signalling is tightly controlled and is dependent on the context of the Hh signal. This is most apparent during development of the neural tube in mammals; Shh is secreted from the notochord and floor plate and diffuses across the ventral neural tube which creates a concentration gradient across this region (Jessell, 2000, Patten and Placzek, 2000). The cells exposed to different concentrations of Shh differentiate into 5 different neuronal subtypes (Marti and Bovolenta, 2002).

1.4.1.6. The hedgehog target genes

Due to its diverse array of functions during development and homeostasis, Hh pathway activation can have a wide variety of consequences within the tumour microenvironment. The Hh pathway is critical for the developing embryo especially

as it has control over cell proliferation and survival. The tumour is able to hijack this signalling pathway to promote tumour proliferation and survival through the upregulation of fibroblast growth factor (FGF) (Sherman et al., 2017), insulin like growth factor binding protein 6 (IGFBP6) (Hao et al., 2013), histone deacteylase (HDAC) (Lee et al., 2013b), telomerase reverse transcriptase (TERT) cyclin D1 (Mille et al., 2014), B-cell lymphoma-2 (Bcl-2)(Han et al., 2009) and nuclear factor kappa-light-chain-enhancer of activated B cells (NF-κB) (Hanna and Shevde, 2016). The upregulation of TERT also allows cells to transform to neoplastic cells with unlimited replicative capability (Mazumdar et al., 2013). Hh pathway activation also leads to an upregulation of inflammatory cytokines in the tumour microenvironment including nucleotide-binding oligomerisation domain-containing protein 2 (NOD2) (Ghorpade et al., 2013), tumour necrosis factor-alpha (TNF-α), interleukin-1-Beta (IL-1β) and interleukin-6 (IL-6) (Li et al., 2015) which are involved in tumour development. The Hh pathway has also been associated with inducing angiogenesis as this is a necessary requirement during the development of the embryo. This is achieved through the upregulation of VEGF (Pinter et al., 2013), FGF, vascular endothelial growth factor receptor (VEGFR) (Hong et al., 2013) and cysteine-rich angiogenic inducer 61 (CYR61)(Harris et al., 2012). The Hh pathway is involved in the differentiation of cells in development; in the tumour this facilitates metastases and invasion which is achieved by the upregulation of matrix metalloproteinases and activation of the transforming growth factor beta-1 (TGF-β) (Choe et al., 2015).

1.4.2. The Wnt signalling pathway

1.4.2.1. Post-translational modifications of Wnt ligands

Wnt ligands are glycoproteins approximately 40kDa in size and contain many cysteine residues, which are critical in the formation of disulphide bonds which occur during appropriate folding of the protein. To date, 19 Wnt ligands have been identified (Mason et al., 1992). Immature Wnt ligands undergo post translational modification in

the endoplasmic reticulum (ER). Firstly, N-linked oligosaccharide chains are added to the peptide backbone, however the biological function of this modification is not clear (Reichsman et al., 1996). The next step is the addition of a palmitate group by the O-acetyl transferase Porcupine (PORCN) which is present in the ER (Tanaka et al., 2002). The addition of the palmitate group has been associated with the successful trafficking and secretion of Wnt ligands from the donor cell, by targeting the Wnt ligands to the cell membrane. The palmitate moiety has also been identified as playing a role in ensuring the appropriate folding of the proteins so they do not get retained by the ER (Mikels and Nusse, 2006). One theory also suggests that the lipid modification has an important role after the secretion of Wnt as it targets the ligand to the cell membrane arguing; that it controls the spatial distribution of Wnt ligands after secretion (Vincent and Dubois, 2002).

1.4.2.2. The canonical Wnt signalling pathway

Just as there are many Wnt ligands there are also many different Wnt receptors. There are 10 known human Wnt receptors known as Frizzled (Fzd) receptors which are 7-pass transmembrane proteins. All Fzd receptors have an extensive extracellular domain which has a cysteine rich site which binds Wnt ligands (Hsieh et al., 1999, Wu and Nusse, 2002). In addition, there are low density lipoprotein (LDL) receptor related proteins 5 and 6 (LRP5 and LRP6), which are required for active Wnt signalling. Different Wnt and Fzd receptor combinations are responsible for the activation of either the canonical or non-canonical Wnt signalling pathway (Dijksterhuis et al., 2014).

In the absence of Wnt ligands a scaffolding protein, Axin interacts with the β-Catenin degradation complex which consists of glycogen synthase kinase 3 (GSK3), casein kinase 1-alpha (CK1α) and adenomatosis polyposis coli (APC). In a complex together they organise the phosphorylation of β-Catenin at serine 45 by CK1α followed by threonine 41, serine 37 and serine 33 by GSK3 (Kimelman and Xu, 2006). This

process targets the β-Catenin for ubiquitination and subsequent degradation (Figure 1.6.) (MacDonald et al., 2009).In the presence of Wnt ligand, a Fzd-LRP5/6 receptor complex forms; this complex recruits Axin which disrupts the GSK3/CK1α/APC degradation complex (Mao et al., 2001). Wnt binding to the Fzd-LRP-5/6 receptor complex also results in the stabilisation of Axin. The disruption of the β-Catenin degradation complex leads to the stabilisation and cytoplasmic accumulation of β-Catenin which then translocates to the nucleus (Komiya and Habas, 2008). The mechanism by which the nuclear translocation occurs is not well understood as β-Catenin does not contain a nuclear localisation sequence, neither does this process involve Ran-mediated nuclear transport or importin proteins (Fagotto et al., 1998). One theory suggests β-Catenin may combine with other proteins which are in the process of nuclear import such as Axin (Cong and Varmus, 2004). Once in the nucleus β-Catenin behaves as a transcriptional co-activator in complex with LEF/TCF transcription factors; this complex binds to the promoter region of target genes (Clevers, 2006) (Figure 1.6.). Changes in the mRNA level of *AXIN2* is most commonly used to identify changes in canonical Wnt pathway activation (Jho et al., 2002).

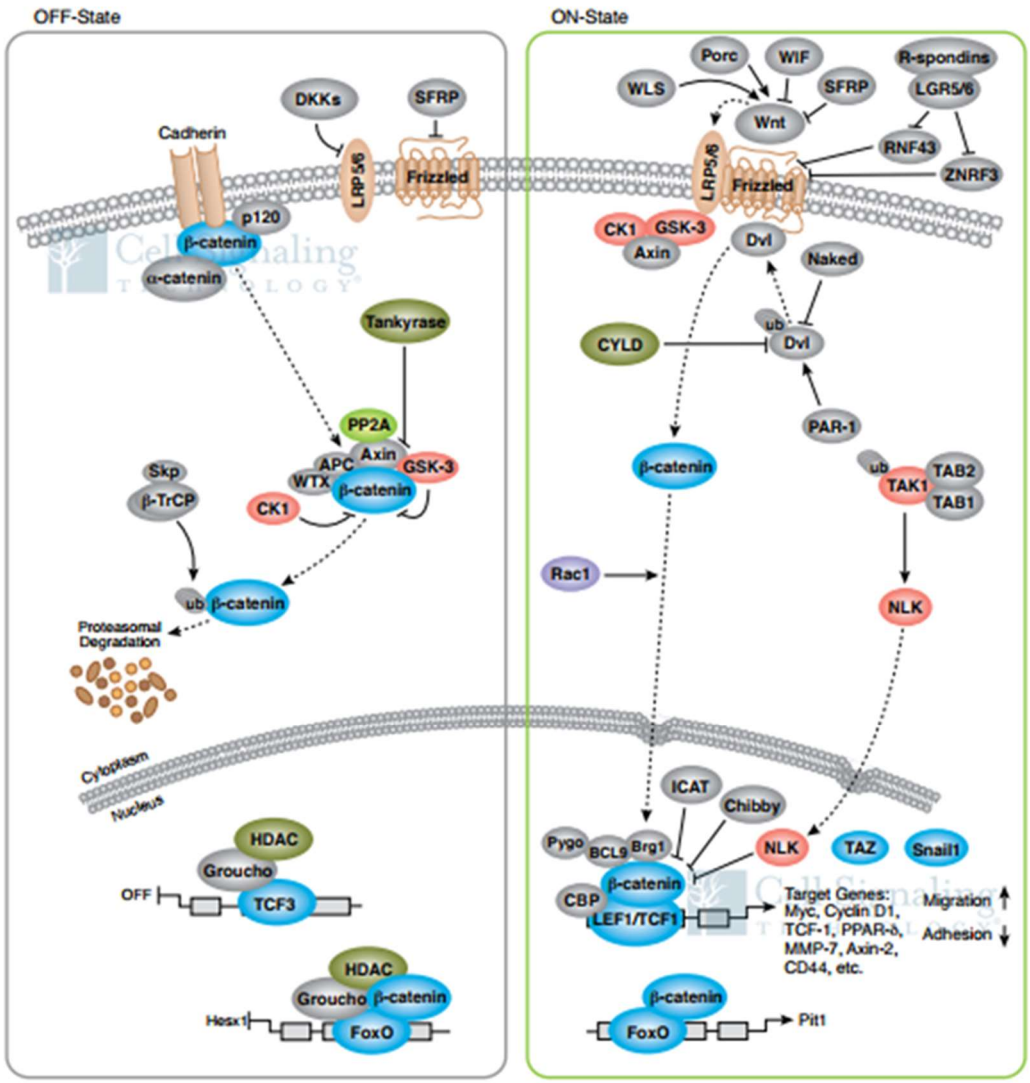

Figure 1.6. Wnt/β-Catenin signalling pathway

Canonical Wnt signalling in the presence and absence of Wnt ligands. Illustration reproduced courtesy of Cell Signalling Technology, Inc (www.cellsignal.com).

1.4.2.3. The non-canonical Wnt signalling pathway

Non-canonical Wnt signalling is described as Wnt pathway activation with downstream effectors which are not β-Catenin-TCF/LCF (Gomez-Orte et al., 2013). There are two main forms of non-canonical Wnt signalling, the planar cell polarity (PCP) and the Wnt/Ca^{2+} pathways. These pathways are both believed to inhibit canonical Wnt/β-Catenin signalling (Bernard et al., 2008). Firstly, the PCP pathway is

activated when a Wnt ligand (specific to this pathway) binds to a Fzd receptor which is in complex with a co-receptor ROR1/2, Ryk or PTK7. Upon binding, the ligand-receptor complex is internalised and a downstream signalling cascade of Rho and Rac GTPases, Rho-kinase (ROCK) and c-Jun N-terminal kinase (JNK) results in the activation of target genes (Yang and Mlodzik, 2015), which are responsible for tissue polarity and cell motility (Walck-Shannon and Hardin, 2014, Sedgwick and D'Souza-Schorey, 2016). The Wnt/Ca^{2+} pathway once activated triggers downstream signalling of a standard GPCR signalling pathway (De, 2011), eventually resulting in the activation of nuclear factor associated with T-cells (NFAT) which activates genes associated with cell fate and migration (Gomez-Orte et al., 2013).

1.4.2.4. Wnt signalling in development

Wnt signalling is indispensable in the developing embryo (Holstein, 2012), the complexity of this signalling pathway comes from the multitude of Wnt ligands and Fzd receptor combinations which can result in the activation of canonical, PCP or Wnt/Ca^{2+} signalling pathways (Kikuchi et al., 2009). Wnt ligands are long range (120μm) signalling molecules which affect cellular fate in a concentration dependant manner (Serralbo and Marcelle, 2014). One theory suggests that long range Wnt signalling is achieved through the interaction between the membrane of cells and the palmitoyl group on the Wnt ligand itself (Takada et al., 2006). Extracellular heparin sulfate proteoglycans (HSPG) have also been suggested as one method of stabilisation and transport of Wnt ligands (Fuerer et al., 2010). The role of the Wnt signalling pathway can be divided into four specific roles: axis patterning, control of cell fate, cell proliferation and cell migration. In a developing embryo Wnt signalling has been implicated in the development of the anteroposterior and dorsal ventral axis (Hikasa and Sokol, 2013). Wnt signalling has an important role in the determination of cell fate in a variety of cell types including the differentiation of pluripotent stem cells into progenitor cells of the mesoderm and endoderm (Nusse, 2008). Wnt

signalling is involved in the development of many tissues throughout the body such as gut, germ cell, hair follicle, lung, nephron and ovary (Verzi and Shivdasani, 2008, Cantu and Laird, 2013, Choi et al., 2013, De Langhe and Reynolds, 2008, Schmidt-Ott and Barasch, 2008, Vainio et al., 1999). During development embryonic signalling pathways such as the Wnt pathway control cell proliferation which is required on a large scale in a growing organism (Willert and Jones, 2006). Cell migration is also a critical part of development as it allows the movement required for the body axis patterning, tissue formation and limb induction, this is achieved through both activation of the canonical Wnt signalling pathway and the PCP pathway (Sedgwick and D'Souza-Schorey, 2016).

1.4.2.5. Wnt signalling target genes

The Wnt signalling pathway is diverse in development and has a wide variety of functions, especially in the activation and maintenance of stem cells which are present throughout the tissues of the body (Nusse, 2008). In the adult organism Wnt signalling maintains rapidly proliferating cell populations such as the epithelium of the crypt cells of the villi in the gut, the hair follicle and skin epidermis through the modulation of the *Lgr5* gene (Haegebarth and Clevers, 2009). During normal tissue homeostasis the stem cell pools which are present in each of these tissues are able to differentiate into a variety of cell lineages, however during tumour growth this property leads to an increased cell proliferation and differentiation. Another Wnt target gene is *c-Myc* which controls cell fate and apoptosis in normal tissues, however during neoplastic transformation it is involved in the switching to glycolysis only metabolism of glucose (Warburg Effect) (Pate et al., 2014). *Cyclin D1* is also under transcription control of the Wnt signalling pathway; in thyroid tumour development it is associated with metastases (Zhang et al., 2012). It has an extensive assortment of target genes which includes many genes which in neoplastic cells would be able to influence the tumour growth and metastases (Ramakrishnan and Cadigan, 2017).

1.5. Aims

PDAC represents a devastating disease with a high unmet therapeutic need. The combination of late diagnosis, poor response to current chemotherapy and the lack of a genetically defined targeted therapy results in a poor prognosis with a low median survival for patients. Moreover, the discrepancy between *in vitro* efficacy of chemotherapeutic agents and clinical outcomes highlights a need for better targeted therapies, but also the necessity for the development of *in vitro* assays that take into account the PDAC tumour microenvironment. The aim of this project was to establish an in vitro model for use in pre-clinical drug development which incorporates PDAC cells and CAFs, the most abundant non-cancerous cell type of the PDAC tumour microenvironment.

1.6. Objectives

1. Create a reproducible 3D co-culture model using CAFs isolated from the PDAC tumour microenvironment.
2. Determine if active Hedgehog signalling is achieved in an *in-vitro* model Transwell model of CAFs and tumour cells
3. Establish whether the Canonical Wnt signalling pathway is involved in the cross-talk between CAFs and tumour cells.
4. Investigate the effect of a 3D co-culture model on the efficacy of Gemcitabine *in vitro.*

2. Materials and Methods

2.1. Materials

2.1.1. Consumables

The following items were purchased from Corning Inc. (USA): All tissue culture flasks (catalogue numbers 430641, 430825, 43001); 96-Well Clear Flat Bottom Ultra Low Attachment Microplates (catalogue number 3474).

Nunc Cryovials (catalogue number 479-1235) disposable sterile scalpels (catalogue number 233-5364) and Superfrost plus adhesion slides (631-0446) were all purchased from VWR.

The following kits, stains and antibodies were all purchased from Abcam (UK): Human Sonic Hedgehog ELISA Kit *(ab100639)* Human Dickkopf-1 ELISA Kit *(ab100501)* Picro-Sirius Red Stain Kit *(ab150681)* Anti-alpha smooth muscle Actin antibody *(ab7817)* Anti-Rabbit IgG Alexa Fluor 488 *(ab150077)* Anti-Sonic Hedgehog antibody *(ab73958)* Rabbit Polyclonal IgG Isotype control *(ab27478)* Anti-wide spectrum Cytokeratin antibody *(ab9377)* Anti-Vimentin antibody *(ab92547)* Anti-CD68 antibody *(ab125212)* Anti-Desmin antibody (*ab32362).*

Unless otherwise specified in parentheses, all materials not listed above were purchased from Sigma-Aldrich (UK).

2.1.2. Primers

The primers used in this project were purchased from Primer Design and were ordered to ensure they spanned intronic regions to remove the likelihood of contaminating genomic DNA being amplified. The efficiency of these primers was determined by comparing the gradient of the expression curve of the gene amplified (using a serial dilution of a positive control sample) and the curve produced using the housekeeping gene Glyceradehyde 3-phosphate dehydrogenase (GAPDH).

Primer	Forward Primer (5' – 3')	Reverse Primer (3' – 5')
GAPDH	Primer design protected sequence	
RPLP0	CCATTGAAATCCTGAGTGATGTG	CGAACACCTGCTGGATGAC
ACTB	CTCTTCCAGCCTTCCTTCCT	CGTACAGGTCTTTGCGGATG
GLI1	CCAGCCAGAGAGACCAACA	GCATCCGACAGAGGTGAGA
SMO	ACCACCTACCAGCCTCTCTC	CCCACAAAACAAATCCCACTCA
PTCH1	CACCATCCTCGGCGTTCT	TGGGCAGGCGGTTCAAG
Shh	CCAGAAACTCCGAGCGATTTA	GCCAAAGCGTTCAACTTGTC
AXIN2	CCAAGTGTCTCTACCTCATTTCC	GCGGCTCTCCAACTCCAG
LEF1	CCGAAGAGGAAGGCGATTTAG	CTGAGAGGTTTGTGCTTGTCT
SFRP1	CATGACGCCGCCCAATG	CCTCAGATTTCAACTCGTTGTC
SFRP4	GATGATGCTTCTTGAAAATTGCTTAG	GGGGGATTACTACGACTGGTG
PORCN	CTGCTGTCCCTGGCTTTTAT	CGATGCTGGTGCGAACA

Table 2.7. Forward and reverse primer sequences used throughout this project

2.2. Methods

2.2.1. Specimen collection

Pancreatic specimens were obtained from patients undergoing surgery to remove a portion of the pancreas with curative intent at the Royal Liverpool University Hospital with local ethical approval and fully informed consent. Patients with PDAC were selected for this project. Histopathologists Professor Fiona Campbell or Dr. Timothy Andrews performed a gross analysis of the specimen and immediately selected "fibrous appearing" pancreatic tissue for isolation of CAFs and epithelial cancer cells,

and “normal appearing” tissue clearly separated from the boundary of the tumour for isolation of Normal Activated Fibroblasts (NAFs). The specimen provided was split in half with one half used for isolation of cells (Section 2.2.2.) and the other half fixed and prepared for staining (Section 2.2.4.).

2.2.2. Isolation of cells from the pancreas

2.2.2.1. Isolation of CAFs

CAFs were isolated using the outgrowth method (Apte et al., 1998, Bachem et al., 1998). This method involves the explantation of pieces of fibrotic tissue removed from the pancreas. Once a fibrotic sample had been identified it was placed immediately into ice cold phosphate buffered saline (PBS). Using sterile disposable scalpels the tissue was divided into small pieces (1-2mm^3). These pieces were then arranged in uncoated 6-well tissue culture plates (5-7 pieces/well) and 500µL of growth media (Iscove’s Modified Dulbecco’s Medium (IMDM) supplemented with 20% Fetal Bovine serum (FBS), 2% L-Glutamine and 1% Penicillin Streptomycin) was added carefully to ensure that the tissue pieces were not disturbed. Plates were incubated overnight at 37^oC in a 5% CO_2 air humidified atmosphere. After 24h 500µL of fresh medium was added with care taken not to disturb the tissue, with further medium changes every three days. Cells were seen growing out of the tissue within 24h (Figure 2.1) and continued for approximately 7days. Once wells had reached 80-90% confluence, cells were sub-cultured (Section 2.1.3.2) into T75 flasks at a concentration of 200,000 cells/flask and tissue pieces were discarded.

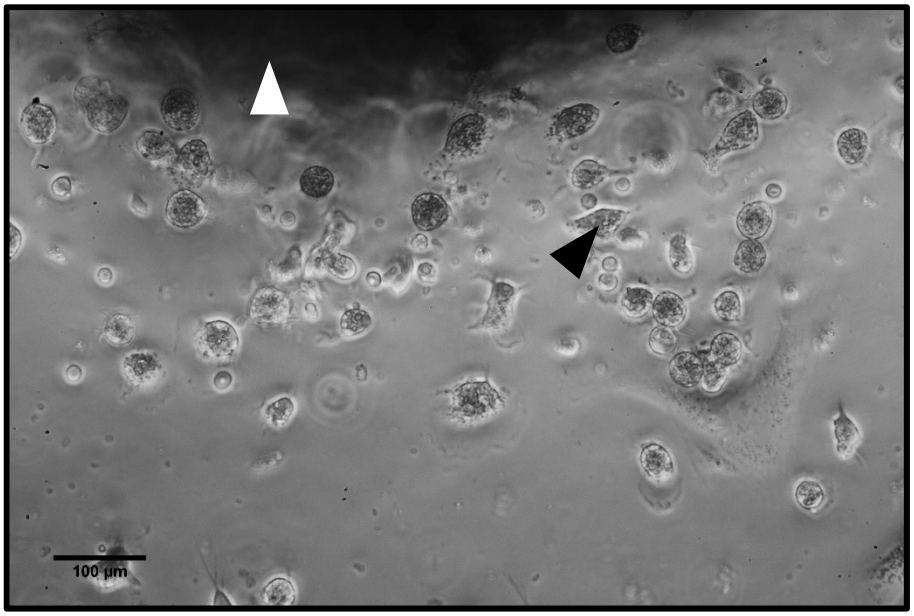

Figure 2.1. Representative Image of cells growing out of tissue pieces

Cells (black arrow) can be observed growing out of the tissue piece (white arrow) from 24h after explantation. This image was taken using Brightfield Microscopy at 20x magnification. Scale bar 100µm.

2.2.2.2. Isolation of epithelial tumour cells

The procedures used to isolate epithelial cancer cells from the pancreas are reviewed in Section 3.2.2.

2.2.2.3. Isolation of normal activated fibroblasts

Normal fibroblasts were isolated from normal appearing tissue adjacent to tumour tissue by my colleague Dr Lawrence Barrera-Briceno using the density gradient method described in Section 3.2.2.

2.2.3. Cell culture

In order to take into consideration the heterogeneity of PDAC, 5 epithelial cancer cell lines (ASPC1, MIAPACA2, PANC1, SUIT2, BXPC3; purchased from the American Type Culture Collection (ATCC)) were selected. These cell lines had varied source, patient gender, mutational status and proliferative capacity (Table 2.1; Figure 2.2).

Cell Line	Source	Mets	Differentiation	*Kras*	*P53*	*P16*	*SMAD4*	Proliferation (Doubling Time)	Ref
ASPC1	Ascites	Yes	Poor	M (12 Asp)	D	Wt	Wt	60h	(Chen et al., 1982)
MIAPACA2	Primary Tumour	ND	Poor	M (12 Cys)	M (248 Trp)	HD	Wt	40h	(Yunis et al., 1977)
PANC1	Primary Tumour	Yes	Poor	M (12 Asp)	M (273 His)	HD	Wt	40h	(Lieber et al., 1975)
SUIT2	Liver Metastases	Yes	Moderate	M	M	M	Wt	38h	(Iwamura et al., 1987)
BXPC3	Primary Tumour	No	Moderate to Poor	Wt	Wt	HD	HD	60h	(Tan et al., 1986)

Table 2.1. Summary of characteristics of pancreatic epithelial cancer cell lines

Characteristics of the pancreatic cancer cell lines used throughout this project including patient information and molecular characteristics such as mutational status of *Kras, P53, P16* and *SMAD4.* Wt indicates a cell line is Wild-type for the gene of interest, M indicates an oncogenic mutation, HD indicates a homozygous deletion. Gene location of mutation provided if known (Deer et al., 2010)

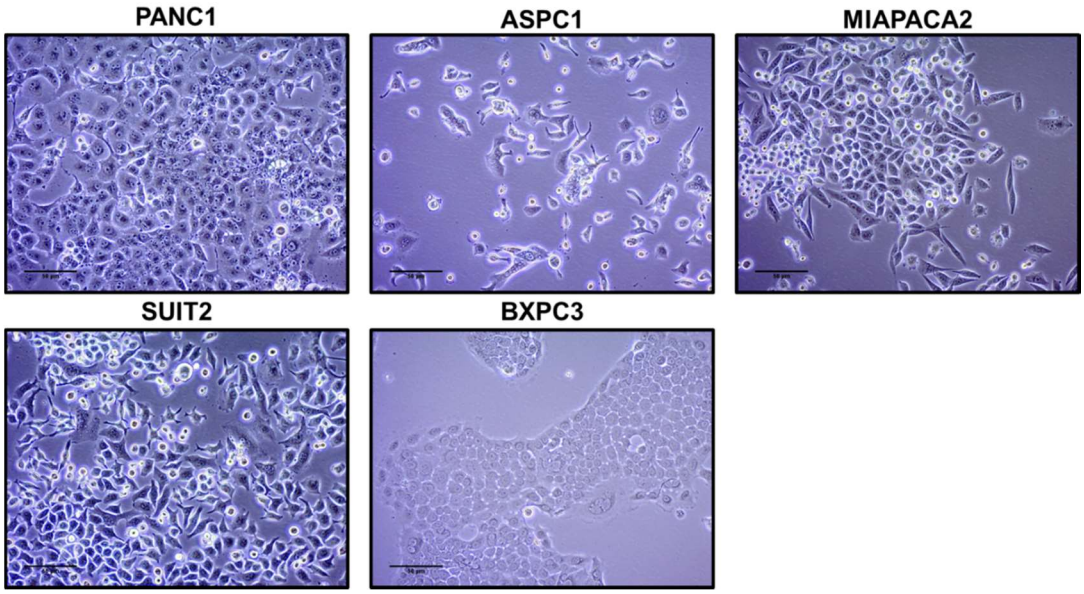

Figure 2.2. Representative Images of pancreatic epithelial cancer cell lines.
Images taken of each cell line under standard growth conditions. Images taken using Brightfield Microscopy at 20x magnification. Scale bar 50µm.

Wnt-3A producing cells (L-Wnt-3A) and Normal pancreatic fibroblasts (NPF) were also purchased from the ATCC.

2.2.3.1. Cell culture conditions

Pancreatic cancer cell lines were cultured in Dulbecco's Modified Eagles Medium (DMEM) supplemented with 10% FBS and the cells were maintained at 37°C in a 5% CO_2 air humidified atmosphere. CAFs, NAFs and Normal Pancreatic Fibroblasts (NPF) were cultured in IMDM supplemented with 10% FBS, 2% L-Glutamine and 1% Penicillin Streptomycin.

2.2.3.2. Maintenance of cells

Once cells had reached 70-80% confluence, the media was removed from the flask. 10mL of PBS was added to wash off any excess media, this was removed and another wash was completed. 2mL of Trypsin-EDTA was then added to each flask. EDTA is a chelating agent which binds calcium and thus prevents the cadherins between cells from binding and forming clumps during detachment. Trypsin is a proteolytic enzyme which cleaves focal adhesion proteins which allow the cells to bind

to each other and the surface of the culture vessel. Both agents have maximal function at 37°C (Freshney and Freshney, 2005) so the flask was incubated at 37°C, 5% CO_2 for approximately 5min (epithelial cancer cell lines) or 10min (CAFs and NAFs). Once the cells were in suspension, 10mL of culture medium was added to each flask and the culture surface was washed twice using this medium to ensure the maximal yield of cells. Cell culture medium must be added in excess in order to quench the trypsin as it contains FBS which inhibits the trypsin. If the trypsinization was allowed to continue it would eventually damage the cell membrane. A 10µL sample of the cells was removed and set aside for counting. The rest of the culture was added to a 15mL centrifuge tube and centrifuged at 400g for 5min. The medium was removed and the pellet re-suspended in an appropriate volume of medium depending on the cell count (Section 2.2.3.3.). The cells were then seeded into a new T75 flask at an appropriate cell density.

2.2.3.3. Cell counting

To quantify the yield of cells from each flask a 10µL aliquot of the cells was taken and 10µL of 0.4% trypan blue was added. Trypan blue is a diazo dye which is commonly used to identify viable cells. As it is a negatively charged molecule it does not cross the cell membrane unless there is membrane damage, therefore it is customarily used to stain dead cells. When a cell suspension has been incubated with trypan blue dead cells appear blue and live cells appear white within a haemocytometer chamber. A haemocytometer was used to count total cell number followed by the live cell number. A haemocytometer is a counting slide used to determine the amount of cells in a liquid sample. The sample is covered with a coverglass which has gridlines etched onto it at a precise distance (250µm) apart which allows the researcher to determine the amount of cells in a specified volume.

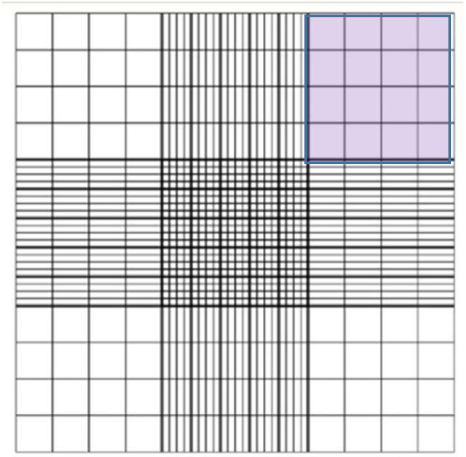

Density calculation:

$$\frac{x}{n} * 10\,000 = cells/mL$$

Figure 2.3 Image of haemocytometer etchings and cell density formula

Typically a haemocytometer comprises 4 large squares (example highlighted in purple) with each representing 1/10,000mL once the coverslip is in place. The formula for calculating the cell density (cells/mL) is given beneath the image of the haemocytometer where x represents cell number and n represents the number of large squares used to generate the cell number. The calculated density does not take into account the initial dilution made using trypan blue (1:2) and therefore the cell density should be adjusted accordingly. Cell viability was determined using (live cell number/Total cell number) x 100.

2.2.3.4. Long-term storage of cells

In order to use cells at a similar passage throughout the project, cells were frozen and kept in liquid nitrogen for long-term storage. In order to create cell banks for this project, cells were cultured in larger culture vessels (T225) and allowed to reach 80-90% confluence. Upon reaching this level, the cells were dissociated from the culture vessel using the method described above (Section 2.2.3.3.). The supernatant was removed and the pellet re-suspended in freezing media (DMEM, 10% FBS, 10% DMSO). The suspension was then aliquoted by 1mL volumes into cryovials at a density of 2 x 10^6 cells/mL. The tubes were transferred to an insulated container and cooled to -80ºC at an approximate rate of 1ºC/min. After 24h the cryovials were transferred to a liquid nitrogen storage container until further use.

2.2.3.5. Recovery of cells

In order to recover cells from long term liquid nitrogen storage a vial was collected and placed on dry ice. 10mL of pre-warmed culture medium was prepared in a centrifuge tube. The cryovial was partially submerged in a water bath at 37°C and agitated until the cell suspension had thawed. The cell suspension was then transferred to the prepared centrifuge tube. This was then placed in a centrifuge and spun at 400g for 5min. The freezing medium was removed and the pellet was re-suspended in fresh medium. The cells were then transferred to a T75 and put into a 37°C, 5% CO_2 air humidified incubator overnight. The following day the cells were checked to determine if the cells were recovering and had adhered to the flask appropriately; the media was refreshed if necessary.

2.2.4. Tissue staining

2.2.4.1. Tissue processing

At specimen collection a part of each sample was taken and fixed in 4% paraformaldehyde (PFA) solution in PBS (Affymetrix), which penetrates the tissue at 1mm/h. The tissue was incubated at 4°C overnight to ensure it was thoroughly fixed.

The role of tissue fixation is to preserve the morphological and physical characteristics of the tissue at a given point in time. PFA fixes the cells by forming crosslinks between proteins. These crosslinks are methylene bridges formed between nitrogen containing side chains of basic amino acids. The fixed tissue was placed in a cassette and stored in 4% PFA solution until processing. The cassettes were then loaded into a Leica TP1020 tissue processor and dehydrated using the following conditions:

1. 1x wash 70% (v/v) methanol
2. 1x wash 90% (v/v) methanol
3. 5x wash 100% methanol
4. 3x wash of Xylene for 1h each
5. 2x wash in molten paraffin wax at 65°C

This tissue processing step is necessary as melted paraffin wax is hydrophobic; the water present in the tissue must be removed before embedding can occur. This process is carried out step-wise in increasing concentrations of ethanol until a water-free solution is reached. It is carried out in this manner to avoid the tissue distortion which could occur if the tissue was immediately immersed in 100% ethanol. An intermediate solvent (Xylene) is then used in a process commonly referred to as “clearing”. This solvent is immiscible with both ethanol and paraffin wax and therefore displaces the ethanol before eventually being displaced by the paraffin wax. Xylene also has a role in removing fat from the tissue specimens which can prevent wax infiltration.

2.2.4.1.1. Paraffin embedding

Once the tissue had been processed, the cassettes were placed in a paraffin wax reservoir at 65ºC in a Leica 61160 embedding station. Tissues were removed from the cassettes and positioned in a metal mould of the appropriate size, and the mould was filled with paraffin wax. The moulds were then placed on an ice plate to solidify. After approximately 2h in the ice tray the paraffin embedded samples were removed from the moulds and stored at room temperature for sectioning at a later date.

2.2.4.1.2. Sectioning

Tissue specimens were kept on ice for 1h before sectioning. Cooling the tissue blocks allows for thinner sections as it increases the structure of the wax. The block was then placed in a Leica RM2245 microtome ensuring the blade would cut straight across the block, and the blocks were sectioned (section thickness set at 4µm). Animal tissue is commonly sectioned at 4µm as it is the average diameter of a cell, and a monolayer of cells is desirable for clarity of images. Once a ribbon of sections was obtained, it was floated on the surface of a water bath (40-45ºC) to flatten the sections. Tweezers

were used to separate the sections which were then picked up using microscope slides and stored at 37°C overnight in a slide rack.

2.2.4.2. Haematoxylin and Eosin staining

Haemotoxylin and Eosin (H&E) is the most commonly used staining system in medical pathology (Fischer et al., 2008). It contains two dyes, the first Haemotoxylin is a dye which is used to stain acidic structures purple/blue. Acidic structures in the cell include heterochromatin which is found in the nucleus and ribosomes which are found in the ER. Eosin stains basic material a pink colour; the cytoplasm of a cell contains proteins which are basic, therefore the cytoplasm of a cell appears pink (Figure 2.4).

H&E staining was completed using a Leica Autostainer XL using the following steps:

1. Xylene dip to remove the paraffin wax (5min)
2. 2x wash in xylene
3. 2x wash in 100% ethanol (30s; Shaking)
4. 2x wash in 95% ethanol (30s; Shaking)
5. 2x wash in 70% ethanol (30s; Shaking)
6. Rinse with tap water (2min)
7. Haematoxylin stain (10min)
8. Rinse with running tap water (5min)
9. Acid water (0.25% HCl/dH_2O)- (30s)
10. Rinse with running tap water (2min)
11. Scott's tap water (30s; Shaking)
12. Rinse with running tap water (2min)
13. 1x wash in 100% ethanol (30s)
14. Eosin stain (2min)
15. 100% ethanol to remove eosin (1min)
16. 2x wash 100% ethanol (30s;Shaking)

17. 3x wash in xylene (30s)
18. Mount coverslips

Once coverslips had been added the slides were left overnight at room temperature to dry.

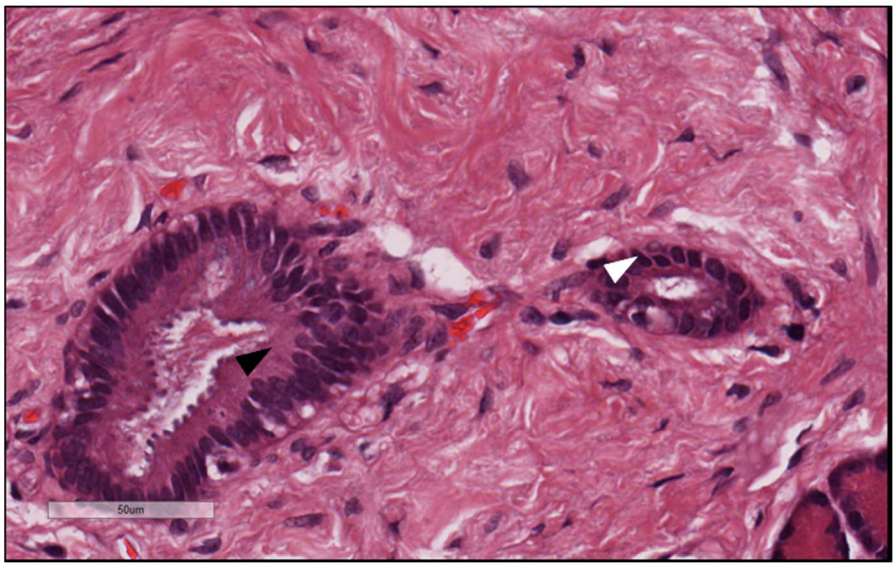

Figure 2.4. Example of H&E stained section

H&E stained section of a PDAC tumour, which allows the visualisation of the cellular structures of the tissue. The cytoplasm of epithelial ductal cells is stained pink (black arrow). Stroma surrounding the ducts is identified based on the morphology of the cells; nuclei are stained purple/blue (white arrow). Scale bar 50µm.

2.2.4.3. Picro-Sirius red staining (connective tissue stain)

Picro-Sirius Red stain is used to visualise (using standard bright field microscopy) collagen I and III fibres (red) in addition to muscle fibres (yellow) and cell cytoplasm (yellow) (Figure 2.5.).

Picro-Sirius Red staining was carried out manually using the following steps:

1. Xylene dip to remove the paraffin wax (5min)
2. 2x wash in xylene (30s)
3. 2x wash in 100% ethanol (30s; Shaking)
4. 2x wash in 95% ethanol (30s; Shaking)
5. 2x wash in 70% ethanol (30s; Shaking)
6. Rinse - running tap water (2min)
7. Picro-Sirius Red Stain (30min)

8. 2x wash in acetic acid solution (1min)
9. Rinse in 100% ethanol (30s)
10. 2x wash in 100% ethanol to dehydrate (1min)
11. Mount coverslips

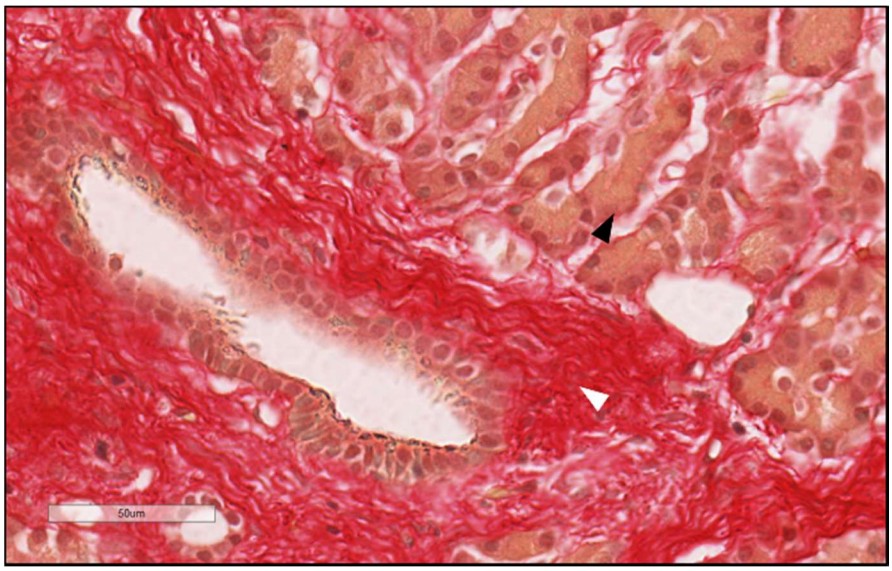

Figure 2.5. Picro-Sirius red stained section PDAC microenvironment
An example of a Picro-Sirius Red stained section of a PDAC tumour, which allows the histological visualisation of connective tissue (collagen I and III). The cytoplasm of epithelial ductal cells and acinar cells are stained a yellow/pink colour (black arrow) with collagen fibres appearing red (white arrow). Scale bar 50µm.

2.2.5. Immunohistochemistry (IHC)

In order to visualise the expression of various proteins within the tumour microenvironment or normal adjacent tissue, IHC was used. Deparaffinisation and antigen retrieval was performed using a PT-Link (Dako) which is a module that combines the process of deparaffinization, rehydration and epitope (antigen) retrieval. Antigen retrieval is necessary due to the formation of methylene bridges during the fixation process which cross-links proteins and can conceal the antigens preventing antibody binding. The PT-Link uses heat-induced antigen retrieval with target retrieval solutions at pH6 and pH8 (Dako). Once the slides had undergone antigen retrieval using the PT-Link, slides were placed on a staining tray and covered with Tris-

buffered saline with 0.1% Tween (TBST) ensuring full coverage of all the slides. The TBST was removed and the sections were dried carefully with a paper towel. The slides were covered with 1% hydrogen peroxide in methanol for 10min. The slides were washed three times for 1min with TBST. The slides were blocked with 10% goat serum in PBS for 30min at room temperature. The primary antibodies were made up in blocking solution according to the concentrations below (Table 2.2.). 200µL of antibody solution was added to each slide, ensuring each section was covered completely. The slides were incubated in primary antibody or isotype control overnight at 4^{o}C. An isotype control is a negative control used to measure the level of non-specific background signal caused by the primary antibody binding to non-specific Fc receptors on the surface of cells. Isotype controls are matched to both the host species and working concentration of the primary antibody. The following day the primary/isotype antibody was removed and the slides were washed with TBST, three times for one minute each. The excess TBST was removed using a paper towel, and Horse Radish Peroxidase (HRP) conjugated secondary antibody was added to the slides and incubated at room temperature for 60min. The secondary antibody was removed and the slides were washed again with TBST. 500µL of 3, 3'-diaminobenzidine (DAB) chromogen was added to each slide and incubated at room temperature for 10min. The DAB/chromogen was washed off with TBST. The slides were then counterstained with haemotoxylin. Coverslips were added using DPX mountant which was added using a Pasteur pipette. The slides were then left overnight to dry.

Antibody	Antibody Stock [µg/mL]	Dilution	pH	Matched Isotype control	Isotype Stock [µg/mL]	Dilution	Secondary
αSMA	200	1:50	9	IgG2a	50	1:200	Mouse
Cytokeratin	200	1:300	6	IgG	1000L	1:1500	Mouse
Shh	200	1:100	6	IgG	1000	1:500	Mouse
β-Catenin	250	1:500	9	IgG	1000	1:2000	Mouse

Table 2.2. Summary of IHC antibody dilutions

2.2.6. Immunocytochemistry (ICC)

Coverslips were sterilised in ethanol, washed in PBS and placed in the wells of a 24-well plate. 12,000 cells were seeded in each well in 1mL of complete growth media. These cells were monitored until they reached 80% confluency, at which point the media was removed and the wells washed twice with 1mL PBS at room temperature. The cells were fixed in 500µL of 4% PFA which was added to each well and incubated at room temperature for 10min. The 4% PFA was removed then replaced with 1mL of PBS and the plate was wrapped in parafilm and stored at 4°C.Once the plates were removed from 4°C they were washed 3 times with TBS at room temperature. The cells were permeabilised using PBS containing 0.1% Triton X-100 for 10min. Triton X-100 is a non-ionic detergent which can solvate cellular membranes, forming small pores which allows the antibodies to access the cells. The coverslips were then incubated with 1% hydrogen peroxide in methanol to block endogenous peroxidases. 500µL was added to each well and this was incubated for 30min. The plates were washed 3 times with 1mL of TBS before the addition of 500µL blocking solution (TBS containing 10% goat serum and 1% bovine serum albumin (BSA)). Blocking solution is used to reduce the non-specific binding of secondary antibodies. This step is crucial to decrease the cross reactivity of endogenous immunoglobulins and the secondary

antibodies. The cells were blocked for 30min at room temperature after which the blocking solution was removed and primary antibodies, diluted in blocking solution, were added to the wells. Table 2.3 details the respective dilutions of the primary antibodies used.

Antibody	Antibody stock [µg/mL]	Dilution	Matched Isotype control	Isotype control stock [µg/mL]	Dilution
αSMA	200	1:500	IgG2A Mouse	50	1:125
Vimentin	1000	1:1000	IgG1 Mouse	1000	1:1000
Desmin	200	1:500	Normal Rabbit IgG	200	1:500
Cytokeratin	200	1:300	IgG Mouse	1000	1:1500
CD68	200	1:500	Normal Rabbit IgG	200	1:500

Table 2.3. Primary Antibodies with dilution factors and the appropriate isotype controls

The plate was incubated with primary antibodies at 4^{o}C overnight after which it was removed and the wells washed with 1mL TBS 3 times. Both rabbit and mouse HRP-conjugated secondary antibodies were diluted 1:100 in blocking solution and incubated for 30mins at room temperature. The secondary antibody was removed

from all wells and washed 3 times with TBS. 500µL of DAB chromogen (Dako) was added to each well and the plate was incubated for 10min. DAB is oxidised in the presence of peroxidase and hydrogen peroxide which produces a brown stain, therefore in the presence of HRP-conjugated secondary antibodies a brown colour is observed. The plate was rinsed with water for approximately 5min, at which point no excess stain was evident in the run-off. The plates were counterstained with 500µL per well Haematoxylin for 2min. The plate was then rinsed with tap water for approximately 2min at which point no excess stain was evident in the run-off. The coverslips were carefully removed from the wells using forceps and dried off by gentle tapping on absorbent tissue paper. The coverslips were then mounted onto slides using 1 drop of mounting glue per coverslip. The slides were then left to dry at room temperature until they were imaged.

2.2.7. Immunofluorescence (IF)

Immunofluorescence (IF) staining was used to stain 3D cell cultures and 2D co-cultures of CAFs and epithelial cancer cell lines. 3D cell cultures which had been fixed embedded and mounted on slides were deparaffinised before the staining procedure was carried out (described in section 2.2.4.2.). For 2D co-cultures CAFs and PANC1 cells were seeded in 96-well, black, clear bottom, Cell Carrier plates (PerkinElmer, UK) at different ratios and left for 24h to adhere; monocultures were also seeded for comparison. The cells were dosed with gemcitabine using a D300 digital liquid dispenser (Tecan). After 48, 72 and 96h the media was removed from the plates and the cells were washed twice with PBS ensuring the complete removal of liquid from the wells each time. The cells were fixed with 100µL of 4% PFA per well, for 10min at room temperature. If the cells were being stained immediately the protocol was continued but it was possible to remove the PFA and add 100µL of PBS to each well and the plates could be stored at 4°C until the staining could be continued. In these experiments cells were fixed when their time points dictated but all plates were

stained at the same time to avoid variation in the staining. Once the plates were removed from 4°C they were washed once with PBS (100µL per well) before progressing onto the staining protocol.

The samples were permeabilised with 0.1% (v/v) Triton X-100 in PBS and incubated for 30min at room temperature. The plates/slides were then washed twice for 5min in PBS. The plates were then washed with 5% (v/v) goat serum in PBS for 1h at room temperature before the addition of primary antibodies diluted in blocking solution (dilutions summarised in Table 2.4).

Primary Antibody	Dilution	Secondary/ Fluorophore	Excitation/Emission maxima (nm)
Mouse monoclonal [1A4] to alpha smooth muscle actin	1:400	Alexa-488	Excitation 490 Emission 524
Rabbit polyclonal to wide spectrum cytokeratin	1:200	Alexa-594	Excitation 590 Emission 617

Table 2.4 Summary of IF Antibody Conditions

The cells were incubated with both primary antibodies or isotype controls overnight at 4°C. The following day the antibodies were removed and the plates were washed three times with PBS for 5min each. Secondary antibodies were diluted 1:500 and incubated for 1h at room temperature. The secondary antibodies were removed and the nuclei were stained with 4', 6-diamidino-2-phenylindole (DAPI) at a 1:10,000 dilution for 10min at room temperature. DAPI is a fluorescent stain which binds to Adenosine-Thymidine regions of DNA, and is excited by ultraviolet light (358nm) with an emission maximum of 461nm. The plates were then washed 3 times for 5min in PBS. The staining was visualised using an Operetta High-Content Imaging system (PerkinElmer).

Using dual staining within the direct co-cultures (section 2.2.4.6.) it was possible to differentiate cancer cells (CTK stained) from CAFs (αSMA stained). Using the isotype controls to remove background fluorescence, it was possible to distinguish αSMA positive cells from CTK positive cells. αSMA staining was used to determine CAFs which were then subtracted from the total nuclei count. 5 regions were imaged in each well at 10x magnification, with each condition run in duplicate. The data was presented as a percentage of the DMSO control.

2.2.8. Molecular biology

2.2.8.1. RNA extraction from cells

To extract RNA from each sample of cells an Aurum total RNA mini kit was used. When each sample was ready for RNA isolation the sample was washed twice with PBS ensuring that all excess was carefully removed. In a T75 flask 350μL of lysis buffer was used, in the experiments which used 6-well plates 150μL per well was used. The lysis buffer contained within the kit is a composition of guanidine thiocyanate (GTC) and β-mercaptoethanol which rapidly lyses the cells and inactivates RNases. GTC is typically used to lyse cells for RNA extraction as it is a chaotropic compound which is very effective at denaturing proteins including cellular membranes. It is used in conjunction with a reducing agent such as β-mercaptoethanol which denatures the RNases by breaking disulphide bonds. If β-mercaptoethanol was not used the RNases would degrade the RNA present in the sample and prevent RNA extraction. Once the lysis buffer had been added to the vessel it was aspirated and dispensed over the cells to help with the lysis. After 5min incubation at room temperature the lysate was collected and stored at -80^{o}C until required. If RNA was being isolated immediately an equal volume of 70% (v/v) ethanol was added to the culture vessel to reduce the viscosity of the lysis buffer. The lysis solution was then added to the silica membrane column contained within the kit. The

spin column was mounted within a cap-less wash tube, and centrifuged for 30s at 21,000g and the filtrate was discarded. 700µL of low stringency wash solution was added to the spin column and it was centrifuged for 30s at 21,000g and the filtrate was discarded. DNase was then added to the column and incubated for 30min at room temperature to remove any contaminating genomic DNA. Two additional wash steps using 700µL of high stringency and low stringency wash solution were performed before the total RNA was eluted from the column and collected in a sample collection tube. When eluting total RNA extracted from primary fibroblasts, 30µL of elution solution was used and 80µL was used for all cell lines. RNA was stored at -80°C until required.

2.2.8.2. RNA quantification

The concentration of total RNA was measured using a NanoDrop 2000 UV-Vis Spectrophotometer (Thermo Scientific) at 260nm. The NanoDrop was blanked using the RNA elution buffer and then 1µL of sample was loaded onto the NanoDrop and the reader closed such that the sample was in direct contact with the optical surfaces. The concentration of the RNA was determined and the 260:280 and 260:230 ratios were used to indicate the quality of the total RNA sample. The 260:280 ratio is used to assess the purity of the RNA; if the ratio is ~2.0 the sample is considered pure, however if the ratio is much lower it indicates the presence of protein, phenol or contaminants which absorb light at ~280nm. The 260:230 ratio is used as a secondary measure of contamination with a 260:230 ratio of 2.0-2.2nm deemed pure. If the ratio is lower it indicates the presence of contaminants that absorb at 230nm such as EDTA or carbohydrates.

2.2.8.3. cDNA synthesis

RNA samples were reverse transcribed into cDNA using the QuantiTect Reverse Transcription Kit. In addition to the total RNA samples, a cDNA-free negative control and a reverse transcriptase free control was prepared. All kit components were

thawed at room temperature and the template RNA was thawed on ice. All kit components were centrifuged before use and then left on ice once thawed. Up to 1µg of RNA was added to a 0.2mL tube and the sample made up to a total volume of 12µL with DNase free water. 2µL of genomic DNA wipeout buffer was added and this reaction was incubated for 2min at 42°C and then placed on ice. The reverse-transcription master mix contains 4µL of Quantiscript RT Buffer, 1µL of reverse transcriptase and 1µL of RT primer mix. The master mix was made up in batches, added to all sample tubes, and the reaction was incubated at 42°C for 15min followed by 95°C for 3min. cDNA was immediately stored at -20°C.

2.2.8.4. Quantitative real time polymerase chain reaction (qRT-PCR)

One of the most robust research tools available to study relative gene expression is qRT-PCR. It is used in a variety of areas of scientific research including forensic, clinical and diagnostic. In 1986 Kary Mullis described his invention of the polymerase chain reaction (PCR) method (Mullis et al., 1986) and Michael Smith and colleagues described the establishment of oligonucleotide-based, site-directed mutagenesis and its development for protein studies (Smith, 1982). In 1993 Higuchi *et al*. (Higuchi et al., 1993) discovered that a fluorescent label could be incorporated into the accumulating PCR product which would allow the whole process to be quantified (Figure 2.6.).

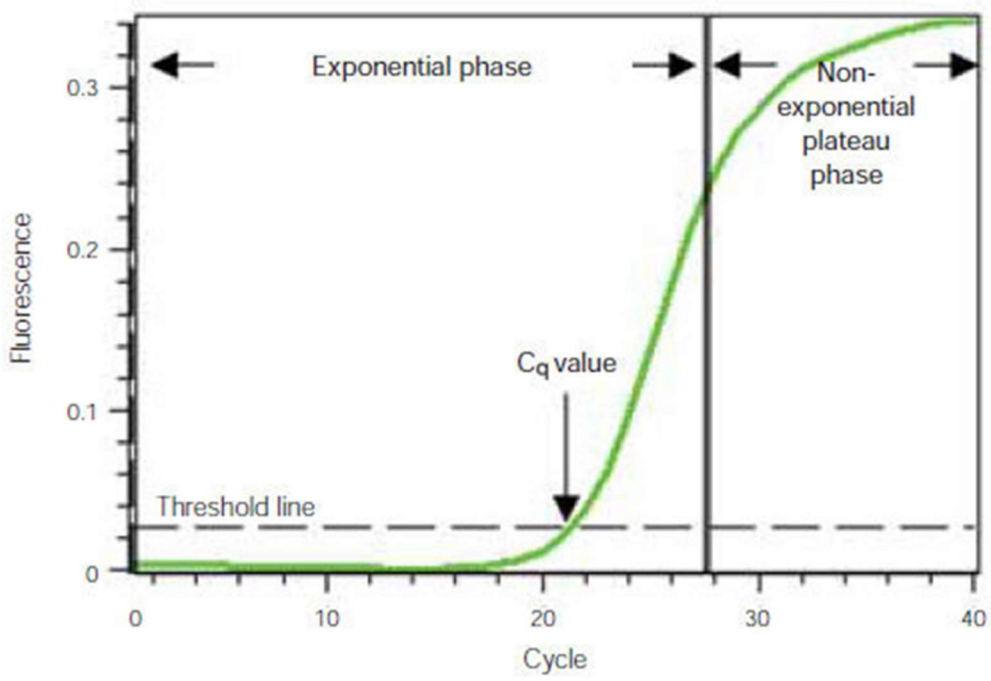

Figure 2.6. Example of qRT-PCR amplification plot

Fluorescence levels are not detected until the amplified PCR product overcomes the threshold, PCR product accumulates exponentially. The cycle number at which the threshold is overcome is known as the quantification cycle (C_q). C_q values are measured during the exponential phase of amplification when the PCR reagents are in excess. This image was reproduced (without permission) from the Biorad qPCR Manual.

As the quantity of the PCR product increases this correlates with an increase in the intensity of the fluorescent signal. In order to investigate changes in gene expression using qPCR, RNA was extracted from cell cultures and cDNA was synthesised using the methods outlined above. To amplify a specific genetic target it is necessary to choose forward and reverse primers with sequences that correspond to matching sequences at the 3' to 5' and 5' to 3' ends of the sequence to be amplified. The amplification process involves an exponential phase during which the number of molecules doubles with each amplification cycle. This plateaus at the point the reaction reagents are consumed. The amount of PCR-end product is used to calculate the amount of genetic starting material using a known standard. The amount of DNA is measured within the exponential phase in real-time (Shipley, 2006). There

are two methods of quantification currently in use: one uses a sequence specific DNA probe the other involves the incorporation of a non-specific fluorescent dye.

The sequence specific probe method uses an oligonucleotide with a specific sequence which hybridises with the target gene and the activity of Taq DNA polymerase (an enzyme isolated from *Thermus aquaticus* DNA polymerase; (Holland et al., 1991)). The oligonucleotide sequence labelled with a fluorescent reporter and a quencher which inhibits the fluorescent signal. When the amplification process is underway the Taq polymerase removes the oligonucleotide sequence which removes the quencher from the probe allowing the fluorescent reporter to emit light (520nm) This model requires the specificity of both the forward and reverse primers and the oligonucleotide probe.

The non-specific probe method involves the use of a fluorescent dye (SYBR Green) which binds to all double stranded DNA present in the sample. The amplification process depends on the specificity of the forward and reverse primers to the cDNA template, the SYBR Green dye will bind to all double stranded DNA. The pitfall of this method is the potential to produce false positive signals which are a result of the dye binding to non-specific double stranded DNA sequences. The dissociation curve can give the user insight into the purity of the amplification, the dissociation curve shows the correlation between SYBR Green labelling and the dissociation temperature which is shown as ΔFluorescence/ΔTemperature against temperature. The dissociation (melting) point (Tm) is the time point at which all of the double stranded DNA has dissociated and corresponds to the peak of the dissociation curve. If there are multiple peaks present on the dissociation curve this can indicate non-specific double stranded PCR products.

During this project both methods outlined above were utilised, the Taqman probe based design was used for the genetic profile arrays, and the SYBR Green method was used for all other genetic analyses. For every rt-PCR reaction there is a baseline signal which generally falls between 3-15 cycles during which the fluorescent signal

is too low to be detected and is therefore considered background. The threshold cycle is the level which indicates a statistically significant increase in signal, and is set carefully to ensure pertinent signals are differentiated from background signals. The C_t value is the cycle number at which the reaction is higher than the threshold cycle (Figure 2.6.) The C_t value allows the calculation of the starting DNA copy number present in the initial sample. As the starting template amount increases the C_t value will decrease. To remove variability related to the amount of target DNA added to the reaction mixture, the efficiency of the RNA extraction and cDNA synthesis the expression of the target gene is normalised to an endogenous control (this is a gene which is expressed in all samples and is referred to as a housekeeping or reference gene). All qPCR reactions were performed in green shell 96-well plates (Biorad Laboratories), each reaction mixture contained 1µL of primers (forward and reverse), 10µL of 2x SYBR Green Master mix and 9µL of cDNA template (10ng per reaction with the remaining volume made up with DNase free water). All reactions were run in triplicate. The PCR reactions were performed using a CFX96 real time PCR detection system (Bio-rad laboratories) using the PCR conditions outlined in Table 2.5.

Hold	**PCR (39 cycles)**	
	Melt	**Anneal/Extend**
95ºC	95ºC	60ºC
10min	0.15min	1min

Table 2.5. PCR conditions
Summary of the conditions used to amplify cDNA in the PCR reaction

Data Analysis

The C_t values measured for the genetic target were normalised using the C_t value obtained from the reference gene in the same cDNA sample. In addition to this, the

target gene was analysed in the experimental sample and compared with a comparator sample. For example: *Treated* versus *Untreated*

Gene expression is expressed as $2^{-\Delta\Delta Ct}$

$\Delta C_t = C_t$ Target Gene - C_t Reference Gene (GAPDH)

$\Delta\Delta C_t = \Delta C_t - C_t$ Comparator Sample

2.2.9. Enzyme-linked immunosorbent assay (ELISA)

2.2.9.1. Quantification of Shh Secretion

To investigate the level of Shh produced by cells exposed to different serum concentrations, a quantitative human Shh ELISA was used. To collect samples for this assay 10,000 cells per well were seeded in a 96-well plate in triplicate per serum concentration. The serum concentrations used were 1%, 5% and 10%. Supernatants were harvested at 24, 48 and 72h. To harvest the supernatant the plate was centrifuged at 400g for 5min and the supernatant was transferred immediately to a fresh 96-well plate and stored at -20°C. This method of analysis was developed in order to replace radioimmunosorbent techniques which involved the use of radiolabelled antibodies and was first described in 1960 (Yalow and Berson, 1960). An alternative was sought due to the inherent risk involved in the use of radioactive particles. In 1971 a substitute was discovered which utilised enzymes conjugated to antibodies rather than isotopes (Engvall and Perlmann, 1971)(Figure 2.7.). The assay kit comprised a 96-well plate which had been pre-coated with an antibody specific for Human Shh, thus any Shh present in the samples will become bound by the immobilised antibody. 100µL of sample or standard (standard curve concentrations: 2000, 800, 320, 128, 51.2, 20.5, 8.2 and 0pg/mL) was added to each well in duplicate. The wells were washed to remove anything which remained unbound and a biotinylated anti-Human Shh antibody was added. The plate was then washed again before the addition of HRP-conjugated streptavidin. Streptavidin tetramers have a high affinity for Biotin and together they form an exceptionally strong

non-covalent bond. This interaction is therefore frequently utilised in research as it can withstand extremes of temperature and pH (Green, 1975). The wells were washed for a final time and a 3,3′,5,5′-Tetramethylbenzidine (TMB) substrate solution was added and incubated for 30min at room temperature. The HRP present catalyses the conversion of TMB into a coloured product depending on the amount of secondary antibody present which is directly proportional to the amount of bound Shh in the well. A stop solution was added to the plate which changes the colour from blue to yellow and the absorbance was measured using an Envision multilabel plate reader (Perkin Elmer) at 450nm.

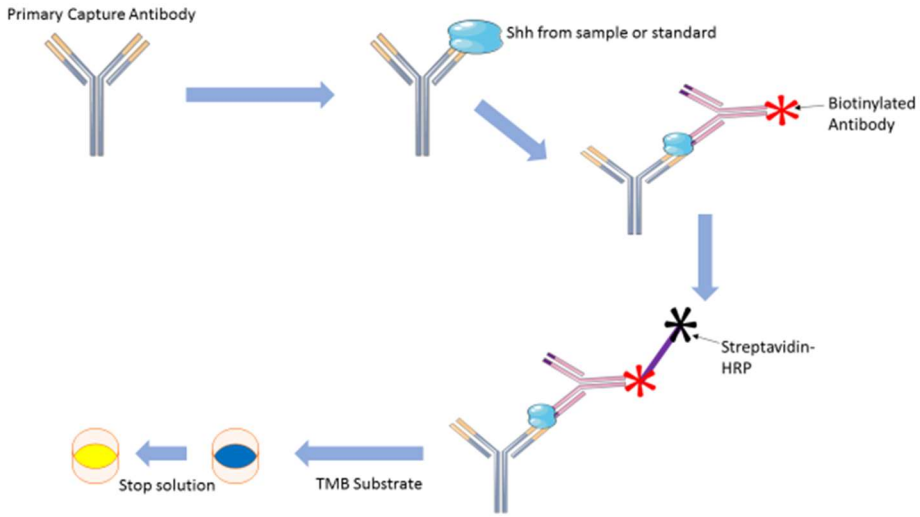

Figure 2.7. Summary of ELISA Technique

2.2.9.2. ELISA for DKK1

To investigate the levels of DKK1 produced by epithelial cancer cells and CAFs a quantitative human DKK1 ELISA kit was used. 10,000 cells per well were seeded in a 96-well plate in triplicate per serum concentration. Supernatants were harvested at 72h. To harvest the supernatant the plate was centrifuged at 400g for 5min and the supernatant transferred immediately to a fresh 96-well plate and stored at -20^{o}C (For full methodology of ELISA see section 2.2.5.2.).

2.2.10. BCA assay to determine protein concentration

In order to determine that the level of secretion of various molecules (Shh, Dkk1 and Collagen1a1) by cells was related to factors other than cell number, the protein concentration for each sample was determined. This was achieved by comparing the samples against a set of known standards which, for the purpose of this experiment was BSA. Protein concentration was determined by the bicinchoninic acid (BCA) protein assay using the manufacturer's protocol. This assay utilises a reaction whereby Cu^{2+} is reduced by proteins to form Cu^{1+} in alkaline conditions. This reduction can be mediated by cysteine, tryptophan and tyrosine residues, and the peptide bond. The greater the reduction of Cu^{2+} ions, the higher the protein concentration. The BCA forms a blue/purple coloured complex with the reduced Cu^{1+} in alkaline conditions, which has an absorption maxima of 562nm. Therefore with higher protein concentrations the solution will be less blue / purple and more green in colour. Eight parts of each of the protein standards (0-2000 μg/ml in duplicate) were mixed with 1 part of the BCA working reagent (containing 0.08% copper sulphate pentahydrate) in a 96-well plate. In addition to the standards, the cell homogenate (neat and diluted 10-fold) was also mixed in the same proportions with the BCA working solution. The plate was then incubated for 30min at 37°C. The absorbance of each sample was then measured at 562nm and a standard curve constructed using Graphpad Prism analysis software using the results obtained from the protein standards. Using this standard curve, the protein concentration of the homogenate could be determined by interpolation.

3. Characterisation of cells isolated from the pancreas and their use in a 3D model of PDAC

3.1. Introduction

PDAC is characterised by a desmoplastic stroma which can encompass greater than 70% of the tumour volume and is believed to be involved in the poor clinical outcome of this disease (Farrow et al., 2008, Waghray et al., 2013, Ghaneh et al., 2007). More sophisticated models of this disease are required to understand the complex interactions between the cancer cells and the cells which make up the stroma such as CAFs. The initial aim of this project was to isolate and characterise pancreatic cells and develop a model which incorporates the most prominent aspect of the tumour microenvironment, namely CAFs. The stroma consists of CAFs, ECM proteins, inflammatory cells and enlarged nerves. The amount of stroma present in a tumour varies greatly between patients, however a greater stromal compartment has been linked to a significantly poorer outcome for the patient (Erkan et al., 2008). Despite the presence of a large stromal component of PDAC being known for 20 years, its contribution to tumorigenesis, resistance to therapy and metastasis remains poorly understood. In 1982, Watari and colleagues reported the presence of star shaped, vitamin-A storing cells in the mouse pancreas (Watari et al., 1982). However it was not until approximately 20 years later that these cells were first isolated, characterised, and their importance in the mechanism of pancreatic fibrosis began to be elucidated (Apte et al., 1998, Bachem et al., 1998). Fibrosis is a critical feature of both chronic pancreatitis and pancreatic cancer; it is understood to be the deposition of excessive amounts of extracellular matrix in response to a disruption in the balance between deposition and degradation of ECM. CAFs were discovered to play an important role in pancreatic fibrogenesis with activated CAFs found to be the source of collagen deposition in response to pancreatic injury (Haber et al., 1999). In this

chapter the method used to isolate primary CAFs is described. Their characterisation using the expression of a panel of markers and their ability to secrete ECM, specifically Collagen1a1 is also described.

In recent years controversy has arisen in the field regarding the role of CAFs in the PDAC tumour microenvironment, initially CAFs were believed to be involved in maintaining a tumour supportive microenvironment and contributing to resistance to chemotherapies has been identified (Sherman et al., 2017, Olive et al., 2009). However, it has also been discovered that pharmacological and genetic removal of the tumour results in more aggressive and reduced survival in mice suggesting that the stroma also as a role in restraining the tumour (Rhim et al., 2014, Lee et al., 2014).

To determine the effect of including CAFs in drug screening models it was necessary to develop a model which allowed the cells to interact with a similar level of complexity as they do in the tumour microenvironment. In this chapter the characterisation of a 3D co-culture model of PDAC is described.

3.2. Methods

3.2.1. Isolation of cancer-associated fibroblasts (CAFs)

This method is described in section 2.2.2.1.

3.2.3. Generation of a 3D co-culture model

A methylcellulose stock solution was created by dissolving 6g of methylcellulose powder in 250mL of IMDM which was pre-warmed to 60^{o}C. Fresh media supplemented with 20% FBS was used to dilute the stock solution 1:1, and this solution was then mixed overnight at 4^{o}C. The solution was aliquoted and centrifuged for 2h at 5000rpm. The clear viscous supernatant was used for the spheroid formation assay. For the spheroid formation assay the stock solution was diluted 1:5. 20µL drops of methylcellulose supplemented media containing 20,000 cells were pipetted onto the lid of 6-well plates with approximately 9 drops per well. The wells were filled

with 2mL of PBS solution. Hanging drops were suspended over the wells containing PBS and cultured under normal culture conditions (5% CO_2, at 37ºC) for 7d which allowed the formation of spheroids. In order to harvest the spheroids 10µL of cell media was carefully pipetted under the spheroids which allowed each spheroid to be collected using a sterile spatula. Spheroids were placed into one well of a 96-well round bottom plate and washed twice with PBS. The cells were then fixed overnight at 4ºC using 4% PFA and the following morning the spheroids were embedded in Histogel (Thermo Scientific Richard-Allan Scientific) processed and sectioned (Section 2.2.4.1.2 and 2.2.4.1.3).

3.3. Results

3.3.1. Sample collection and isolation of CAFs

Isolation of cells from “fibrous” appearing tissue was completed in collaboration with Dr Lawrence Barrera. Isolation of cells from “normal” appearing tissue was completed by Dr Lawrence Barrera. Pathologists (Professor Fiona Campbell and Dr Tim Andrews) performed gross analysis of the specimen to identify “normal” appearing tissue, which is yellow in colour and “fibrous” appearing tissue which typically appears white and is hard when touched. In order to isolate cells from the PDAC microenvironment it was necessary to collect tissue samples from patients undergoing pancreatic resection at Royal Liverpool University Hospital. Figure 3.1A shows representative images from two of the specimens collected highlighting the difference in morphology between normal pancreatic tissue and tissue taken from an area of fibrosis. In the tumour section it is possible to visualise tumour cells embedded in the desmoplastic stroma (Figure 3.1A, black arrow). IHC analysis of αSMA and pan-cytokeratin stained tumour cores (Figure 3.1B & C) displayed strong αSMA positive staining in the stroma consistent with its expression in activated fibroblasts. Pan-cytokeratin staining was found in the cytoplasm of epithelial cells which was consistent with previous reports (Erkan et al., 2012a, Erkan et al., 2008). Tumour

sections were taken from each specimen collected and stained for αSMA and pan-cytokeratin in order to visualise the morphology of the tumour specimens used to isolate cells.

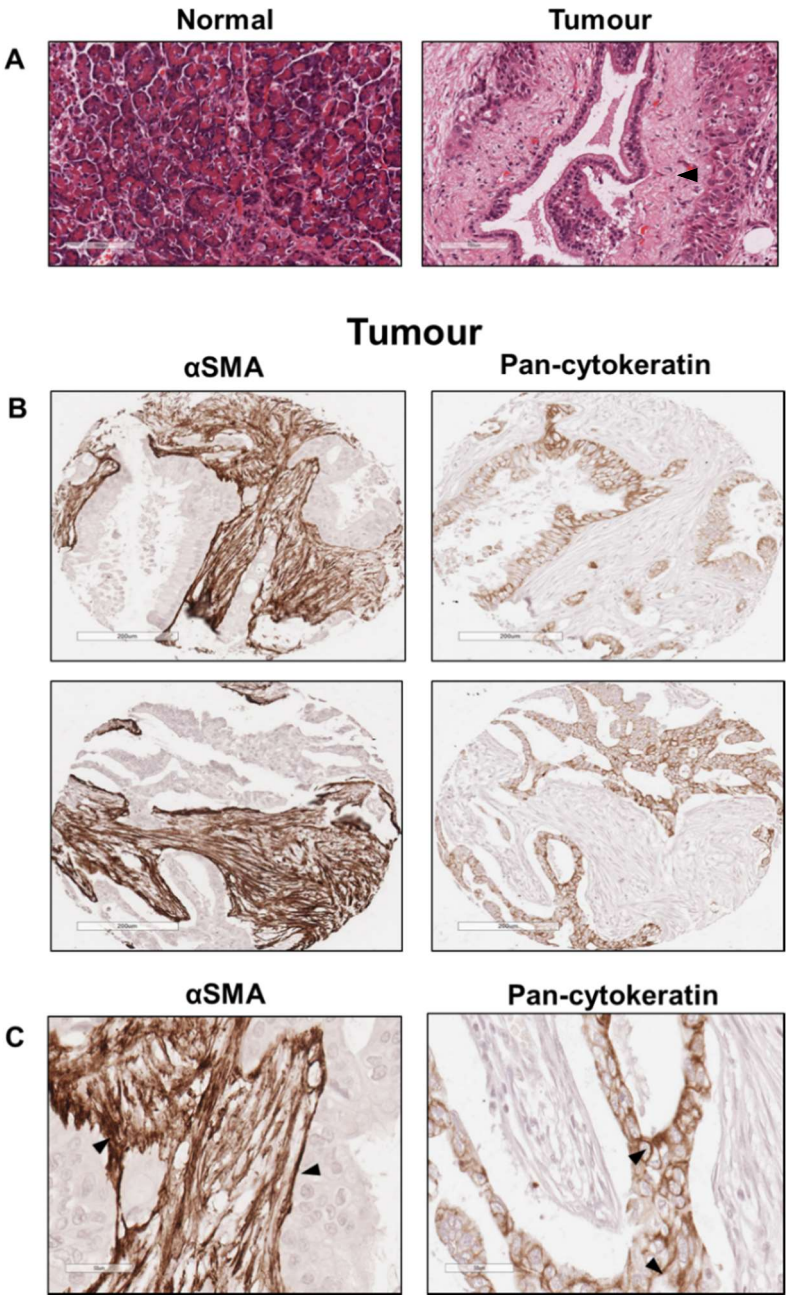

Figure 3.1. Representative Images of staining of normal tissue compared with tumour tissue

A: Haematoxylin and Eosin staining of normal appearing tissue and tumour tissue sections taken from specimens used to obtain CAFs. Normal histology section showing a standard arrangement of pancreatic acinar cells. Tumour section shows a prominent desmoplastic stroma surrounding tumour cells (black arrow). **B:** Tumour cores stained for αSMA and Pan-cytokereratin. Representative pairs of serial tumour cores clearly show stromal elements stained positively for αSMA (left image) and tumour cells stained positively for Pan-cytokeratin (right image). Positive αSMA staining indicates the presence of activated CAFs in the pancreatic tumour microenvironment. Epithelial cancer cells are stained positive for Pan-cytokeratin. Scale bar 200μm. **C:** Higher magnification images of tumour cores stained for αSMA and Pan-cytokereratin. Higher magnification (20x magnification) images show strong αSMA positive

staining of stromal elements (black arrows). Pan-cytokeratin staining shows the morphology of the tumour cells (black arrows).Scale bar 50μm.

3.3.2. Characterisation of CAFs using fibroblast markers

Isolation of cells using the outgrowth method can yield a mixed population of cells as the tumour microenvironment contains a variety of cells types. Therefore it was necessary to determine the purity of the cell populations using a selection of markers to characterise CAFs or contaminating cells such as macrophages or epithelial cells. It was important to investigate the purity and heterogeneity of all cells isolated from the pancreas at the earliest possible passage using a panel of markers; αSMA stains positively smooth muscle cells and pericytes of blood vessels, therefore it was combined with staining for the intermediate filament protein vimentin which is expressed in stromal cell lineages. Desmin is also an intermediate filament protein which positively stains up to 20% of CAFs (Apte et al., 1998). CAFs are identified by their myofibroblast-like phenotype and expression of αSMA, Vimentin and desmin. All of the fibroblasts isolated (both from normal and tumour tissue) showed 80% or above expression of αSMA and Vimentin. There was minimal expression of Desmin. All isolated fibroblast cultures were negative for CTK and CD68 which indicated that they were free from contaminating cell types (Table 3.1, Figure 3.2.).

Sample ID	Diagnosis	Normal/Fibrous	αSMA	Vimentin	Desmin	CTK	CD68
R2796	Mucinous Cystic Neoplasm	Normal	90%	98%	0%	0%	0%
R2797	Duodenal Adeno-carcinoma	Normal	80%	80%	0%	0%	0%
R2951	Intraductal papillary mucinous neoplasm	Normal	80%	100%	0%	0%	0%
R3030	PDAC	Fibrous	100%	80%	1%	0%	0%
R3072	PDAC	Fibrous	90%	100%	0%	0%	0%
R3088	PDAC	Fibrous	80%	85%%	2%	0%	0%
R3104	PDAC	Fibrous	100%	100%	1%	0%	0%
R2875	PDAC	Fibrous	90%	90%	0%	0%	0%

Table 3.1 Samples used in this study and their expression of CAF markers

The characteristics of samples collected by myself and Dr L. Barrera which were used in this study. The percentage of marker expression was estimated by myself and Dr L. Barrera independently and then compared and the average calculated. This estimation was achieved by approximation of the percentage of positive cells within 3 fields of view/cover slide.

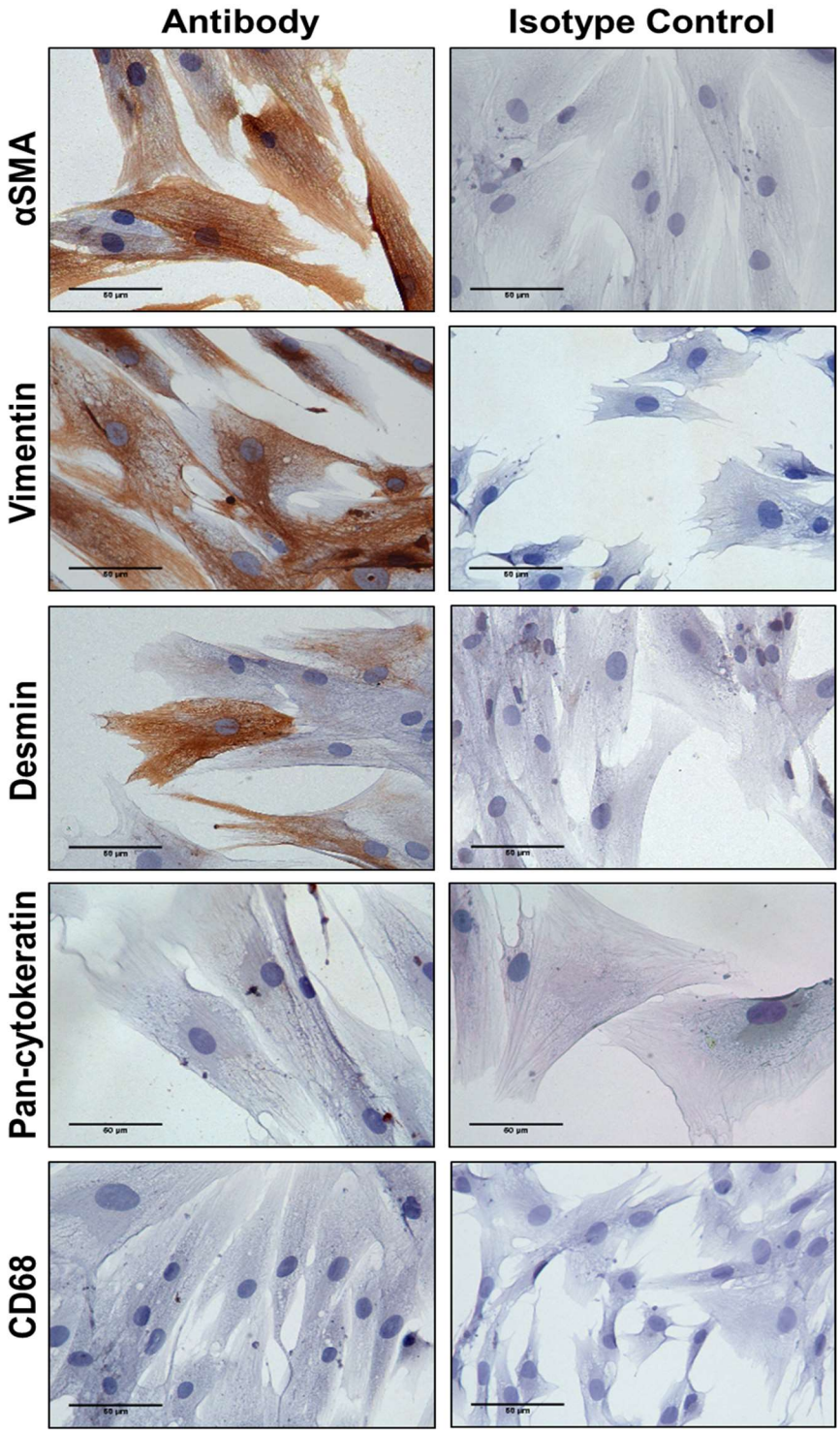

Figure 3.2. Characterisation of CAFs using expression of various markers

Expression of CAF (R3088) marker proteins demonstrated by ICC in CAFs. Alpha smooth muscle actin (α-SMA), Vimentin and Desmin are commonly expressed in CAFs (Apte et al., 1998). Pan-cytokeratin and CD68 were used to identify if contaminating cells were present in these primary cultures. As a negative control, cells were incubated with an isotype matched control antibody, at the same concentration as the primary antibody. Scale bar 50μm.

3.3.3. Characterisation of CAFs using collagen production

Having established that the isolated CAFs express the appropriate markers it was also necessary to determine the functionality of the CAFs isolated which was established using the ability of the CAFs to secrete collagen 1a1. A major component of the pancreatic tumour microenvironment is collagen; it has been established that CAFs are the source of the deposition of the excessive amount of extracellular matrix (Bachem et al., 2005). Figure 3.3.A shows the co-localisation of αSMA positive cells and the deposition of collagen using Picro Sirius Red staining which was consistent with previous reports (Apte et al., 2004). In order to determine that the isolated CAFs exhibited a similar phenotype in culture, the level of secreted collagen1a1 was quantified using an ELISA. All 3 CAF lines secreted significantly more collagen than pancreatic cancer cell lines (Figure 3.3B). This clearly demonstrates that the isolated CAF cells not only express the protein markers associated with CAFs, but also secrete collagen consistent with their physiological function.

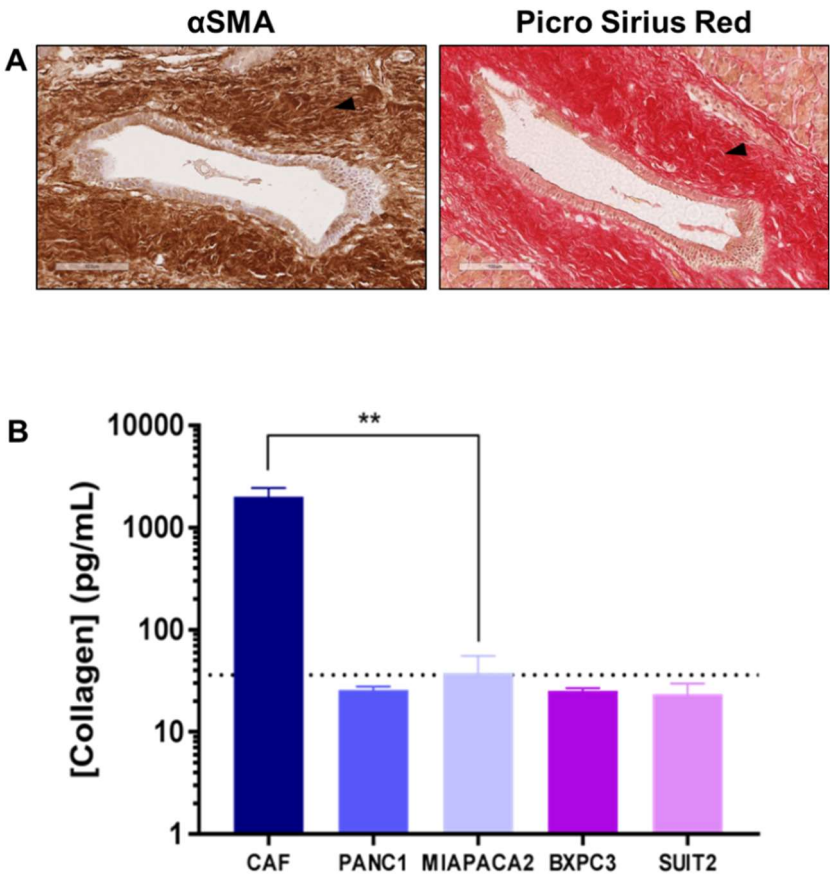

Figure 3.3. Collagen production in CAFs compared to a panel of pancreatic cancer cell lines
A: A representative image of serial sections of pancreatic cancer showing co-localisation of Picro Sirius Red and αSMA. **B:** CAFs secrete significantly more collagen than pancreatic cancer cell lines. Quantification of Col1a1 was determined using a standard curve for comparative analysis. ** indicates significance with $p<0.0014$ (N=3) in collagen secretion between CAFs and MIAPACA2, the level of collagen secreted by the other cell lines was below the limit of detection (shown as a dotted line) of the ELISA therefore statistics could not be performed.

3.3.4. Isolation of epithelial tumour cells

In order to best model the PDAC tumour microenvironment I sought to combine isolated tumour cells with CAFs. However, despite using a variety of techniques I was unable to isolate epithelial cells. The methods used and the results obtained are detailed below. The first method used was the outgrowth method (Erkan et al., 2012a), unfortunately within 7 days CAFs outgrew the cultures and the epithelial cancer cells did not survive (Figure 3.4.).

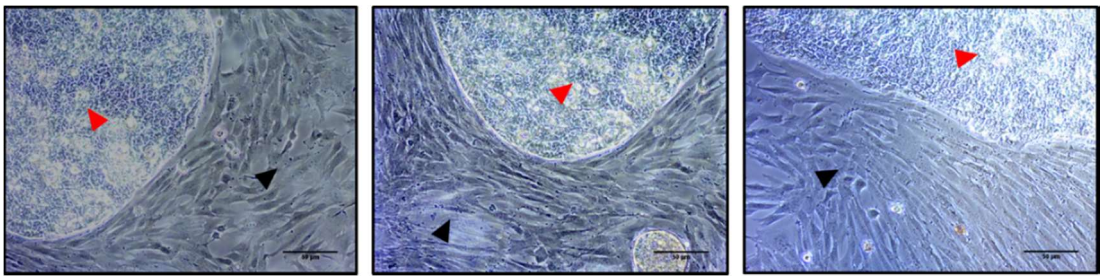

Figure 3.4. Morphologically different cell types isolated using the outgrowth method

Representative images of cells growing out of tissue explants after 7 days. It is possible to distinguish between two morphologically different cell types. Black arrows indicating CAFs and red arrows indicating what is believed to be epithelial tumour cells. Scale bar 50µm.

There are two methods generally used for the removal of contaminating fibrolasts from primary epithelial cell cultures. The first is the use of a sterile canula to mechanically remove fibroblasts from cultures. This method was trialled and was found to be ineffective due to the rapid recovery of the CAFs from this treatment. The second method for removal of contaminating fibroblasts is selective trypsinization, which is possible due to the fact that CAFs do not adhere to the culture vessel as strongly as epithelial tumour cell lines (Felix Rückert, 2012). However, over time the selective trypsinization process appeared to damage the epithelial cells as fewer cells survived each round. The next method attempted was the use of selective media to attempt to reduce the growth of CAFs within the mixed cultures. The following media formulations were used:

- Dulbecco's Modified Eagle's Medium (Supplemented with 10% FBS)
- Dulbecco's Modified Eagle's Medium (Supplemented with 20% FBS)
- Keratinocyte-Serum Free Medium
- Dulbecco's Modified Eagle's Medium/HAMS F-12 Nutrient Mixture (Supplemented with 10% FBS)
- Dulbecco's Modified Eagle's Medium/HAMS F-12 Nutrient Mixture (Supplemented with 20% FBS)

- “Dresden” modified DME medium - Dulbecco’s Modified Eagle’s Medium(Supplemented with 20% FBS) with Keratinocyte-Serum Free Medium in a 2:1 ratio (Ruckert et al., 2012)

In all cases the CAFs maintained their growth rate and appeared to be resistant to changing the culture conditions, therefore it was necessary to develop an alternative method to separate the cell populations.

Epithelial cancer cells were removed from the well surface using cloning rings, however once they had been removed they did not reattach to the new culture vessel. In order to determine why the epithelial cells would not reattach, trypsin was substituted for other, milder dissociation solutions such as Accutase. However, substitution of trypsin with Dispase and Accutase also resulted in a lack of epithelial cell reattachment. The mechanical dissociation of the cells using a sterile spatula was also unsuccessful. To ensure that the epithelial cells were in sufficient contact with the culture vessel surface, the volume of media was reduced to encourage cellular attachment. The epithelial cancer cells were seeded into a 96-well plate to reduce the size of the culture vessel, therefore reducing the area available for the cells to re-attach encouraging cell-cell communication.

The second most commonly used method for the isolation of primary epithelial cells is the use of digestive enzymes to break down connective tissue and produce a suspension of cells (Owens et al., 1976, Chifenti et al., 2009, Kalinina et al., 2010). The only cells which survived this treatment were CAFs, most likely because approximately 80% of the PDAC tumour microenvironment is made up of stromal cells, and therefore CAFs are the more abundant cell type. After two separate experiments this method was deemed unsuitable. The next method utilised was the use of density gradients in an attempt to capture fractions which contained epithelial cells. Unfortunately this method was unsuccessful after three attempts, with the only cells proliferating from these cultures being CAFs. The presence of CAFs and cancer cells in mixed cultures isolated from tumour specimens was investigated using ICC

staining for αSMA and Pan-cytokeratin. It was found that mixed cultures contained both α-SMA positive cells and Pan-cytokeratin positive cells, which indicates the presence of both CAFs and epithelial cancer cells (Figure 3.5).

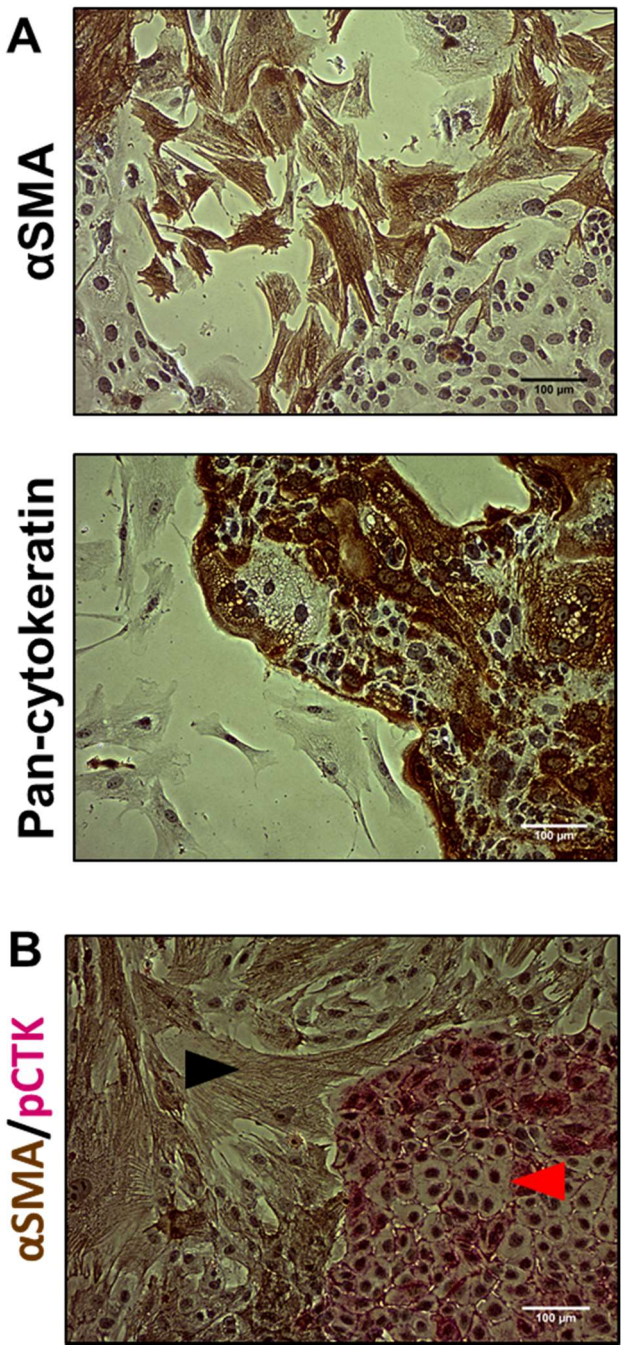

Figure 3.5. Expression of αSMA and pan-cytokeratin in mixed cultures of CAFs and cancer cells isolated from PDAC specimens

A: Representative images of mixed cultures showing CAFs positively stained for αSMA and cancer cells positively stained for pan-cytokeratin. **B:** Representative image of a mixed culture of CAFs and cancer cells dual stained for αSMA (black arrow) and pan-cytokeratin (red arrow).Scale bar 100µm.

It was possible to visualise colonies of cancer cells growing out of tumour pieces in addition to CAFs (Figure 3.4.). However upon attempting to dissociate them using various techniques (see section 3.1.2) the epithelial cells would not successfully re attach resulting in a loss of the sample. Given the difficulties with maintaining freshly isolated epithelial cells from pancreatic cancer patient samples an alternative was required in order to model the interaction between epithelial and fibroblast cells. A panel of 5 well-characterised pancreatic cancer cell lines was selected (PANC1, SUIT2, MIAPACA2, ASPC1 and BXPC3) (Lieber et al., 1975, Iwamura et al., 1987, Yunis et al., 1977, Chen et al., 1982, Tan et al., 1986) to best match patient variation due to their diverse origins (Table 2.1.). The expression of pan-CTK and αSMA in the 5 cell lines chosen and a CAF line was determined using IF (Figure 3.6.). As expected the 5 PDAC cell lines expressed pan-CTK and the CAF line was negative and only the CAF line was positive for αSMA (Figure 3.6.).

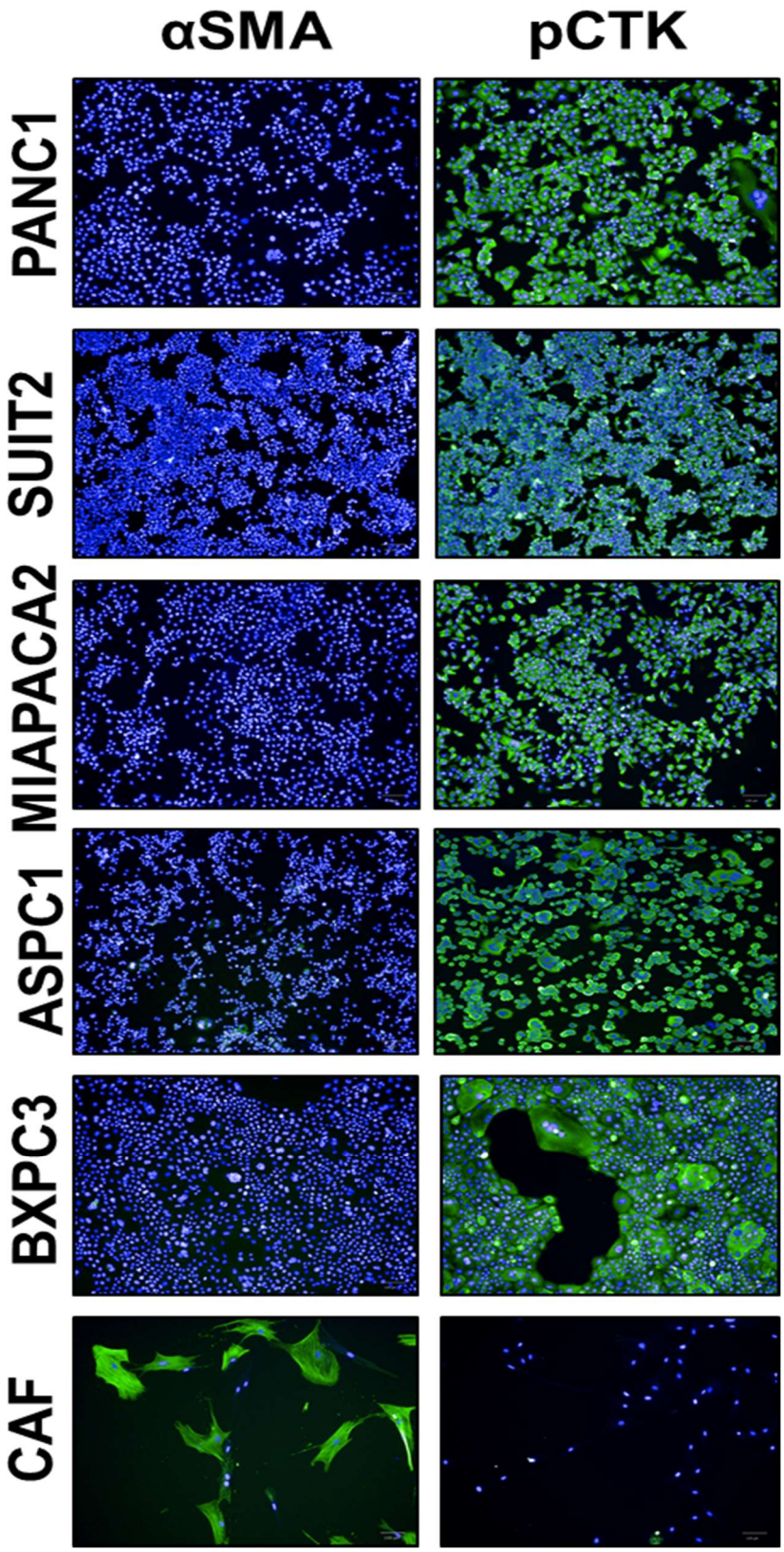

Figure 3.6. Immunofluorescence images of cancer cell lines and CAF stained for αSMA and pan-cytokeratin

Cancer cell lines are negative for αSMA expression and positive for pan-cytokeratin, CAFs are positive for αSMA expression and negative for pan-cytokeratin.

3.3.5. 3D model of pancreatic cancer

The importance of the tumour microenvironment in PDAC has become increasingly clear in recent years, specifically the role of CAFs in the production of a desmoplastic stroma which has been implicated in resistance to chemotherapy, metastasis and maintenance of a tumour supportive microenvironment (Erkan et al., 2012b, Farrow et al., 2008). However, despite such knowledge there has been little progress in the development of drug discovery models which include CAFs. In order to identify the complex interactions between CAFs and cancer cells, the effect of CAFs on tumour cell growth and the role of CAFs in reducing the efficacy of chemotherapy, more sophisticated models of the tumour microenvironment are required. 3D models have been shown to more accurately represent the behaviour of tumour cells *in vivo (Wu and Swartz, 2014, Nyga et al., 2011),* however these models have been lacking in pancreatic cancer due to the inability to recreate the stroma. Recently methods have been developed to create 3D co-culture models which include CAFs (Ware et al., 2016b). In order to create a reproducible 3D co-culture model for use in drug screening assays it was necessary to characterise how these cells interact in 3D and to elucidate the effect of introducing CAFs into a 3D model of PDAC. There were clear morphological differences between the spheroids formed from mono-cultures of different pancreatic cancer cell lines: BXPC3, PANC1 and ASPC1 formed spheroid structures in the absence of CAFs, whereas SUIT2 and MIAPACA2 formed disintegrated and loose structures (Figure 3.7).

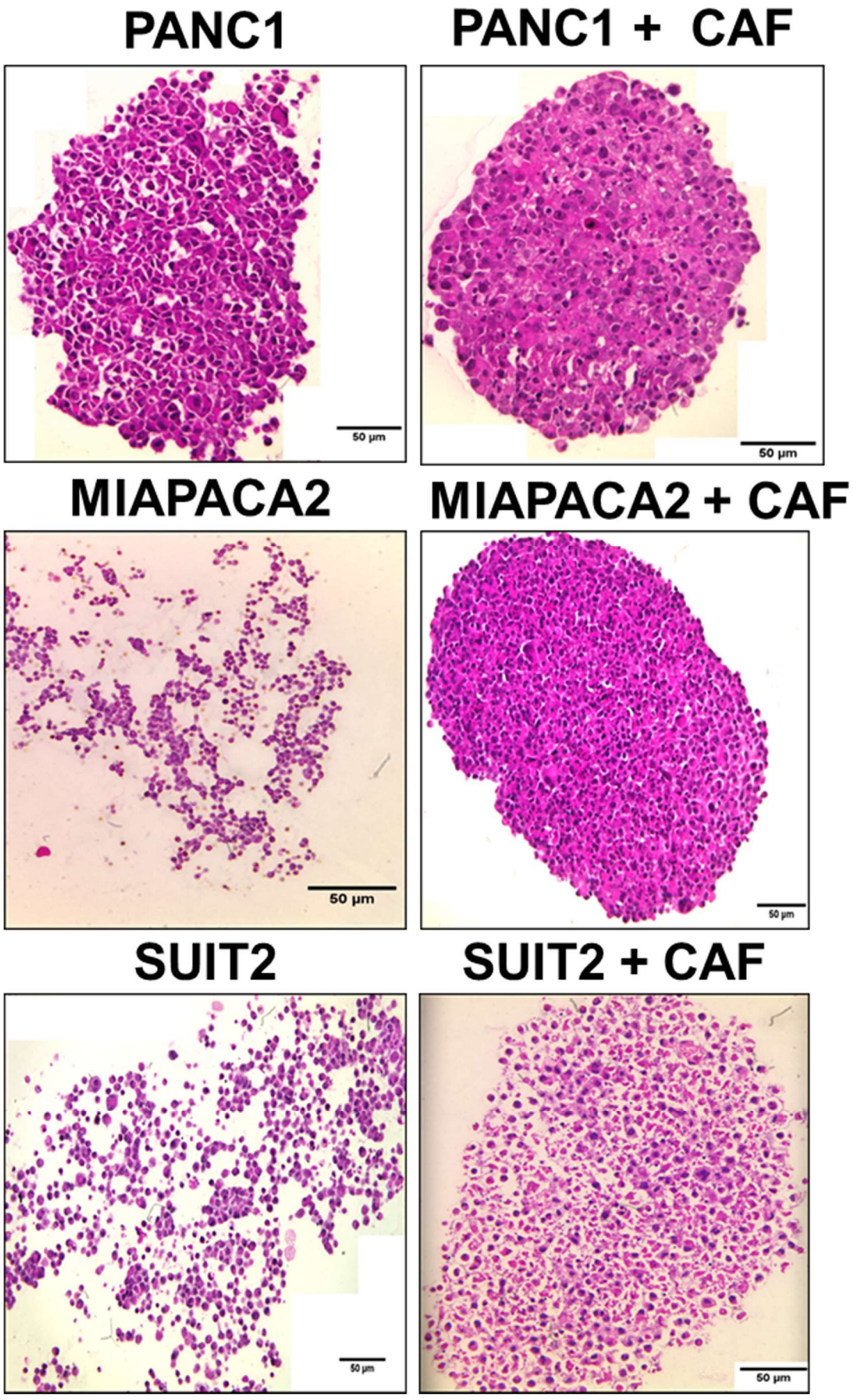
PANC1
PANC1 + CAF
MIAPACA2
MIAPACA2 + CAF
SUIT2
SUIT2 + CAF
50 µm

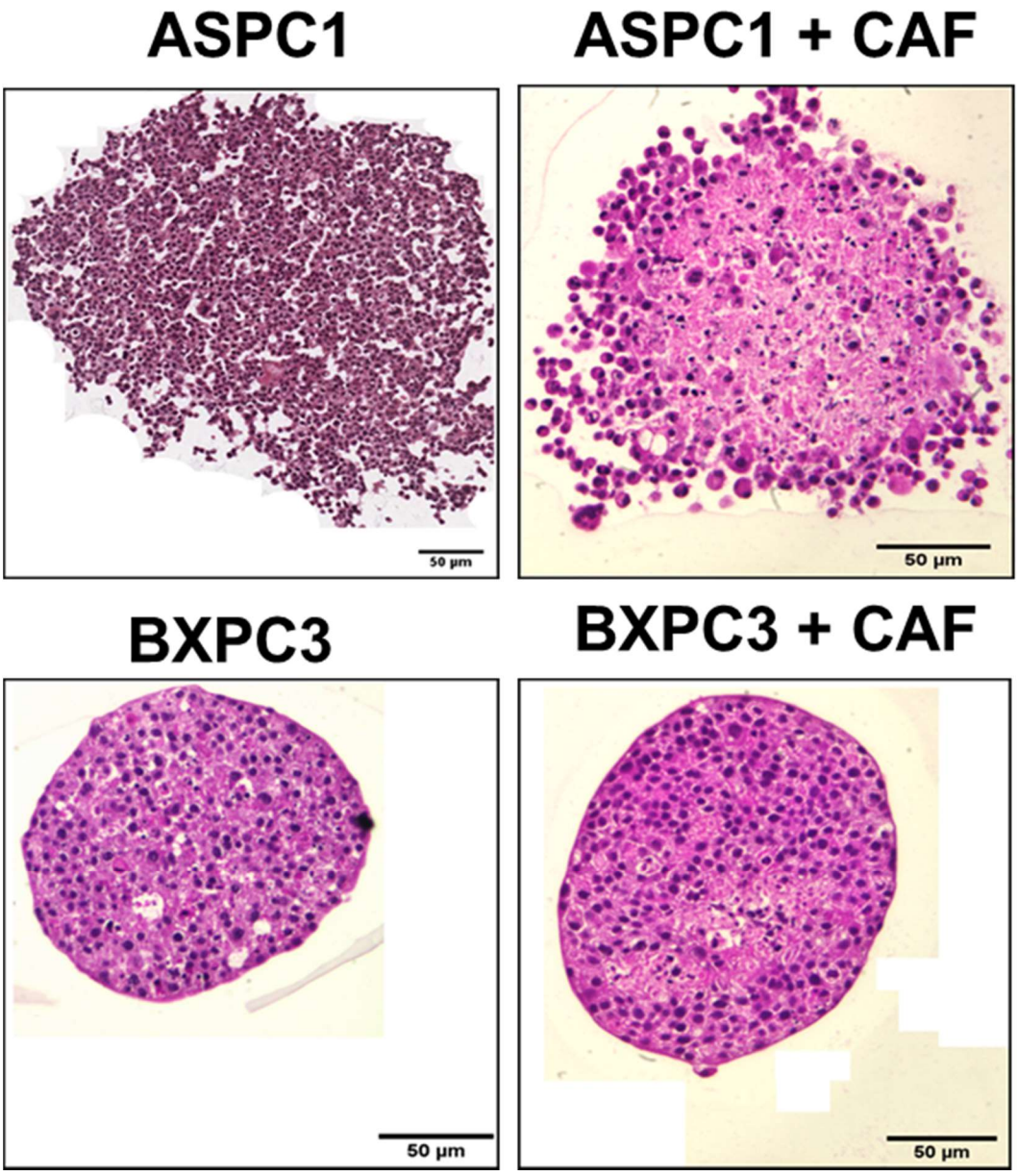

Figure 3.7. Histological analysis of PDAC spheroids after 1 week in culture

Representative H&E images of cancer cell lines in 3D culture alone and in the presence of CAFs in a 1:2 ratio of CAFs:cancer cells. Brightfield microscopy indicates differences in morphology between cells cultured alone and in the presence of CAFs. Overall the addition of CAFs visibly increases the density of the spheroids. Scalebar 50µm.

In order to quantify the effects of including CAFs on the morphological phenotype of spheroids, the parameters of diameter and circularity were measured (Figure 3.8, Figure 3.9.). PANC1, SUIT2 and MIAPACA2 spheroids showed an increase in circularity upon addition of CAFs (Figure 3.9). In the case of SUIT2 and MIAPACA2

it was not possible to measure circularity in the absence of CAFs as they did not maintain a spheroid structure and therefore statistical analysis was not performed. PANC1 spheroids had an increase in circularity in the presence of CAFs with a mean circularity of 0.82±0.02 alone compared to 0.96±0.02 in the presence of CAFs ($p=0.0023$, $N=3$).

Upon co-culturing BXPC3 cells with CAFs, the resulting spheroids appeared to have a similar shape which is verified by a statistically similar circularity score (0.988, 0.985 and 1.000 for mono-BXPC3, mono-CAF and co-culture respectively; Figure 3.9). However, despite having the same number of cells the co-culture was significantly smaller in diameter than BXPC3 alone (241.2μm and 377.3μm; Figure 3.8) suggesting the addition of CAFs causes the spheroids to be more structurally compact. Similarly PANC1, MIAPACA2, and SUIT2 cell lines also appeared to be more dense in the presence of CAFs compared to when they were cultured alone (Figure 3.7.).

Staining of spheroids created using PANC1, MIAPACA2 and CAFs was carried out in order to investigate the orientation and spatial distribution of the cells within the co-culture models.

In both MIAPACA-CAF and PANC1-CAF spheroids it appears that αSMA positive cells (CAFs) are found throughout the spheroid rather than confined to a specific area (such as the centre) (Figure 3.10.). This is consistent with the model of the PDAC tumour microenvironment created by Ware and colleagues, who describe a stroma rich spheroid model with collagen deposition throughout their spheroids (Ware et al., 2016b). Together this suggests this model replicates the distribution of αSMA positive cells throughout the PDAC tumour microenvironment and resembles the pathology of the disease in an *in vitro* model.

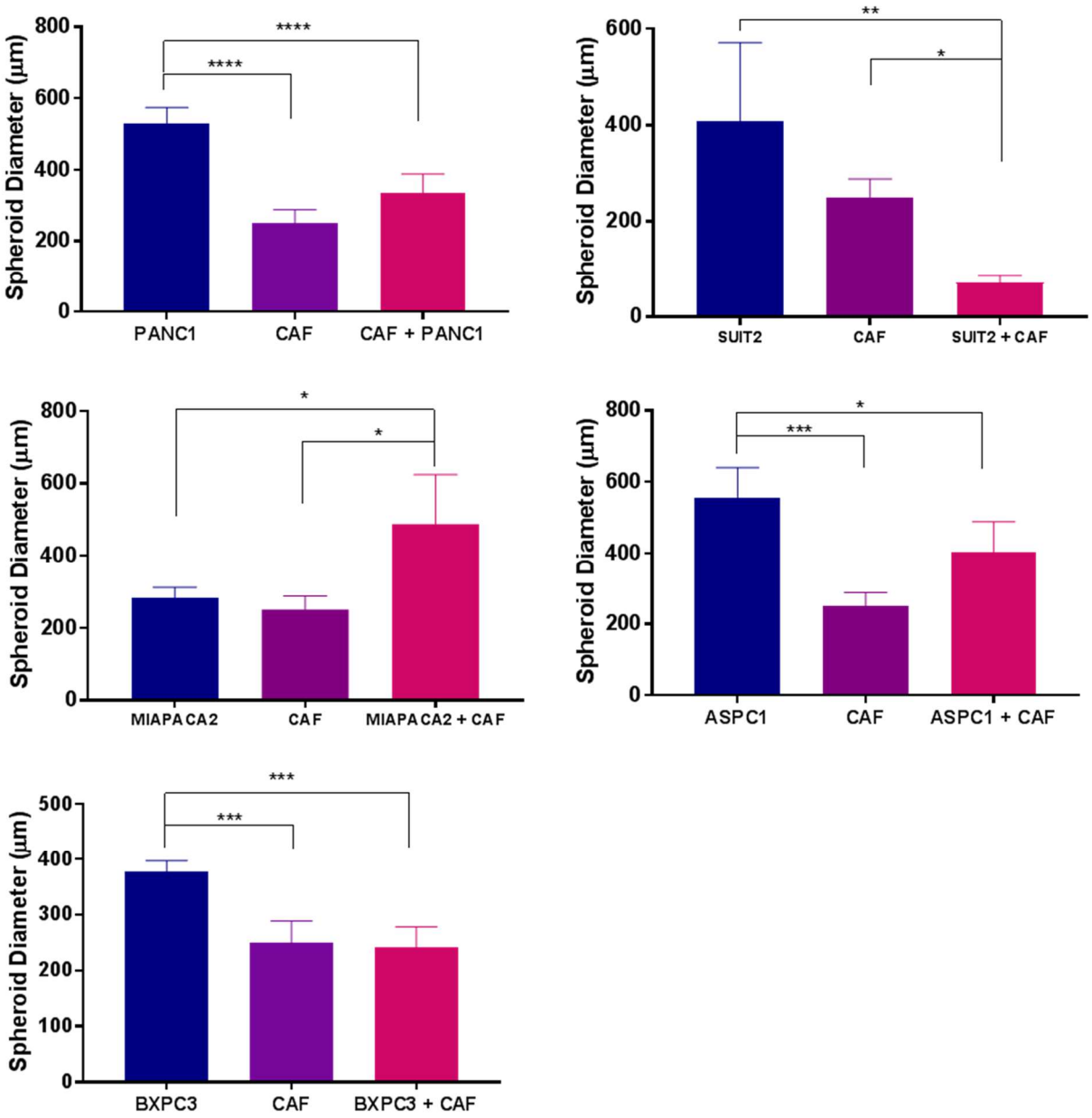

Figure 3.8. Diameter of spheroids in the presence and absence of CAFs

Brightfield microscopy allowed the measurement of the diameter of the spheroids. All spheroids except MIAPACA2 cells showed a decrease in spheroid diameter with the presence of CAFs.

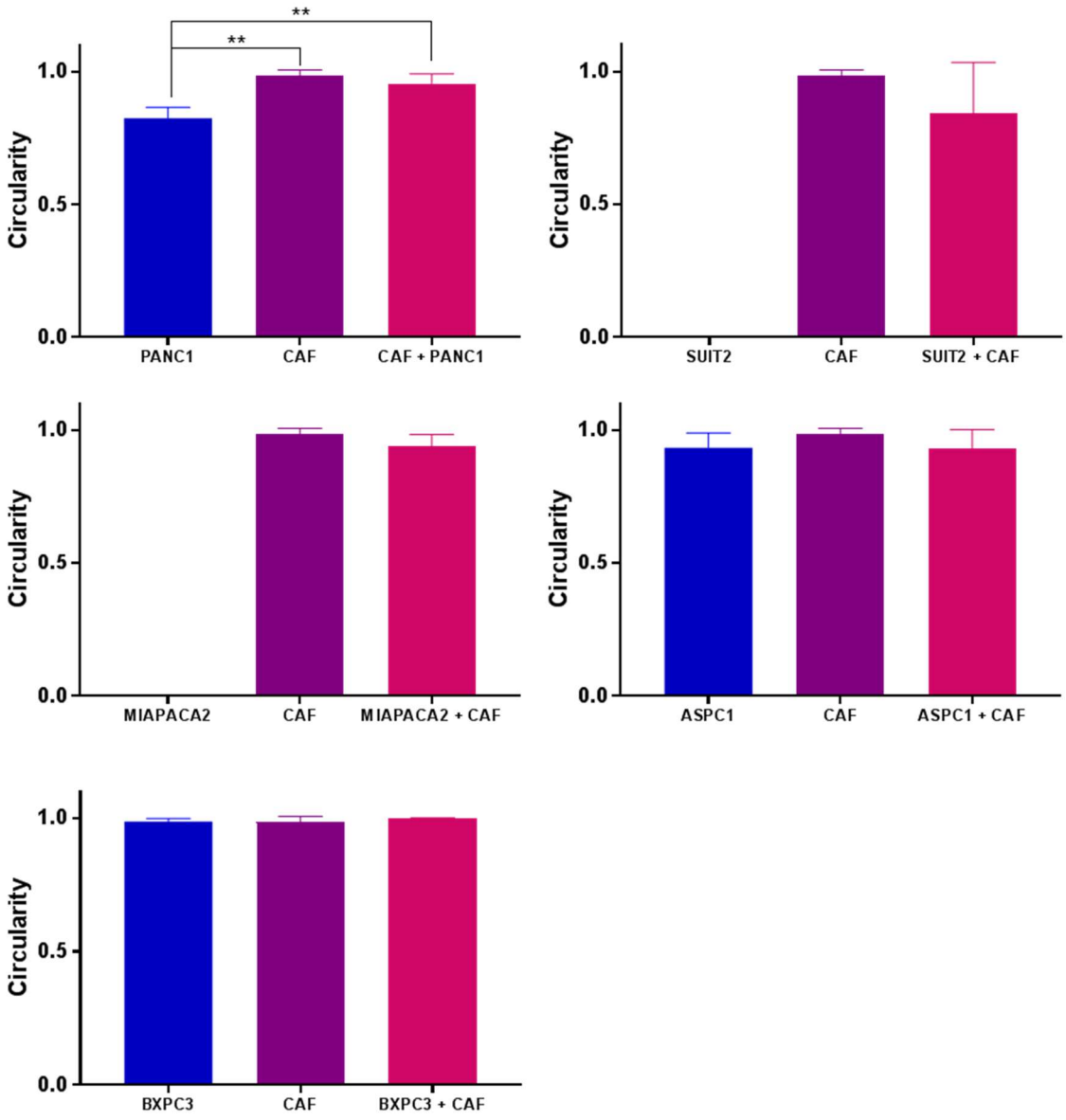

Figure 3.9. Circularity of spheroids in the presence and absence of CAFs

As an indicator of the morphological differences between the spheroids. The circularity of the spheroids was measured using the formula below:

$$\text{Circularity} = 4\pi \frac{\text{Area of spheroid}}{\text{Perimeter of spheroid}^2}$$

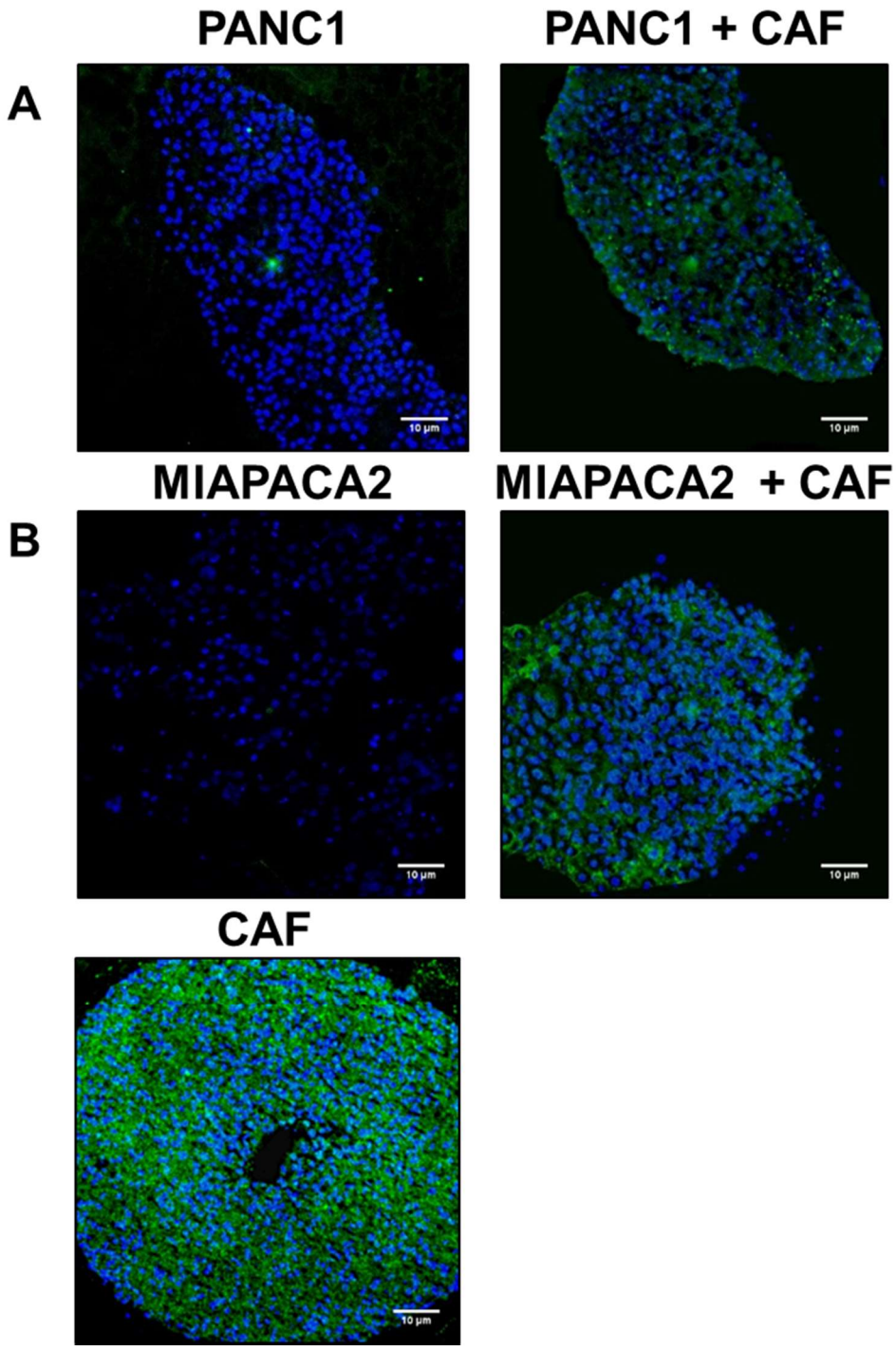

Figure 3.10. Characterisation of the 3D co-culture model

A: 3D cultures of cancer cell lines (PANC1, MIAPACA2) alone or in co-culture with CAFs stained for αSMA. Co-cultures show the presence of αSMA positive cells dispersed throughout the spheroid. **B:** 3D culture of CAFs (40,000 cells) showing strong positive staining throughout the spheroid.Scalebar 10µm.

3.4. Discussion

CAFs have been found to be the main cell type involved in the maintanence of the stroma and deposition of abundant extracellular matrix proteins (Apte et al., 2004, Wilson et al., 2014). It has been established that a high activated stroma index (αSMA/collagen) results in a poorer prognosis for patients (Erkan et al., 2008). Given such a crucial role for CAFs within PDAC, it is necessary to develop models which include elements of the stroma. The initial aim of my project was to isolate and characterise cells from the PDAC microenvironment. CAFs were successfully isolated from human PDAC tissue samples and characterised using a panel of CAF specific markers. The presence of positve αSMA and vimentin and an absence of CTK and CD68 (Figure 3.2) is consistent with previous reports (Apte et al., 1998, Apte et al., 2004) and therefore show that the isolated and cultured CAFs exhibit a morphology consistent with those observed in tissue. The fact that CAFs secrete Col1a1 in culture demonstrates that the isolated CAFs were phenotypically functional. Taken together these data suggest that the CAFs used throughout this project represent a suitable model of CAFs found within the PDAC tumour microenvironment.

In order to recapitulate the tumour microenvironment it would have been preferable to isolate primary epithelial tumour cells from patients, however this was not possible. In lieu of isolated primary epithelial cells a panel of 5 pancreatic cancer cell lines was chosen. These cells have previously been shown to offer a suitable model of PDAC (McConkey et al., 2010) and therefore were considered to be a good alternative to primary epithelial cells. 3D cell culture has been shown to provide cellular genetic profiles which more closely resemble the clinical genetic profiles than 2D cell cultures (Kenny et al., 2007). *In vivo* cells are ellipsoidal, have complex 3D interactions and form elaborate cellular structures. It is impossible to recreate this *in vitro* but 3D models are closer than unsophisticated 2D models (Nelson and Bissell, 2005, Shield et al., 2009). Consistent with these findings, the data presented above describes an

appropriate 3D model of PDAC, which mimics tumour morphology and the presence of stromal cells (CAFs). The addition of CAFs changed the morphology of the spheroids; they visibly appeared to be more densely packed. In all cell lines except MIAPACA2 the addition of CAFs to the model caused a decrease in diameter. This could be due to the fact that MIAPACA2 did not form structurally robust spheroids when they were cultured alone. These findings indicate that the CAFs may be providing structural support for the growth of cancer cells. This is consistent with the findings above showing that the 3 CAF cell lines tested secreted significantly more collagen than the epithelial cells. Collagen maintains tissue structure in a healthy pancreas. In the PDAC tumour microenvironment homeostatic control of collagen deposition is lost and CAFs secrete over 3-fold what benign fibroblasts would secrete in healthy tissue (Ryschich et al., 2009). During tumour progression the role of collagen fibres also changes dramatically and they become aligned (Egeblad et al., 2010). This can lead to an increase in interstitial pressures due to compactness of the microenvironment (McConnell et al., 2016) and create migratory corridors which makes collagen fibres complicit in tumour invasion (Provenzano et al., 2008, Riching et al., 2014). Preliminary staining showed the location of αSMA positive cells dispersed throughout the co-culture model which was consistent with the findings of Ware and colleagues who found collagen deposited throughout the spheroids they had created indicating the distribution of CAFs (Ware et al., 2016a, Ware et al., 2016b). This is similar to tumour architecture and the presence of collagen deposits suggests this model with functionally active CAFs is a model which closely resembles the PDAC tumour microenvironment. The importance of CAFs within the pancreatic tumour microenvironment is clear; these cells have a complex and intricate relationship with cancer cells resulting in tumour progression. Understanding the key mechanisms that underpin the pro-oncogenic relationship between cancer cells and CAFs is therefore key to devloping treatment for PDAC. One such mechanism thought to contribute toward PDAC progression are the embryonic signalling

pathways (Morris et al., 2010, Bai et al., 2016, Zhang et al., 2013). The cross-talk between CAFs and cancer cells of these signalling pathways must therefore be characterised *in vitro* in order to determine how these cells communicate *in vivo.* The co-culture model presented herein provides an ideal platform by which this relationship may be investigated.

4. Hedgehog signalling in the PDAC tumour microenvironment

4.1. Introduction

In 2003 Thayer and colleagues observed aberrant Shh ligand expression in early pancreatic cancer precursor lesions (Thayer et al., 2003). This finding has since been corroborated in KRAS driven mouse models of PDAC (Hingorani et al., 2005) suggesting that Shh has an important role in the initiation and progression of PDAC. Indeed, abnormal expression of Hh ligands has been observed in other solid tumours including prostate, colon and breast (O'Toole et al., 2011, Sheng et al., 2004, Wang et al., 2013). Perhaps more surprisingly however, in PDAC there appeared to be no activated Hh signalling within the tumour epithelial cells (Yauch et al., 2008) suggesting that aberrant Shh signalling may be a product of cross talk between CAFs and epithelial cancer cells. Hh signalling has been implicated in the formation of the stroma through the activation of CAFs (Bailey et al., 2008). The development of PDAC with its associated desmoplastic stroma alters the architecture of the pancreas. This can, in part be due to excessive proliferation of activated CAFs (αSMA positive) that secrete large amounts of ECM preventing blood perfusion, oxygen diffusion and effects the distribution of nerves throughout the parenchyma (Erkan et al., 2012b) . The presence of the desmoplastic stroma presents a physical barrier to drug delivery due to its effect on the blood perfusion of the PDAC microenvironment (Provenzano and Hingorani, 2013). Therefore, antifibrotic agents such as Vitamin E and Hh pathway inhibitors, aimed at depleting the stroma offered a promising therapeutic approach. In a KPC model of PDAC (mouse model produced from a mixed genetic background which develops and has similar pathological features of the human disease (Lee et al., 2016)), treatment of tumour bearing mice with IPI-926 (a small molecule SMO inhibitor created by Infinity Pharmaceuticals) resulted in collapse of the stroma which allowed for increased perfusion and, when combined with

Gemcitabine resulted in an increased survival rate (Olive et al., 2009) . However, despite the hopeful results in these pre-clinical studies, the Phase 2 clinical trial of IPI-926 in combination with Gemcitabine (IPI-926-03 trial; NCT01130142) showed reduced survival in patients compared to the placebo arm. Further studies into Hh signalling in the pancreatic tumour microenvironment showed that genetic deletion of *Shh* or inhibition of SMO during tumour formation resulted in a reduced tumour mass which corresponded to a decreased desmoplastic stroma. However, unexpectedly these tumours showed a much more lethal phenotype (Rhim et al., 2014, Lee et al., 2014). Such a surprising finding demonstrates that, despite a clear role for the Hh signalling pathway in PDAC, the precise manner by which it functions within the mircroenvironment has yet to be elucidated.

I therefore sought to determine whether the Hh pathway was active in an *in vitro* model of PDAC, and whether Redx SMO inhibitors could be used to block this activation.

4.2. Methods

4.2.1. ELISA for Shh

To investigate the level of Shh produced by cultured cells, a quantitative human Shh ELISA Kit was used. Samples were prepared using the following method: cells were seeded in triplicate at 10,000 cells per well in a 96-well plate and grown in the presence of differing FBS concentrations (1%, 5% or 10% FBS). After 24, 48 and 72h, the plate was spun at 400g for 5min and the supernatant transferred immediately to a fresh 96-well plate and stored at -20^{o}C. For a full description of the technique see Section 2.1.6.1.

4.2.2. Recombinant Shh treatment optimisation

To determine the optimal concentration of recombinant Shh (rShh) able to cause the greatest upregulation of the Hh pathway in CAFs, a titration of rShh was performed

at 3 different time points (24, 48 and 72h) using one example of CAFs (R3104). 50,000 CAFs per well were seeded onto 6-well plates and left to adhere under standard culture conditions overnight. The following day the growth media was changed to serum free IMDM. The serum starvation step is necessary in order to measure changes in Hh pathway activation as serum is rich in growth factors and proteins and may therefore negate the cells' dependency on embryonic cell signalling pathways. After 24h of serum starvation the cells were treated with either IMDM containing 1% FBS or serum-free IMDM with either 0.25, 0.5, 1, 2 or 3 µg/mL of rShh in duplicate per condition. This concentration range was chosen to confirm literature reports showing that treatment with rShh could induce an upregulation in *GLI1* mRNA (Hwang et al., 2012). RNA was isolated after 24, 48 and 72h and Hh pathway activation was analysed using changes in the mRNA level of *GLI1.*

4.2.3. Inhibition of Hh pathway in a 2D model

Once the optimal rShh concentration and time point required for the largest detectable activation of the Hh pathway had been selected, the effect of Redx SMO inhibitors on Hh pathway activation in CAFs was investigated. 50,000 CAFs were seeded per well of a 6-well plate, the cells were left overnight in an incubator (37ºC, 5% CO_2 air humidified atmosphere). The following day the media was replaced with IMDM (2% L-Glutamine, 1% Penicillin Streptomycin) supplemented with either 1% FBS or 2µg/mL of rShh and containing Redx SMO inhibitors. The plate was then incubated for a further 24h (37ºC in a 5% CO_2 air humidified atmosphere; for plate map see Table 4.1). At 24h RNA was isolated and changes in *GLI1* mRNA were analysed using q-PCR (Section 2.1.5.4.). 2 technical replicates were included on each plate which was repeated in 3 individual CAF lines (isolated from 3 different patients).

1% FBS IMDM 0.1% DMSO	2µg/mL rShh in IMDM 0.1% DMSO	2µg/mL rShh in IMDM 0.1% DMSO
2µg/mL rShh in IMDM 1000nM Redx Inhibitor	2µg/mL rShh in IMDM 100nM Redx Inhibitor	2µg/mL rShh in IMDM 10nM Redx Inhibitor

Table 4.1. 6-Well plate map summarising the conditions used to investigate the inhibition of Hh pathway in CAFs.

4.2.4. Transwell co-culture for Hh pathway activation

Transwell co-culture allows for the analysis of changes in Hh pathway genes in CAFs when PANC1 cells and CAFs are cultured in the same well. The Transwell co-culture model used in this project involved the separation of epithelial cancer cells from CAFs using a permeable membrane to allow paracrine signalling to occur with a physical barrier between the two cell populations. 6-well Transwell polycarbonate membranes (Corning Life-sciences) were used with a pore size of 0.4µm, which does not permit the migration of cells through the membrane but does allow the passage of proteins and signalling molecules such as Shh and Wnt. During the optimisation of this experiment various epithelial cell:CAF ratios and time points were explored until the optimal conditions to give the highest activation of Hh pathway was determined. Optimisation experiments were carried out in duplicate using one exemplar CAF cell line (R3215) with the final conditions repeated in duplicate with 3 CAF lines (R3030, R3072 and R3088). 1 week before the Transwell experiment was carried out, cells were transferred from DMEM (supplemented with 10% FBS) to IMDM (supplemented with 10% FBS, 2% L-Glutamine and 1% Penicillin Streptomycin). This was done to ensure that changes in mRNA expression could not be attributed to a change of growth medium. An empty 6-well plate was filled with 2mL per well of growth medium, the Transwell inserts were added and 50,000 PANC1 cells or CAFs were loaded onto the insert in 2mL of media. In the empty Transwell plate 50,000 PANC1 cells or CAFs were seeded in 2mL of growth medium and the cells were allowed to adhere

overnight. Cells in the Transwell plate were serum starved for 24h and cells on the Transwell inserts were placed in IMDM (5% FBS, 2% L-Glutamine and 1% Penicillin Streptomycin) for 24h. Following this, all media was removed from both Transwell chambers and the inserts were placed in their corresponding wells following the plate map below (Table 4.2.). This was repeated in 3 individual CAF lines. To investigate tumour cell paracrine signalling to CAFs in this Transwell model, it was decided that CAFs should be seeded on the bottom chamber. This is because the yield of RNA from the plate was greatly decreased when CAFs were seeded on the inserts despite cell adherence and growth being unaffected (Figure 4.1.). This could be due to the difference in the growth area on the Transwell insert compared to the bottom chamber. 2mL of fresh IMDM (5% FBS, 2% L-Glutamine and 1% Penicillin Streptomycin) was added to the top and bottom chambers in each well.

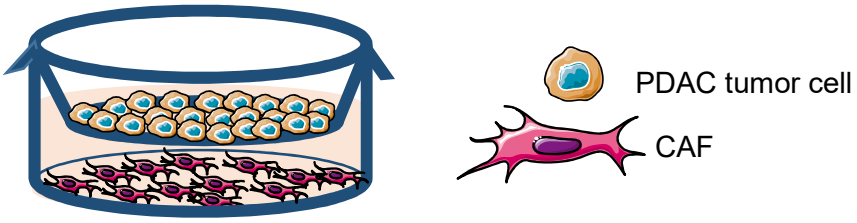

Figure 4.1: Schematic of transwell co-culture model illustrating assay setup.

Top Chamber	CAF 50,000 cells	PANC1 50,000 cells	PANC1 50,000 cells
Bottom Chamber	CAF 50,000 cells	CAF 50,000 cells	PANC1 50,000 cells

Table 4.2: Platemap of conditions used in a Transwell model

RNA was isolated from both chambers after 48h and the difference in Hh pathway activation between CAFs cultured with either CAFs or PANC1 cells was measured by RT-PCR (section 2.2.5.4.). Hh pathway activation was described using changes in

mRNA level of *GLI1, SMO* and *PTCH1* as these are the main effectors of the Hh pathway (Choudhry et al., 2014).

4.2.5. Hh pathway inhibition in a Transwell co-culture model

Using the Transwell co-culture model developed above, it was possible to investigate how effective Redx SMO inhibitors would be in a model which allowed paracrine signalling between epithelial cancer cells and CAFs. The method used is identical to section 4.2.4 with the addition of either Redx SMO inhibitor (10mM stock in DMSO, final DMSO concentration 0.1%) or vehicle control (0.1% DMSO) to all wells (see Table 4.3 for plate map).

Top Chamber	CAF 50,000 cells 0.1% DMSO	PANC1 50,000 cells 0.1% DMSO	PANC1 50,000 cells 1000nM (Redx Compound A)
Bottom Chamber	CAF 50,000 cells 0.1% DMSO	CAF 50,000 cells 0.1% DMSO	CAF 50,000 cells 1000nM (Redx Compound A)
Top Chamber	CAF 50,000 cells 0.1% DMSO	PANC1 50,000 cells 0.1% DMSO	PANC1 50,000 cells 1000nM (Redx Compound B)
Bottom Chamber	CAF 50,000 cells 0.1% DMSO	CAF 50,000 cells 0.1% DMSO	CAF 50,000 cells 1000nM (Redx Compound B)

Table 4.3 Platemap of condition used in a Transwell model to investigate if Redx SMO inhibitors could reduce activation of Hh pathway in CAFs

RNA was isolated from cells in both chambers after 48h and the difference in Hh pathway activation between CAFs cultured with CAFs/PANC1 cells in the absence or presence of Redx SMO inhibitors was investigated by RT-PCR (section 2.2.5.4.). Hh pathway activation was determined using changes in mRNA level of *GLI1.*

4.2.6. Taqman Array for Hh pathway

A human Hh pathway TaqMan Array (Thermo Fisher Scientific) was used to compare the differential expression of Hh pathway associated genes in CAFs and NAFs compared with a normal pancreatic fibroblast cell line (NPF; purchased from ATCC). The array plate contained 44 Hh associated genes *(BCL2, BNC1, BTRC, CREBBP, CSNK1A1, CSNK1D, CSNK1E, CSNK1G1, CSNK1G2, CSNK1G3, dhh, DISP1, DISP2, E2F1, FBXW11, FOXA2, GAS1, GLI1, GLI2, GLI3, GSK3B, HHIP, IFT52, IFT88, ihh, LRP2, MTSS1, MYF5, PRKACA, PRKACB, PRKACG, PRKX, PRKY, PTCH1, PTCH2, RAB23, Shh, SMO, STIL, STK36, SUFU, ZIC1, ZIC2, ZIC3)* and 4 control genes (*18S, GAPDH, GUSB* and *HPRT1*) in duplicate. The genes included in this array are from the vertebrate Hh family of associated genes. CAFs, NAFs and NPFs were cultured in IMDM (10% FBS, 2% L-Glutamine, 1% Penicillin Streptomycin) and were allowed to reach 80% confluence at which point their RNA was isolated. The cDNA was diluted with a volume of DNase free water to a concentration of 1ng/μL which corresponds to 10ng/reaction. The array plate was centrifuged at 1000rpm for 2min, each well was loaded with 10μL of cDNA and 10μL of mastermix. The mastermix used was TaqMan Fast Universal PCR Master Mix (2X), no AmpErase UNG (AppliedBiosystems). The plate was centrifuged for a second time at 1000rpm for 2min and then loaded into a T100 Thermal Cycler (Biorad) and the plate was run according to the cycle detailed in Table 2.5. The fluorophore used with TaqMan was carboxyfluorescein (FAM).

4.3. Results

4.3.1. Shh expression and secretion

In order to confirm the presence of aberrant Shh expression in the pancreatic tumour microenvironment, IHC analysis was performed (See section 2.2.4.4.). Figure 4.2 shows that Shh was expressed in epithelial cells lining ducts in the pancreatic tumour microenvironment compared to an absence of strong positive staining in the acini and

ducts of normal tissue (Figure 4.2A-B). When strong positive Shh staining was compared using a positive pixel count algorithm the difference between tumour and normal tissue was shown to be statistically significant (p=0.0008) (Figure 4.2C). It is interesting to note that the Shh staining in the epithelial cells surrounding ducts shows strong positive staining in a perinuclear compartment in a pattern reminiscent of that observed in staining for the golgi/ER (Figure 4.2.B). This spatial staining is consistent with the presence of Shh precursors which are targeted to the golgi/ER for post-translational modification of the addition of a cholesterol moiety prior to secretion (Eaton, 2008).

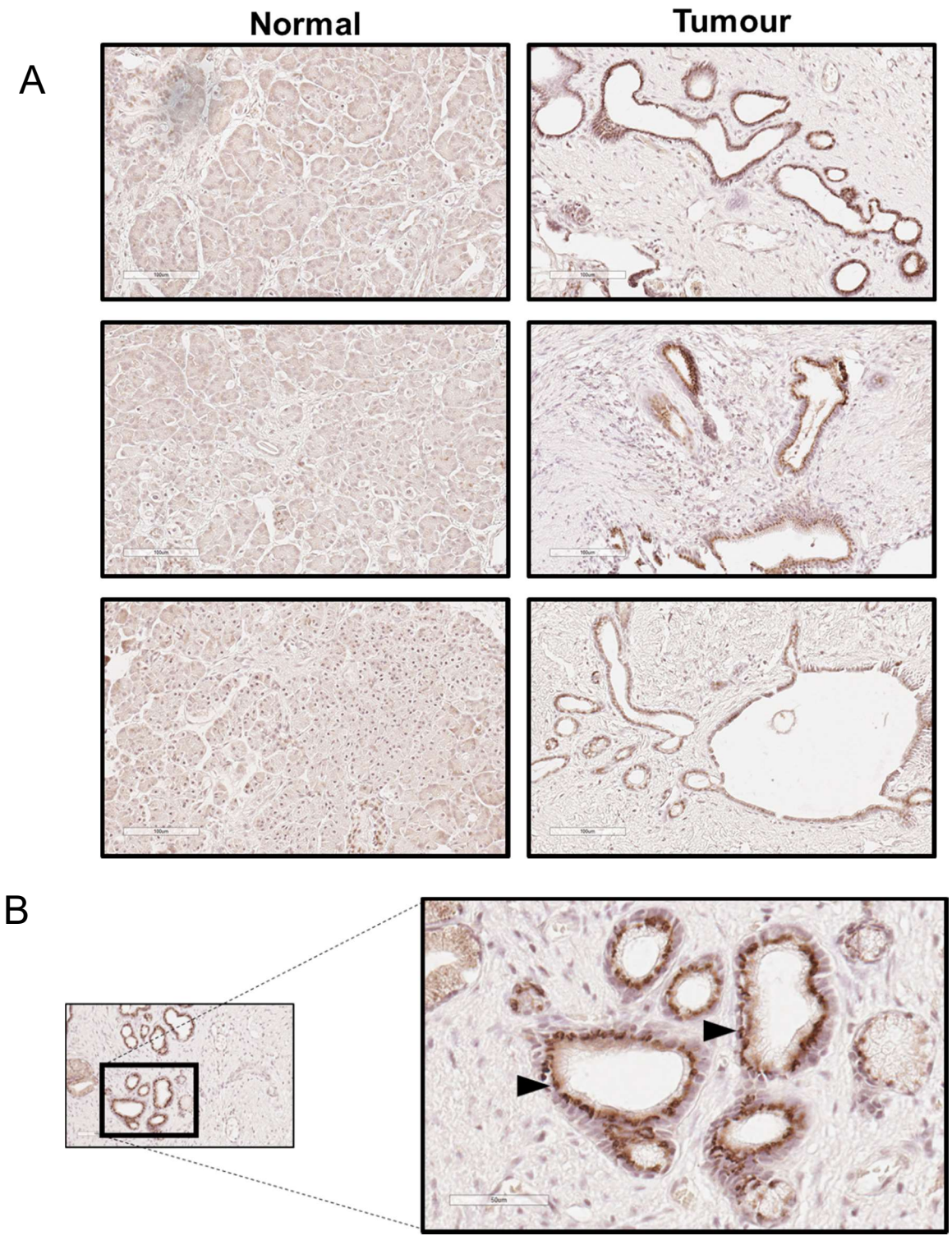
A
Normal
Tumour
B

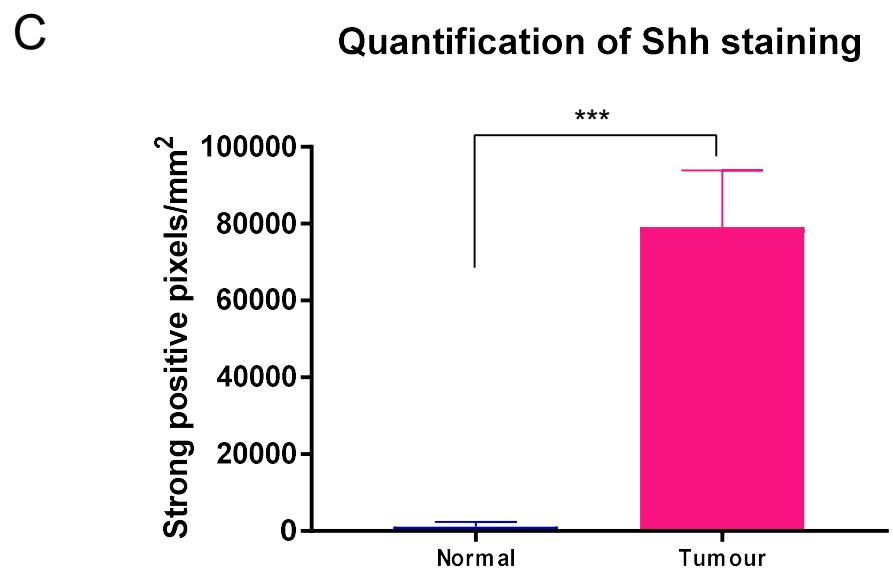

Figure 4.2.Shh staining in the pancreatic tumour microenvironment

A: IHC analysis of Shh staining in tissue isolated from normal appearing tissue compared with fibrous appearing tissue from PDAC specimens. There is no specific positive staining in normal pancreatic acini compared to strong positive staining in pancreatic tumour cells in PDAC samples. Scale bar: 100µm. **B**: Higher magnification image of a pancreatic tumour showing strong perinuclear staining in tumour cells. Scale bar: 50µm**. C**: Quantification of staining in Normal compared with Tumour specimens using Aperio Imagescope to isolate and count strong positive pixels. To quantify staining three areas were chosen per sample. This data shows the comparison of 3 normal vs 3 tumour specimens. P value = 0.0008.

As discussed in Section 3.3.4. it was not possible to isolate primary pancreatic tumour cells from tumour specimens, therefore it was necessary to establish the expression of Shh in a panel of established pancreatic cancer cell lines. To this end, PANC1, MIAPACA2, SUIT2, ASPC1 and BXPC3 cell lines were fluorescently labelled using anti-Shh antibodies and DAPI nuclei stain (Section 2.2.4.6.) (Figure 4.3).

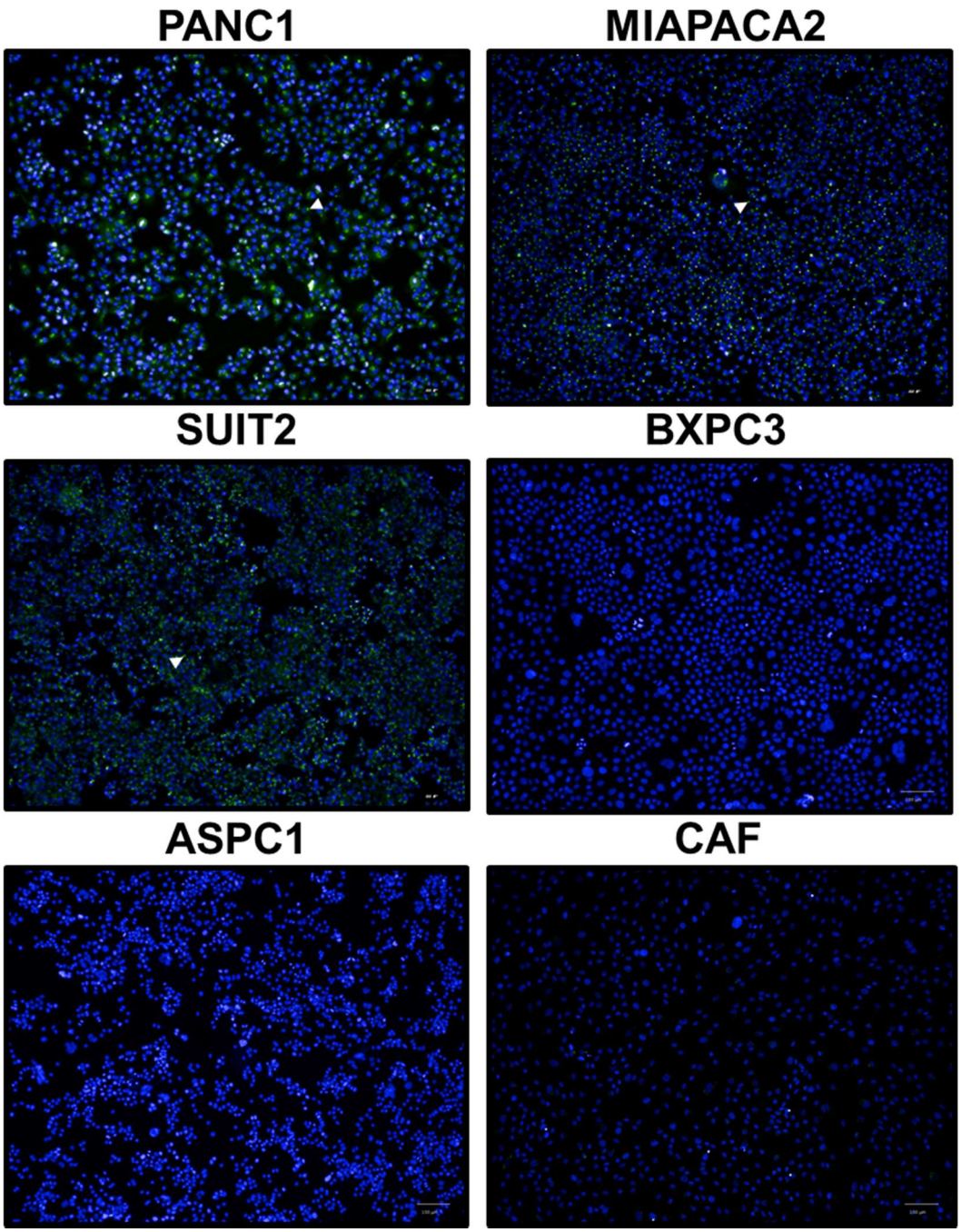

Figure 4.3. Shh expression in pancreatic cancer cell lines

Representative images of pancreatic cell lines and a CAF isolate (R3104). All cells were stained for Shh expression (green) and counterstained with the nuclei dye DAPI (blue). An isotype control was used to remove background fluorescence.

Figure 4.3. shows that PANC1, MIAPACA2 and SUIT2 express Shh in a homogenous manner. Moreover, the positive Shh staining in these cell lines is also in a perinuclear compartment in a pattern reminiscent of that observed in staining for the golgi/ER which is similar to that observed in tumour cells in the PDAC tumour microenvironment (Figure 4.3, Figure 4.1A & B). However, Shh staining was minimal/absent in BXPC3, ASPC1 and CAF despite similar cell numbers present. The absence of staining in the CAF cells was similar to the lack of Shh present in the stromal cells of the pancreatic tumour microenvironment (Figure 4.2A & B). The presence of Shh within the cells may not necessarily translate into secreted Shh which is crucial for effective modelling of paracrine Hh signalling between CAFs and epithelial cells. I therefore sought to quantify the level of Shh secreted by each cell line using a quantitative ELISA for human Shh.

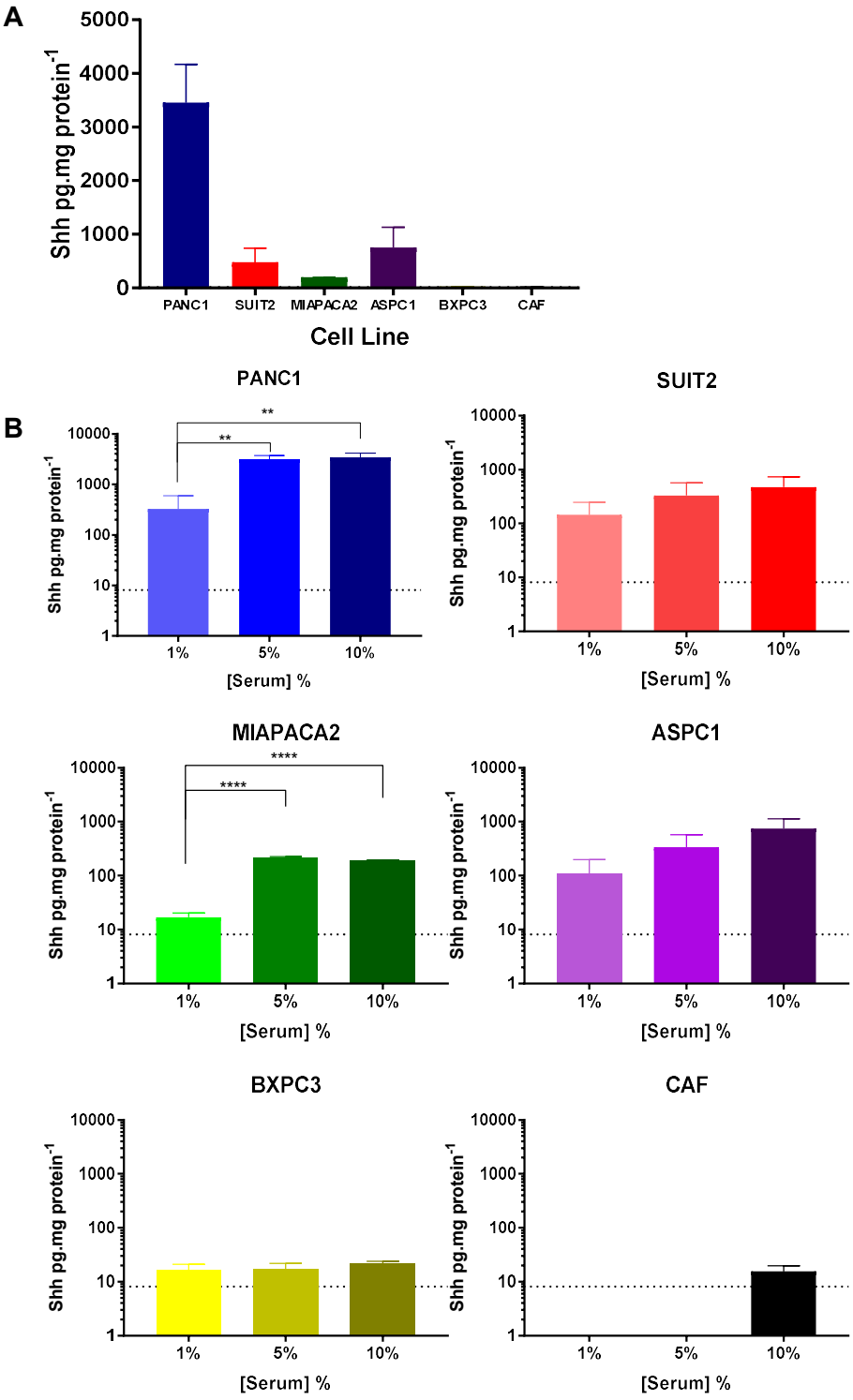

Figure 4.4. Secretion of Shh by pancreatic cancer cell lines and CAFs at varying serum concentrations

A: Shows the levels of Shh secretion from PDAC cancer cell lines compared to CAFs under standard culture conditions (10% Serum). CAFs secrete below the limit of detection for this ELISA therefore statistical analysis was not appropriate. **B**: Shows the effect of different serum (FBS) concentrations on the secretion of Shh secretion in PDAC cancer cell lines and CAFs. Dotted line indicates the limit of detection for the ELISA.

It was necessary to investigate not only the Shh expression level in the various cancer cell lines but also their ability to produce Shh ligand in low serum conditions. In standard culture conditions (10% FBS) Shh was detected in the supernatants of all 5 PDAC cell lines (Figure 4.4A). However only PANC1 cells secrete significantly more Shh than CAFs when compared using a one-way ANOVA ($p<0.0001$; Figure 4.4A). PANC1 and MIAPACA2 cells secrete significantly more Shh when they are cultured in 10% and 5% serum compared to 1% serum condition. No Shh was detected in CAF supernatants (Figure 4.4.) which is consistent with the absence of Shh expression in the cells (Figure 4.3). In stark contrast, all 5 PDAC lines secreted detectable levels of Shh in each of the 3 serum conditions with PANC1 cells exhibiting the most secreted Shh in all 3 conditions with a mean of 3451.4±415.9, 3175±314.5 and 329.1±156.2 pg.mg protein^{-1} in 10, 5 and 1% serum respectively (Figure 4.3 B). The lack of detectable Shh in CAF supernatant at 1% and 5% serum makes direct statistical comparison unfeasible for these conditions.

4.3.2. Hh pathway in CAFs

Having established that the PDAC cell lines used in this project secrete Shh the next step was to investigate whether differences in the expression of Hh pathway genes exist between activated fibroblasts isolated from the tumour microenvironment compared with fibroblasts isolated from normal appearing tissue.

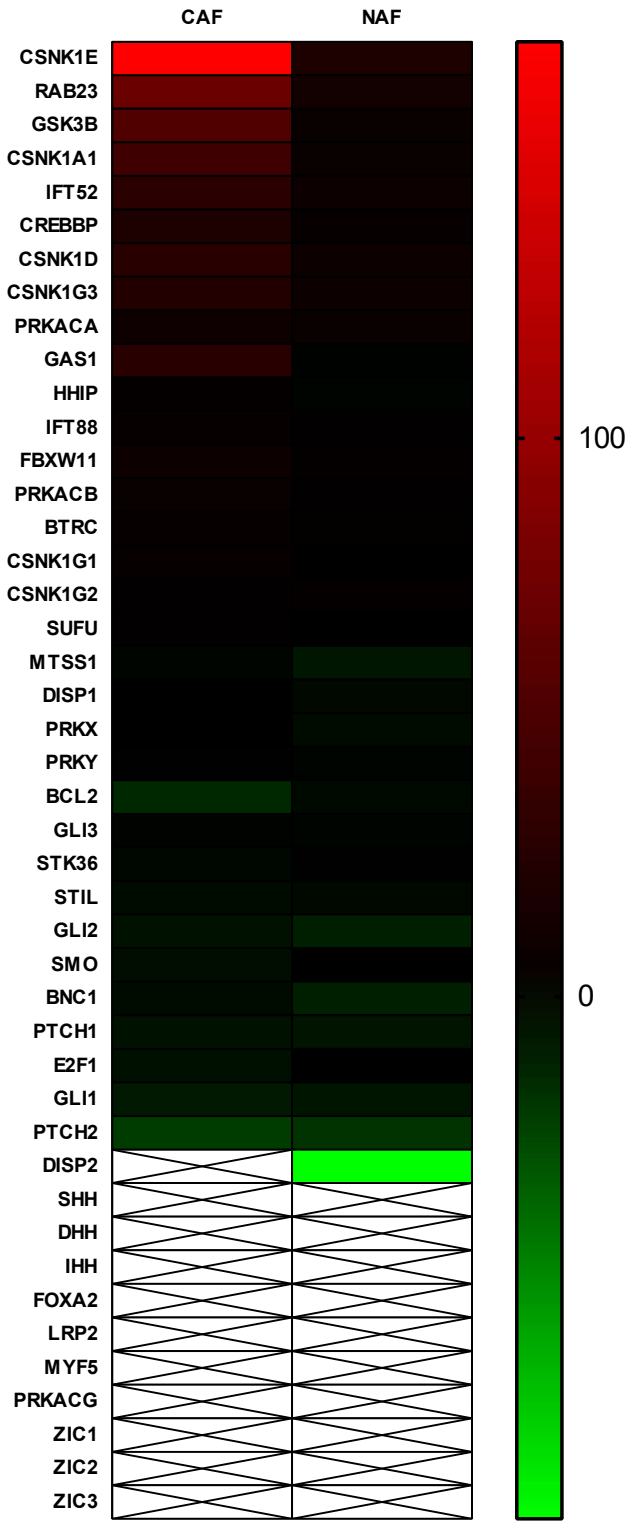

Figure 4.5. Differentially expressed genes in CAFs and NAFs

Differentially expressed genes in CAFs and NAFs using a normal pancreatic fibroblast line (Purchased from ATCC) as a control fibroblast line, gene expression profiles were obtained by Taqman mini array. Upregulation of genes of interest is indicated by red colour, downregulation is shown using green. The discovery analysis (Benjamini, Krieger and Yekutieli, with Q = 1%. Computations assume that all rows are sample from populations with the same scatter (SD)) identified three statistically significant gene differences CSNK1E1 ($p<1x10^{-14}$), RAB23 (p=0.000004) and GSK3β (p=0.0001).

Analysis of both CAFs (N=3) and NAFs (N=3) show three significantly upregulated genes in CAFs which are associated with the Hh pathway *CSNK1E1, RAB23* and *GSK3β* (Figure 4.5). Casein Kinase1E1 and GSK3β are involved in the proteolytic processing of the GLI transcription factors in response to the released repression of SMO upon binding of a Shh ligand to its receptor PTCH11 (Aikin et al., 2008). RAB23 is a regulator of the Hh pathway as it is involved in the control of intracellular vesicles; PTCH11 and SMO are continually trafficked between the cytoplasm and cell membrane through vesicles, therefore this protein is essential for effective Hh signalling (Eggenschwiler et al., 2001). Another finding from this gene expression panel was a lack of gene expression relating to the Hh ligands, Shh, ihh and dhh in both CAFs and NAFs. Interestingly, there appeared to be no significant changes in the downstream Hh pathway components such as *PTCH1, SMO* and *GLI1* (Figure 4.5). Together these data demonstrate that Hh signalling is not active in CAFs and NAFs when they are cultured alone suggesting that Hh signalling does not occur in an autocrine manner. However, they are capable of responding to Hh ligand in a paracrine fashion as they have downstream Hh signalling components. This is also consistent with the lack of mRNA for Hh ligands in CAFs and NAFs.

4.3.3. Hh pathway activation in CAFs in response to Hh stimulus

Having established that pancreatic cancer cells secrete Shh whereas CAFs do not, it was necessary to determine if it was possible to activate the Hh signalling pathway in the CAFs. This is because the CAFs, despite lacking Hh ligand, clearly express the components necessary for responding to external Hh ligand (Figure 4.5). Should the CAFs respond then it was also important to determine the most appropriate time point at which to measure the activated Hh signalling for future experiments.

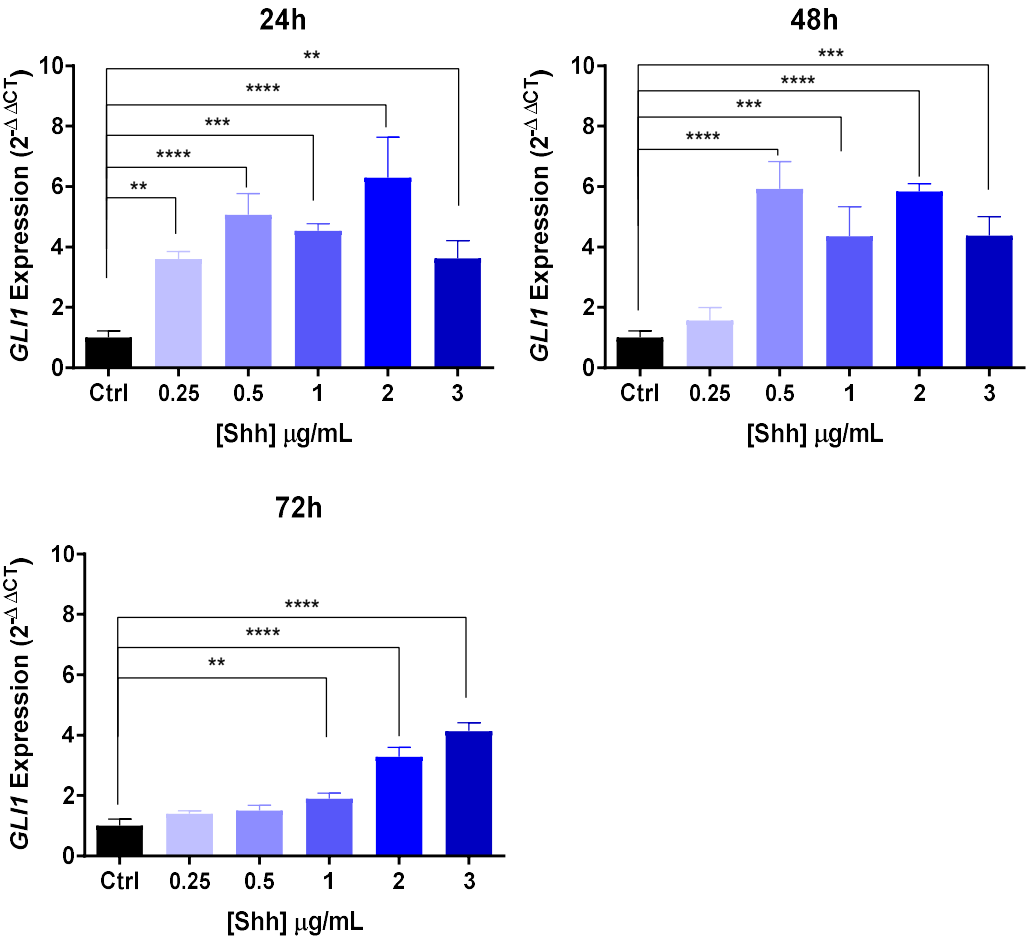

Figure 4.6. Time-course of GLI1 induction in pancreatic CAFs.

Graphs showing *GLI1* expression (RT-PCR) in CAFs exposed to different concentrations of recombinant Shh (0.25, 0.5, 1 ,2 and 3 µg/mL) for 24, 48 and 72h. Gene expression was normalised to *GAPDH* and compared to expression of *GLI1* in CAFs cultured in IMDM (1% FBS, 2% L-Glu, 2% PenStrep). Each bar represents the $^{\Delta\Delta}$Ct gene expression of 3 experiments using the same CAF line, R3104.

At 24h post stimulation of CAFs, a significant upregulation in *GLI1* mRNA expression could be observed across all rShh concentrations (Figure 4.6.). At 48h concentrations >0.25µg/mL showed a significant upregulation of *GLI1* mRNA (Figure 4.5). At 72h only 1, 2 and 3 µg/mL were able to elicit a significant upregulation in *GLI1* (Figure 4.6). This could be due to the mechanism of Hh pathway activation. For example, during development of the neural progenitor regions of the brain in mammals, Shh produces a rapid response in GLI1 expression which is lost over time (Cohen et al., 2015). This is important in as neural development requires varying duration and level of Shh signal (Cohen et al., 2015) . Similar temporal signalling is also present in the JAK/STAT and Wnt pathway and is referred to as ligand pulsing (Bachmann et al., 2011, Hernandez et al., 2012). This could explain why only the higher concentrations of rShh elicit a response at 72h. Once it was established that there was a significant upregulation of Hh pathway activity in CAFs from as early as 24h and using the lowest concentration (0.25µg/mL) of rShh, it was then necessary to investigate if exposing CAFs to conditioned media from PDAC cell lines induced a change in *GLI1* expression. This was to determine if the cross talk between these cell types could be recapitulated in an *in vitro* model.

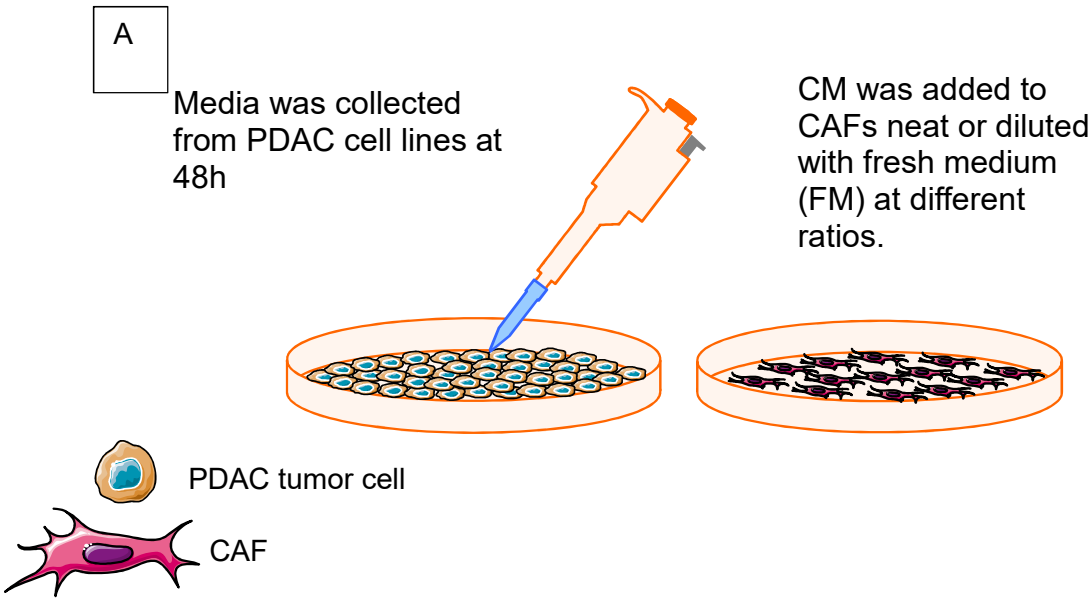

B

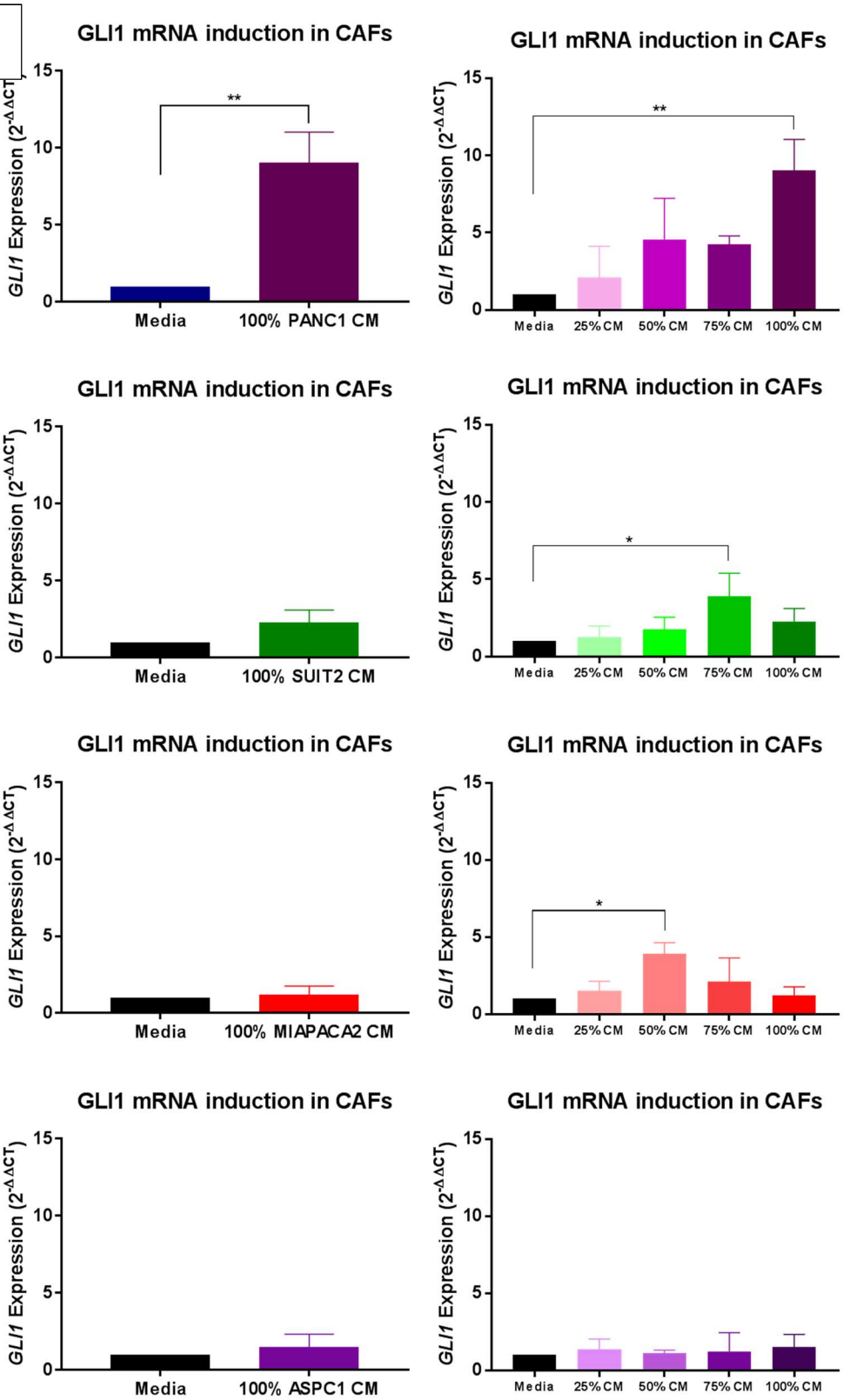
GLI1 mRNA induction in CAFs
GLI1 Expression (2-ΔΔCT)
15
10
5
0
**
Media
100% PANC1 CM
GLI1 mRNA induction in CAFs
GLI1 Expression (2-ΔΔCT)
**
Media
25% CM
50% CM
75% CM
100% CM
GLI1 mRNA induction in CAFs
GLI1 Expression (2-ΔΔCT)
Media
100% SUIT2 CM
GLI1 mRNA induction in CAFs
GLI1 Expression (2-ΔΔCT)
*
Media
25% CM
50% CM
75% CM
100% CM
GLI1 mRNA induction in CAFs
GLI1 Expression (2-ΔΔCT)
Media
100% MIAPACA2 CM
GLI1 mRNA induction in CAFs
GLI1 Expression (2-ΔΔCT)
*
Media
25% CM
50% CM
75% CM
100% CM
GLI1 mRNA induction in CAFs
GLI1 Expression (2-ΔΔCT)
Media
100% ASPC1 CM
GLI1 mRNA induction in CAFs
GLI1 Expression (2-ΔΔCT)
Media
25% CM
50% CM
75% CM
100% CM

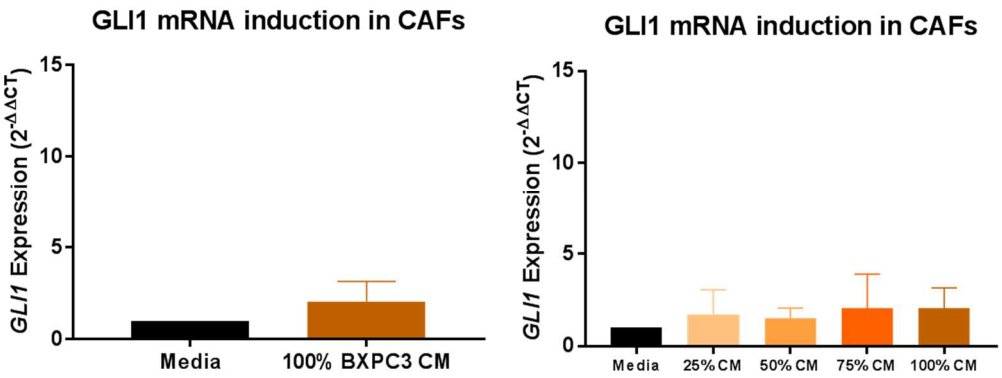

Figure 4.7. Induction of *GLI1* mRNA in response to conditioned medium from pancreatic cancer cell lines

A: Schematic illustrating conditioned medium assay setup.

B: Graphs showing *GLI1* expression (RT-PCR) in CAFs exposed to conditioned media (IMDM supplemented with 5% FBS, 1% L-Glutamine, 2% Penicillin streptomycin) from pancreatic cancer cell lines either undiluted, or diluted with fresh media. Gene expression was normalised to *GAPDH* and compared to expression of *GLI1* in CAFs cultured in IMDM (1% FBS, L-Glutamine, 2% Penicillin streptomycin). Each bar represents the $^{\Delta\Delta}$Ct gene expression of 3 different CAF lines (R3088, R3072 and R3030) with 2 technical replicates per cell line. Statistical significance was determined using an ordinary one way ANOVA.

Figure 4.7. shows that it was possible to detect significant changes in *GLI1* expression in CAFs in response to conditioned media from PANC1, SUIT2 and MIAPACA2 cells. Interestingly, this response corresponded well to the levels of Shh produced by the pancreatic cancer cell lines (Fig 4.4A) with the same rank order of PANC1, SUIT2 and MIAPACA2 for both Shh secretion and conditioned media response. PANC1 cells were found to secrete the most Shh (3451.0± 415.9pg.mg protein^{-1}) and they stimulated the largest upregulation of *GLI1* mRNA in CAFs (9.04-fold), followed by SUIT2 (472.2±153.4 pg.mg protein^{-1}) which produced the next largest upregulation of GLI1 mRNA (3.89-fold). The only other cell line to produce a change in *GLI1* mRNA was MIAPACA2 (3.89-fold) which was also found to produce relatively high levels of Shh (192.7±2.647 pg.mg protein^{-1}). The only anomaly was in the case of ASPC1 which did not produce a significant *GLI1* mRNA induction despite secreting a higher level of Shh than SUIT2 and MIAPACA2 cells (748.5± 220.7 pg.mg protein^{-1}). Despite the detection of Shh secretion by ASPC1 using ELISA (Figure 4.4.A) which is consistent with the findings of Li and colleagues who found that ASPC1 cells secreted Shh (Li et al., 2014) there did not appear to be any expression of Shh detected using IF in ASPC1 cells (Figure 4.3). Together this data suggests that the Shh secreted from ASPC1 is not functionally active (Figure 4.7.).

Once it had been established that CAFs were responsive to both rShh and Shh produced by pancreatic cancer cell lines it was possible to determine if changes in *GLI1* induction could be inhibited using small molecule SMO inhibitors developed by Redx Pharma.

Redx compounds A-E significantly reduced the response to rShh ligand as demonstrated by a reduced induction of *GLI1* mRNA. For example 1000nM Redx compound A reduced the induction of GLI1 mRNA from 6.2±1.3 to 1.8±0.3 fold (Figure 4.8). The ability of SMO inhibitors to reduce GLI1 induction in response to

rShh stimulation demonstrates that Redx SMO inhbitors are effective at reducing the activation of Hh pathway in CAFs induced by rShh.

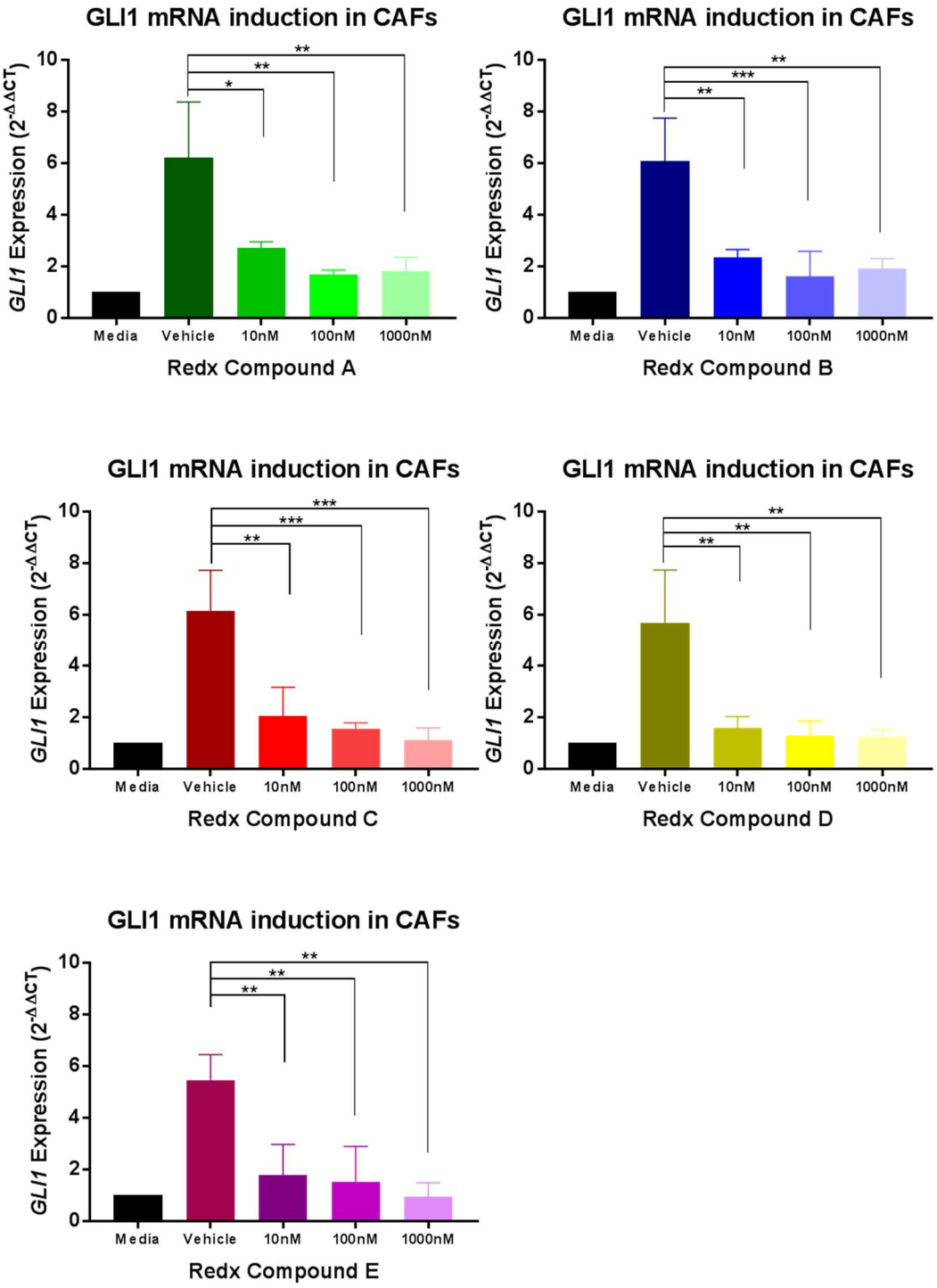

Figure 4.8. rShh-mediated GLI1 induction in the presence of Redx SMO inhibitors

Graphs showing *GLI1* expression (RT-PCR) in CAFs exposed to media (IMDM 1% FBS, 1% L-Glutamine, 2% Penicillin streptomycin) supplemented with 2µg/mL of rShh in the presence of either a vehicle control (0.1% DMSO) or Redx SMO Inhibitors (0, 10nM, 100nM and 1000nM). Gene expression was normalised to GAPDH and compared to the expression of *GLI1* in CAFs cultured in (1% Serum Media). Each bar represents the $^{\Delta\Delta}$Ct gene expression of 3 experiments using 3 individual CAF lines (3 replicates/cell line). Statistical significance was determined using an ordinary one way ANOVA.

Once the efficacy of Redx SMO inhibitors had been established using GLI1 mRNA expression, it was important to determine if this resulted in any change in GLI1 protein expression. Therefore, Redx compounds A and B were selected to determine whether the reduction in GLI1 mRNA would translate into a reduction of GLI1 protein, measured using IF.

IF labelling of GLI1 revealed that exposure of CAFs to 2µg/mL rShh resulted in increased GLI1 protein expression (Figure 4.9A). However, when cells were treated with 1000nM of Redx compound (A or B) this staining was almost completely ablated (Figure 4.9A). This reduction was highly significant when compared using an ordinary ANOVA with a p value of $p<0.0001$ (Figure 4.9B). These data are consistent with the mRNA expression data (Figure 4.8.) thus demonstrating that the reduction in GLI1 mRNA expression by Redx SMO inhibitors is translated to a reduction in GLI1 protein.

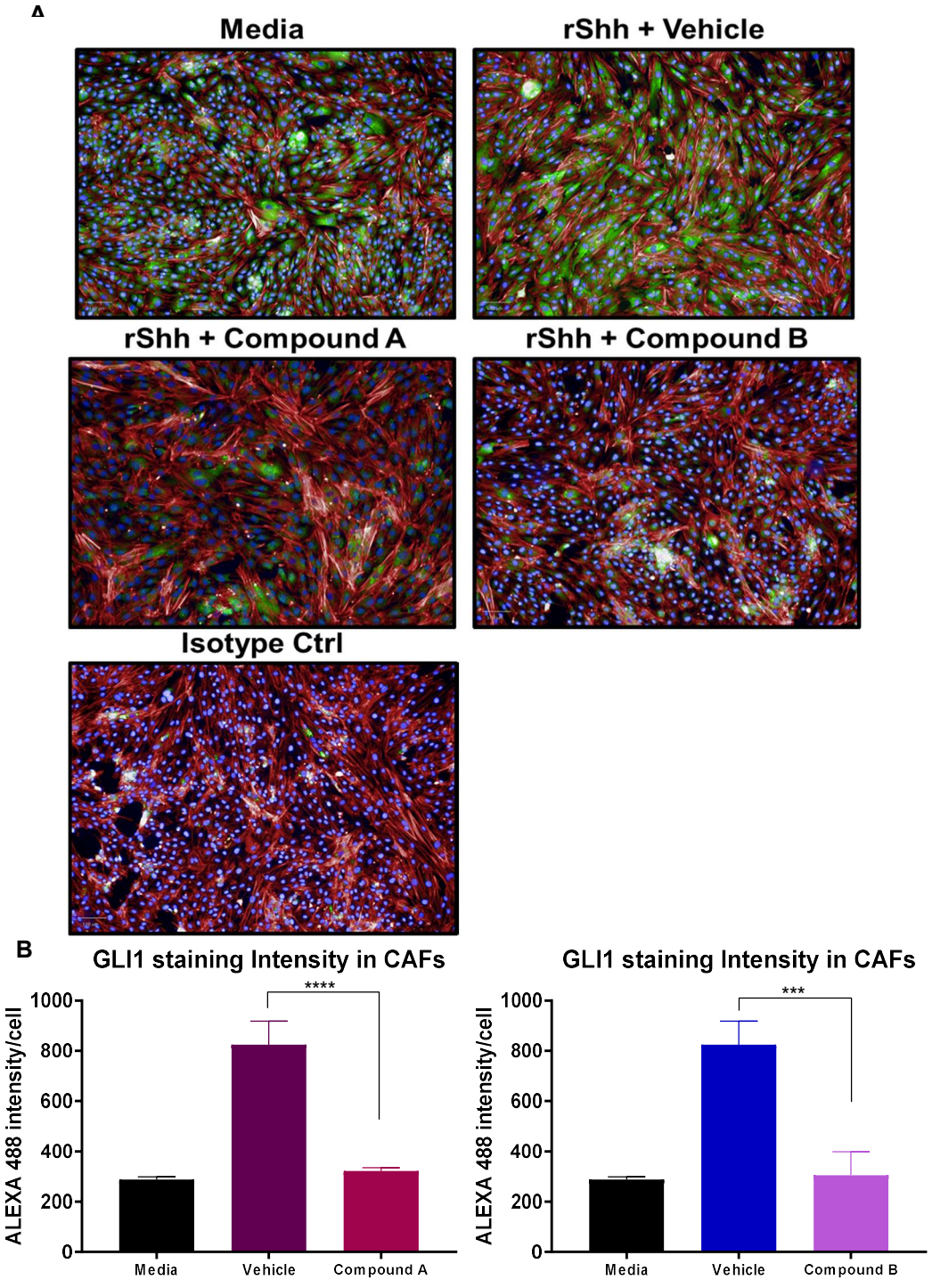

Figure 4.9. Loss of GLI1 stimulation in response to Redx SMO Inhbitors

GLI1 expression was measured in CAFs in 1% media, Vehicle (rShh + 0.1% DMSO) and Stimulation + Compound treatment (rShh + SMO inhibitors 1000nM). **A: Representative Images of experimental conditions**. Nuclei stained with DAPI (blue), Actin stress fibres stained with Phalloidin (Red) and GLI1 is labelled with an anti-GLI1 antibody followed by an ALEXA-488 conjugated secondary antibody (green). Isotype control, was used to exclude background fluorescence is also shown. **B: Quantitative analysis of GLI1 staining intensity** .GLI1 staining intensity per cell was measured using an Operetta HTS imaging system (PerkinElmer). Each bar represents mean ± SEM GLI1 staining intensity. 3 wells per condition with 3 regions of interest (ROI) per well. Cells touching or crossing a ROI border were automatically excluded to reduce variation. Statistical significance was determined using an ordinary one way ANOVA. *** indicate a $p<0.0001$

4.3.6. Transwell co-culture model of CAFs and PANC1 cells

Having established that CAFs not only express the proteins capable of responding to Shh stimulation, but also exhibit Shh pathway activation (GLI1 induction) in response to rShh, it was important to determine whether CAFs responded to endogenous levels of Hh activation. This was necessary in order to determine if co-culture models of CAFs and cancer cells exhibit similar Hh pathway activation when cultured in the same well. This was achieved using a Transwell system. Firstly, it was critical to establish appropriate experimental conditions which resulted in an upregulation of the Hh pathway. PANC1 cells were chosen for use in this model as they produce the most Shh relative to the other pancreatic cancer cell lines used in this project (Figure 4.4 A) and their conditioned media induced the largest *GLI1* mRNA upregulation in CAFs (Figure 4.7).

A Transwell co-culture model of CAFs and PANC1 cells showed that after 24h neither a 1:1 or 1:2 ratio of CAF:PANC1 elicited an increase in *GLI1, SMO* and *PTCH1* mRNA which suggests that 24h is not sufficient time for Shh concentrations to overcome the threshold required to activate Hh signalling in CAFs (Figure 4.10.). At 48h a 1:1 ratio gave the largest combined induction of *GLI1* and SMO mRNA with a fold induction of 5.63±1.37 and 8.57±1.25 respectively (Figure 4.10.). This was consistent with the induction of *GLI1* mRNA which was achieved using recombinant ligand (~6-fold; Figure 4.8.). Consequently, these conditions were chosen for future experiments. Increasing the ratio to 1:2 (CAF:PANC1) did not result in a further increase of *GLI1* induction, however there was an upregulation of *SMO* 9.23±0.62 fold and *PTCH1* 7.55±1.27 fold mRNA (Figure 4.10.). At 72h using a 1:1 ratio of CAF:PANC1 there was a 3.88±2.09 fold upregulation of *GLI1* mRNA, 1.50±0.61 fold upregulation of *SMO* and 3.78±1.05 upregulation of *PTCH1* (Figure 4.10.). This could suggest that the maximal activation of Hh signalling is achieved at 48h whereas at 72h Hh pathway activation level is reduced. This could be a consequence of a decrease in Shh

secretion by PANC1 cells as the nutrients present in the Transwell become depleted. The reduced activation of Hh pathway activation at 72h was consistent with the data achieved using rShh ligand (Figure 4.6.) suggesting response to Shh ligand is rapid and the *GLI1* mRNA levels decrease over time if the signal is not maintained.

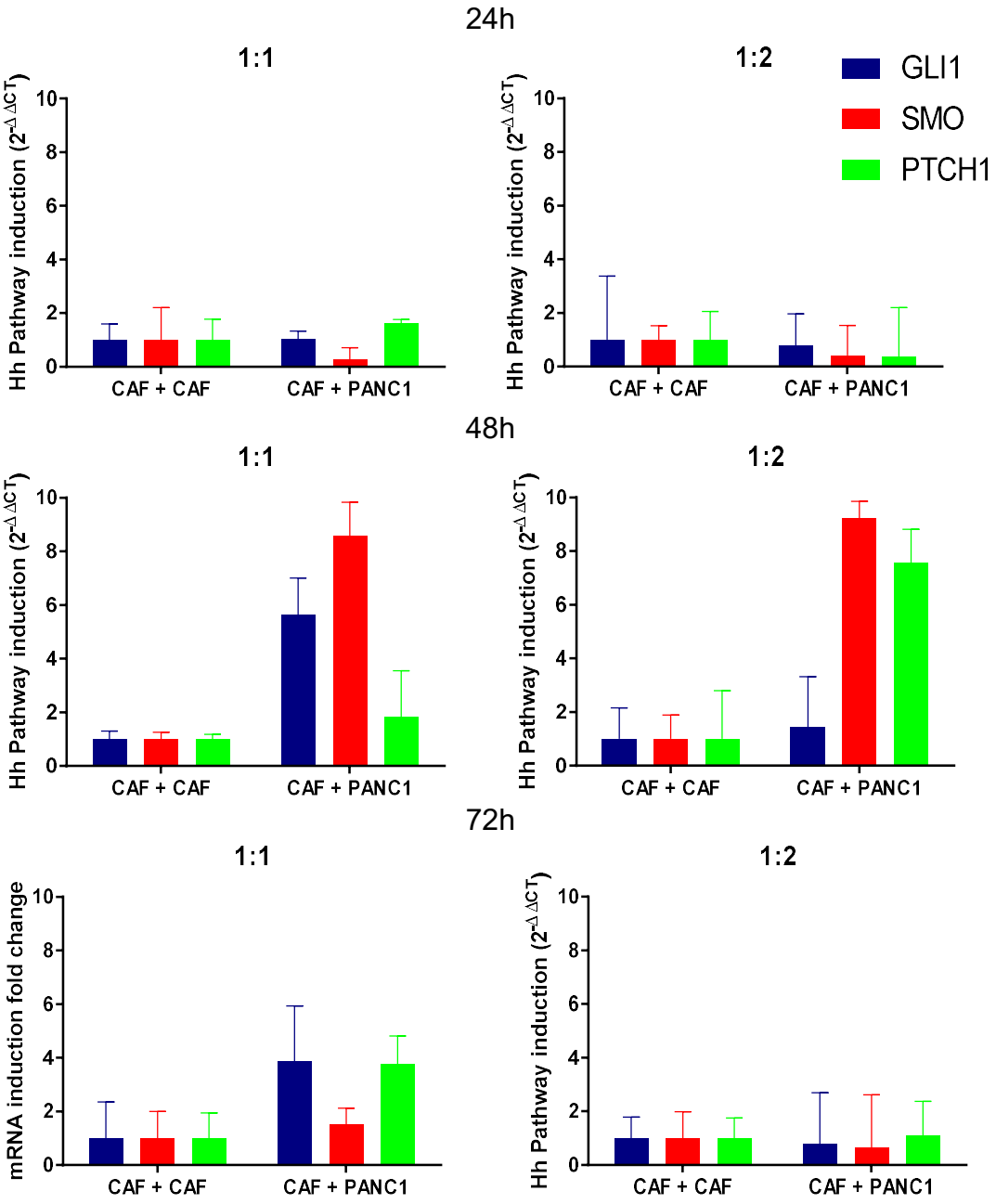

Figure 4.10. Upregulation of Hh signalling pathway in CAFs in a Transwell co-culture model

Graphs showing *GLI1, PTCH1* and *SMO* expression (RT-PCR) in CAFs cultured in the same well as PANC1 cells at either 1:1 ratio or 1:2 (CAF:PANC1) ratio for 24, 48 and 72h. Each bar represents the $^{\Delta\Delta}$Ct gene expression of 1 experiments using 2 replicates. Statistical analysis was not performed as this was a preliminary optimisation experiment and was not replicated in multiple CAF lines.

Having established the 1:1 ratio of CAF:PANC1 cells at 48h induced the greatest upregulation of *GLI1* mRNA expression in CAF R3104, it was necessary to confirm upregulation of the Hh pathway using multiple primary CAF lines to ensure that changes in *GLI1* expression were a consistent finding and not specific to CAFs isolated from one specific patient. The Hh pathway was activated in CAF cell lines R3088, R3072 and R3030 when they were cultured in the same well as PANC1 cells as demonstrated by the significant (p=0.0007) upregulation of GLI1 mRNA expression (Figure 4.11).

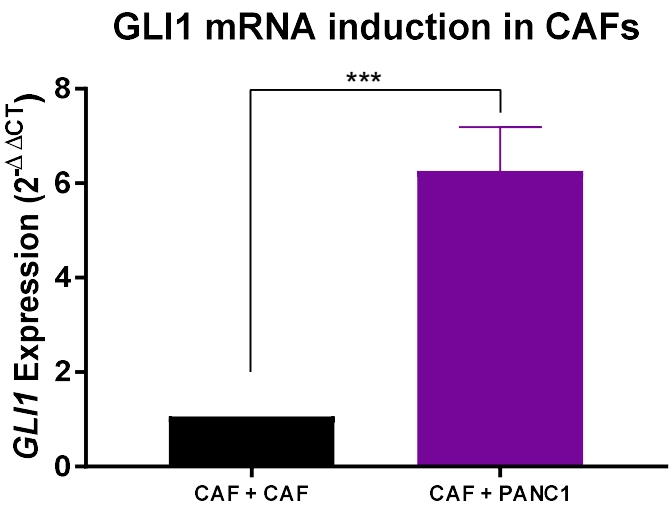

Figure 4.11. Upregulation of *GLI1* in a Transwell co-culture model

Graph showing *GLI1* expression (RT-PCR) in CAFs cultures in the same well as PANC1 cells at a 1:1 ratio for 48h. Each bar represents the $^{\Delta\Delta}$Ct gene expression of 3 CAF lines (R3088, R3072, R3030) (3 replicates per cell line). Statistical significance was determined using an ordinary one way ANOVA. *** represents p= 0.0007 taking into consideration the standard deviation of the calibrator sample (CAF+CAF)

Having established that a Transwell model of CAFs and PANC1 cells results in Hh pathway activation in CAFs, I sought to determine if this was an appropriate model to test the efficacy of Redx SMO inhibitors. In the presence of 1000nM Redx compound

A and Redx compound B, the induction of GLI1 mRNA was reduced from 6.05±0.68 fold to 2.22±0.41 fold, and to 1.20±0.31 fold respectively (Figure 4.12.). This demonstrates that it was possible to inhibit Hh pathway activation in a paracrine model of Hh signalling using Redx SMO inhibitors.

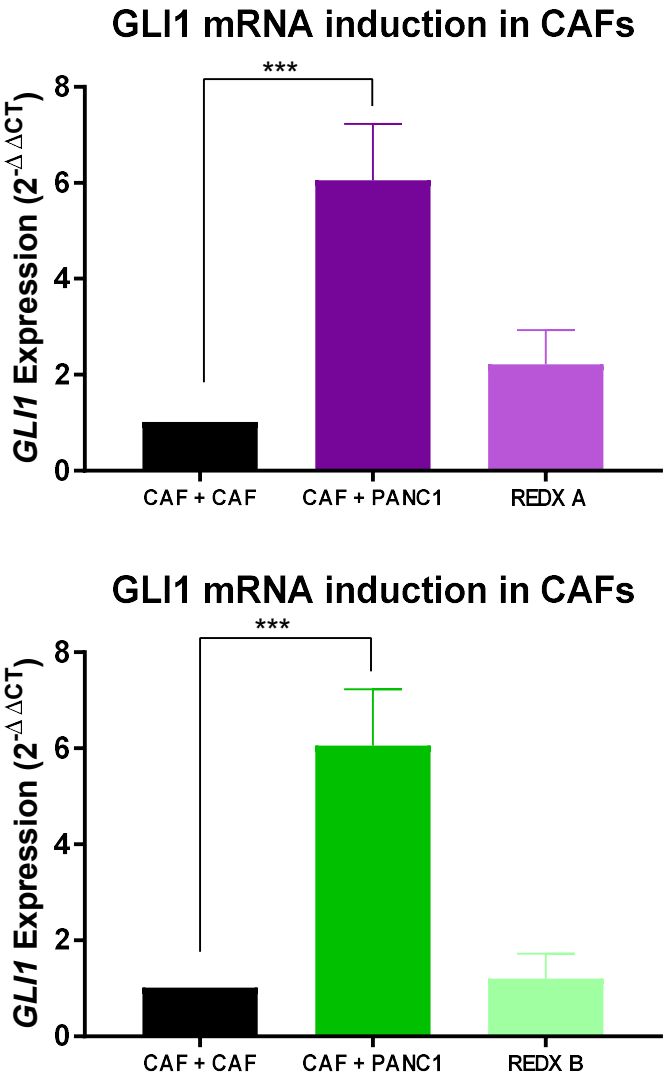

Figure 4.12. Inhibition of Hh pathway in a Transwell co-culture model

Graph showing *GLI1* expression (RT-PCR) in CAFs cultured in the same well as PANC1 cells at a 1:1 ratio for 48h in the presence of Redx SMO inhibitors (1000nM) or a vehicle control (0.1% DMSO). RNA was isolated from CAFs at 48h. Gene expression was normalised to GAPDH and compared to the expression of *GLI1* in CAFs cultured alone. Each bar represents the $^{\Delta\Delta}$Ct gene expression of 3 CAF lines R3088, R3072 and R3030 (3 replicates per cell line). Statistical significance was determined using an ordinary one way ANOVA. *** represents $p<0.0006$ taking into consideration the standard deviation of the calibrator sample (CAF+CAF)

4.4. Discussion

The importance of the tumour microenvironment in facilitating tumour progression and metastases has been well studied (Carr and Fernandez-Zapico, 2016, Feig et al., 2012, Apte and Wilson, 2012, Apte et al., 2013). However conflicting evidence has implicated the tumour stroma in both a tumour supportive and a tumour restraining role (Rhim et al., 2014, Rucki and Zheng, 2014). One critical pathway involved in the formation of the desmoplastic stroma in PDAC is the Hh signalling pathway (Thayer et al., 2003). The results in this chapter demonstrate the presence of aberrant Shh expression present in the pancreatic tumour microenvironment (Figure 4.1) specifically in the pancreatic tumour cells, which is consistent with previous reports (Bailey et al., 2008, Thayer et al., 2003). To create an *in vitro* model which incorporates aspects of the tumour microenvironment and which has appropriate signalling between the cell types it was necessary to discover which pancreatic cancer cell lines expressed Shh in a similar pattern to tumour cells observed in the PDAC tumour microenvironment (Figure 4.3). Using IF to visualise Shh expression, PANC1, SUIT2 and MIAPACA2 cells expressed Shh in a perinuclear pattern (Figure 4.3.) which indicates localisation to the golgi/ER which was in the same location as Shh expression observed in pancreatic ductal epithelial cells (Figure 4.2). This confirms that with regards to Hh signalling, these cell lines were appropriate to represent PDAC tumour cells. Once it had been established that the pancreatic cancer cell lines chosen to represent PDAC mirrored the spatial expression of Shh in epithelial cancer cells, the next step was to determine if the expression of Shh correlated to secretion of the ligand. PANC1 cells secreted the greatest amount of Shh ligand (3.4ng.mg protein^{-1}) with the other cell lines secreting detectable amounts of Shh (0.5, 0.19, 0.75 and 0.02 ng.mg protein^{-1} for SUIT2, MIAPACA2, ASPC1 and BXPC3 respectively; Figure 4.4A). The secretion of Shh was impacted by nutrient deprivation in the cases of PANC1 and MIAPACA2 (Figure 4.4 B). This observation

was significant as it was critical to isolate which cell lines could activate Hh signalling *in vitro*, and to determine under what condition it would be possible to maintain active Hh signalling. It was established that Shh secreting cell lines could maintain secretion under conditions of 5% serum-containing media, however there was a significant loss when exposed to 1% serum-containing media. The finding that Shh secretion is detected in nutrient deprived conditions indicated that Shh secretion levels could vary as the tumour develops and conditions within the tumour microenvironment decline. The expression of Shh is detected throughout PDAC progression even in precursor lesions as early as PanIN1a (Thayer et al., 2003), however as the desmoplastic stroma develops it alters the architecture of the pancreas; capillaries are compressed which creates a nutrient deprived, hypoxic microenvironment (Rasheed et al., 2012) . Therefore the finding that nutrient deprived conditions (1% serum) has a significant impact of Shh secretion in PANC1 and MIAPACA2 cells suggests that the conditions within the tumour could have an impact on Shh secretion.

My finding of little difference in expression of Hh pathway-associated genes in NAFs and CAFs is intriguing. Only three genes (CSNK1E1, GSK3β and RAB23) were significantly differentially expressed between the two cell types with each found to be differentially upregulated in CAFs compared to NAFs. All three genes are involved in active Hh signalling. CSNK1E1 and GSK3β are part of the degradation complex for GLI2 and GLI3 which is necessary for GLI1 activation, GLI2 specifically is targeted for phosphorylation by CSNK1E1 (Riobo and Manning, 2007). RAB23 acts downstream of SMO and upstream of the GLI proteins and is involved in the subcellular localisation of downstream Hh pathway effectors; it is involved in preventing the activation of GLI proteins in the absence of Hh ligand stimuli (Eggenschwiler et al., 2006). These genes are not the main effectors of the Hh signalling pathway (PTCH1, SMO and GLI1)(Briscoe and Therond, 2013). This suggests that the presence of active Hh signalling in the PDAC tumour

microenvironment is not due to the general upregulation of Hh pathway machinery in CAFs, but rather increased stimulation from PDAC cancer cells in the tumour microenvironment. This is supported by the lack of expression of *Shh, ihh* and *dhh* in CAFs and NAFs (Figure 4.5) which is consistent with previous reports that Hh signalling in the PDAC tumour microenvironment occurs in a paracrine fashion with Shh being secreted from epithelial cells and acting upon cells of the stroma (Yauch et al., 2008).

Consistent with CAFs expressing components of the pathway allowing them to respond to active Hh signalling, treatment with rShh induced *GLI1* expression. Moreover, Shh secreted from a physiological source (pancreatic cancer cell lines) was also able to elicit the induction in *GLI1* expression, as demonstrated by incubation of CAFs with conditioned media from Shh secreting PANC1, SUIT2 and MIAPACA2 cells. The only cell line which secreted Shh and did not cause an upregulation in *GLI1* was ASPC1 cells. One of the obstacles of using conditioned media from cell lines is the inability to determine the exact composition of the media as cells secrete a variety of signalling molecules. Therefore it is possible that ASPC1 cells are secreting factors which result in the antagonism of the Hh pathway for example through the activation of Hedgehog Inactivating Protein or Suppressor of Fused (SuFu) which both result in the inhibition of Hh pathway activation (Merchant and Matsui, 2010, Velcheti and Govindan, 2007). The maximal *GLI1* upregulation using recombinant ligand was 6.31-fold when CAFs were treated with 2µg/mL rShh for 24h (Figure 4.6.). The maximal upregulation measured in response to Shh present in conditioned media was a 9.04-fold upregulation of *GLI1* mRNA using 100% PANC1 conditioned medium (Figure 4.7.). A drawback of conditioned media experiments is the possibility that the cancer cells have diminished the nutrient supply in the media and this could have a negative impact on the growth or response of CAFs. To overcome this, a dilution of the conditioned media was made using fresh growth

media to ensure that the maximal *GLI1* induction was observed (Figure 4.7). Interestingly, the cell lines with the fastest growth rates, SUIT2 and MIAPACA2 (Table 2.1.) showed a maximal *GLI1* induction in CAFs when the conditioned media from these cell lines was diluted with fresh media to replace nutrients. This indicates that the nutrient content of the conditioned media could have an effect on Hh signalling in CAFs.

Once it had been established that CAFs were responsive to external Hh stimuli using both rShh and conditioned media from CAFs, it was possible to determine if SMO inhibitors could inhibit the induction of *GLI1* in CAFs. The stimulation of Hh pathway using rShh was diminished in the presence of Redx SMO inhibitors at the lowest concentration tested (10nM; Figure 4.8), and corresponded to reduced expression of GLI1 in CAFs (Figure 4.9). Modulating the Hh signalling pathway which is involved in the maintenance of the pancreatic tumour microenvironment as a treatment option for PDAC has been trialled with IPI-926, however the positive results obtained in mice did not translate to positive clinical outcomes for human patients (Olive et al., 2009). The ability to model the tumour microenvironment *in vitro* to provide more information surrounding the mechanism of action of the complex signalling pathways involved in the PDAC tumour microenvironment would be beneficial in drug screening models in order to predict the efficacy of treatments before they reach the clinic. Using a Transwell co-culture model which contained PANC1 cells, it was possible to investigate the function of Redx SMO inhibitors in a model that incorporates two cell types (Figure 4.10). Redx SMO inhibitors tested in this model showed a reduction in *GLI1* induction compared with the Transwell co-culture alone (Figure 4.11). Together these results suggest that Hh signalling occurs in a paracrine manner via the activation of downstream Hh signalling in CAFs in response to secretion of Shh ligand from epithelial cells lining ducts in the PDAC tumour microenvironment. Treatment of CAFs with rShh or conditioned media from Shh producing cells result in the

upregulation of *GLI1* mRNA which was blocked using Redx SMO inhibitors at concentrations as low as 10nM. These data are consistent with reports that found that Hh pathway inhibitors were much more potent against mesenchymal cells than cancer cell lines (Yauch et al., 2008). These results corroborate studies indicating that the Hh pathway facilitates cross talk between cancer cells and CAFs (Yauch et al., 2008, Bailey et al., 2009) thus providing a tumour supportive environment. Using Transwell co-culture models allows the cross talk between CAFs and cancer cells which provides an effective research tool in the investigation of signalling pathways involved in PDAC. The data presented in this chapter would suggest that preclinical models that do not include stromal elements such as CAFs may not bet adequate for testing PDAC therapies as the stroma plays an important role in supporting tumour progression, metastasis and chemotherapy resistance (Apte and Wilson, 2012, Apte et al., 2013).

5. Wnt/ β-Catenin signalling in the PDAC tumour microenvironment

5.1. Introduction

In various cancers such as colorectal and cutaneous melanoma, mutations of Wnt pathway signalling components (*APC, LRG5, LRP6, AXIN, CTNNB1*) are common (Zhan et al., 2017) However these mutations are rare in PDAC and the role of Wnt signalling in PDAC development and progression is not well understood (Zhan et al., 2017). Despite the lack of mutations, aberrant localisation (cytoplasmic and nuclear) of β-Catenin is found in approximately 65% of PDAC cases (Zeng et al., 2006). In a healthy human pancreas, β-Catenin is found at the cell membrane; nuclear and cellular localisation is associated with canonical pathway activity (Zeng et al., 2006). Surprisingly, studies have revealed that Wnt/ β-Catenin signalling seemingly antagonises KRAS driven acini-ductal-metaplasia (ADM) and subsequent PanIN formation, until the cells have been directed into a metaplastic lineage at which point the cells develop a reliance on Wnt/ β-Catenin signalling and other developmental signalling pathways (Morris et al., 2010). Wnt/ β-Catenin signalling has also been implicated in the PDAC tumour microenvironment, wherein nuclear localisation of β-Catenin is observed in PDAC cancer cell lines in response to being cultured on collagen type 1 This results in increased expression of Wnt target genes *c-myc* and *cyclin D1* and an increased growth rate of the cells (Koenig et al., 2006). Given the presence of aberrant Wnt signalling in the PDAC tumour microenvironment, the aim of this chapter was to determine if the Wnt/ β-Catenin signalling pathway is involved in the crosstalk between PDAC cancer cells and CAFs.

5.2. Methods

5.2.1. Taqman array for Wnt pathway

In order to investigate the Wnt pathway gene expression profile for PDAC cancer cells compared with normal pancreas ductal (HPDE) cells a human Wnt pathway TaqMan

Array plate (Applied Biosystems) was used. The array plate contained 92 Wnt associated genes (*APC, AXIN1, AXIN2, BTRC, CSNK1A1, CSNK1D, CSNK1G1, CSNK1G2, CSNK1G3, CSNK2A1, CSNK2A2, CSNK2B, CTNNB1, CTNNBIP1, CXXC4, DACT1, DKK1, DKK2, DKK3, DKK4, DVL1, DVL2, DVL3, EP300, FBXW11, FGF4, FOXN1, FRAT1, FRAT2, FRZB, FZD1, FZD10, FZD2, FZD3, FZD4, FZD6, FZD7, FZD8, FZD9, GSK3A, GSK3B, KREMEN1, KREMEN2, LEF1, LRP5, LRP6, MYC, NKD1, NLK, CBY1, PITX2, PORCN, PPP2CA, PPP2R1A, PYGO1, PYGO2, RHOU, SENP2, SFRP1, SFRP2, SFRP4, SFRP5, SLC9A3R1, TCF7, TCF7L1, TCF7L2, TLE1, TLE2, TLE3, TLE4, TLE6, WIF1, WISP1, WNT1, WNT10A, WNT10B, WNT11, WNT16, WNT2, WNT2B, WNT3, WNT3A, WNT4, WNT5A, WNT5B, WNT6, WNT7A, WNT7B, WNT8A, WNT8B, WNT9A, WNT9B*) and 4 control genes (*18S, GAPDH, GUSB* and *HPRT1)* in duplicate. The genes included in this array are mainly from the vertebrate Wnt family of associated genes including inhibitors of the Wnt pathway including secreted frizzled related proteins and the Disheveled family. RNA was isolated from flasks once the cells reached 80% confluence which had been cultured in complete growth medium, the RNA was quantified and reverse transcription performed on the total RNA samples. The cDNA was diluted with a volume of DNase free water to a concentration of 1ng/μL which corresponds to 10ng/reaction. The array plate was centrifuged at 1000rpm for 2min, each well was loaded with 10μL of cDNA and 10μL of mastermix. The mastermix used was TaqMan Fast Universal PCR Master Mix (2X), no AmpErase UNG (AppliedBiosystems). The fluorophore used with TaqMan was carboxyfluorescein (FAM). The expression profiles of the pancreatic cancer cell lines (PANC1, MIAPACA2 and BXPC3) were compared with the ductal cell line HPDE as a control. The expression profiles of 3 CAF lines were compared with 3 NAF lines using normal pancreatic fibroblasts (NPF) as a control.

5.2.2. L-Wnt-3A conditioned medium

L-Wnt-3A is a mouse fibroblast cell line which constitutively produces Wnt-3A (Willert et al., 2003). The cells were produced by the transfection of L-M(TK-) cells with the Wnt-3A expression vector. The secretion of Wnt ligands depends on their palmitoylation, a post translation modification which is required for Wnt ligand to be effectively trafficked out of the cell (Mikels and Nusse, 2006). This palmitoylation step is catalysed by the o-acetyl-transferase Porcupine (PORCN) (Voloshanenko et al., 2013). Wnt secretion can be inhibited in the donor cells by inhibition of PORCN using Redx small molecule inhibitors. In order to generate L-Wnt-3A conditioned medium (CM) 1 million cells per T75 flask were seeded. Two flasks were seeded: one was seeded in L-Wnt-3A culture medium (DMEM, 4.5g/mL glucose, 10% FBS, 1% Geneticin) with 0.1% DMSO, and the other was seeded in L-Wnt-3A culture medium with 100nM Redx compound F. An empty flask was also filled with culture medium and incubated with the other flasks for 72h to generate control media, at which point the L-Wnt-3A cells had reached 80% confluency. The CM was removed from the cells and centrifuged at 400g for 5min, and then sterile filtered using a 2µm filter. This CM was then added to PDAC cancer cell lines, CAFs and NAFs which had been seeded at 50,000 cells per well in 6-well plates 24h previously. The RNA was isolated after the cells had been incubated with CM for 24h. Changes in *AXIN2* level were measured using qRT-PCR. To determine if the effect of the CM was concentration-dependent the stock amount was diluted with fresh growth media to the following concentrations: 25%, 50%, 75% and 100% CM.

5.2.3. Transwell co-culture for Wnt pathway activation

The optimal ratio of PDAC cells to CAFs found to cause an activation of Wnt pathway was a 1:2 ratio for 72h. An empty 6-well plate was filled with 2mL per well of growth medium, the Transwell inserts were added and 100,000 PANC1 cells or 50,000 CAFs were loaded onto the insert in 2 mL of media. In the empty Transwell plate 100,000

PANC1 cells or 50,000 CAFs were seeded in 2mL of growth medium, and the cells were allowed to adhere overnight. Cells in the Transwell plate were serum starved for 24h. At this point all the media was removed from both Transwell plate and inserts and the inserts were placed in their corresponding wells (Table 5.1.) and the wells were filled with 3mL of medium (5% Serum IMDM) . To investigate the effect of a Transwell co-culture model on Wnt pathway activation in CAFs and PANC1s in this model RNA was isolated from all chambers after 72h.

Top	CAF 50,000cells	PANC1 100,000cells	PANC1 100,000cells
Bottom	CAF 50,000cells	CAF 50,000 cells	PANC1 100,000cells

Table 5.1. Platemap of Transwell co-culture model

5.2.3. Wnt pathway inhibition in a Transwell co-culture model

Using the Transwell co-culture model developed above, it was possible to investigate how effective a Redx PORCN inhibitor would be at inhibiting canonical Wnt signalling in a model which allowed paracrine signalling between PDAC cells and CAFs. The method used is described above with the addition of 0.1% DMSO to all wells. Table 5.2. shows the platemap used.

Top	PANC1 100,000cells 1000nM Redx PORCN Inhibitor	PANC1 100,000 cells	PANC1 100,000 cells
Bottom	CAF 50,000 cells 1000nM PORCN Inhibitor	CAF 50,000 cells	PANC1 100,000 cells

Table 5.2. Platemap of Transwell co-culture model with Redx PORCN inhibitor

5.3. Results

5.3.1. β-Catenin Expression in the PDAC tumour microenvironment

To investigate the presence of active canonical Wnt signalling in the PDAC tumour microenvironment IHC analysis was performed (method described in Section 2.2.4.4.) to determine the location of β-Catenin in the PDAC tumour microenvironment compared to normal pancreatic tissue. In the normal pancreas β-Catenin forms part of the E-cadherin-catenin complex which maintains the intracellular adhesion which is believed to be disrupted during pancreatic tumorigenesis (Li and Ji, 2003). Consistent with previous reports β-Catenin is localised to the cell membrane of normal pancreatic acini (Figure 5.1.B) which undergoes redistribution to cytoplasmic and nuclear location in epithelial cancer cells (Figure 5.1.A&C) (Zeng et al., 2006, Pasca di Magliano et al., 2007).

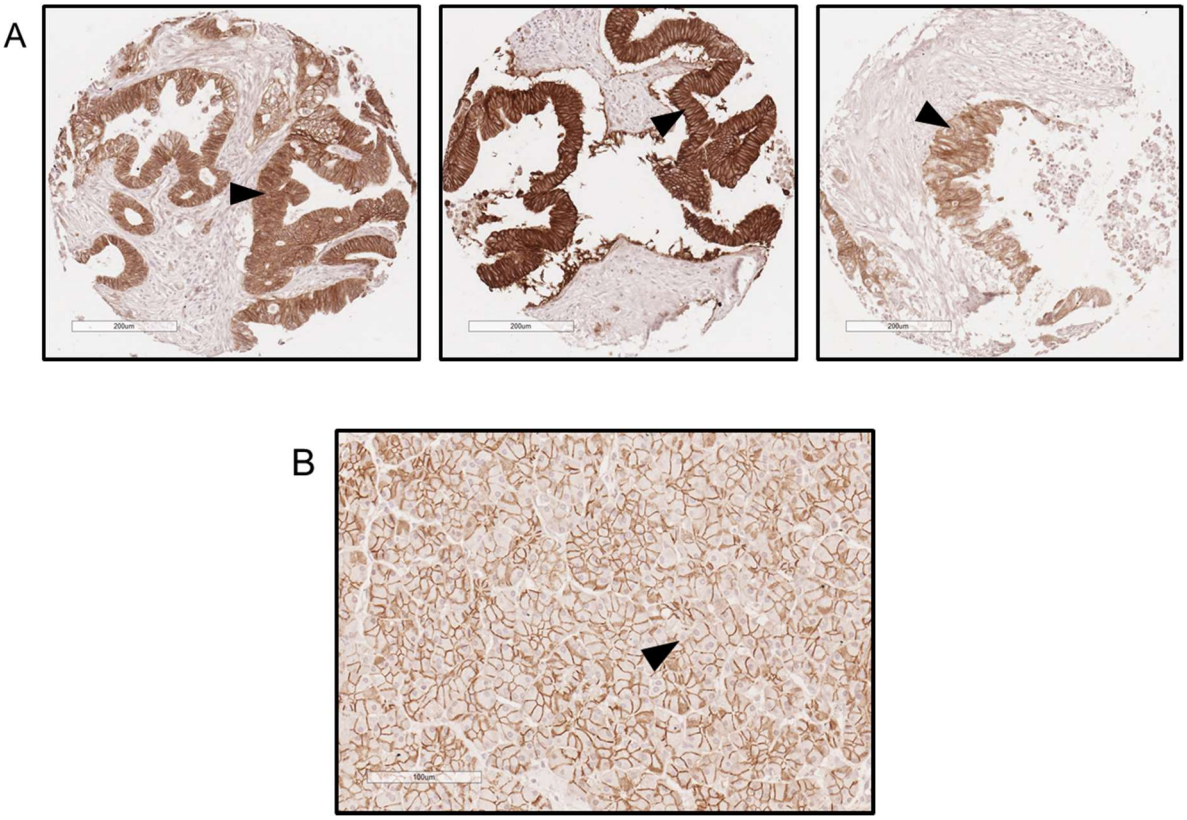

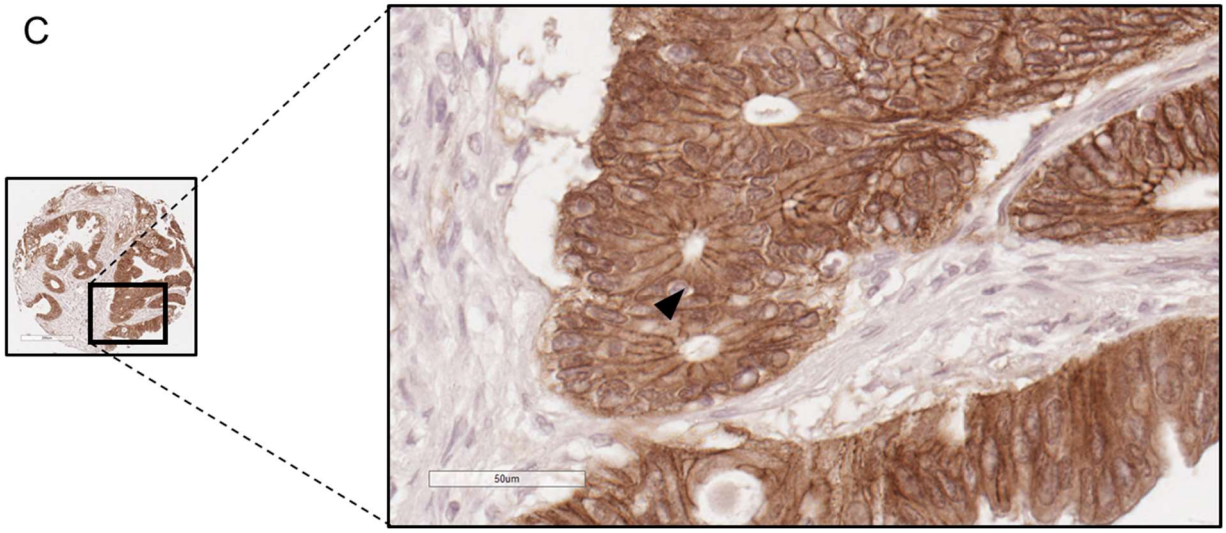

Figure 5.1. β-Catenin staining in the PDAC tumour microenvironment

A: IHC of tumour cores stained for β-Catenin showing that positive staining is restricted to tumour cells. (black arrows). Scale bar 200μm **B**: Representative image of tissue isolated from normal appearing tissue stained using IHC for β-Catenin. The staining appears to be found restricted to the cell membrane of the normal pancreatic acini (black arrow).Scale bar 100μm **C**: Higher magnification image of tumour core (40x) showing the localisation of β-Catenin in the cell membrane and cytoplasm of tumour cells (black arrow).Scale bar 50μm.

5.3.2. Expression of Wnt Signalling associated genes in pancreatic cancer cell lines

Unlike the Hh pathway the role of the Wnt pathway in PDAC tumorigenesis is not well understood. I sought to determine if any pattern of gene expression was common to pancreatic cancer cell lines to elucidate the role of PDAC tumour cells in canonical Wnt signalling. 3 pancreatic cancer cell lines were chosen for this study: PANC1, MIAPACA2 and BXPC3. Their expression of genes associated with Wnt signalling was compared with a normal pancreatic ductal cell line HPDE. There did not appear to be a clear pattern of Wnt associated genes commonly expressed in all three cancer cell lines investigated (Figure 5.2.). These well characterised cell lines were chosen to represent patient variation as they have diverse genetic origins (Table 2.1.) however this could also be responsible for the differences in expression of Wnt associated genes. Wnt ligands associated with both canonical and non-canonical Wnt

pathways were found to be upregulated in the PDAC cell lines (Figure 5.2.). Wnt5B was upregulated in PANC1 (38.2-fold) and unchanged in MIAPACA2 (1.2-fold) and BXPC3 (0.56-fold) when compared to the HPDE control. A threshold of ±4-fold was recommended in the manufacturers guide to identify biologically significant changes using this array format. Wnt10A was found to be upregulated in BXPC3 (22.9-fold) and PANC1 cells (7.5-fold) and unchanged in MIAPACA2 cells (0.4-fold). Wnt11 was found to be upregulated in BXPC3 (17.7-fold) and PANC1 cells (5.6-fold) and downregulated in MIAPACA2 cells (0.02-fold) (Figure 5.2.). Wnt4 was upregulated in BXPC3 (40.9-fold) and PANC1 cells (4.7-fold) and was unchanged in MIAPACA2 cells (0.83-fold). LRP5 was upregulated in PANC1 (8.3-fold) and BXPC3 cells (5.9 fold) and unchanged in MIAPACA2 cells (0.4-fold).

A larger sample size including of representative PDAC cells would be required to determine if any Wnt signalling pathway component expression is common to PDAC. Nevertheless, unlike the findings in Hh pathway components (Section 4.3.2) the data presented in Figure 5.2. suggests that there is no universal PDAC expression profile for Wnt pathway components.

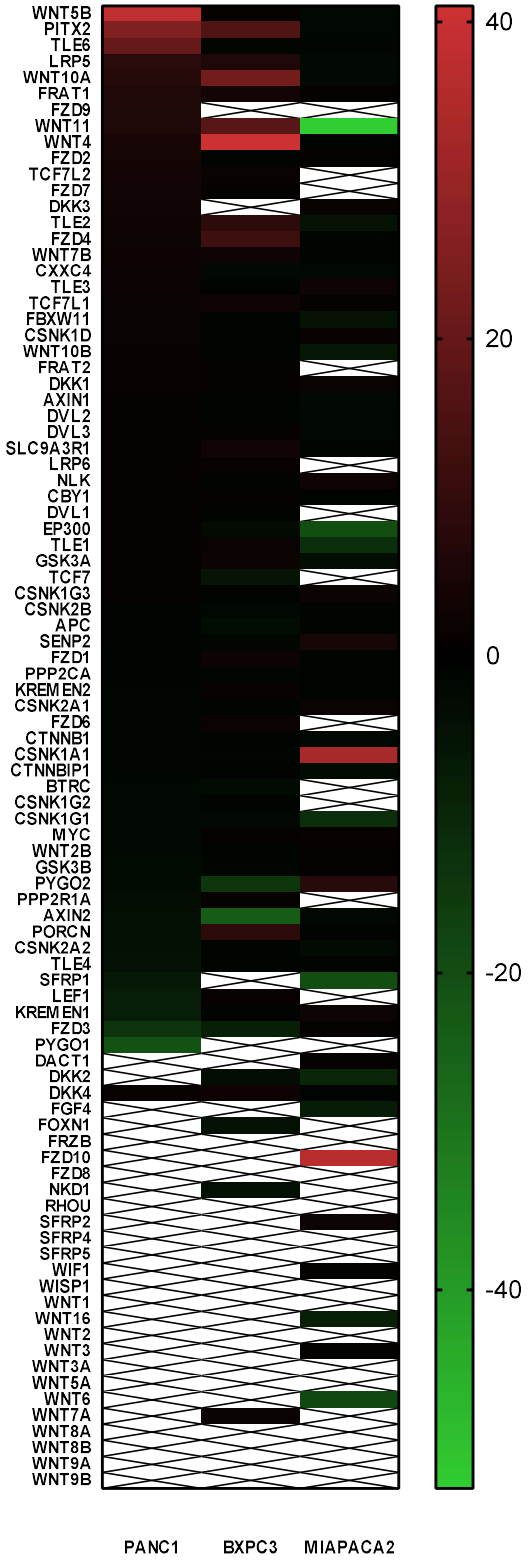

Figure 5.2. Differentially expressed WNT signalling genes in pancreatic cancer cell lines

Differentially expressed genes involved in WNT Signalling in 3 pancreatic cancer cell lines (PANC1, BXPC3 and MIAPACA2) using a normal ductal cell line as a control (HPDE). Gene expression profiles were obtained by Taqman mini array. Upregulation of genes of interest is indicated by red colour, downregulation is shown using green.

5.3.3. Expression of Wnt Signalling associated genes in pancreatic CAFs and NAFs

Having established that there was no consensus secretion of Wnt ligand or expression of Fzd receptors in pancreatic cancer cell lines the next step was to determine if there were any differentially expressed Wnt associated genes between CAFs isolated from the PDAC tumour microenvironment and NAFs isolated from normal appearing tissue.

22 genes were found to be differentially regulated in CAFs compared with NAFs (N=3) (Figure 5.3.), including Wnt signalling pathway components such as *AXIN2, LEF1* and *LRP5. FZD3 and FZD9* were also found to be upregulated which indicates the ability of CAFs to respond to Wnt ligands. *SFRP4* and *FRZB* were also found to be upregulated in CAFs 249-fold and 8-fold respectively (Table 5.1.). *DKK1,* an antagonist of the Wnt pathway was also found to be downregulated in CAFs 0.1-fold compared to 0.4-fold in NAFs. DKK1 has two mechanisms of action depending on whether it is antagonising canonical or non-canonical Wnt signalling. Canonical Wnt signalling was the focus of this project due to the presence of cytoplasmic and nuclear accumulation in early PDAC lesions (PanIN) right through disease progression (Al-Aynati et al., 2004, Zeng et al., 2006, Pasca di Magliano et al., 2007) . It has also been suggested that levels of β-Catenin accumulation also correlates with PanIN grade (Al-Aynati et al., 2004) . A more functional role for canonical Wnt signalling in PDAC tumour maintenance and progression has been suggested whereby increased Wnt signalling is associated with increased tumour cell survival (Pasca di Magliano et al., 2007). However, the presence of non-canonical Wnt ligand such as Wnt5a, commonly abberant in PDAC, indicates non-canonical Wnt signalling may also have a role in PDAC development (Pilarsky et al., 2008).

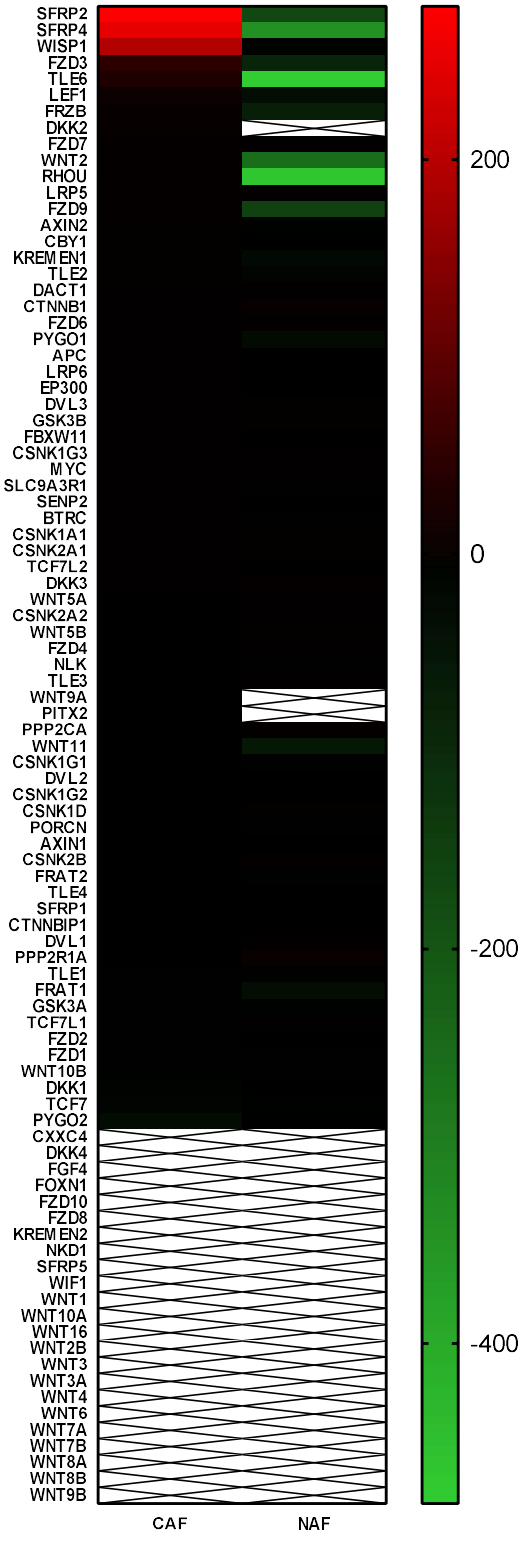

Figure 5.3. Differentially expressed Wnt/ β-Catenin genes in CAFs vs NAFs

Differentially expressed genes in CAFs and NAFs using a normal pancreatic fibroblast line as a control fibroblast line, gene expression profiles were obtained by Taqman mini array. Upregulation of genes of interest is indicated by red colour, downregulation is shown using green. CAF lines used (R3030, R3088, R3072), NAF lines used (R2796, R2797, R2951).

Gene	P value	CAF Mean	NAF Mean	Difference	q value
SFRP4	4.2E-11	249.7	-340.1	589.9	4.6E-10
RHOU	1.6E-10	3.9	-464.7	468.6	1.4E-09
FZD3	3.3E-09	48.2	-88.0	136.2	2.4E-08
FZD9	4.4E-09	3.3	-154.3	157.6	2.7E-08
WISP1	2.2E-08	194.5	-7.5	202.0	1.2E-07
PYGO1	3.4E-08	1.6	-24.1	25.7	1.6E-07
WNT11	1.2E-07	-0.1	-54.6	54.5	5.1E-07
FRZB	1.4E-07	7.9	-73.0	80.9	5.1E-07
LEF1	1.4E-07	12.7	-32.5	45.2	5.1E-07
PPP2R1A	1.6E-06	-2.2	9.2	-11.4	5.3E-06
DKK1	8.9E-06	-8.6	-2.3	-6.3	2.8E-05
KREMEN1	5.0E-05	2.8	-22.1	25.0	1.5E-04
AXIN2	5.8E-05	3.3	-6.3	9.6	1.6E-04
PYGO2	6.5E-05	-28.3	-1.2	-27.0	1.7E-04
NLK	9.7E-04	0.1	-4.0	4.1	2.3E-03
DVL1	1.0E-03	-1.9	2.1	-4.1	2.3E-03
DKK3	2.0E-03	1.1	5.4	-4.3	4.4E-03
FZD7	2.4E-03	4.9	1.7	3.3	4.6E-03
CSNK1G1	2.4E-03	-0.1	-2.6	2.5	4.6E-03
CSNK2B	3.3E-03	-1.5	4.8	-6.3	6.2E-03
LRP5	3.7E-03	3.4	1.4	1.9	6.7E-03
TCF7	3.9E-03	-13.7	-6.7	-6.8	6.7E-03

Table 5.1. Summary of differentially expressed genes in CAFs vs NAFs

Differentially expressed genes in CAFs and NAFs using a normal pancreatic fibroblast line as a control fibroblast line, gene expression profiles were obtained by Taqman mini array. The discovery analysis Benjamini, Krieger and Yekutieli (with Q = 1%) was used to identify differentially expressed genes

These data suggest that, unlike the Hh pathway, no clear donor/acceptor role for paracrine signalling exists between CAFs and PDAC cancer cells. Therefore I sought to determine if CAFs and PDAC cancer cells were susceptible to exogenous Wnt ligand stimulation

5.3.4. Wnt pathway activation in pancreatic cells in response to Wnt stimulus

Wnt pathway stimulation was achieved using an L-Wnt-3A cell line (Willert et al., 2003). This method was chosen over the use of recombinant Wnt ligands due to inconsistencies which have been reported in the use of commercially available Wnt-3A due to misfolded or proteolytically cleaved protein products (Cajanek et al., 2010).

Changes in *AXIN2* mRNA induction were used to investigate Wnt/ β-Catenin signalling activity; *AXIN2* is commonly used to determine Wnt pathway activity as it has been found to be induced by Wnt ligands (Jho et al., 2002). It was possible to detect significant changes in response to CM from L-Wnt-3A cells in CAF, NPF and PANC1 cells (Figure 5.4.). Different concentrations of L-Wnt-3A CM was used to investigate whether the *AXIN2* response in cells was concentration-dependant and if there was any detrimental effect on *AXIN2* induction by using undiluted CM which was potentially nutrient depleted after 72h in culture with L-Wnt cells. The response observed in CAFs was concentration-dependant with the maximal induction of *AXIN2* when CAFs were exposed to 100% CM from L-Wnt-3A cells (fold change: 73.0±12.8, p=0.0003). NPF cells had a maximal AXIN2 induction with 75% CM (fold change: 17.3±1.7, p<0.0001). PANC1 cells had a maximal *AXIN2* induction with 50% CM (fold change: 28.3±3.0, p=0.0001). The effect of nutrient deprivation on Wnt signalling was most apparent in PANC1 cells. These cells had the greatest induction of *AXIN2* mRNA in CM which was diluted with 50% fresh growth medium. This is most likely related to the fact that the population doubling time of PANC1 cells is much quicker than the CAFs and NPFs (approximately 40, 72 and 72-96h respectively) which suggests they are more metabolically active and require more nutrients.

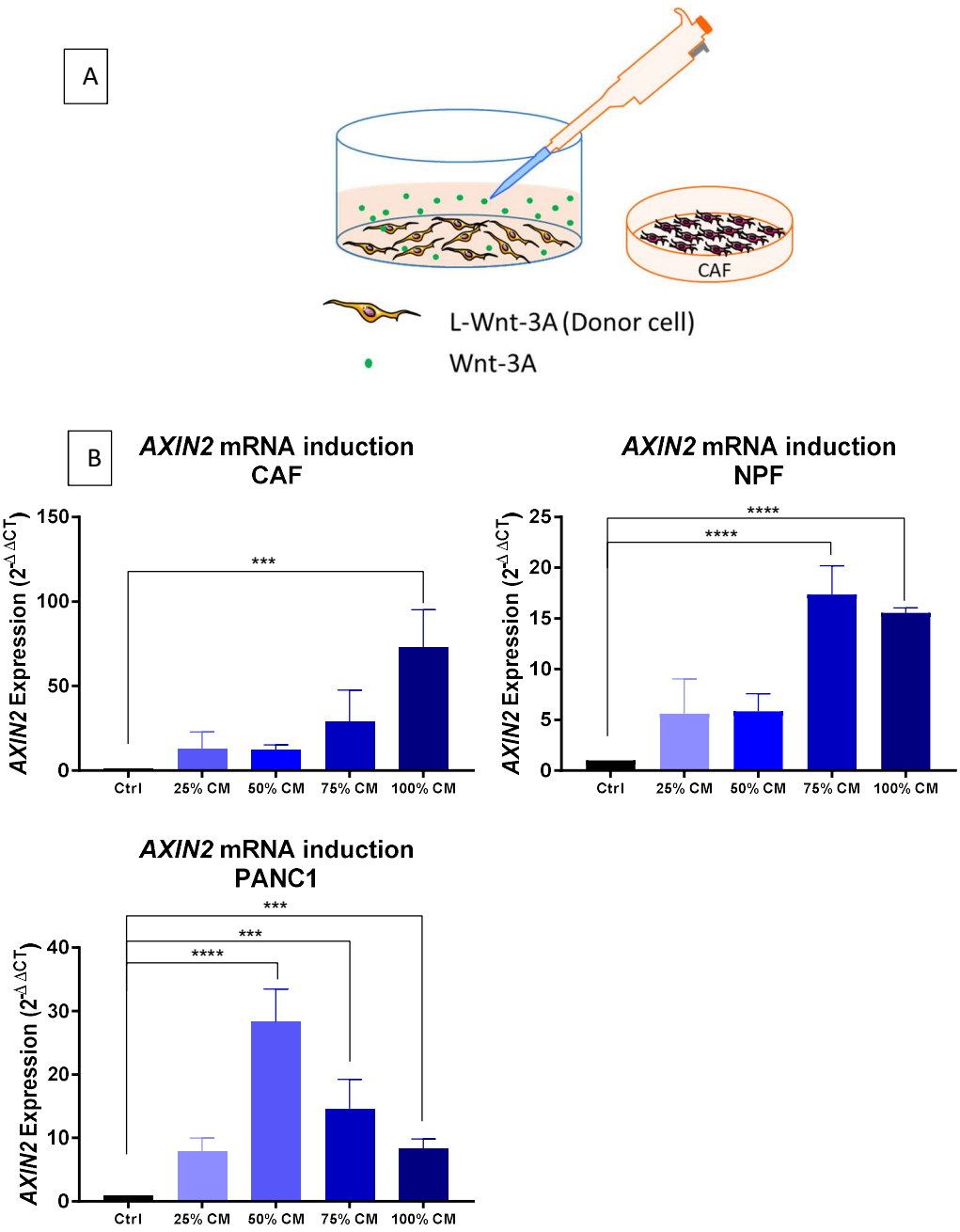

Figure 5.4. Induction of *AXIN2* mRNA in PANC1, CAF and NPF in response to conditioned medium from L-Wnt-3A cells

A: Schematic of assay setup

B:Graphs showing *AXIN2* expression (RT-PCR) in CAF, NPF and PANC1 cells exposed to conditioned media (DMEM supplemented with 10% FBS) from L-Wnt-3A cells either undiluted, or diluted with fresh media. Gene expression was normalised to *GAPDH* and compared to expression of *AXIN2* in CAF, NPF and PANC1 cells cultured in DMEM (10% FBS incubated in an empty flask). Each bar represents the $^{\Delta\Delta}$Ct gene expression of 3 experiments using the 3 different CAF lines (R3088, R3072 and R3030) or 3 different experiments (NPF, PANC1) Statistical significance was determined using an ordinary one way ANOVA

Given that it was possible to activate Wnt signalling in CAFs, NPFs and PANC1 cells, I sought to determine whether it was possible to reduce this activation using a Redx PORCN inhibitor (Redx Compound F) in PDAC cancer cell lines. PORCN is a protein involved in the post translational modification of Wnt ligands which is required for their successful secretion from Wnt producing cells (Takada et al., 2006). Inhibition of PORCN has resulted in effective inhibition of Wnt signalling which has highlighted PORCN as an important target in oncology (Liu et al., 2013) . The induction of *AXIN2* mRNA in PANC1 cells when they were exposed to CM from L-Wnt-3A cells and the vehicle (0.1% DMSO) was 8.3±0.9-fold (p=0.0002) upregulation which decreased to 1.1±0.5-fold in the presence of a Redx PORCN inhibitor. This loss of AXIN2 induction was also observed in MIAPACA2 (fold change: 5.5±0.5 decreased to 1.4± 0.2, p=0.0001) and BXPC3 cells (fold change: 42.6±10.9 decreased to 1.8±0.4, p=0.0085) (Figure 5.5.).

A

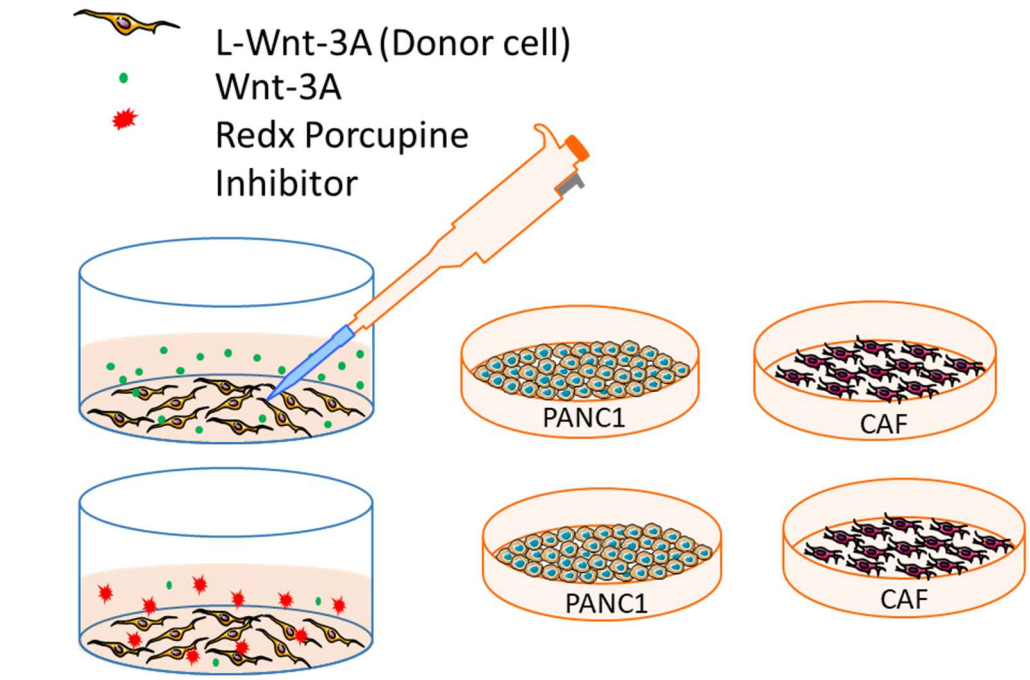

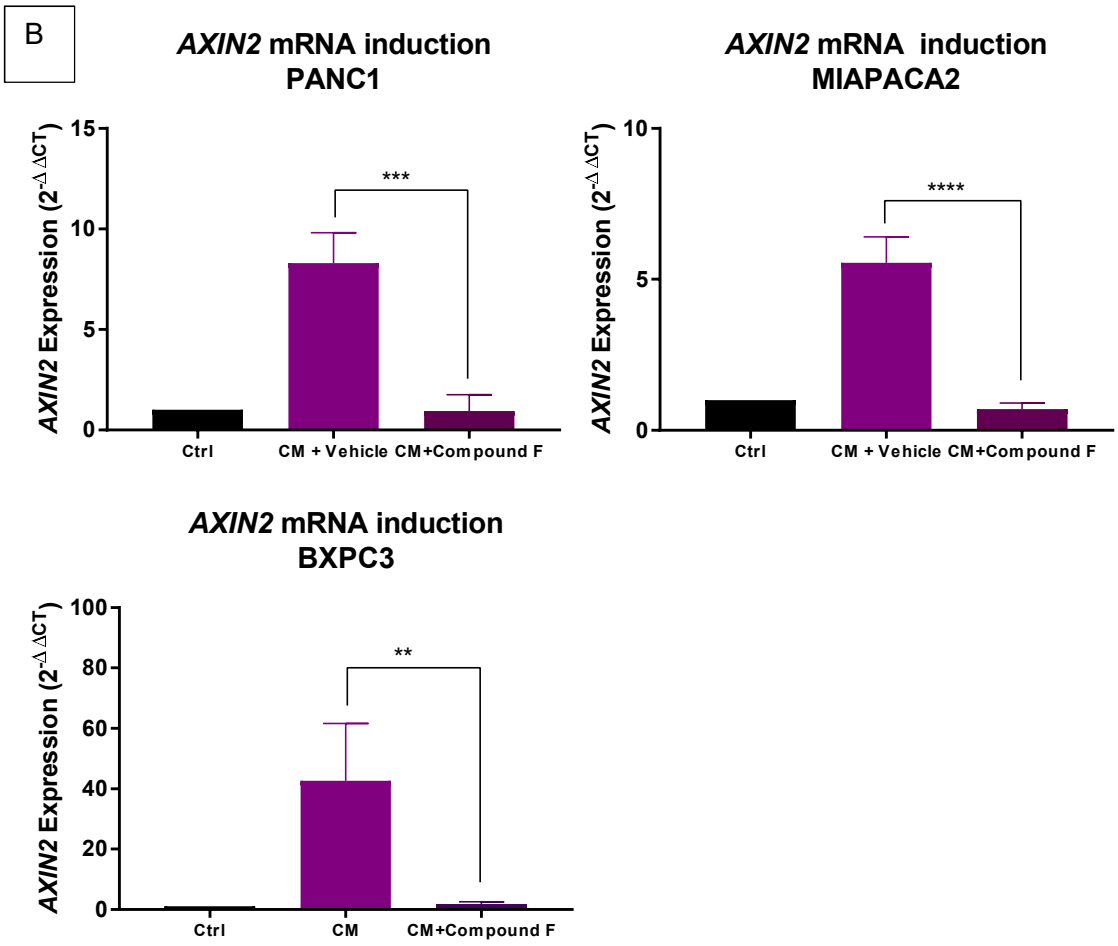

Figure 5.5. *AXIN2* mRNA induction in pancreatic cancer cell lines in the presence of conditioned medium from L-Wnt-3A cells and a Redx PORCN inhbitor

A: Schematic representation of assay setup

B: Graphs showing *AXIN2* expression (RT-PCR) in PANC1, MIAPACA2 and BXPC3 cells exposed to 100% CM (DMEM 10% FBS) from L-Wnt-3A cells in the presence or absence (Vehicle 0.1% DMSO) or Redx PORCN inhibitor. Gene expression was normalised to GAPDH and compared to the expression of *AXIN2* in PANC1, MIAPACA2 and BXPC3 cultured in (DMEM 10% FBS, conditioned in an empty flask). Each bar represents the $^{\Delta\Delta}$Ct gene expression of 3 experiments. Statistical significance was determined using an ordinary one way ANOVA.

It was established that the PDAC cell lines tested had different levels of *AXIN2* induction in response to CM from L-Wnt-3A cells and regardless of the level of *AXIN2* induction, it was reduced in the presence of Redx PORCN inhibitors. I therefore sought to determine whether CAFs and NAFs had a similar response to exogenous Wnt ligand provided by the L-Wnt-3a cells and whether this could be reduced by the presence of Redx PORCN inhibitors. There was a marked difference between the

activation of Wnt pathway in CAFs compared to NAFs. In CAFs induction of *AXIN2* in the presence of CM from L-Wnt-3A cells (vehicle 0.1% DMSO) was 73.0±12.8-fold which was reduced to 13.9±8.2-fold (p=0.0073) in the presence of a Redx PORCN inhibitor. In NAFs induction of AXIN2 in the presence of CM from L-Wnt-3A cells (vehicle 0.1% DMSO) was 16.9±5.2-fold which was reduced to 2.8±1.1-fold in the presence of a Redx PORCN inhibitor (Figure 5.6.).

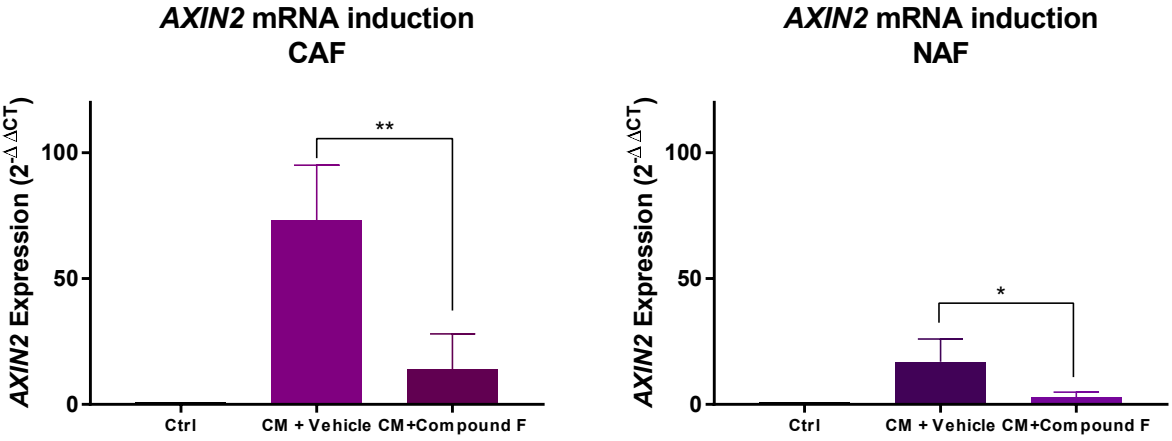

Figure 5.6. Differing Induction of *AXIN2* mRNA CAF and NAF in response to conditioned medium from L-Wnt-3A cells

Graphs showing *AXIN2* expression (RT-PCR) in CAFs and NAFs exposed to 100% CM (DMEM 10% FBS) from L-Wnt-3A cells in the presence or absence (Vehicle 0.1% DMSO) or Redx PORCN inhibitor. Gene expression was normalised to GAPDH and compared to the expression of *AXIN2* in CAFs and NAFs cultured in (DMEM 10% FBS, conditioned in an empty flask). Each bar represents the $^{\Delta\Delta}$Ct gene expression of 3 cell lines (CAF: R3088, R3030, R3072) (NAF; R2797, R2796, R2951). Statistical significance was determined using an ordinary one way ANOVA.

It was determined that there was a significant difference in response to Wnt stimulus depending on whether the cells had been isolated from either the PDAC microenvironment (CAFs) or normal appearing tissue (NAFs). NAFs had a similar induction of *AXIN2* (16.9-fold, Figure 5.6.) to NPF cells (17.3-fold, Figure 5.4) which indicated that NAFs more closely resemble the NPF cell line. In order to investigate the response of other Wnt associated genes the induction of *LEF1* was examined. Lymphoid enhancing binding factor 1 (LEF1) is a transcriptional promoter which forms

a complex with β-Catenin in the nucleus, which stimulates the transcriptional activation of Wnt target genes (Komiya and Habas, 2008). *LEF1* expression has been found to be increased in the presence of active Wnt signalling (Planutiene et al., 2011, Filali et al., 2002) . There was found to be a significant induction of *LEF1* mRNA in NPF cells in response to L-Wnt-3A when exposed to 100% CM. There was a 4.2±0.4 ($p=0.0016$)-fold upregulation of *LEF1* mRNA (Figure 5.7.). Treatment with a Redx PORCN inhibitor also reduced the induction of LEF1 in NPF's from 4.9±0.3-fold to 2.0±0.4-fold upregulation ($p=0.005$, Figure 5.7.).

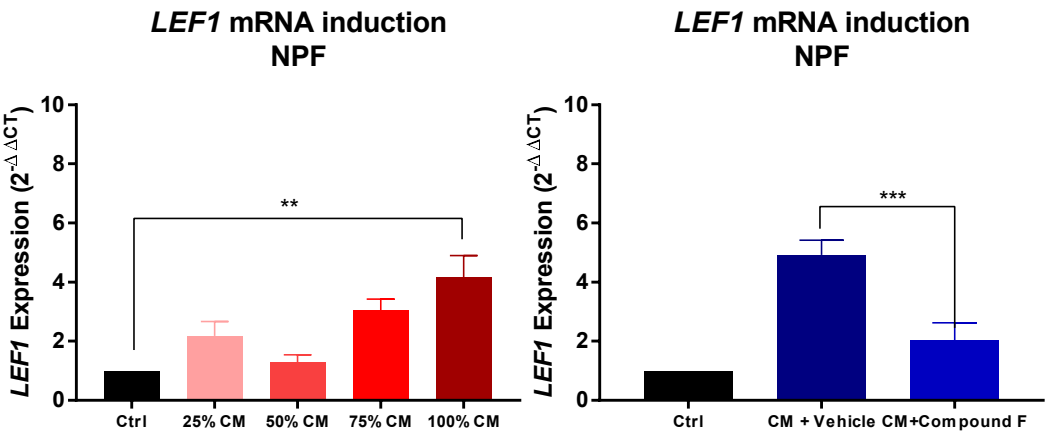

Figure 5.7. Induction of *LEF1* mRNA in NPF in response to conditioned medium from L-Wnt-3A cells and the effect of PORCN inhibition on LEF induction

Graphs showing *LEF1* expression (RT-PCR) in NPF cells exposed to CM (DMEM 10% FBS) from L-Wnt-3A cells either diluted with fresh growth media (DMEM 10% FBS)(left panel). Graphs showing *LEF1* expression (RT-PCR) in NPF cells exposed to CM (DMEM 10% FBS) from L-Wnt-3A in the presence or absence (Vehicle 0.1% DMSO) or Redx PORCN inhibitor (right panel). Gene expression was normalised to GAPDH and compared to the expression of *LEF1* in NPFs cultured in (DMEM 10% FBS, conditioned in an empty flask). Each bar represents the $^{\Delta\Delta}$Ct gene expression of 3 experiments. Statistical significance was determined using an ordinary one way ANOVA.

5.3.5. Transwell co-culture model of CAFs and PANC1 cells

Having established that both pancreatic fibroblasts and pancreatic cancer cell lines responded to exogenous Wnt signal provided by L-Wnt-3A cells, I sought to investigate whether culturing CAFs and pancreatic cancer cell lines in the same well resulted in an induction in Wnt signalling. At 24h and 48h a 1:1 or 1:2 ratio of PANC1:CAF cells did not result in an induction of either *AXIN2* or *LEF1* (Figure 5.8.). At 72h using a 1:1 ratio there was an induction of AXIN2 (4.8±2.2-fold) and LEF1 (3.3±2.1-fold)(Figure 5.8.). Using a 1:2 ratio of PANC1:CAF there was a greater induction of *AXIN2* (10.9±1.9 fold), however there was no change in *LEF1* mRNA (Figure 5.8.)

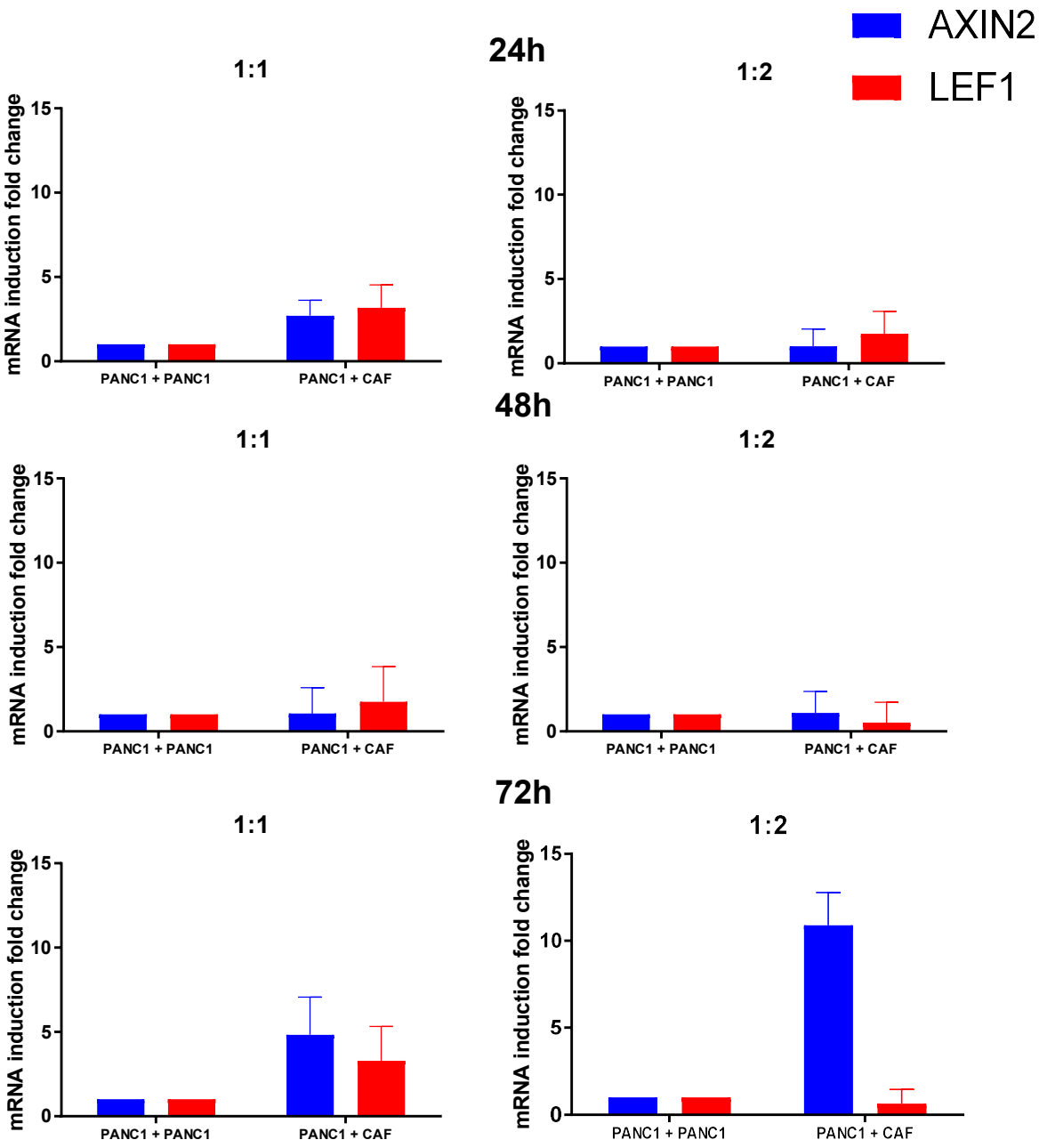

Figure 5.8. Upregulation of Wnt signalling pathway in PANC1 cells in a Transwell co-culture model

Graphs showing *AXIN2* and *LEF* expression (RT-PCR) in PANC1 cells cultured in the same well as CAFs cells at either 1:1 ratio or 1:2 (PANC1:CAF) ratio for 24, 48 and 72h. Each bar represents the $^{\Delta\Delta}$Ct gene expression of 1 experiments using 2 replicates. Statistical analysis was not performed as this was a preliminary optimisation experiment and was not replicated in multiple CAF lines.

This model was used to investigate whether induction of *AXIN2* mRNA in PANC1 cells in response to being cultured with CAFs could be reduced using a Redx PORCN

inhibitor. It was found that addition of the Redx PORCN inhibitor to a Transwell co-culture model of PANC1 cells and CAFs reduced the induction of AXIN2 mRNA from 7.1±0.7-fold to 1.7±0.8fold upregulation (Figure 5.9, p=0.0011).

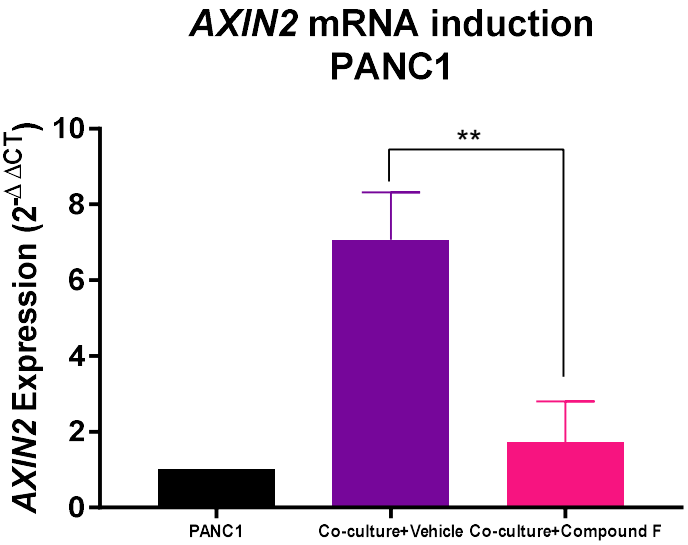

Figure 5.9. Loss of *AXIN2* induction in PANC1 cells in a Transwell co-culture model when treated with Redx PORCN inhibitor (Compound F)

Graphs showing *AXIN2* expression (RT-PCR) in PANC1 cells cultured in a Transwell with CAFs presence or absence (Vehicle 0.1% DMSO) or Redx PORCN inhibitor. Gene expression was normalised to GAPDH and compared to the expression of *AXIN2* in PANC1. Each bar represents the $^{\Delta\Delta}$Ct gene expression in PANC1 cells of 3 experiments carried out with three independent CAF lines (CAF: R3088, R3030, R3072)). Statistical significance was determined using an ordinary one way ANOVA.

There was a marked upregulation of *AXIN2* mRNA in response to being cultured in the same well as CAFs, I therefore sought to investigate whether there was any impact on Wnt signalling in CAFs when they were cultured with MIAPACA2 and PANC1 cells. As it had been previously established that both PDAC cancer cell lines and CAFs were responsive to exogenous Wnt ligand (Figure 5.4, Figure 5.5 and Figure 5.6.). There was found to be no upregulation of *AXIN2* in CAFs in response to being co-cultured in a Transwell with PANC1 or MIAPACA2 cells (Figure 5.10). However, *PORCN* mRNA was significantly upregulated in CAFs in a Transwell co-culture with PANC1 cell lines which indicates an upregulation of Wnt secretion (3.9±0.6-fold, p=0.0018, Figure 5.10.). This suggests that Wnt signalling is occurring

in a paracrine fashion in this model with Wnt ligand being secreted from CAFs and activating downstream Wnt signalling in PANC1 cells.

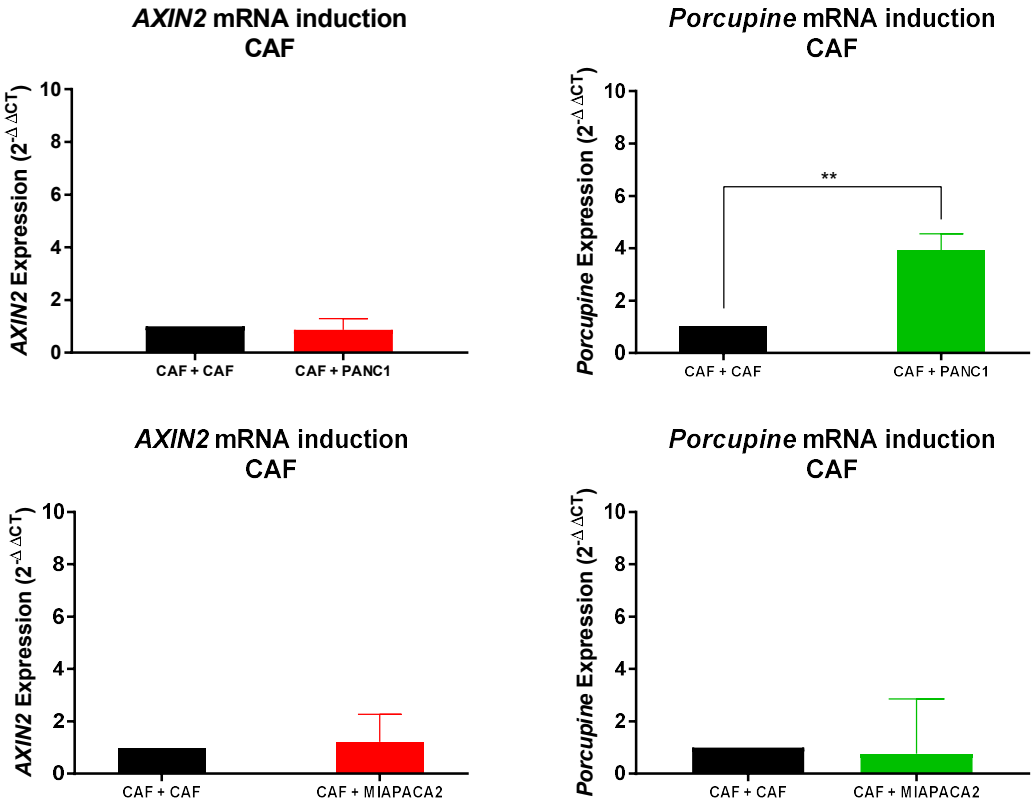

Figure 5.10. Induction of *PORCN* in CAFs when co-cultured with PANC1 cells in a Transwell model

Graphs showing *AXIN2 and PORCN* expression (RT-PCR) in CAFs cultured in a Transwell with PANC1 or MIAPACA2 cells. Gene expression was normalised to GAPDH and compared to the expression of *AXIN2* in CAFs cultured alone. Each bar represents the $^{\Delta\Delta}$Ct gene expression in CAFs (3 independent CAF lines: R3088, R3030, R3072)). Statistical significance was determined using an ordinary one way ANOVA

Using the Taqman mini array for Wnt/ β-Catenin signalling it had been established that there was a significant upregulation of *SFRP4* mRNA in CAFs compared with NAFs (Figure 5.3, Table 5.1), therefore the effect of a Transwell co-culture model on the mRNA of these genes was investigated. *SFRP1* and *SFRP4* mRNA was upregulated (3.55±1.11-fold) and (15.4±0.4-fold) in CAFs when they were cultured with PANC1 cells (Figure 5.11.). There was no induction of *SFRP1* and *SFRP4* when CAFs were cultured with MIAPACA2 cells (Figure 5.11.).

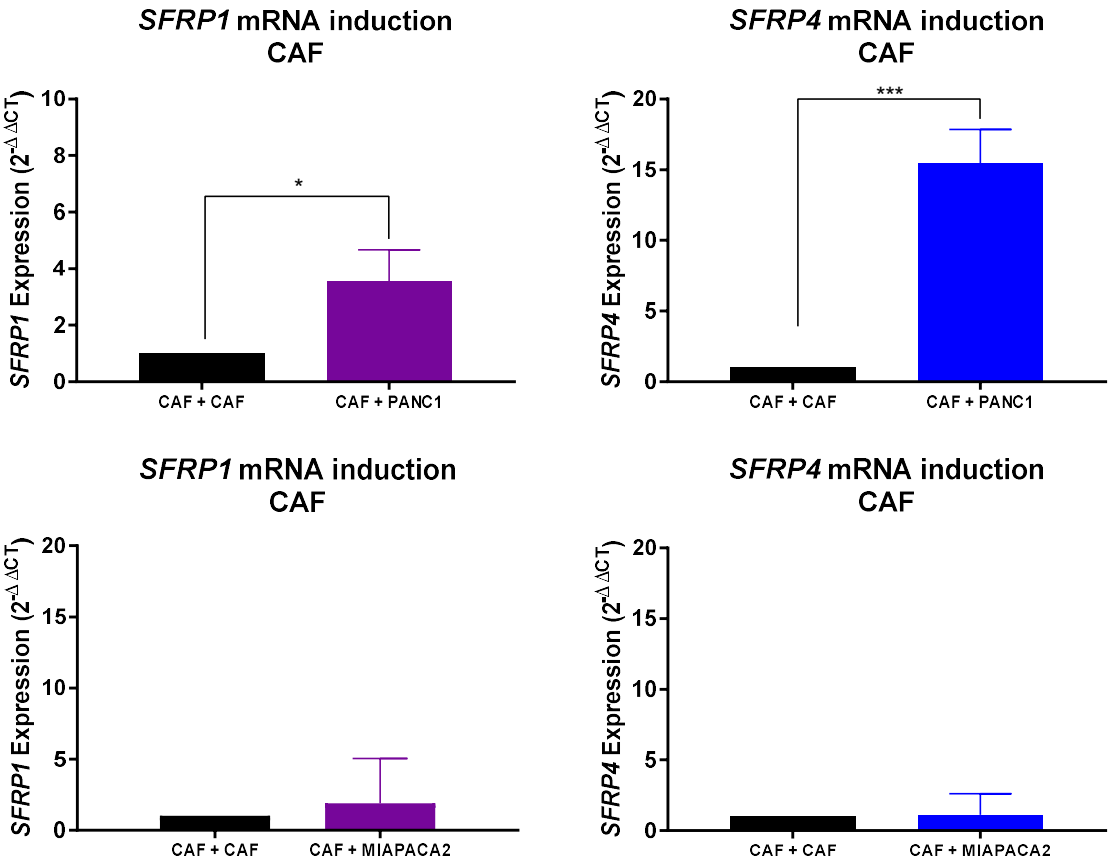

Figure 5.11. Induction of *SFRP1 and SFRP4* in CAFs when cultured with PANC1 cells in a Transwell co-culture model

Graphs showing *SFRP1 and SFRP4* expression (RT-PCR) in CAFs cultured in a Transwell with PANC1 or MIAPACA2 cells. Gene expression was normalised to GAPDH and compared to the expression of *AXIN2* in CAFs cultured alone. Each bar represents the $^{\Delta\Delta}$Ct gene expression in CAFs (3 independent CAF lines: R3088, R3030, R3072)). Statistical significance was determined using an ordinary one way ANOVA

5.3.6. DKK1 secretion by CAFs and pancreatic cancer cell lines

DKK1, an antagonist of Wnt pathway, was found to be downregulated in CAFs (Figure 5.3, Table 5.1), I therefore considered whether this was consistent with the secretion of DKK1 in CAFs compared to PDAC cell lines. This was investigated using an ELISA. All of the pancreatic cancer cell lines with the exception of MIAPACA2, secreted significantly more DKK1 than CAFs (Figure 5.12.).

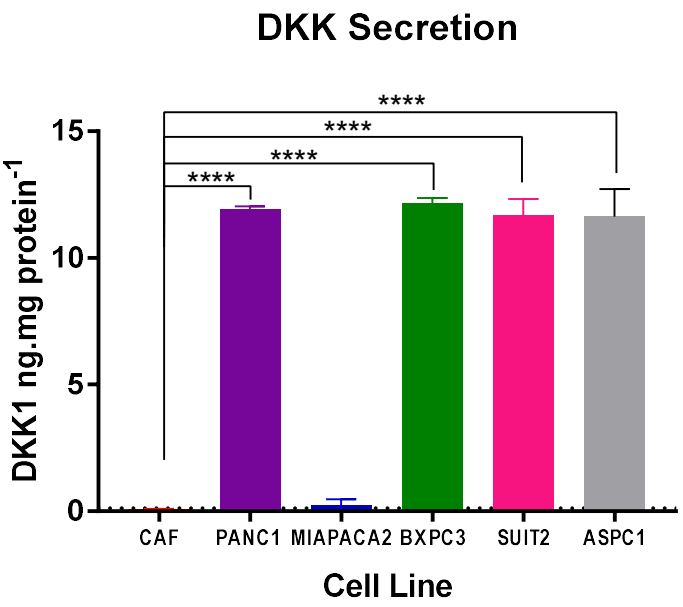

Figure 5.12. Secretion of DKK1 by pancreatic cancer cell lines and CAFs

PANC1, BXPC3, SUIT2 and ASPC1 cells secrete significantly more DKK1 than CAFs under standard culture conditions (10% Serum), **** indicates significance with $p<0.0001$ indicates significance (N=3). Supernatants were collected and tested for the presence of DKK1 using a quantitative sandwich ELISA (abcam). Bars represent supernatants collected from 3 experiments compared to the protein concentration of each experiment collected at the same time as the supernatants were harvested.

5.4. Discussion

Like the Hh pathway, the Wnt signalling pathway is an embryonic signalling pathway that has been implicated in the development of the pancreas (Wells et al., 2007). Mutations in genes associated with the Wnt pathway are uncommon in PDAC unlike other cancers such as colorectal, esophageal and gastric (Zhan et al., 2017, Novellasdemunt et al., 2015, Boynton et al., 1992, Chiurillo, 2015). However, despite the lack of mutations there is an accumulation of cytoplasmic/nuclear β-Catenin in approximately 65% of PDAC patients beginning in precursor lesions (Zeng et al., 2006). This suggests a role for canonical Wnt signalling in the tumorigenesis of PDAC. It was demonstrated that PDAC tumour cores showed cytoplasmic localisation of β-Catenin (Figure 5.1 A&C) compared with normal tissue which showed β-Catenin expression restricted to the cell membranes in acinar cells (Figure 5.1 B). The presence of cytoplasmic localisation of β-Catenin in PDAC suggests this marker could

be used to predict the prognosis of patients. In non-small cell lung cancer and colorectal cancer cytoplasmic accumulation of β-Catenin correlates with a poorer outcome for patients (Li et al., 2013, Brabletz et al., 2001). In order to investigate the mechanism of Wnt signalling in the PDAC microenvironment, the expression of Wnt pathway associated genes in CAFs, NAFs and PDAC cell lines was measured using a Taqman mini array. PANC1 cells showed an upregulation of Wnt5B which was consistent by the findings of Saitoh and Katoh (Saitoh and Katoh, 2002). Wnt5B is associated with non-canonical Wnt pathway; Wnt5B secretion from PANC1 cells has been found to be secreted in exosomes in a paracrine fashion (Harada et al., 2017). Wnt5B has been found to be highly expressed in breast cancer and head and neck squamous cell carcinoma (Klemm et al., 2011, Deraz et al., 2011); its expression is associated with a more invasive phenotype in both tumours. Wnt10A was found to be upregulated in both PANC1 and BXPC3 cells (Figure 5.2.); Wnt10A is associated with canonical Wnt pathway activation and has been found to be deregulated in leukaemia (Memarian et al., 2009). LRP5, a Fzd co-receptor associated with the canonical Wnt pathway, was also found to be upregulated in PANC1 and BXPC3 cells (Figure 5.2.) which suggests the potential for active canonical Wnt signalling in these cell types. However, there was not a clear pattern of Wnt expression genes which clarified a mechanism for Wnt signalling in the PDAC tumour microenvironment. 22 Wnt pathway associated genes were found to be differentially expressed in CAFs compared to NAFs. Among these genes were SFRP and Frzb. These molecules have traditionally been referred to as antagonists of the Wnt pathway as they bind Wnt ligands and prevent binding to Frizzled receptors (Lavergne et al., 2011). Evidence has emerged that restoring pancreatic CAFs to their quiescent phenotype using retinoic acid results in secretion of SFRP4 and eventually leads to a reduction of β-Catenin translocation to the nucleus which results in increased apoptosis of cancer cells (Froeling et al., 2011). However, there are conflicting reports that during development SFRP molecules act to increase the signalling range of Wnt ligands by

behaving as extracellular transporters (Mii and Taira, 2009, Esteve et al., 2011). DKK1 was found to be down regulated in CAFs. During canonical Wnt signalling DKK1 binds receptor Kremen1 and 2 which form a complex with DKK1 and the LRP co-receptors and eventually lead to endocytosis of LRP's removing them from the plasma membrane preventing the binding of Wnt ligands (Mao et al., 2002). Additionally, *DKK1* has been found to be a target gene of β-Catenin/TCF pathway which suggests a negative feedback loop exists between β-Catenin nuclear accumulation and Wnt pathway inhibition (Niida et al., 2004). Additionally, *AXIN2* and *LEF1* were found to be upregulated in CAFs compared to NAFs (Figure 5.3.). Both genes are main effector of the canonical Wnt pathway (MacDonald et al., 2009), suggesting that CAFs are responsive to canonical Wnt ligands. Taken together there is no clear evidence which cell type is the donor/acceptor in the PDAC tumour microenvironment or if both are responsive to Wnt signalling.

Using conditioned media from L-Wnt-3A cells it was possible to elicit an upregulation in *AXIN2* mRNA in both fibroblasts and pancreatic cancer cell lines (Figure 5.4, Figure 5.5). This response was reduced if the L-Wnt-3A cells were cultured in the presence of a PORCN inhibitor developed by Redx Pharma. This suggests that both epithelial and CAF cells in the pancreatic tumour microenvironment are responsive to paracrine Wnt signalling. This is in stark contrast to the expression of Hh signalling pathway components (Figure. 4.4) whereby an absence of Shh, dhh and ihh suggests that clear donor/acceptor roles exist between Shh-producing epithelial cells and responsive CAFs. Such a lack of defined roles for CAFs and PDAC cancer cells with respect to Wnt signalling in PDAC is reflective of the many diverse roles for Wnt signalling during disease and development. For example, in colon cancer Wnt ligand secretion has been found to be elevated in cancer stem cells and has been implicated in the maintenance of the tumour supportive microenvironment (Malanchi et al.,

2011),whereas, in lung fibrosis Wnt ligands have been found to be upregulated in fibroblasts (Baarsma et al., 2011).

Interrogation of the Wnt pathway-associated genes from Transwell co-cultures of both PDAC cancer cell lines and CAFs revealed *AXIN2* mRNA induction in PANC1 cells in the presence of CAFs, an effect that was inhibited by a Redx PORCN inhibitor (Figure 5.9). Two possible mechanisms could explain this: either paracrine signalling exists between CAFs and PANC1 cells in this model, with CAFs secreting Wnt ligands which are activating downstream signalling in the PANC1 cells; or the CAFs are possibly stimulating an autocrine signalling loop in the PANC1 cells. There is evidence for autocrine activation of Wnt/ β-Catenin signalling pathway in cancer cells in mammary tumours (Bafico et al., 2004), however an autocrine signalling mechanism has not been identified in PDAC. Further investigation revealed that *PORCN* mRNA was upregulated in CAFs when they were cultured with PANC1 cells, which suggests that CAFs are responsible for Wnt secretion as PORCN is involved in the post translational modification of Wnt ligands which is required for their successful secretion from Wnt producing cells (Takada et al., 2006). When CAFs were cultured with MIAPACA2 cells no *PORCN* mRNA upregulation was observed, however MIAPACA2 cells showed a Wnt pathway expression profile which had very few similarities to PANC1 and BXPC3 cells (Figure 5.2.). This suggests that the Wnt signalling pathway is behaving in a mechanistically different way in MIAPACA2 cells.

DKK1 was found to be downregulated in CAFs, therefore the secretion of DKK1 in pancreatic cancer cell lines and CAFs was investigated using an ELISA (Figure 5.12). It was found that pancreatic cancer cell lines secrete significantly more DKK1 than CAFs. DKK1 has been found to be a target gene of β-Catenin/TCF pathway which suggests a negative feedback loop exists between β-Catenin nuclear accumulation and Wnt pathway inhibition (Niida et al., 2004). DKK1 has been found to be present in the PDAC tumour microenvironment, and is associated with a more aggressive

phenotype in pancreatic cancer cells (Takahashi et al., 2010). The presence of an auto-inhibitory feedback mechanism in the PDAC tumour microenvironment could be a result of the deregulation of Wnt signalling pathway in the tumour cells.

The data presented within this chapter show that the Wnt pathway is clearly active within PDAC cell lines and suggests paracrine signalling between CAFs and PDAC cancer cells. However, the increased presence of endogenous Wnt pathway inhibitors together with the lack of a clear Wnt pathway expression profile for epithelial and CAFs means the role of non-canonical Wnt signalling and how this relates to canonical signalling must first be defined specifically within the context of PDAC in order to draw firm conclusions based on the data presented herein.

6. Incorporating aspects of the PDAC tumour microenvironment in drug screening models

6.1. Introduction

In vitro 2D monolayer cell based assays have been used as a critical part of the drug discovery process for decades (Lovitt et al., 2014, Fang and Eglen, 2017, Horvath et al., 2016). The limitations of these assays have been more widely exposed as the importance of the tumour microenvironment in drug delivery has become clearer. 2D monolayer assays do not accurately represent the 3D cellular environment within a tumour which also includes the untransformed cells and the tumour microenvironment. Unlike other tumours murine models for PDAC there remains a limited amount of models which actually represent human disease (Herreros-Villanueva et al., 2012). This could be a contributing factor to the low success rate of compounds reaching clinical development; currently approximately 10% of compounds pass phase III clinical trials with many compounds failing because there is a lack of clinical efficacy or toxicities (Ledford, 2011). The *in vitro* profile for Gemcitabine, the current standard of care for PDAC shows cytotoxic activity against cancer cells *in vitro*, however this does not translate to clinical efficacy (Lee et al., 2013a). Paclitaxel was suggested as a potential alternative treatment for PDAC as it also shows cytotoxic activity against cancer cells *in vitro* (Liebmann et al., 1993). Due to reduced drug delivery it did not show any improvement on Gemcitabine (Liebmann et al., 1993). This was somewhat overcome by using albumin bound Paclitaxel which increased drug delivery, however it was also associated with increased toxicities and can therefore only be used in high performing patients (Adamska et al., 2017). In the case of pancreatic cancer the discrepancy between clinical efficacy and *in vitro* models could be due to simplistic 2D monolayer assays not allowing for the complex interactions between tumour cells and the stroma. A variety of signalling pathways including Hh and Wnt/ β-Catenin allow a dynamic cross-talk between CAFs and

tumour cells which results in increased ECM deposition, cancer cell proliferation, and migration (von Ahrens et al., 2017, Weekes and Winn, 2011). My own research (Chapters 3 and 4) on the Hh and Wnt/ β-Catenin signalling pathways provides evidence for significant crosstalk between CAFs and pancreatic cancer cells. Given the low success rates of standard chemotherapy regimens, targeting these signalling pathways in PDAC has gained more attention in recent years (Gore and Korc, 2014). However, research has implicated the tumour microenvironment not only in upregulating signalling pathways which support tumour growth but in modulating the efficacy of the chemotherapy itself (Hessmann et al., 2017, Richards et al., 2017). In order to investigate the efficacy of compounds to treat malignancies which have an active tumour microenvironment more sophisticated screening models must be produced which incorporate the microenvironment. Attempts have been made to include aspects of the tumour microenvironment *in vitro*, however the majority of these models involve 2D co-cultures (Haqq et al., 2014). 3D cultures have an advantage over 2D culture systems as the cells are able to organise into tissue like structures allowing the cells to establish cell-cell contacts and ECM deposition which have been established as playing a role in a tumour's response to chemotherapeutic agents (Estrada et al., 2016). 3D cultures have been found to be more resistant to both chemo and radio therapeutic targeting (Longati et al., 2013), however despite this knowledge validated 3D culture systems are not commonly used *in vitro* to screen compounds. In this chapter, the effect of including CAFs in both 2D and 3D co-culture models on the efficacy of chemotherapeutic agents used to treat PDAC were investigated.

6.2. Methods

6.2.1. 2D Cell proliferation assay

The appropriate seeding density for each cell line was determined using cell growth over time to ensure that the cells were in the exponential growth phase when they

were treated. Cells were seeded at their pre-determined seeding density (Table 6.1) in 100µL of medium and left for 24h to adhere in 96-well flat, white, clear bottom plates (Greiner Bio-One). The following day cells were treated with either Gemcitabine or Paclitaxel using a D300 digital liquid dispenser (Tecan). The plates were placed in an incubator (37°C, 5% CO_2) for 72 and 96h. CellTitre-Glo was prepared using the manufacturer's instructions. At the appropriate time point, plates were removed from the incubator and allowed to equilibrate to room temperature for 30min. 10µL of CellTitre-Glo® reagent was added to each well and the plates were sealed with a black plate seal and placed on an orbital shaker for 10min. Luminescence was read using an EnVision plate reader (PerkinElmer). The luminescent signal generated is in direct proportion to the amount of ATP in the well, which is required for the conversion of luciferin to oxyluciferin in the presence of assay reagents. Cell viability was determined and compared to a DMSO control which was set at 100%.

Cell Line	Cell number (cells/well)
PANC1	1,000
SUIT2	500
MIAPACA2	1,000
BXPC3	2,000
ASPC1	4,000
CAF	4,000

Table 6.1. Cell Seeding Densities for 2D Proliferation Assays

6.2.2. Chemotherapy pulsing

Chemotherapy pulsing was used to determine the effect of mimicking clinical dosing of chemotherapeutic agents in an *in vitro* assay on the viability of pancreatic cancer cell lines. The cMAX (maximum serum concentration of drug in humans) of Gemcitabine (74.4± 11.3 (µM)) and Paclitaxel (4.5 ± 0.4 (µM)) (Fogli et al., 2002)

was used to calculate an approximate exposure time such that it matched the total exposure determined by the AUC.

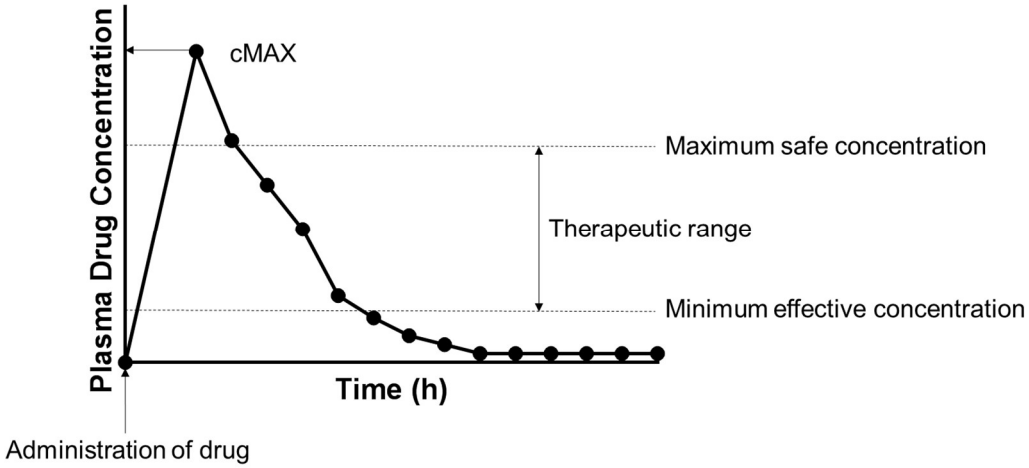

$$\text{Time (h)} = \frac{\text{Area Under Curve (µg/mL)}}{\text{cMAX (µg/mL)}}$$

$$0.83\text{h} = \frac{9.3\ (\text{AUC h x µg/mL})}{11.15\ (0.5\text{cMAX µg/mL})}$$

$$0.83\text{h} \times 60 = 50.0\text{min}$$

Figure 6.1. Example of the plasma concentration-time curve

A typical example of a plasma-concentration over time curve showing pharmacokinetic and pharmacodynamic parameters after a single drug treatment. The Area Under the Curve (AUC) value for Gemcitabine (9.3 ± 1.8 (h × µg/ml)) and Paclitaxel (15.8 ± 1.1 (h × µmol/l)) were used to determine the length of time the cells were exposed to drug at 0.5 cMAX and 0.1 cMAX, using the formula above.

This assay was set up using the design outlined is Section 6.2.1. Once cells had been incubated overnight in order to adhere, Gemcitabine and Paclitaxel were pulsed onto the cells for length of time each drug is present in serum at a given concentration (Table 6.2.). Once the pulse was completed, media was replaced with fresh vehicle (DMSO) containing media. For comparison cells were also treated with the mean IC_{50} (96h), which had been previously established for each cell line (Section 6.3.1.).

Chemotherapy	0.5 cMAX (μM)	Time (min)	0.1 cMAX (μM)	Time (min)
Gemcitabine	37.21	50	7.44	250
Paclitaxel	2.25	420	0.45	2100

Table 6.2 Experimental conditions of chemotherapy pulsing experiment

6.2.3. Transwell co-culture model

To determine if the addition of CAFs could have an effect on the sensitivity of epithelial cells to Gemcitabine in a Transwell co-culture model, CAFs and PANC1 cells (1:1 ratio) were seeded onto a 96-well Transwell plate with CAFs and PANC1 on the bottom and top chambers respectively. To control for cell number, Transwell plates were also seeded with CAFs alone or PANC1 alone. The cells were left for 24h to adhere. The following day they were treated with Gemcitabine using a digital liquid dispenser D300 (Tecan). After 72h cell viability was measured using the CellTitre-Glo procedure described in section 6.2.1.

6.2.4. 3D Co-culture model

Using the Promega 3D CellTiter-Glo cell viability assay it was possible to determine the amount of viable cells in 3D multicellular spheroids of pancreatic cancer cell lines and CAFs. It was first necessary to determine the appropriate seeding density, which was achieved by dosing 3D mono-cultures of PANC1 cells which had been seeded at different densities. The cells were seeded in Ultra-Low Attachment (ULA) plates at different seeding densities and incubated for 24h to form spheroids. The cells were then treated with Gemcitabine and incubated for 48, 72, and 96h. The CellTiter-Glo 3D reagent was thawed at 4^{o}C overnight and then placed in a 22^{o}C water bath for 30min before use. The plate containing the spheroids was equilibrated for 30min at room temperature. 50μL of CellTiter-Glo 3D was added to each well and placed on an orbital plate shaker for 5min. The cell lysate and CellTiter-Glo reagent was moved

to a flat, clear bottom 96-well plate, incubated for a further 25min (room temperature) and then the luminescent signal was measured using an EnVision multilabel plate reader (Perkin Elmer). To determine the effect of co-culturing CAFs and epithelial cells in a 3D culture model had on the sensitivity to Gemcitabine, the above method was repeated with a 1:1 ratio of CAFs and PANC1 cells.

6.3. Results

6.3.1. Proliferation of pancreatic cell lines cultured in 2D is inhibited by Gemcitabine and Paclitaxel

In order to determine the effect of the addition of CAFs to drug screening models, it was first necessary to establish the effect of Gemcitabine and Paclitaxel on pancreatic cancer cell lines and CAFs in a traditional 2D screening model. All 5 pancreatic cell lines tested (PANC1, SUIT2, MIAPACA2, BXPC3 and ASPC1) were sensitive to both Gemcitabine and Paclitaxel at 72 and 96h (Figure 6.2, Figure 6.3, Figure 6.4. and Figure 6.5.) with an IC_{50} for Gemcitabine 338nM (SUIT2) and Paclitaxel 5.73nM (PANC1) in the least sensitive cell lines at 72h. In contrast to this nM and in some cases, pM potency, CAF proliferation at 72 and 96h remained >50% of the DMSO control even in the presence of the highest concentration of either Gemcitabine or Paclitaxel (10μM). As 50% inhibition of growth was not achieved an IC_{50} value was not calculated and the CAFs were deemed resistant to Gemcitabine and Paclitaxel. These data are consistent with previous findings that CAFs are resistant to chemotherapeutic agents (Fang and Eglen, 2017, Richards et al., 2017).

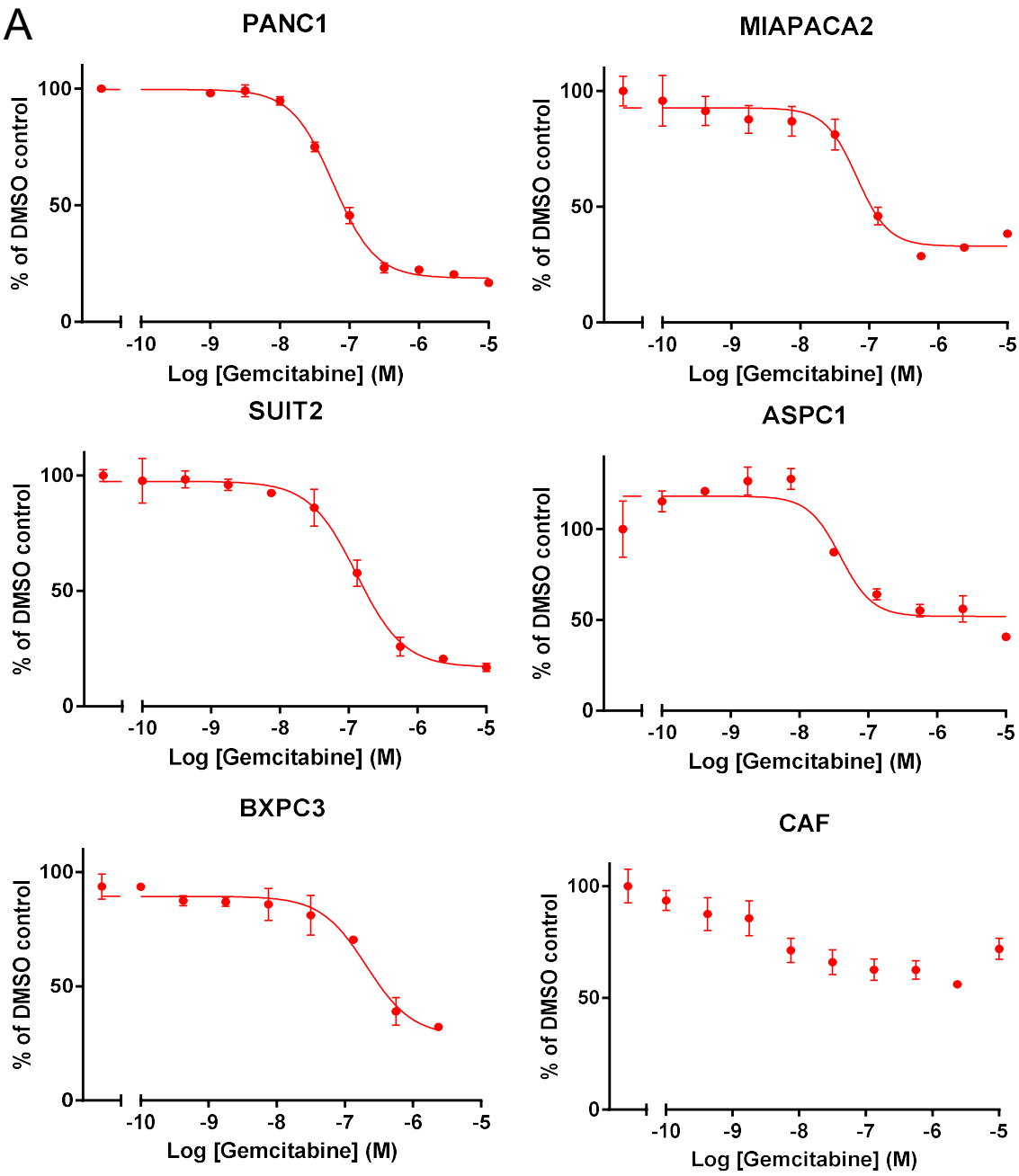
A
PANC1
MIAPACA2
SUIT2
ASPC1
BXPC3
CAF
% of DMSO control
Log [Gemcitabine] (M)
100
50
0
-10
-9
-8
-7
-6
-5

B

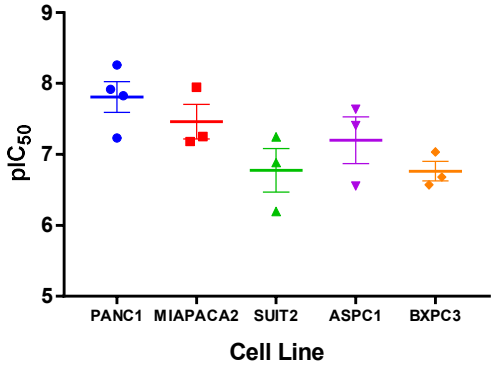

C

Cell line	Average pIC_{50} (M)
PANC1	7.81±0.21
MIAPACA2	7.46± 0.25
SUIT2	6.47 ±0.38
ASPC1	7.2±0.33
BXPC3	6.77±0.14
CAF	≤5.00

Figure 6.2. Pancreatic cancer cell lines are sensitive to Gemcitabine at 72h

A: Representative graphs of a 2D cell proliferation assay. Cells were exposed to increasing concentrations of Gemcitabine, at 72h cell viability was measured using Cell-Titre Glo. Data were fitted to a sigmoidal dose-response curve and the pIC_{50} was determined using GraphPad Prism 5.0. The data are shown as mean ±S.D. of one assay performed in triplicate, normalised to a DMSO control which was set at 100%. **B:** Shows the mean pIC_{50} with S.E.M for the multiple screening runs (three or greater) for each cell line. Summary table of average pIC_{50} for each cell line. **C**. Summary table of average pIC_{50} values obtained for each cell lines.

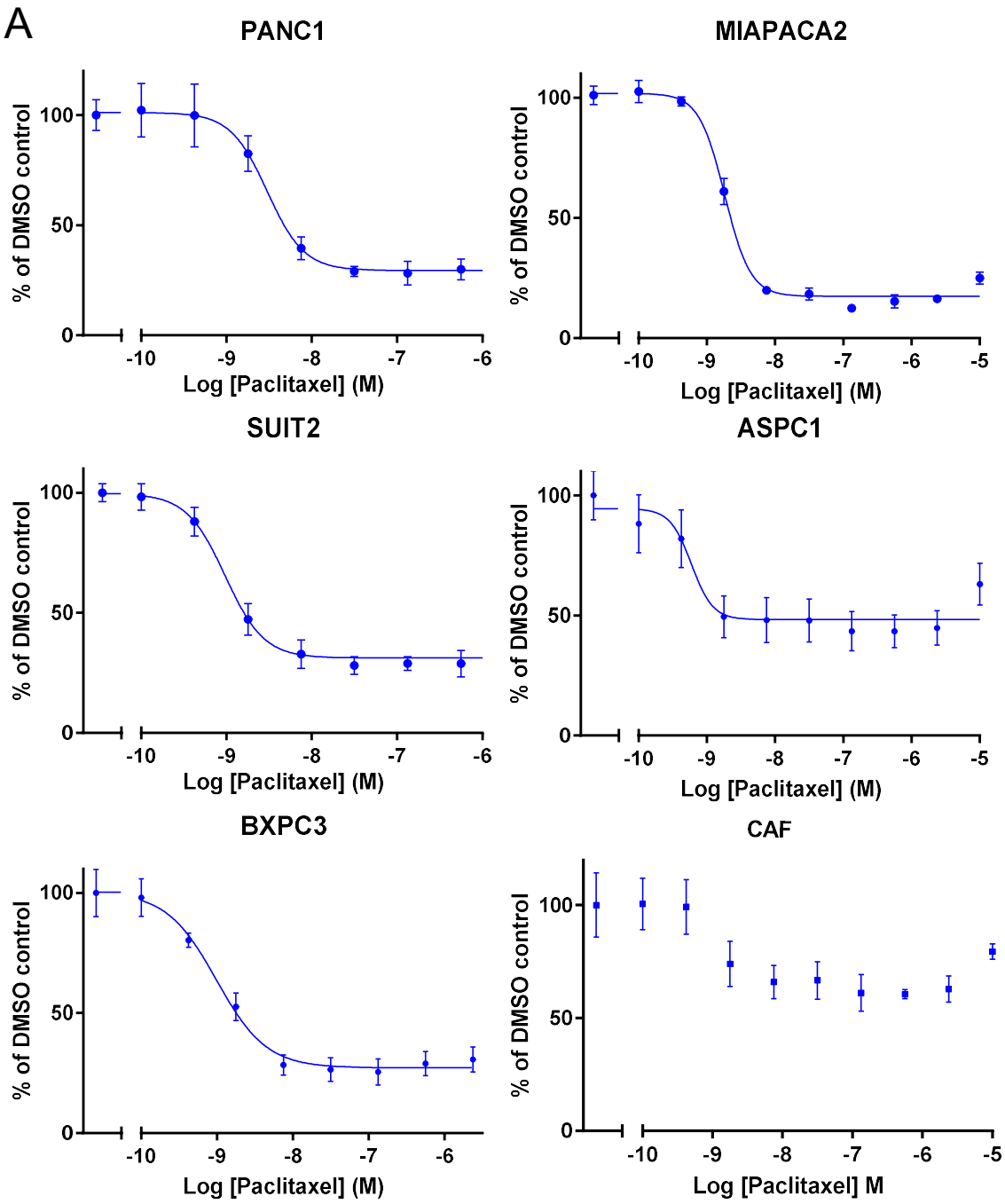
A
PANC1
MIAPACA2
SUIT2
ASPC1
BXPC3
CAF
% of DMSO control
Log [Paclitaxel] (M)
Log [Paclitaxel] M
100
50
0
-10
-9
-8
-7
-6
-5

B

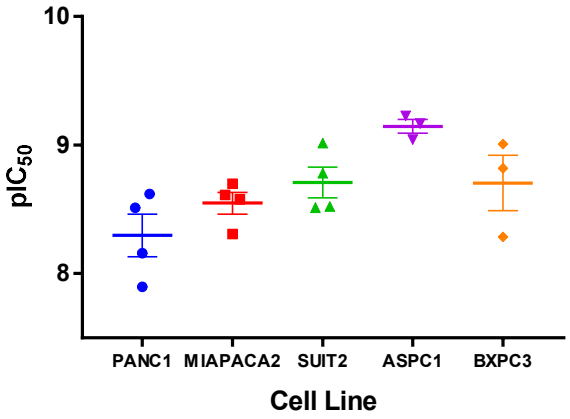

C

Cell line	Average pIC_{50} (M)
PANC1	8.27 ±0.17
MIAPACA2	8.55 ±0.09
SUIT2	8.71 ±0.12
ASPC1	9.15 ±0.05
BXPC3	8.70 ±0.22
CAF	≤5.00

Figure 6.3. Pancreatic cancer cell lines are sensitive to Paclitaxel at 72h

A: Representative graphs of a 2D cell proliferation assay. Cells were exposed to increasing concentrations of Paclitaxel, at 72h cell viability was measured using Cell-Titre Glo. Data were fitted to a sigmoidal dose-response curve and the pIC_{50} was determined using GraphPad Prism 5.0. The data are shown as mean ±S.D. of one assay performed in triplicate, normalised to a DMSO control which was set at 100%. **B:** Shows the mean pIC_{50} with S.E.M for the multiple screening runs (three or greater) for each cell line. C. Summary table of average pIC_{50} for each cell line.

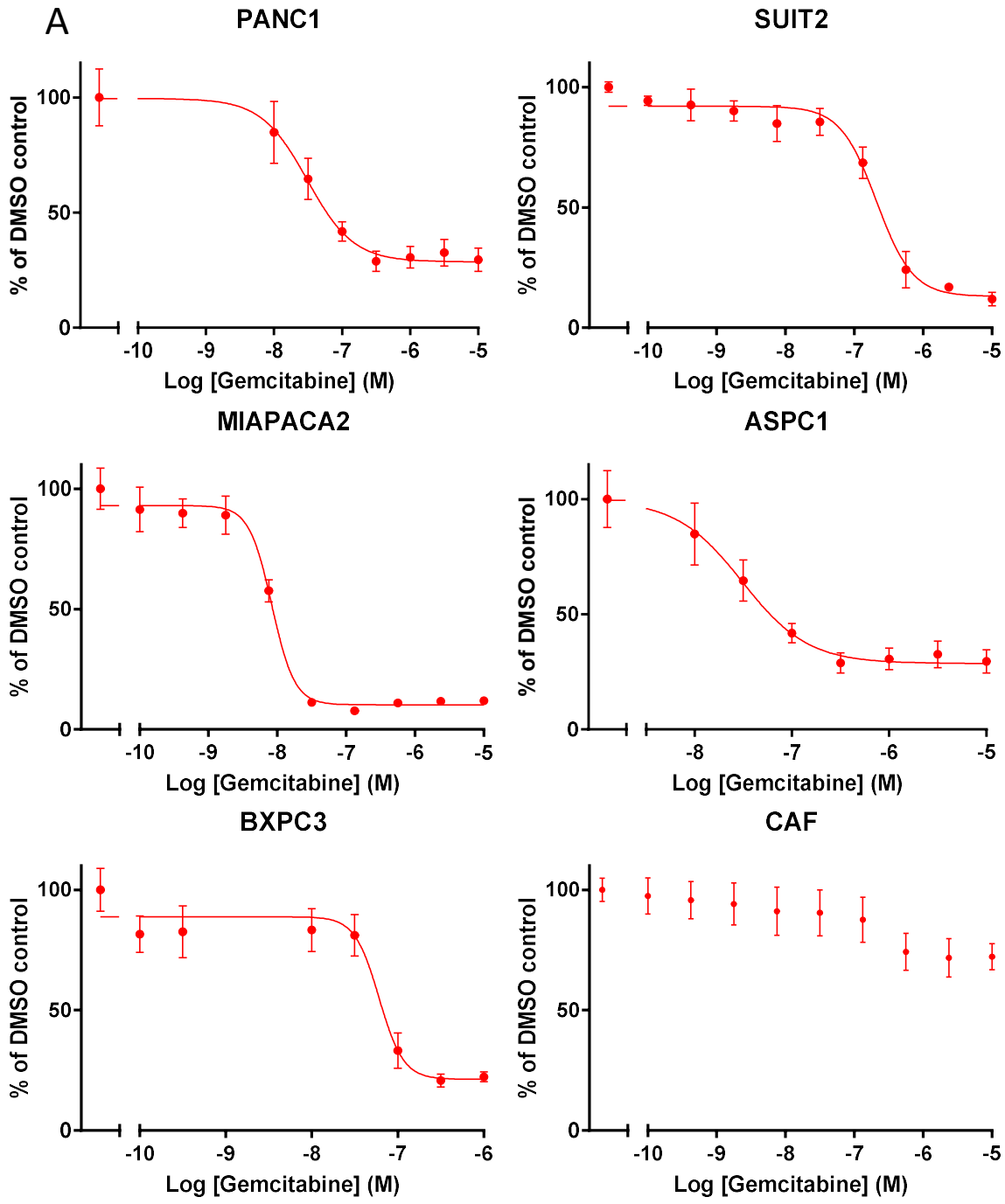
A
PANC1
SUIT2
MIAPACA2
ASPC1
BXPC3
CAF
% of DMSO control
Log [Gemcitabine] (M)
100
50
0
-10
-9
-8
-7
-6
-5

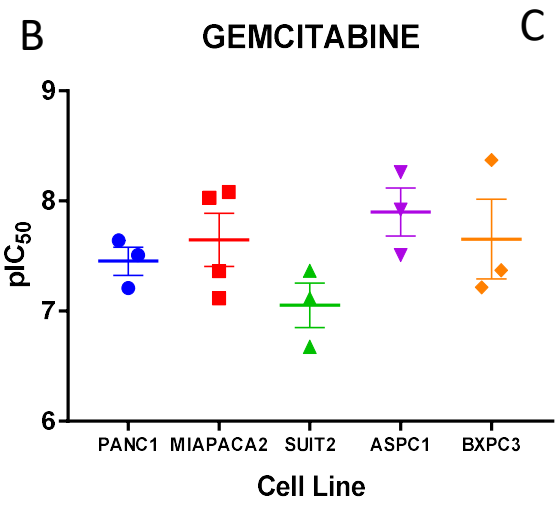

Cell line	Average pIC_{50} (M)
PANC1	7.45 ±0.13
MIAPACA2	7.65 ±0.24
SUIT2	7.05 ±0.20
ASPC1	7.99 ±0.22
BXPC3	7.65 ±0.36
CAF	≤5.00

Figure 6.4. Pancreatic cancer cell lines are sensitive to Gemcitabine at 96h

A: Representative graphs of a 2D cell proliferation assay. Cells were exposed to increasing concentrations of Gemcitabine, at 96h cell viability was measured using Cell-Titre Glo. Data were fitted to a sigmoidal dose-response curve and the pIC_{50} was determined using GraphPad Prism 5.0. The data are shown as mean ±S.D. of one assay performed in triplicate, normalised to a DMSO control which was set at 100%. **B:** Shows the mean pIC_{50} with S.E.M for the multiple screening runs (three or greater) for each cell line. **C**. Summary table of average pIC_{50} for each cell line.

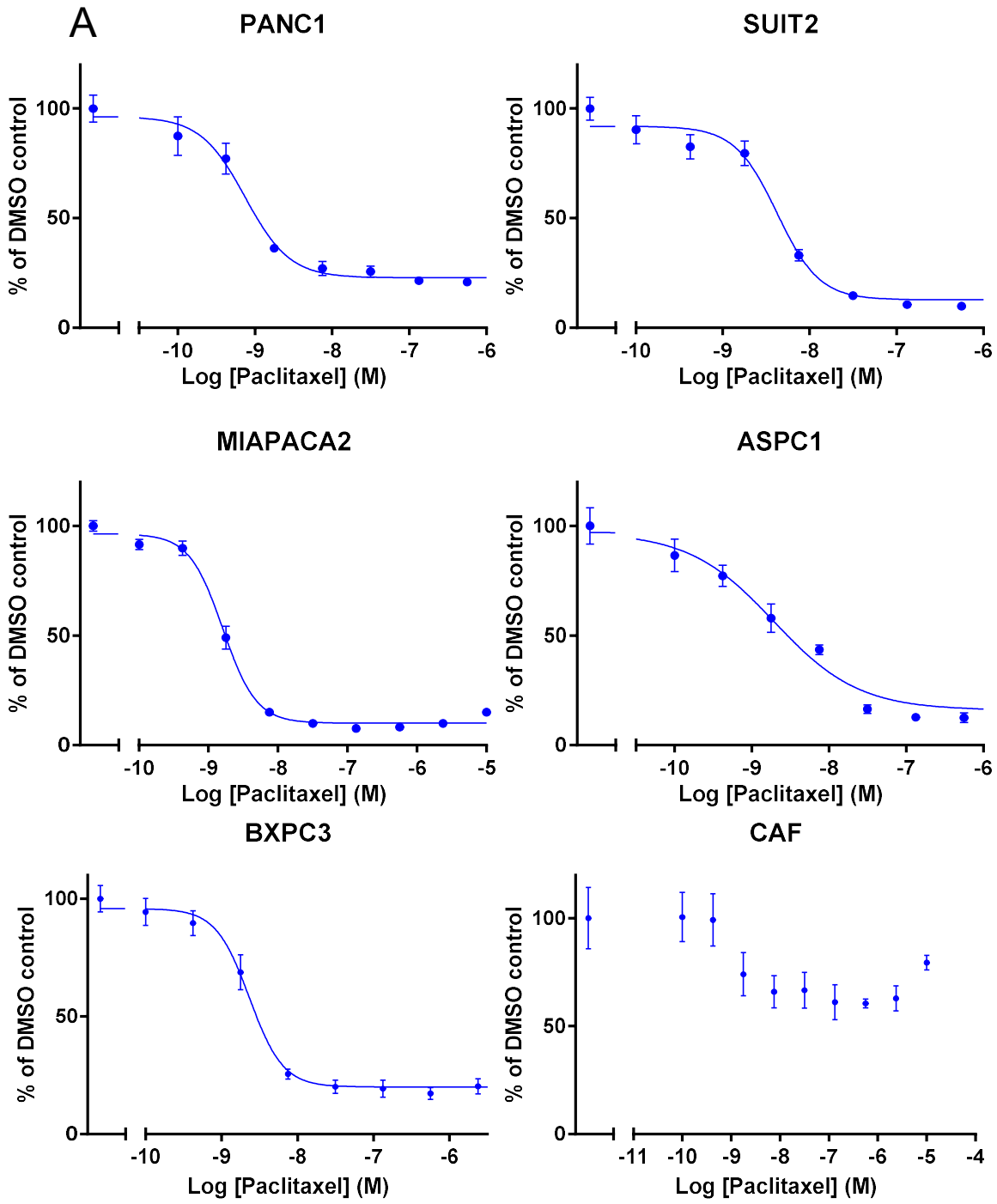
A
PANC1
SUIT2
MIAPACA2
ASPC1
BXPC3
CAF
% of DMSO control
Log [Paclitaxel] (M)

B

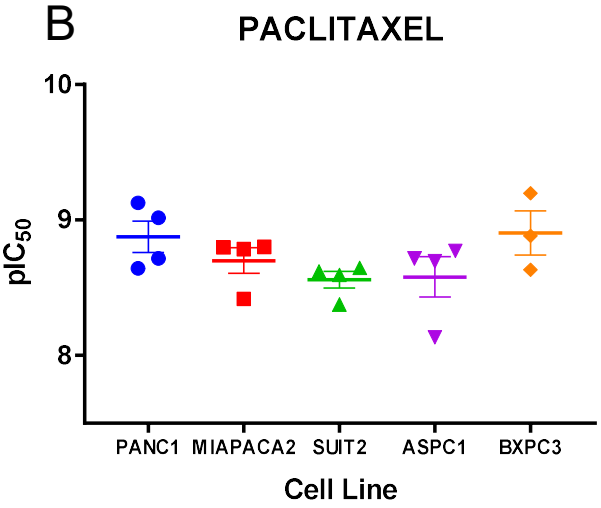

C

Cell line	Average pIC_{50} (M)
PANC1	8.88 ±0.12
MIAPACA2	8.70 ±0.09
SUIT2	8.56 ±0.06
ASPC1	8.58 ±0.15
BXPC3	8.90 ±0.16
CAF	≤5.00

Figure 6.5. Pancreatic cancer cell lines are sensitive to Paclitaxel at 96h

A: Representative graphs of a 2D cell proliferation assay. Cells were exposed to increasing concentrations of Paclitaxel, at 96h cell viability was measured using Cell-Titre Glo. Data were fitted to a sigmoidal dose-response curve and the pIC_{50} was determined using GraphPad Prism 5.0. The data are shown as mean ±S.D. of one assay performed in triplicate, normalised to a DMSO control which was set at 100%. **B:** Shows the mean pIC_{50} with S.E.M for the multiple screening runs (three or greater) for each cell line. **C.** Summary table of average pIC_{50} for each cell line.

6.3.2. Chemotherapy pulsing as an alternate method for dosing cells during in vitro drug screening assays

Drug screening assays in the pharmaceutical industry are designed with a variety of factors in consideration such as pharmacological relevance, reproducibility, quality and importantly cost (Hughes et al., 2011). In PDAC research the standard, mono-2D cell based assay is still the most widely used to compare the anti-proliferative effect of drugs on pancreatic cancer cells (Awasthi et al., 2013). However, the findings presented in chapters 3-5 strongly suggest that CAFs contribute to a dynamic tumour supportive microenvironment exhibiting active signalling pathways which support tumour growth and metastases, as found by others (Farrow et al., 2008, Waghray et al., 2013). A mono-2D cell based assay does not take into consideration factors within the tumour microenvironment which can affect chemotherapeutic agents. Neither does it take into account length of time and concentration of drug that the cancer cells within the tumour are exposed to. In a 2D mono culture based assay, compounds are ranked based on their potency whereby cells are continuously exposed to a compound. However, this does not replicate the *in vivo* situation as compounds are rapidly cleared by the host. One method of investigating the effect of chemotherapeutic agents on cancer cells is using a dosing schedule which mimics the clinical exposure of cells to drug as closely as possible within the limits of *in vitro* testing. Once it had been established that pancreatic cancer cell lines were sensitive to treatment with chemotherapeutic agents (Gemcitabine and Paclitaxel) at both 72 and 96h, the effect of a clinical dosing regimen was investigated.

Using a clinical dosing regimen PANC1 cells did not show any increase in cell viability when treated with 37.21μM for 50min (0.5 cMAX)(Figure 6.6.). However when treated with 7.44μM for 250min (0.1 cMAX) they appeared to have a normal cell growth until 72h after which point there was a reduction in cell viability (Figure 6.6.). SUIT2 and MIAPACA2 showed a reduction in cell viability which fell below 0h in all 3 conditions (0.5 cMAX, 0.1 cMAX and IC_{50}) which suggests cell death (Figure 6.6.). ASPC1 cells

were sensitive to 0.5 and 0.1 cMAX as there was no increase in cell viability after dosing with these concentrations (Figure 6.6.). There was no effect on BXPC3 cell viability when treated with the (previously determined) IC_{50} of Gemcitabine (22.4nM) at 96h (Figure 6.4.). CAFs retained their resistance to Gemcitabine and there was minimum effect on cell viability under three conditions.

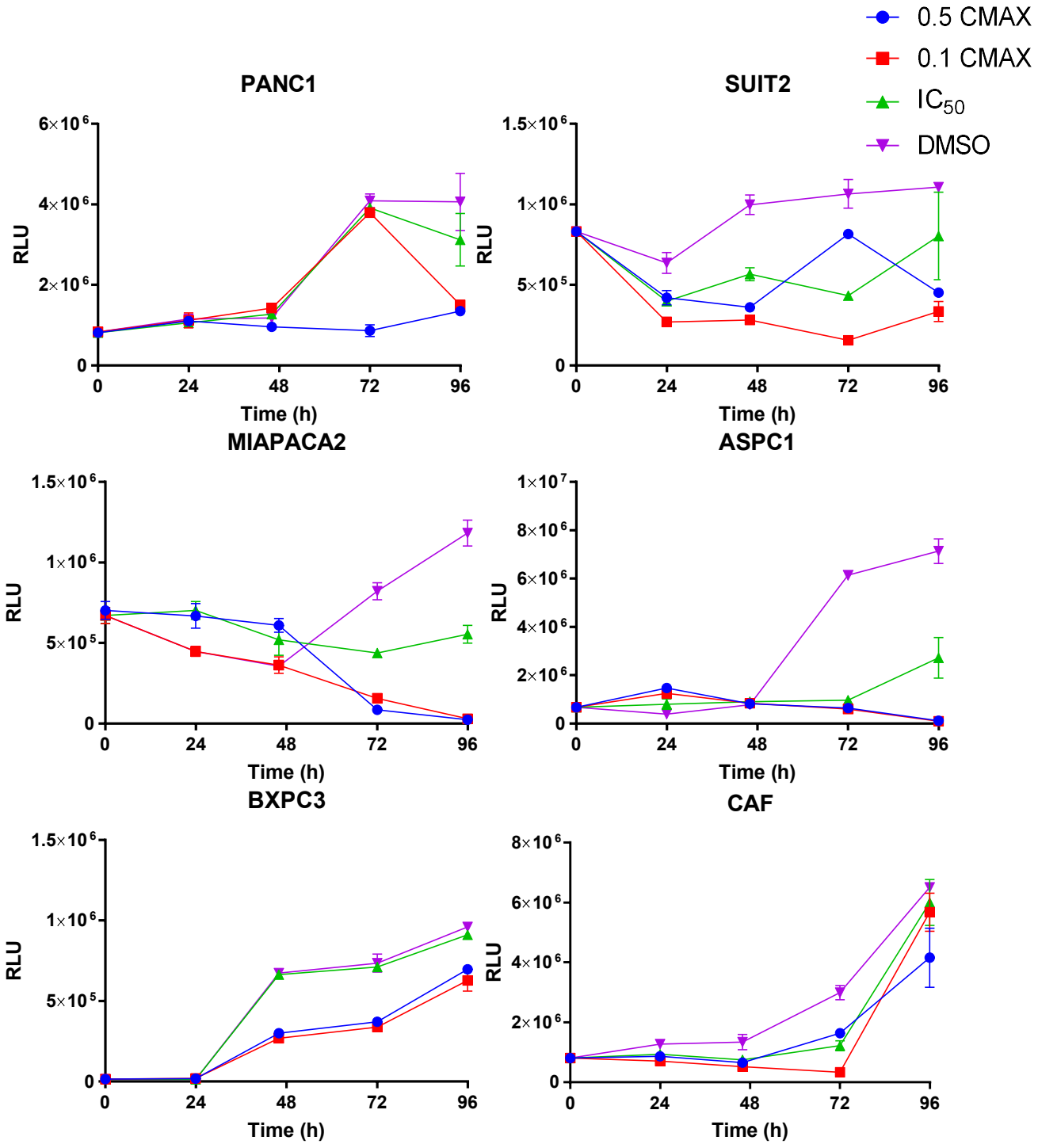

Figure 6.6. Cell Viability of pancreatic cancer cell and CAFs after pulsing with Gemcitabine

Representative graphs of a 2D cell proliferation assay. Cells were exposed to Gemcitabine concentrations which corresponded to 0.5 cMAX, 0.1 cMAX, IC_{50} and a DMSO control. At 24, 48, 72 and 96h cell viability was measured using Cell-Titre Glo. Data was analysed using GraphPad Prism 5.0. The data are shown as mean ±S.D. of one assay performed in triplicate.

Using a clinical dosing regimen to dose cells with Paclitaxel SUIT2 and MIAPACA2 showed a decrease in cell viability in all 3 conditions (IC_{50}, 2.25μM for 420min (0.5 cMAX) and 0.45μM for 2100min (0.1 cMAX)) which was below that detected at the 0h time-point and indicates that there was cell death in response to treatment (Figure 6.7). PANC1 cells did not proliferate after dosing with 0.5 cMAX, though there was a slight increase in viable cells when treated with 0.1 cMAX (Figure 6.7.). However, dosing with the previously determined IC_{50} (96h time point; 1.3nM) appeared to prevent proliferation up to 72h after dosing before the cells appeared to recover such that there was no difference in cell proliferation between the IC_{50} and vehicle (DMSO) control (Figure 6.7). ASPC1 cells were sensitive to dosing with both 0.5 cMAX and 0.1 cMAX as there was no increase in viable cells up to 96h after dosing (Figure 6.7.). BXPC3 cells showed a decrease in proliferation when treated with 0.5 cMAX and 0.1 cMAX and there was a slight decrease in viable cells when BXPC3 were treated with the pre-determined IC_{50} (1.3nM Figure 6.5.). CAFs were sensitive to Paclitaxel using this model and did not recover from dosing with 0.5 and 0.1 cMAX as there was no increase in cell proliferation (Figure 6.7.). As it was not possible to determine an IC_{50} for CAFs the highest IC_{50} determined for the pancreatic cancer cell lines was used which was SUIT2 (2.8nM, Figure 6.5.). This did not have any effect on the proliferation of CAFs (Figure 6.7.).

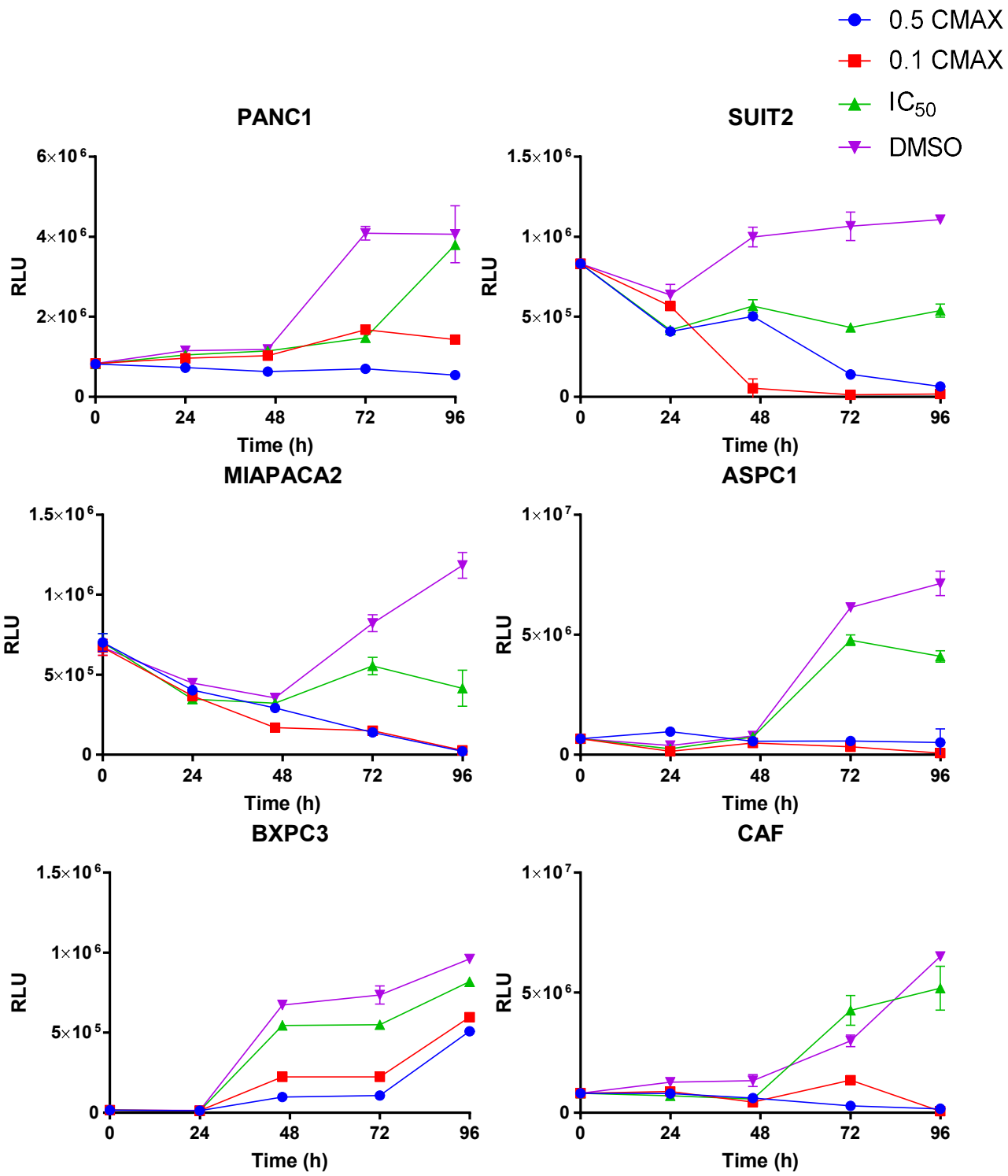

Figure 6.7. Cell Viability of pancreatic cancer cell and CAFs after pulsing with Paclitaxel

Representative graphs of a 2D cell proliferation assay. Cells were exposed to Gemcitabine concentrations which corresponded to 0.5 cMAX, 0.1 cMAX, IC_{50} and a DMSO control. At 24, 48, 72 and 96h cell viability was measured using Cell-Titre Glo. Data was analysed using GraphPad Prism 5.0. The data are shown as mean ±S.D. of one assay performed in triplicate.

Figures 6.6 and 6.7 show that, rather than better modelling the efficacy drop-off between *in vitro* testing and clinical observation, mimicking the clinical AUC by pulsing with either 0.5 or 0.1 cMAX had a more marked anti-proliferative effect at 96h than dosing with the pre-determined IC_{50}. It is therefore clear that the dosing regimen is not responsible for the discrepancy between clinical and *in vitro* efficacy and that an alternative model should be sought.

6.3.3. CAFs reduce the anti-proliferative effect of Gemcitabine in 2D co-culture models

To investigate the effect of including CAFs in drug screening assays, a direct 2D co-culture model was used. The addition of CAFs to a 2D model to create a direct co-culture showed a reduction in the anti-proliferative effect of Gemcitabine (Figure 6.8.). Gemcitabine exposure to PANC1 cells alone gave an IC_{50} of 63.1nM whereas the addition of CAFs caused a decrease in sensitivity (Gemcitabine IC_{50}: 9 PANC1:1 CAF, 331.1nM; 1 PANC1:1 CAF, 301.9nM; 1 PANC1:9 CAF, 436.5nM).

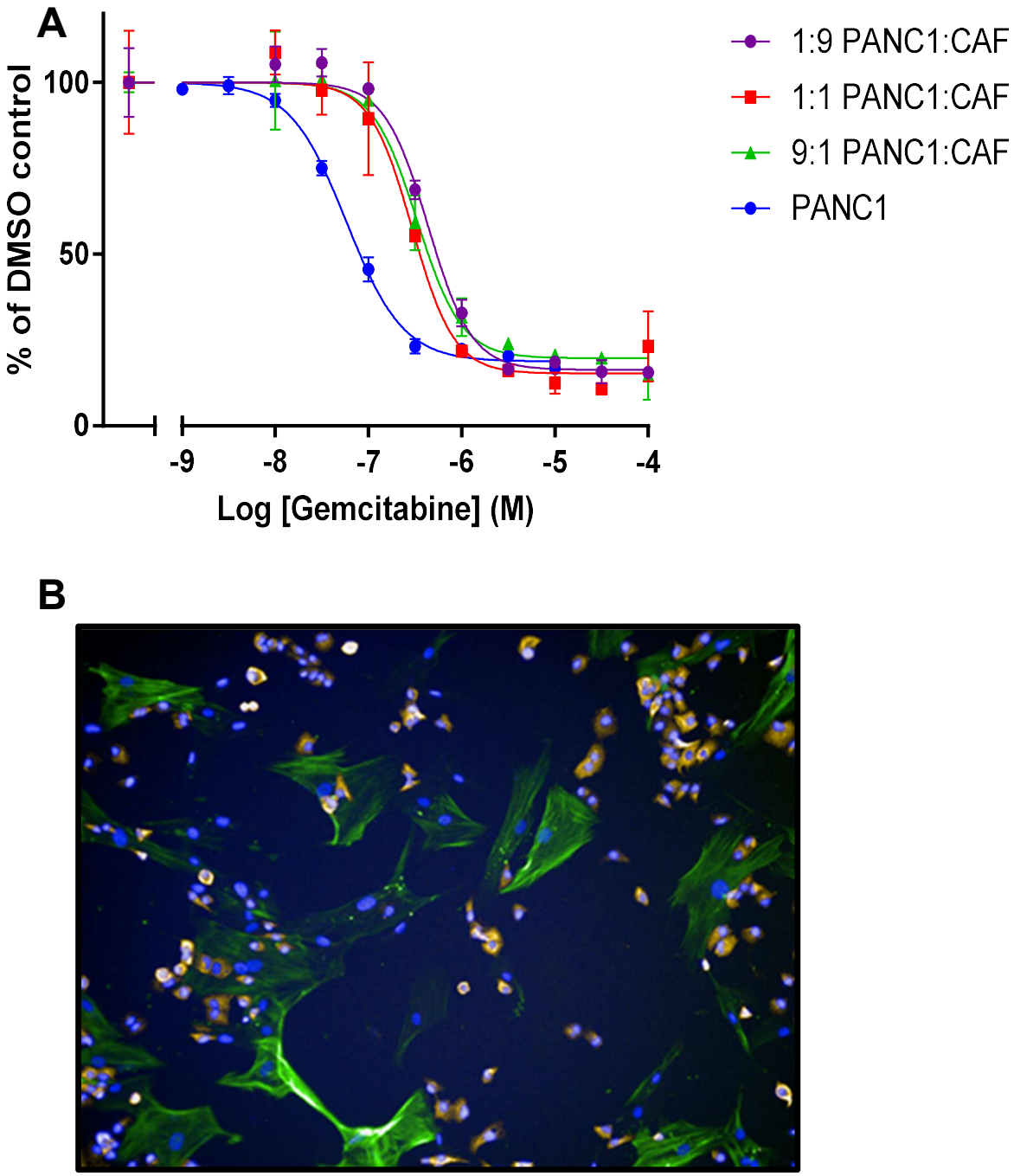

Figure 6.8. Addition of CAFs to a 2D screening model reduces the anti-proliferative effect of Gemcitabine on PANC1 cells

A: Representative graph of a 2D cell proliferation assay. Cells were exposed to Gemcitabine and a DMSO control. At 72h cell viability was determined using a nuclei count which was achieved by staining the cells with DAPI, anti-α-SMA-488 and anti-CTK-594. Nuclei which were associated with areas of positive α-SMA-488 staining were considered to be CAFs and excluded from nuclei count. Data were analysed using GraphPad Prism 5.0. The data are shown as mean ±S.D. of one assay performed in triplicate. **B**: Example image from this assay showing anti-α-SMA-488 (Green) and anti-CTK-594 (Yellow) and nuclei (Blue). Average nuclei count was measured using an Operetta (Perkin Elmer), using 4 areas of interest per well.

In order to confirm that co-culture with CAFs with PANC1 cells were responsible for the reduction in the anti-proliferative effect of Gemcitabine in PANC1 cells, the effect of CAFs on the Gemcitabine IC_{50} in PANC1 cells was investigated using a Transwell co-culture model. A ratio of 1:1 of each cell type was chosen as it was clear from the co-culture model described above (Figure 6.8.) that the ratio of CAFs to epithelial cells did not significantly impact the Gemcitabine IC_{50}.

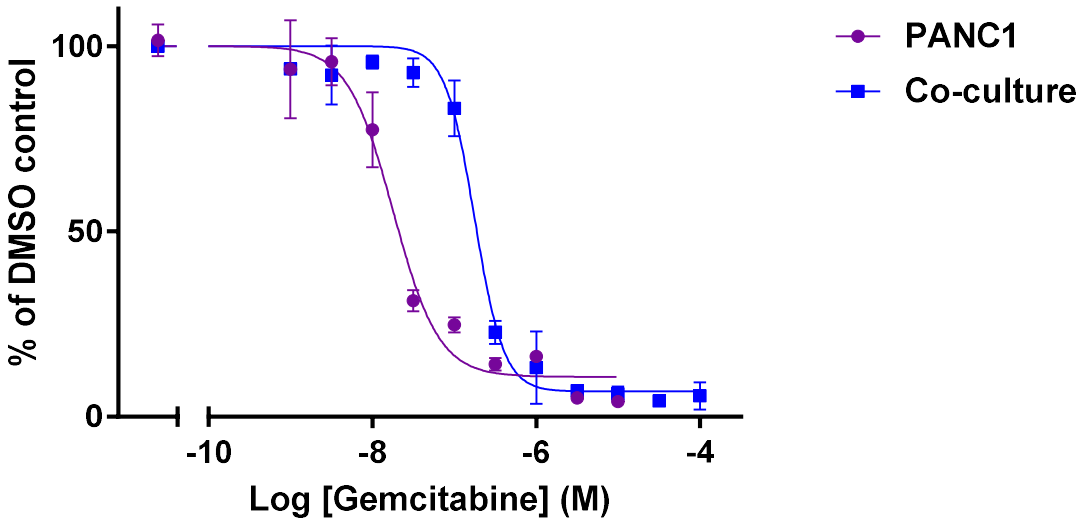

Figure 6.9. CAFs reduce the anti-proliferative effect of Gemcitabine in a Transwell model
PANC1 cells were cultured on Transwell (Top) inserts alone or in the presence of CAFs (Bottom) 1;1 ratio. Cells were cultured for 72h in the presence of gemcitabine. Proliferation of PANC1 cells was measured using Cell Titre Glo.

The co-culture of CAFs with PANC1 cells in a Transwell system dramatically reduced the anti-proliferative effect of Gemcitabine (Figure 6.9.). This reduction resulted in a 10-fold decrease in Gemcitabine potency (pIC_{50} from 7.7±0.16 to 6.3±0.13M, N=3). Such a significant reduction in potency (P value = 0.0036) is consistent with the direct co-culture model (Figure 6.8.) and suggests that CAFs are able to reduce the anti-proliferative effect on Gemcitabine even in a model wherein the cells are not in direct co-culture.

6.3.4. CAFs reduce the anti-proliferative effect of Gemcitabine in a 3D co-culture model

To develop a model which more closely mimics the PDAC tumour microenvironment allowing a physical interaction between the tumour cells and CAFs, a 3D co-culture model was used. Initially, it was necessary to determine an optimal cell density for this model. Due to the limitations of the assay it was found that in order to measure any response to Gemcitabine the spheroids had to be reduced in size to 1,000 cells/well (Figure 6.10.) as any increase in cell number caused assay saturation.

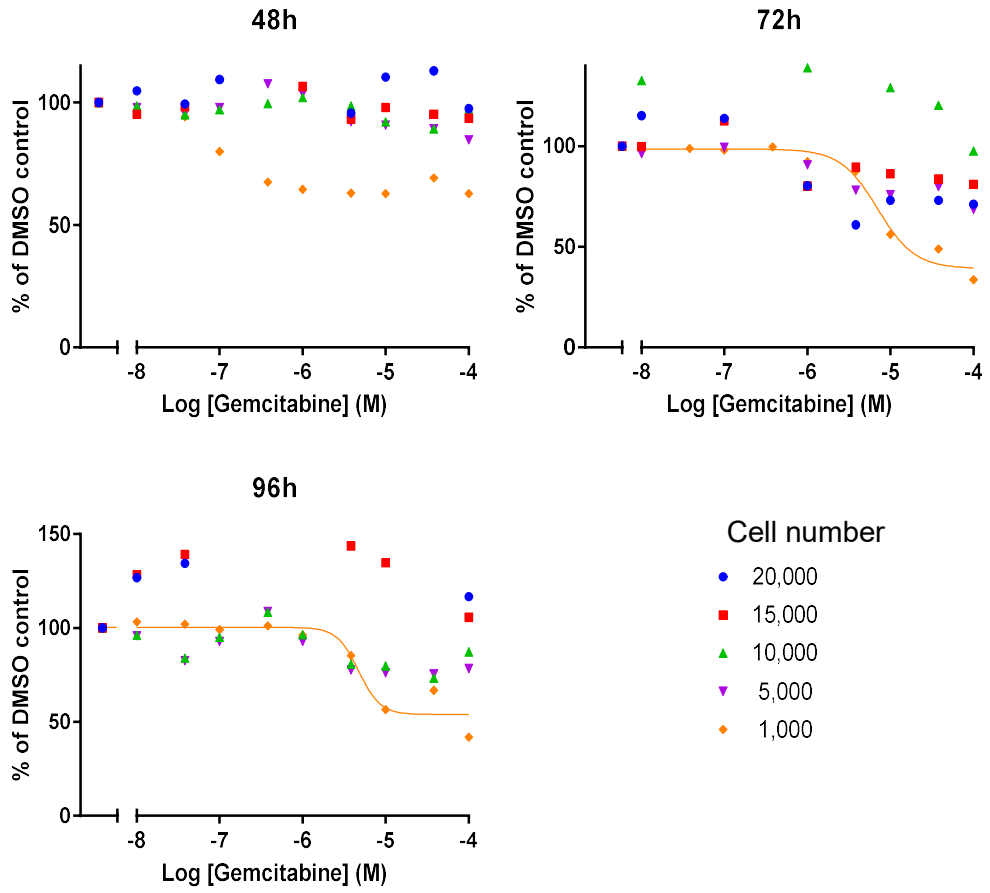

Figure 6.10. Optimisation of pancreatic cancer cell number in a 3D drug screening model
PANC1 cells were plated at varying cell densities in ULA plates and left overnight in order to form spheroids. At 24h the spheroids were treated with Gemcitabine or a DMSO control. At 24, 48 and 72h after dosing cell viability was determined using 3D Cell Titre Glo. Spheroids were resistant to Gemcitabine treatment when they were cultured at 20,000, 15,000, 10,000, 5,000 cells/ spheroid. At 1,000 cells/ spheroid at 72 and 96h there was an anti-proliferative effect dependant on Gemcitabine concentration.

CAFs were found to be resistant to Gemcitabine in 3D culture regardless of the cell density (Figure 6.11.). It was not possible to calculate an IC_{50} as there was not a 50% decrease in ATP concentration using up to 50μM Gemcitabine. There was a slight decrease in cell proliferation in the 10,000 and 1,000 cell conditions; however this was not marked enough to consider the CAFs sensitive to Gemcitabine in this model.

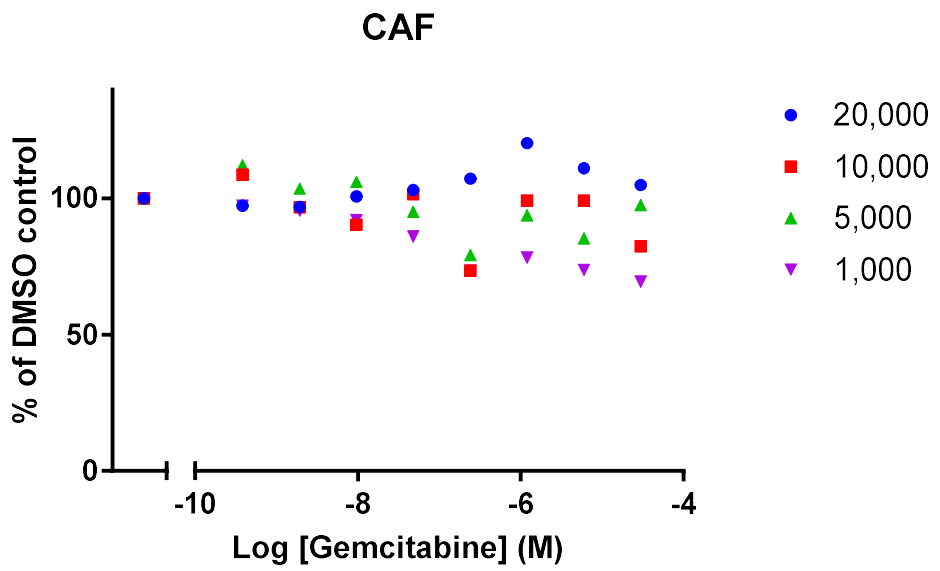

Figure 6.11. CAFs are resistant to gemcitabine in a 3D cell culture model

CAFs were plated at varying cell densities in ULA plates and left overnight in order to form spheroids. At 24h the spheroids were treated with Gemcitabine or a DMSO control. At 72h after dosing cell viability was determined using 3D Cell Titre Glo. Spheroids were resistant to Gemcitabine treatment when they were cultured at 20,000, 15,000, 10,000, 5,000 and 1,000 cells/ spheroid.

Once an appropriate cell number had been established a 3D co-culture was tested using this model. A 1:1 ratio of pancreatic cancer cell to CAFs was used as this ratio had been shown to effect drug potency in both co-culture and Transwell 2D models (Figure 6.8, Figure 6.9.). The anti-proliferative effect of Gemcitabine was reduced in all cases in which pancreatic cancer cells were cultured with CAFs: PANC1 cells cultured in 3D alone gave a pIC_{50} 6.1 ±0.13M which was reduced to a pIC_{50} ≤4.30M (Figure 6.12, Table 6.1.). The pIC_{50} of SUIT2 cells was reduced from 6.6 ±0.22M to ≤4.30, though in this case the cell proliferation was reduced to approximately 58%. MIAPACA2 cells when cultured alone in 3D gave a pIC_{50} of 7.5 ±0.19 which was reduced to ≤5.50 (Figure 6.12, Table 6.1.). BXPC3 had a pIC_{50} of 7.3 ±0.24 which was reduced to ≤5.00, in this case there also appeared to be an effect on cell proliferation, however this was not marked enough to be able to determine a pIC_{50} (Figure 6.12, Table 6.1.). Together these data suggest that CAFs have a significant effect on chemotherapeutic resistance in the PDAC tumour microenvironment.

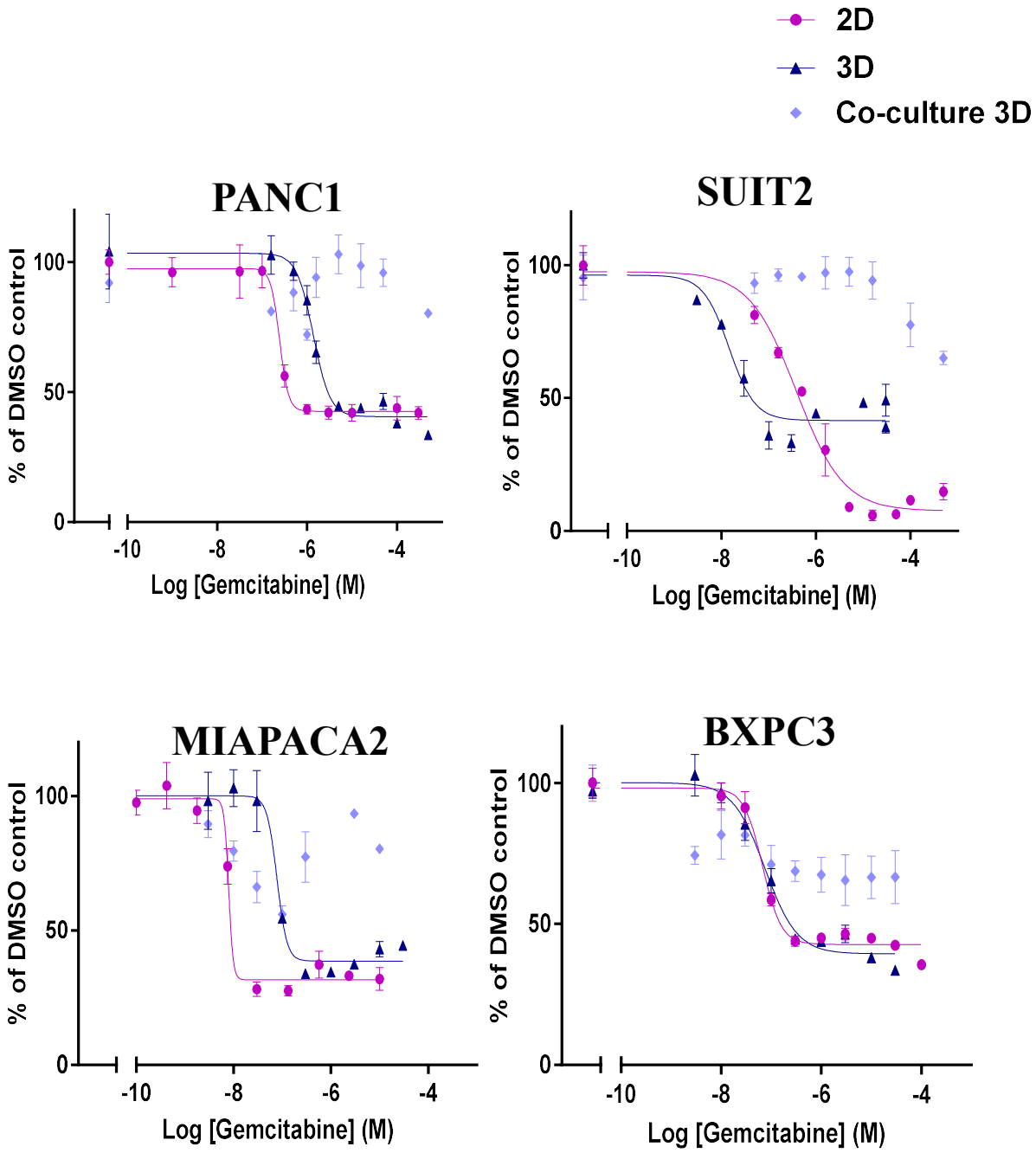

Figure 6.12. CAFs are resistant to Gemcitabine in a 3D co-culture model

Representative graphs of 2D and 3D Cultures generated using normal tissue culture (2D) or ultra-low attachment plates (3D), whereby cells were seeded and left overnight to form spheroids at which point they were treated with Gemcitabine. At 72h spheroids were lysed and ATP concentration was determined using 3D Cell Titre Glo. When cells were cultured in 3D with CAFs the anti-proliferative effect of gemcitabine was reduced (N=3).

	2D Mean pIC_{50} (M)	3D Mean pIC_{50} (M)	3D Co-Culture Mean pIC_{50} (M)
PANC1	6.9 ±0.17	6.1 ±0.13	≤4.30
BXPC3	7.3 ±0.34	7.3 ±0.24	≤5.00
MIAPACA2	8.2 ±0.09	7.5 ±0.19	≤5.50
SUIT2	6.4 ±0.41	6.6 ±0.22	≤4.30

Table 6.1. Comparison of average pIC50's of Gemcitabine of pancreatic cancer cells in 2D, 3D and in 3D co-culture models with CAFs (N=3)

6.4. Discussion

Only 20% of patients are diagnosed with resectable tumours; the vast majority of patients have locally advanced or metastatic disease by the time of diagnosis (Heestand et al., 2015). In the more common event that a tumour is not resectable, the current standard of care is Gemcitabine treatment. This however, has limited efficacy with a median survival of less than 6 months (Hidalgo, 2010). During *in vitro* testing of Gemcitabine and Paclitaxel (Figure 6.3, 6.4, 6.5. and 6.6.), pancreatic cancer cells appear to be sensitive to both chemotherapies, which would suggest they would be effective therapies for PDAC. Conversely, both drugs appeared ineffective with regards to the proliferation of CAFs. Both of these drugs target the rapidly proliferating epithelial cancer cells. Gemcitabine is a nucleoside analogue which inhibits DNA synthesis when dFdCTP is incorporated into DNA which prevents DNA polymerases from functioning past the incorporation (Huang et al., 1991). This traps cells within the S phase of the cell cycle preventing further cell proliferation. In addition, Gemcitabine also targets the enzyme ribonucleotide reductase (RNR). The diphosphate analogue binds to the RNR active site and inactivates the enzyme irreversibly. Once RNR is inhibited, the cell cannot produce the deoxyribonucleotides required for DNA replication and repair this leads to cell cycle arrest and apoptosis (Cerqueira et al., 2007).

Paclitaxel functions by binding to the β-subunit of tubulin, which is a protein highly involved in the structure of microtubules which need to be fluid in order for a cell to function appropriately (Horwitz, 1994). Paclitaxel binds to tubulin and locks the microtubules in place preventing them from undergoing the dynamic instability which is necessary for chromosome remodelling during mitosis, this causes mitotic arrest (Weaver, 2014). CAFs are untransformed cells and proliferate at a much slower rate than epithelial pancreatic cancer cell lines and this could, in part, explain their resistance to Gemcitabine and Paclitaxel.

In many drug discovery programmes, the anti-proliferative potency of compounds are ranked using IC_{50} values obtained using 2D cell culture. One key difference between this method and *in vivo*/clinical dosing is that the concentration of the compound is sustained throughout the *in vitro* experiment albeit with the potential for cellular enzymatic breakdown of the compound. Due to pharmacokinetics this sustained concentration is not achievable within an animal with the serum concentration often experiencing a sharp peak (cMAX) followed by a rapid decline as the drug is cleared through phase I and II metabolism (Figure 6.1). Therefore one potential explanation of the discrepancy between *in vitro* and clinical efficacy could be the dosing regimen. In order to determine if mimicking *in vivo* drug exposure in an *in vitro* model had any effect on the viability of the cells, chemotherapeutic pulsing was used whereby cells were briefly exposed to either 0.1 or 0.5 cMAX for a time equivalent to the overall clinical exposure (AUC) calculated from literature (Fogli et al., 2002, Wang et al., 2007) reports (Figure 6.1, Table 6.2.) before the media was refreshed. This was then compared to cells exposed continuously to a previously determined IC_{50} concentration. Using this method of the anti-proliferative effect of Gemcitabine and Paclitaxel in pancreatic cancer cell lines was sustained with the exception of BXPC3 which appeared to recover from chemotherapy pulsing over time (Figure 6.6, Figure 6.7). CAFs remained resistant to Gemcitabine (Figure 6.6) however, pulsing with

Paclitaxel reduced the cell viability of CAFs (Figure 6.7). The data comparing dosing regimen would suggest that the discrepancy between *in vitro* and clinical potency is not due to the difference in compound exposure between the two disciplines. However one such limitation of this technique is that the AUC and cMAX calculations were taken from serum concentrations. As discussed before, the desmoplastic reaction reduces the blood perfusion in the PDAC tumour microenvironment and therefore the serum concentration may be far larger than the concentration that the tumour is exposed to. Nevertheless, in all cases, the pulsing was more effective in inhibiting PDAC cell growth than the IC_{50} concentration, suggesting that a specific regimen does not underpin efficacy. Given the resistance of CAFs to Gemcitabine and Paclitaxel, I hypothesized that the interplay between CAFs and epithelial cells may contribute toward the decreased sensitivity of tumour cells to Gemcitabine.

A direct 2D co-culture model was used to investigate the effect of the addition of CAFs to a drug screening model. It was shown that CAFs confer Gemcitabine resistance in this model (Figure 6.8A). However, this model used IF to exclude nuclei which were associated with positive αSMA staining (Figure 6.8B) and therefore did not include PANC1 cells which grew in close proximity to CAFs. In order to confirm this finding a Transwell co-culture model was used. This model in which both cell types were separated by a physical barrier confirmed that culturing CAFs and PANC1 cells in the same well reduced the anti-proliferative effect of Gemcitabine on PANC1 cells (Figure 6.9). 3D models have been developed as the future of pharmacological drug screening assays (Horvath et al., 2016). In order to model the tumour microenvironment in PDAC a 3D co-culture model was used. It was found that culturing the cells in 3D in the presence of CAFs reduced the anti-proliferative effect of Gemcitabine more than in a direct 2D or Transwell co-culture model (Figure 6.12). The presence of CAFs within a 2D co-culture model has an impact on pancreatic cancer cell resistance to Gemcitabine. The 3D co-culture model presented herein

causes a complete loss of the anti-proliferative effect of Gemcitabine and therefore is able to better reflect the chemotherapy resistance which is observed in the clinic and may therefore represent a more sophisticated and ultimately more accurate model by which to predict a new treatment's *in vivo* and subsequently clinical efficacy.

It has been suggested that one method by which CAFs increase resistance to chemotherapy is by the secretion of exosomes which contain micro RNAs that upregulate pathways which are involved in chemotherapy resistance in cancer cell lines (Richards et al., 2017). Therefore in the 3D co-culture model described above the cells are in very close contact with one another and exosome signalling could explain the chemotherapy resistance. Additionally, it was found that pre-treating CAFs with Gemcitabine increased the secretion of these exosomes (Richards et al., 2017). In my model both cell types within the spheroid are exposed to Gemcitabine which could stimulate exosome secretion in the CAFs. Recently it has been discovered that CAFs can behave as scavengers and remove Gemcitabine from the PDAC and tumour microenvironment to reduce its availability for epithelial cancer cells (Hessmann et al., 2017). In the 3D co-culture model the presence of CAFs which are able to scavenge Gemcitabine could be contributing to the reduction in the anti-proliferative effect of Gemcitabine in this model. This is reminiscent of the PDAC tumour microenvironment. The presence of CAFs within the 3D co-culture model has been shown to have increase the denseness and compactness of the spheroids compared with the looser structures of the pancreatic cancer cell mono-cultures (Figure 3.7, Figure 3.8.). This suggests that the interactions between the cancer cells and CAFs leaves less exposed surface area for Gemcitabine uptake by PDAC cells which could also impact chemotherapeutic resistance.

Taken together this provides evidence that the PDAC tumour microenvironment is dynamic in its response to chemotherapeutic agents and CAFs play a much more significant role in chemotherapy resistance than as just a physical barrier to chemotherapy.

7. Discussion

PDAC remains one of the most aggressive cancer types and is the fourth leading cause of cancer-related death worldwide (Garrido-Laguna and Hidalgo, 2015). The overall 5-year survival rate for patients diagnosed with PDAC is less than 5% (Siegel et al., 2015) and it is predicted that PDAC will be the second most lethal cancer-related malignancy by 2030 (Rahib et al., 2014). This poor prognosis is in part due to the fact that most patients are diagnosed with advanced disease. In addition, effective tools for screening for PDAC have not yet been developed which makes early detection of this disease unlikely. Once a patient has been diagnosed, there are limited treatment options available with tumour resection giving the most promising outlook for patients with 5-year survival rising to 15-20% (Oettle et al., 2007). However only 20% of patients presenting with PDAC have a resectable tumour (Malafa, 2015). Despite an increased understanding of PDAC tumour biology over the past 10-20 years this has not translated to treatment breakthroughs against this malignancy. This is partly due to the lack of drug screening models which incorporate the tumour microenvironment. Considering the tumour microenvironment makes up over 80% of the PDAC tumour volume (Feig et al., 2012) this is critical in understanding how drugs impact this tumour.

The initial aim of this project was to isolate cells from the PDAC tumour microenvironment and use the cells to develop and characterise a 3D model of PDAC. The changes wrought on the architecture of the pancreas during tumorigenesis were shown using H&E staining (Figure 3.1A) and include the development of a desmoplastic stroma (Waghray et al., 2013). Activated CAFs are the most abundant cell type of the stromal reaction and are identified by their expression of αSMA, which distinguishes them from cancer cells which express pan-cytokeratin (Apte et al., 1998)(Figure 3.1. B&C). CAFs were isolated using the outgrowth method (Bachem et al., 1998) and were characterised using the expression of markers and their

production of collagen 1a1 (Figure 3.2, Figure 3.3.). In order to accurately represent the PDAC tumour microenvironment it would have been preferable to use only cancer cells freshly isolated from tumour tissue samples in the creation of a 3D model, however after trialling various methods, this was not possible (Section 3.2.2.). The difficulties encountered with isolating PDAC cells is consistent with the findings of Ruckert *et al.* (2012) in which the isolation of pancreatic epithelial cancer cell lines was found to have a remarkably low success rate (~10%) with respect to other tumour cell isolates (Ruckert et al., 2012, Dangles-Marie et al., 2007, DeRose et al., 2011). One method of PDAC epithelial cell isolation which has been reported to have a high success rate is the use of patient derived xenografts (Pham et al., 2016). This method involves the implantation of tumour specimens into immune compromised mice; these xenografts are allowed to develop until they reach 1.5cm in diameter at which point they are passaged into new mice. This method has been shown to maintain epithelial cell markers (EpCAM, CK18 and CK19) and the isolated cells remain negative for CD68 and αSMA which is consistent with the original tumour (Pham et al., 2016). For future experiments, cells derived in this manner, in combination with the CAFs used in this project, would potentially allow for the most accurate *in vitro* modelling of CAF: Tumour cell interactions within the PDAC microenvironment. Given that it was not possible to isolate PDAC cells, commercially available cell lines were used. Commercially available pancreatic cancer cell lines have been suggested as a barrier to the development of new therapies as they do not represent the intra-patient tumour cell heterogeneity that exists in cells isolated from primary samples (Cassidy et al., 2015). However, when modelling complex microenvironments with a particular focus on drug development, there exists a fine balance between best representing the complexity of the disease whilst also ensuring a cost effective and reproducible assay. Therefore, five PDAC cell lines were chosen with particular consideration made to best represent patient heterogeneity whilst also ensuring that the selected cell lines

were well characterised with respect to PDAC research (McConkey et al., 2010, Deer et al., 2010, Gradiz et al., 2016, Dalla Pozza et al., 2015).

In furtherance of the development of a 3D model which incorporated CAFs it was necessary to investigate how CAFs and pancreatic cancer cell lines interacted when co-cultured in 3D. The use of 3D cell cultures in cancer research was first trialled by Sutherland and colleagues as early as 1970 (Sutherland et al., 1970). Since then it has been found that culturing cancer cells in 3D results in the maintenance of structures similar to those present in the primary tumour which differentiates these cultures from standard monolayer cultures (Mueller-Klieser, 1987). Indeed, pancreatic cancer cell lines (PANC1 and BXPC3) were shown to grow successfully in multicellular spheroids (Sipos et al., 2003). However, a 3D spheroid model does not accurately represent the tumour microenvironment as it does not incorporate the plethora of other cells present in the microenvironment such as CAFs, immune cells, nerves or blood cells. Given that the microenvironment plays such a key role in PDAC development and maintenance (Waghray et al., 2013, Wang et al., 2016a, Khan et al., 2015) it was necessary to characterise the effect that the addition of CAFs had on spheroids created from PDAC cell lines. In the case of BXPC3, PANC1 and ASPC1 cells, spheroids formed in the absence of CAFs, however MIAPACA2 and SUIT2 cells formed loose structures which did not resemble spheroids. The addition of CAFs to MIAPACA2 and SUIT2 3D cultures allowed spheroids to form which indicates that the CAFs are able to provide structure, most likely in the form of extracellular matrix which allows the formation of spheroids which could not form when tumour cells are cultured alone. Moreover, there were differences in the diameter of the spheroids between spheroids created from mono and co-cultures (Figure 3.8.). Spheroid co-cultures showed a decrease in diameter compared to pancreatic cancer cell line mono-cultures except in the case of MIAPACA2. However, it was difficult to measure a true diameter in the MIAPACA2 mono-culture spheroids as they did not form structurally

stable spheroids. Circularity was increased in co-cultures of PANC1, SUIT2 and MIAPACA2 compared with mono-cultures of the cancer cell lines (Figure 3.9.). Of all five cell lines used in this project these three are the more rapidly proliferating which could be the reason they require the support of ECM produced by CAFs in order to form structurally stable spheroids in culture. Phenotypic observations show the spheroids which contain CAFs appear to be denser with less spaces observed between the cells in the co-cultures of PANC1, SUIT2 and MIAPACA2 with CAFs (Figure 3.7.). ASPC1 cells show clear structural differences in spheroids created from mono and co-culture with CAFs (Figure 3.7.). Thus, incorporating CAFs, which are responsible for the desmoplastic stromal reaction, into 3D culture clearly affected the morphology of spheroids. This work contributes to the development of *in vitro* models which incorporates the interactions between CAFs and PDAC cancer cells.

The distribution of αSMA positive cells throughout the spheroids (Figure 3.10.) resembles the distribution of CAFs within the PDAC tumour microenvironment (Figure 3.1.) and is consistent with previous reports (Ware et al., 2016b). Unfortunately, due to the time limitations of the project it was not possible to complete the staining necessary to fully elucidate the morphology of the cells within the spheroids. Were this to be investigated further it would require staining for pan-cytokeratin and E-cadherin to visualise the location of the pancreatic cancer cell lines and the junctions between the cells. Nevertheless, the circularity, diameter and morphological differences shown when CAFs are incorporated into the spheroids demonstrate that CAFs markedly affect PDAC spheroids when grown in co-culture. The presence of αSMA positive fibroblasts throughout the co-culture suggests that the cells are distributed in a manner that reflects primary patient samples.

Hh and Wnt/β-catenin signalling pathways are involved in the maintenance of the PDAC tumour microenvironment (Morris et al., 2010, Bai et al., 2016, Bailey et al., 2008, Pilarsky et al., 2008). Consequently, the effect of co-culturing CAFs with PDAC

tumour cells had upon these aberrant embryonic signalling pathways was investigated.

The Hh pathway is activated during the development of the gastro-intestinal (GI) tract. Activation of Hh pathway during GI tract development results in the formation of tissues with duodenal properties rather than pancreatic tissue (Hebrok, 2003). Interestingly the Hh pathway is downregulated during pancreatic development (Hebrok, 2003). Moreover, in the adult pancreas, the Hh pathway is found to be restrained to the β-cells of the endocrine pancreas where it is involved in the production of insulin (Thomas et al., 2000). The Hh pathway can become active in the exocrine pancreas in the event of pancreatic injury where it has a role in tissue regeneration (Fendrich et al., 2008). It is clear therefore, that with particular regard to the pancreas, the Hh pathway is tightly regulated such that its activation is not only limited to specific areas but also in response to specific stimuli, namely insulin secretion.

Mutations in Hh pathway components which lead to constitutive activation of the pathway have been identified in some cancers such as basal cell carcinoma and medullablastoma (Fecher and Sharfman, 2015, Archer et al., 2012). In addition, a subset of solid tumours exhibit aberrant ligand-driven Hh pathway activation including colon, ovarian, small-cell lung and pancreatic cancer (Wang et al., 2013, Szkandera et al., 2013, Savani et al., 2012, Yauch et al., 2008). Various reports have shown that in the case of aberrant ligand expression, the tumour cells are resistant to Shh whereas mesenchymal cells of the stroma are Shh responsive as determined by their upregulation of *GLI1 (Nolan-Stevaux et al., 2009, Tian et al., 2009, Yauch et al., 2008)*. Activation of the Hh pathway in PDAC was initially reported by two independent studies (Nakashima et al., 2006, Kasperczyk et al., 2009). Shh expression is detected from PanIN1 throughout disease progression and this expression has been found to correspond directly with oncogenic Kras expression,

indicating that Shh is downstream of $Kras^{G12D}$ during pancreatic tumorigenesis (Ling et al., 2012). Kras is able to influence Shh expression through the NF-κB pathway; the activation of NF-κB signalling *in vitro* can promote transcriptional activity of Shh (Gu et al., 2016). It has been established that Shh expressed by the tumour cancer cells activate SMO-dependant downstream signalling in CAFs in the pancreatic stroma which leads to desmoplasia (Bailey et al., 2008, Feldmann et al., 2007, Olive et al., 2009). IHC visualisation of Shh ligand within the PDAC tumour microenvironment showed Shh expression in the tumour cells lining pancreatic ducts and was found to be absent in the stroma (Figure 4.2.). This is consistent with previous reports (Rucki et al., 2017, Damhofer et al., 2015) and demonstrates that Shh expression is restricted to the tumour cells of the tumour microenvironment. In 2D culture PANC1, MIAPACA2 and SUIT2 cells expressed markedly more Shh than ASPC1, BXPC3 and CAFs. Moreover, the perinuclear pattern of Shh expression in PANC1, MIAPACA2 and SUIT2 is reminiscent of the Shh expression observed in the PDAC tumour microenvironment. This similarity suggests that, despite the inherent limitations associated with immortalized cell lines, PANC1, MIAPACA2 and SUIT2 represented an appropriate PDAC model with respect to Shh signalling. 4/5 PDAC cell lines tested (PANC1, MIAPACA2 SUIT2 and ASPC1) secreted Shh whereas CAFs did not secrete Shh above the limit of detection of the ELISA. This level of Shh protein in cell supernatants was in broad agreement with the cellular expression level determined by IF, and is consistent with previous reports (Yamazaki et al., 2008). Together these data show that Shh is actively secreted by PDAC cells but not by CAFs suggesting that the tumour-supportive role of the stroma (Erkan et al., 2012b) is not mediated directly through Shh-driven proliferation. Rather through Shh, cancer cells are able to communicate with the surrounding microenvironment which supports cancer progression (Gu et al., 2016).

It was possible to activate Hh signalling in CAFs by treating them with rShh ligand (Figure 4.6). Moreover, Shh secreted by pancreatic cancer cells elicited a downstream signalling response in CAFs *in vitro* (Figure 4.7.) demonstrating the ability of pancreatic cancer cells to influence downstream Hh signalling in CAFs, a fact that was confirmed using a Transwell co-culture model (Figure 4.11.). Although GLI1 expression is accepted as a robust read-out for Hh signalling (Pandolfi and Stecca, 2015) other Hh pathway components such as *PTCH11* and *SMO* are also activated in CAFs. The >5-fold upregulation of *GLI1* and >8-fold upregulation of *SMO* mRNA which indicated an activation of Hh pathway in CAFs following co-culture of CAFs and PDAC cells. Likewise, the >9 fold upregulation of *SMO* and >7 fold upregulation *PTCH11* expression also indicates Hh pathway activity. *PTCH11* is not only the receptor for Shh but is an inhibitor of the Hh pathway through inhibition of SMO (Choudhry et al., 2014, Rimkus et al., 2016), however it is also a target of *GLI1* (Shahi et al., 2010) suggesting an auto-inhibitory feedback mechanism is active in this pathway. Nevertheless, the upregulation of SMO, GLI1 and PTCH1 indicate that CAFs are able to respond to a physiologically relevant level of Hh stimulation provided by PANC1 cells. Introducing SMO inhibitors to the transwell co-culture model resulted in a loss of the upregulation of *GLI1* which shows that this co-culture model of CAFs and PDAC cancer cell lines exhibits regulated and active Hh signalling which can be effectively utilised to assess the efficacy of small molecule inhibitors of Hh pathway components. This may therefore provide a model for exploring the underpinning mechanisms of the signalling pathways involved in the PDAC tumour microenvironment, and whether these pathways can be manipulated to produce a clinical benefit. The ability of these cell types to influence one another *in vitro* provides evidence that models of PDAC need to include CAFs to bridge the gap between *in vitro* and *in vivo* testing. Hh pathway inhibitors (SMO antagonists) have been shown to reduce the growth of pancreatic tumours in mice (Olive et al., 2009, Ozdemir et al., 2015), which emphasizes a role for Hh pathway in PDAC tumour development. SMO

inhibitors trialled in the past have not had positive outcomes in the clinic for PDAC; IPI-926 was combined with Gemcitabine in a clinical trial (IPI-926-03 trial; NCT01130142). Unfortunately, the KPC model used in this study was not able to effectively predict the outcome of the long term effects of stromal depletion. Evidence suggests that depletion of the stroma results in more aggressive and metastatic tumour types (Rhim et al., 2014, Ozdemir et al., 2015). Once the stroma was depleted there was an approximate 3-fold upregulation of blood vessels which is responsible for the transient positive effects of increased drug delivery however eventually the increased blood supply led to an increased metastatic phenotype (Rhim et al., 2014). Nevertheless, such a key paracrine signalling mechanism may therefore represent an ideal drug target for PDAC as evidenced by the ability of Redx small molecule SMO inhibitors to disrupt the induction of GLI1 expression in CAFs. Therefore before any further therapies targeting stromal depletion are developed careful consideration needs to given to other components of the PDAC tumour microenvironment such as vasculature and perhaps stromal depletion in combination with angiogenesis inhibition would be more effective. Perhaps, modelling the complexity of the PDAC tumour microenvironment in *in vitro* models will aid in our understanding of the molecular mechanisms which underpin PDAC tumour maintenance and progression, and whether targeted therapies can be translated to a clinical benefit for patients. Furthermore, in light of the limitations of the KPC mouse model perhaps Hh pathway inhibitors in combination with inhibitors of other pathways which are involved in the PDAC tumour microenvironment, such as Wnt pathway still represent a viable targeted therapy approach for treatment of PDAC.

More recently studies have been published which showed that genetic or pharmacological (Hh inhibitors) depletion of the stroma in KPC mice resulted in poorly differentiated tumours which were found to be phenotypically more aggressive and metastatic (Rhim et al., 2014, Ozdemir et al., 2015). This phenomenon had also been

reported in bladder cancer (Shin et al., 2014). Combined these data indicate that the role of the stroma is variable in PDAC progression and metastases. However, what is clear is that tumour cells and CAFs are part of a dynamic signalling network that allows crosstalk between these cell types.

Unlike the Hh signalling pathway, the role of the Wnt signalling pathway in PDAC is poorly understood. Similar to the Hh signalling pathway, mutations which result in constitutive Wnt pathway activation are rare (Jiang et al., 2013, Weekes and Winn, 2011). Despite this, cytoplasmic β-catenin accumulation (in approximately 65% of PDAC cases) is observed in both PanIn and PDAC (White et al., 2012) (Figure 5.1.). Inhibition of β-catenin using siRNA in pancreatic cancer cell lines has been found to significantly reduce proliferation and increase the apoptosis of cancer cells (Pasca di Magliano et al., 2007) indicating a role for the Wnt pathway in maintenance of PDAC tumorigenesis. The mechanism by which β-catenin relates to disease severity is not clear; Wnt ligands which correspond to canonical Wnt signalling have been found to be over expressed in PDAC (Pasca di Magliano et al., 2007, Sano et al., 2016). Wnt7B and Wnt5A have also been found to be present in the PDAC tumour microenvironment; these Wnt ligands are commonly associated with autocrine Wnt signalling (Arensman et al., 2014, Ripka et al., 2007). In contrast, Wnt5A has also been implicated in playing a paracrine role within the PDAC tumour microenvironment, and co-culture experiments showed that pancreatic cancer cell lines could induce Wnt5A expression in CAFs (Ripka et al., 2007). In order for Wnt5A to activate canonical Wnt signalling it interacts with FZD5 which is typically associated with conditions which result in a dysregulation of tissue homeostasis such as the tissue fibrosis commonly observed during liver cirrhosis (Katoh and Katoh, 2007). This could be a potential mechanism by which Wnt signalling is involved in the desmoplastic reaction of PDAC.

Pancreatic development occurs initially in hypoxic conditions which causes the activation of hypoxia inducible factor-1α (HIF-1α) which in turn activates Notch signalling, this is responsible for the proliferation of naive endocrine cells from progenitor cells (Apelqvist et al., 1999). At approximately day 14 neovascularisation of the pancreas occurs which creates normoxic conditions which inhibits Notch signalling and Wnt/β-catenin signalling is activated this results in the proliferation of cells which form the exocrine pancreas (Wells et al., 2007). The interplay between these developmental signalling pathways which exists during pancreatic development could represent a mechanism by with these pathways are involved in pancreatic tumorigenesis. The Notch signalling pathway has been implicating in controlling epithelial to mesenchymal transition (EMT) and Wnt/β-catenin signalling has been implicated in acinar-ductal metaplasia (ADM) (Gungor et al., 2011, Zhang et al., 2013). It is believed that the crosstalk between these pathways has a role in PDAC development (Hindriksen and Bijlsma, 2012) however the interplay between these pathways has not been elucidated. The β-catenin independent Wnt pathway has also been implicated in the development of vasculature during pancreatic tumour development, in particular Wnt5A has been associated with capillary sprouting (Masckauchan et al., 2006). Targeting angiogenesis in PDAC has been ineffective to date; it has been suggested that one way to overcome this is to target both Hh and Wnt pathways to inhibit the stroma and angiogenesis to increase the efficacy of chemotherapy (Weekes and Winn, 2011). I therefore sought to investigate whether the Wnt pathway had any involvement in the crosstalk between CAFs and pancreatic cancer cells. When CAFs and pancreatic cancer cell lines were exposed to external Wnt signals from Wnt3A producing cells there was an upregulation of *AXIN2* mRNA which indicates an upregulation of the Wnt pathway (Figure 5.4, Figure 5.5.). However, this did not give any indication as to whether one cell type was more likely to be Wnt ligand responsive. A Transwell co-culture model, showed an upregulation of *AXIN2* mRNA in PANC1 cells when they were cultured with CAFs (Figure 5.9.)

however there was no change in *AXIN2* in CAFs (Figure 5.10.) indicating that Wnt ligands are produced by CAFs in the PDAC tumour microenvironment. This paracrine signalling mechanism is the opposite to the observations regarding the Hh pathway wherein the Shh is produced by tumour cells and induces downstream signalling in the CAFs. This is interesting as both Hh and Wnt pathways have similar roles in tissue homeostasis in the adult organism especially with regard to maintenance of stem cell populations and wound repair (Petrova and Joyner, 2014, Mohammed et al., 2016, Bai et al., 2016). That a difference exists in the tumour microenvironment suggests that the tight regulation of these pathways which exists during development and homeostasis is lost when the pathways become aberrantly activated in the tumour.

An array of Wnt pathway associated genes found *SFRP4* to be differentially expressed in CAFs compared to NAFs (Figure 5.3.). Furthermore, culturing CAFs and PANC1 cells in the same well resulted in an upregulation of *SFRP4* mRNA in CAFs (Table 5.1, Figure 5.11). As *SFRP4* has been shown to be an inhibitor of Wnt pathway (Ford et al., 2013, Kawano and Kypta, 2003) this indicates the potential presence of antagonists of Wnt signalling in the PDAC tumour microenvironment. In order to fully understand the role of Wnt signalling in PDAC a much more in-depth study is required. Specifically the determination of which Wnt ligands are present in the PDAC tumour microenvironment and whether they are consistent with canonical or non-canonical Wnt pathway activation is needed. Once it is established which pathway or if all are active in the PDAC tumour microenvironment it would be possible to establish the role of Wnt signalling in PDAC. Different combinations of Wnt ligands and Fzd receptors result in the activation of different downstream Wnt pathways which have different consequences within the cell (van Amerongen, 2012). For example the PCP pathway has a role in tumour cell proliferation and resistance to cell death whereas the Wnt/ β-catenin pathway has been linked with anchorage independent growth and invasion of tumour cells (Daulat and Borg, 2017, Sano et al., 2016).

Nevertheless, the discovery that culturing CAFs and pancreatic cancer cells in the same well induced changes in Wnt pathway activation through upregulation of *AXIN2* in PANC1 cells was sufficient to show these cell types are able to signal to one another in an *in vitro* model. It was also possible to inhibit the upregulation of the Wnt pathway in PANC1 resulting from them being cultured with CAFs in a Transwell co-culture model. This inhibition of Wnt pathway was achieved using a Redx PORCN inhibitor (Figure 5.9.), suggesting that this model can be effectively utilised to assess the efficacy of small molecule inhibitors of the Wnt pathway. The identification of the Wnt pathway being dysregulated in a number of human tumours including pancreatic, has led to the development of pharmacological inhibitors of the pathway. PORCN is an o-acetyl transferase which is required for the palmitoylation of Wnt ligands, a process which is required for their secretion. PORCN inhibitors have been identified as a potential therapeutic to target tumours such as colorectal cancer which is driven by the Wnt pathway (Schatoff et al., 2017) but also tumours which have a propensity to metastasize, such as pancreatic and lung (Zeng et al., 2006, Stewart, 2014). This is due to aberrant Wnt pathway activation being detected in cells identified as cancer stem cells (CSCs) which are believed to be involved in resistance to chemotherapy (de Sousa and Vermeulen, 2016).

The ability of a Transwell co-culture model of CAFs and pancreatic cancer cell lines to cause an upregulation of both Hh and Wnt pathways indicates the importance of models which incorporate CAFs and potentially other aspects of the tumour microenvironment. In order to develop new therapies an agent must undergo rigorous testing in cells and animal models; this process can take over 10 years to complete and cost in excess of £500 million (Dickson and Gagnon, 2004). The development of new therapies in cancer is challenging due to the heterogeneity of tumours and the presence of a complex microenvironment which can affect resistance to therapies and overall disease progression. Drug discovery in the field of solid cancers still relies

heavily on testing the efficacy of new drugs on cancer cell lines grown in 2D, which then progresses to subcutaneous xenograft models (Unger et al., 2014). However, these reductionist models often give results which differ from those achieved in clinical trials (Mak et al., 2014). One reason for this is their inability to predict the effect of the tumour microenvironment on the therapies being tested. Therefore traditional methods of testing drug candidates has been under increasing examination and the development of more clinically relevant models which more effectively predict the clinical outcomes is of great importance in drug development (Santo et al., 2017). The overall aim of this project was to create a reproducible model which incorporated aspects of the PDAC tumour microenvironment to be used to screen new therapies. All of the pancreatic cancer cell lines tested (PANC1, MIAPACA2, SUIT2, BXPC3 and ASPC1) were sensitive to the anti-proliferative effect of chemotherapies such as Gemcitabine and Paclitaxel, however CAFs were found to be resistant at 72 and 96h (Figure 6.2, 6.3, 6.4. and 6.5.). This is consistent with previous reports detailing the efficacy of Gemcitabine *in vitro* in cancer cell lines from many tumour types including pancreatic, non-small cell lung, ovarian and bladder cancers (Rathos et al., 2012, Zoli et al., 1999, Boven et al., 1993, Pace et al., 2000, Hayashi et al., 2011). Gemcitabine targets the rapidly proliferating cancer cells, however in the PDAC tumour microenvironment approximately 80% of the tumour mass is composed of CAFs (Xie and Xie, 2015). Richards and colleagues also found CAFs to be intrinsically resistant to Gemcitabine, and CM from CAFs improved the survival of cancer cell lines treated with Gemcitabine (Richards et al., 2017). 2D co-culture models containing CAFs and PANC1 cells show a reduction in the anti-proliferative effect of Gemcitabine on PANC1 cells in the presence of CAFs (Figure 6.8, Figure 6.9.). Furthermore, 3D co-culture models of CAFs and pancreatic cancer cell lines showed a marked effect on the efficacy of Gemcitabine (Figure 6.12.). There are intrinsic mechanisms of Gemcitabine resistance in PDAC such as levels of hENT1 or dCK expression in tumour cells (Giovannetti et al., 2006, Kroep et al., 2002). However, the data

presented herein suggests that CAFs also have an impact on Gemcitabine resistance which is more complex than simply providing a physical barrier to treatment. Fibroblast drug scavenging is one method by which CAFs affect gemcitabine resistance in PDAC. Hessman and colleagues show that the intracellular concentration of Gemcitabine in CAFs is higher than in tumour cells, suggesting that they remove Gemcitabine from the PDAC tumour microenvironment. This reduces the overall exposure of tumour cells to high concentrations of Gemcitabine and its anti-proliferative effect on cancer cells is therefore diminished (Hessmann et al., 2017). Gemcitabine treatment has also been found to promote secretion of exosomes in CAFs which contain factors which induce expression of SNAIL in tumour cells (Richards et al., 2017). SNAIL expression has been found to promote tumour growth, metastases and chemotherapy resistance (Namba et al., 2015, Kaufhold and Bonavida, 2014). Both the exosome secretory role and the scavenging capacity of CAFs could explain the marked reduction in gemcitabine sensitivity when CAFs were co-cultured with PDAC cancer cell lines. Furthermore, 2D models which are commonly used in drug discovery provide an environment wherein every tumour cell has access to oxygen and nutrients which does not reflect the PDAC tumour microenvironment (Mehta et al., 2012). The deposition of collagen by the isolated CAFs contributed to the dense spheroids formed when in co-culture with PDAC cells. A more compact spheroid (with respect to PDAC cells alone) may help this model mimic the nutrient and oxygen restricted environment of the PDAC microenvironment. The lack of CAFs and 3D models may therefore offer an explanation as to why the ability to rapidly screen compounds in 2D cell assays has not resulted in a corresponding increase in approved drugs from the drug development industry. Developmental signalling pathways such as the Hh and Wnt pathways, which have been shown to be active in the PDAC tumour microenvironment, have also been implicated in mechanisms of Gemcitabine resistance (Jia and Xie, 2015). The efflux transporter ABCB2 is a downstream target of Shh and is believed to be involved in

resistance to Gemcitabine in PDAC (Xu et al., 2013). Wnt signalling has been implicated in increased resistance to Gemcitabine in lung cancer cell lines (Zhang et al., 2013); an increase in Wnt5a expression has been associated with increased resistance to apoptosis in response to Gemcitabine treatment in PDAC (Griesmann et al., 2013). Therefore the models presented in this project provide an accurate method by which compounds could be screened in an assay that takes into account the active Hh and Wnt paracrine signalling between CAFs and epithelial cells. Furthermore, this system accounts for the close 3D interaction and potential scavenging role of CAFs within PDAC. Taking such factors into account is necessary in understanding the molecular mechanisms which contribute to chemotherapy resistance in the PDAC tumour microenvironment.

Models which take into consideration the complexity of the tumour microenvironment are necessary to fully understand the factors which will impact the efficacy of chemotherapies. Together the data presented in this project indicate the intricacies of the signalling cross-talk network between CAFs and pancreatic cancer cell lines. To develop therapies to treat this complex disease it is necessary to utilise models which effectively recapitulate aspects of the native tumour tissue.

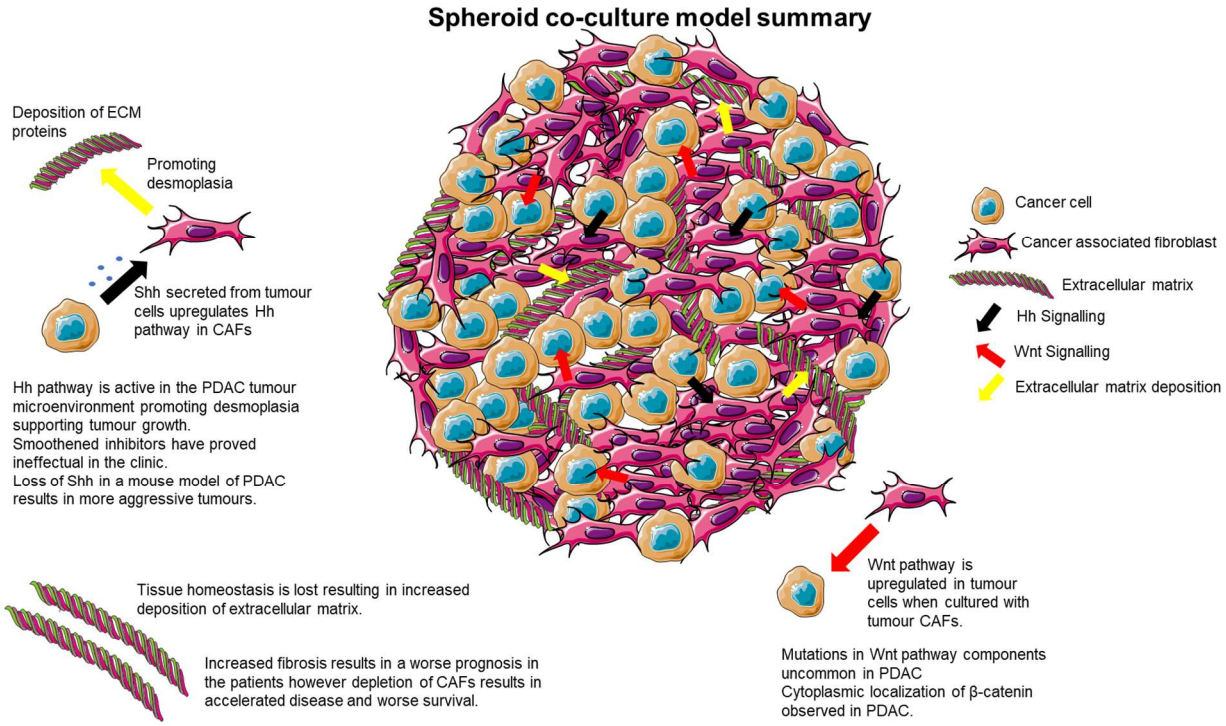

Figure 7.1. Spheroid co-culture model summary

The spheroid co-culture model presented is a mixed culture of CAFS and PDAC cancer cells which more accurately represents the PDAC tumour microenvironment than the standard 2D mono-culture which is most commonly utilised in drug discovery. I have demonstrated that culturing CAFs and PDAC cell lines in the same well (Chapter 5,6) results in active signalling (Hh, Wnt) between CAFs and tumour cells. Therefore it is likely that active signalling exists in the 3D co-culture model presented herein (Black/Red arrows). Additionally, the presence of CAFs in the model will result in the deposition of ECM mimicking the PDAC tumour microenvironment.

Future Directions

In order to continue with this project it is necessary to characterise this model further, I would have liked to stably transfect both the CAFs and tumour cell lines to express an easily identifiable marker such as (GFP or RFP). Once this had been accomplished it would be possible to quantify the proliferation of each cell type over time in the model and on the addition of chemotherapeutic agents, identify which cell type was most affected. In addition it would be interesting to investigate the efficacy of chemotherapies using different dosing methods such as the pulsing method described in chapter 6 (Figure 6.5, Figure 6.6) when they were used in the spheroid co-culture model. The pulsing dosing method more closely mimics the exposure of cells in the PDAC tumour than traditional dosing methods and the more closely we

can recapitulate what is happening in vivo the more chance we have of being able to predict how patients will respond to the chemotherapies.

I was able to establish that culturing CAFs and tumour cells in the same well resulted in active Hh and Wnt signalling. Firstly, I would have like to investigate the levels of Hh and Wnt signalling in the spheroid co-culture model. Then eventually to use the spheroid co-culture model to test investigate combination therapies such as Hh and Wnt pathway inhibitors in combination with Gemcitabine.

References

ADAMSKA, A., DOMENICHINI, A. & FALASCA, M. 2017. Pancreatic Ductal Adenocarcinoma: Current and Evolving Therapies. *Int J Mol Sci,* 18.

AIKIN, R. A., AYERS, K. L. & THEROND, P. P. 2008. The role of kinases in the Hedgehog signalling pathway. *EMBO Rep,* 9**,** 330-6.

AL-AYNATI, M. M., RADULOVICH, N., RIDDELL, R. H. & TSAO, M. S. 2004. Epithelial-cadherin and beta-catenin expression changes in pancreatic intraepithelial neoplasia. *Clin Cancer Res,* 10**,** 1235-40.

ANDERSSON, R., AHO, U., NILSSON, B. I., PETERS, G. J., PASTOR-ANGLADA, M., RASCH, W. & SANDVOLD, M. L. 2009. Gemcitabine chemoresistance in pancreatic cancer: molecular mechanisms and potential solutions. *Scand J Gastroenterol,* 44**,** 782-6.

APELQVIST, A., LI, H., SOMMER, L., BEATUS, P., ANDERSON, D. J., HONJO, T., HRABE DE ANGELIS, M., LENDAHL, U. & EDLUND, H. 1999. Notch signalling controls pancreatic cell differentiation. *Nature,* 400**,** 877-81.

APTE, M. V., HABER, P. S., APPLEGATE, T. L., NORTON, I. D., MCCAUGHAN, G. W., KORSTEN, M. A., PIROLA, R. C. & WILSON, J. S. 1998. Periacinar stellate shaped cells in rat pancreas: identification, isolation, and culture. *Gut,* 43**,** 128-33.

APTE, M. V., PARK, S., PHILLIPS, P. A., SANTUCCI, N., GOLDSTEIN, D., KUMAR, R. K., RAMM, G. A., BUCHLER, M., FRIESS, H., MCCARROLL, J. A., KEOGH, G., MERRETT, N., PIROLA, R. & WILSON, J. S. 2004. Desmoplastic reaction in pancreatic cancer: role of pancreatic stellate cells. *Pancreas,* 29**,** 179-87.

APTE, M. V. & WILSON, J. S. 2012. Dangerous liaisons: pancreatic stellate cells and pancreatic cancer cells. *J Gastroenterol Hepatol,* 27 Suppl 2**,** 69-74.

APTE, M. V., WILSON, J. S., LUGEA, A. & PANDOL, S. J. 2013. A starring role for stellate cells in the pancreatic cancer microenvironment. *Gastroenterology,* 144**,** 1210-9.

ARCHER, T. C., WEERARATNE, S. D. & POMEROY, S. L. 2012. Hedgehog-GLI pathway in medulloblastoma. *J Clin Oncol,* 30**,** 2154-6.

ARENSMAN, M. D., KOVOCHICH, A. N., KULIKAUSKAS, R. M., LAY, A. R., YANG, P. T., LI, X., DONAHUE, T., MAJOR, M. B., MOON, R. T., CHIEN, A. J. & DAWSON, D. W. 2014. WNT7B mediates autocrine Wnt/beta-catenin signaling and anchorage-independent growth in pancreatic adenocarcinoma. *Oncogene,* 33**,** 899-908.

ARVELO, F., SOJO, F. & COTTE, C. 2016. Tumour progression and metastasis. *Ecancermedicalscience,* 10**,** 617.

AWASTHI, N., ZHANG, C., SCHWARZ, A. M., HINZ, S., WANG, C., WILLIAMS, N. S., SCHWARZ, M. A. & SCHWARZ, R. E. 2013. Comparative benefits of Nab-paclitaxel over gemcitabine or polysorbate-based docetaxel in experimental pancreatic cancer. *Carcinogenesis,* 34**,** 2361-9.

BAARSMA, H. A., SPANJER, A. I., HAITSMA, G., ENGELBERTINK, L. H., MEURS, H., JONKER, M. R., TIMENS, W., POSTMA, D. S., KERSTJENS, H. A. & GOSENS, R. 2011. Activation of WNT/beta-catenin signaling in pulmonary fibroblasts by TGF-beta(1) is increased in chronic obstructive pulmonary disease. *PLoS One,* 6**,** e25450.

BACHEM, M. G., SCHNEIDER, E., GROSS, H., WEIDENBACH, H., SCHMID, R. M., MENKE, A., SIECH, M., BEGER, H., GRUNERT, A. & ADLER, G. 1998. Identification, culture, and characterization of pancreatic stellate cells in rats and humans. *Gastroenterology,* 115**,** 421-32.

BACHEM, M. G., SCHUNEMANN, M., RAMADANI, M., SIECH, M., BEGER, H., BUCK, A., ZHOU, S., SCHMID-KOTSAS, A. & ADLER, G. 2005. Pancreatic carcinoma cells induce fibrosis by stimulating proliferation and matrix synthesis of stellate cells. *Gastroenterology,* 128**,** 907-21.

BACHMANN, J., RAUE, A., SCHILLING, M., BOHM, M. E., KREUTZ, C., KASCHEK, D., BUSCH, H., GRETZ, N., LEHMANN, W. D., TIMMER, J. & KLINGMULLER, U. 2011. Division of labor by dual feedback regulators controls JAK2/STAT5 signaling over broad ligand range. *Mol Syst Biol,* 7**,** 516.

BAFICO, A., LIU, G., GOLDIN, L., HARRIS, V. & AARONSON, S. A. 2004. An autocrine mechanism for constitutive Wnt pathway activation in human cancer cells. *Cancer Cell,* 6**,** 497-506.

BAI, Y., BAI, Y., DONG, J., LI, Q., JIN, Y., CHEN, B. & ZHOU, M. 2016. Hedgehog Signaling in Pancreatic Fibrosis and Cancer. *Medicine (Baltimore),* 95**,** e2996.

BAILEY, J. M., MOHR, A. M. & HOLLINGSWORTH, M. A. 2009. Sonic hedgehog paracrine signaling regulates metastasis and lymphangiogenesis in pancreatic cancer. *Oncogene,* 28**,** 3513-25.

BAILEY, J. M., SWANSON, B. J., HAMADA, T., EGGERS, J. P., SINGH, P. K., CAFFERY, T., OUELLETTE, M. M. & HOLLINGSWORTH, M. A. 2008. Sonic hedgehog promotes desmoplasia in pancreatic cancer. *Clin Cancer Res,* 14**,** 5995-6004.

BANGS, F. & ANDERSON, K. V. 2017. Primary Cilia and Mammalian Hedgehog Signaling. *Cold Spring Harb Perspect Biol,* 9.

BAPAT, A. A., HOSTETTER, G., VON HOFF, D. D. & HAN, H. 2011. Perineural invasion and associated pain in pancreatic cancer. *Nat Rev Cancer,* 11**,** 695-707.

BARRETT, M. T., DEIOTTE, R., LENKIEWICZ, E., MALASI, S., HOLLEY, T., EVERS, L., POSNER, R. G., JONES, T., HAN, H., SAUSEN, M., VELCULESCU, V. E., DREBIN, J., O'DWYER, P., JAMESON, G., RAMANATHAN, R. K. & VON HOFF, D. D. 2017. Clinical study of genomic drivers in pancreatic ductal adenocarcinoma. *Br J Cancer,* 117**,** 572-582.

BEACHY, P. A., HYMOWITZ, S. G., LAZARUS, R. A., LEAHY, D. J. & SIEBOLD, C. 2010. Interactions between Hedgehog proteins and their binding partners come into view. *Genes Dev,* 24**,** 2001-12.

BECKER, A. E., HERNANDEZ, Y. G., FRUCHT, H. & LUCAS, A. L. 2014. Pancreatic ductal adenocarcinoma: risk factors, screening, and early detection. *World J Gastroenterol,* 20**,** 11182-98.

BERNARD, P., FLEMING, A., LACOMBE, A., HARLEY, V. R. & VILAIN, E. 2008. Wnt4 inhibits beta-catenin/TCF signalling by redirecting beta-catenin to the cell membrane. *Biol Cell,* 100**,** 167-77.

BIANKIN, A. V., WADDELL, N., KASSAHN, K. S., GINGRAS, M. C., MUTHUSWAMY, L. B., JOHNS, A. L., MILLER, D. K., WILSON, P. J., PATCH, A. M., WU, J., CHANG, D. K., COWLEY, M. J., GARDINER, B. B., SONG, S., HARLIWONG, I., IDRISOGLU, S., NOURSE, C.,

NOURBAKHSH, E., MANNING, S., WANI, S., GONGORA, M., PAJIC, M., SCARLETT, C. J., GILL, A. J., PINHO, A. V., ROOMAN, I., ANDERSON, M., HOLMES, O., LEONARD, C., TAYLOR, D., WOOD, S., XU, Q., NONES, K., FINK, J. L., CHRIST, A., BRUXNER, T., CLOONAN, N., KOLLE, G., NEWELL, F., PINESE, M., MEAD, R. S., HUMPHRIS, J. L., KAPLAN, W., JONES, M. D., COLVIN, E. K., NAGRIAL, A. M., HUMPHREY, E. S., CHOU, A., CHIN, V. T., CHANTRILL, L. A., MAWSON, A., SAMRA, J. S., KENCH, J. G., LOVELL, J. A., DALY, R. J., MERRETT, N. D., TOON, C., EPARI, K., NGUYEN, N. Q., BARBOUR, A., ZEPS, N., AUSTRALIAN PANCREATIC CANCER GENOME, I., KAKKAR, N., ZHAO, F., WU, Y. Q., WANG, M., MUZNY, D. M., FISHER, W. E., BRUNICARDI, F. C., HODGES, S. E., REID, J. G., DRUMMOND, J., CHANG, K., HAN, Y., LEWIS, L. R., DINH, H., BUHAY, C. J., BECK, T., TIMMS, L., SAM, M., BEGLEY, K., BROWN, A., PAI, D., PANCHAL, A., BUCHNER, N., DE BORJA, R., DENROCHE, R. E., YUNG, C. K., SERRA, S., ONETTO, N., MUKHOPADHYAY, D., TSAO, M. S., SHAW, P. A., PETERSEN, G. M., GALLINGER, S., HRUBAN, R. H., MAITRA, A., IACOBUZIO-DONAHUE, C. A., SCHULICK, R. D., WOLFGANG, C. L., et al. 2012. Pancreatic cancer genomes reveal aberrations in axon guidance pathway genes. *Nature,* 491**,** 399-405.

BISHOP, J. M. 1991. Molecular themes in oncogenesis. *Cell,* 64**,** 235-48.

BITGOOD, M. J., SHEN, L. & MCMAHON, A. P. 1996. Sertoli cell signaling by Desert hedgehog regulates the male germline. *Curr Biol,* 6**,** 298-304.

BOVEN, E., SCHIPPER, H., ERKELENS, C. A., HATTY, S. A. & PINEDO, H. M. 1993. The influence of the schedule and the dose of gemcitabine on the anti-tumour efficacy in experimental human cancer. *Br J Cancer,* 68**,** 52-6.

BOYNTON, R. F., BLOUNT, P. L., YIN, J., BROWN, V. L., HUANG, Y., TONG, Y., MCDANIEL, T., NEWKIRK, C., RESAU, J. H., RASKIND, W. H., HAGGITT, R. C., REID, B. J. & MELTZER, S. J. 1992. Loss of heterozygosity involving the APC and MCC genetic loci occurs in the majority of human esophageal cancers. *Proc Natl Acad Sci U S A,* 89**,** 3385-8.

BRABLETZ, T., JUNG, A., REU, S., PORZNER, M., HLUBEK, F., KUNZ-SCHUGHART, L. A., KNUECHEL, R. & KIRCHNER, T. 2001. Variable beta-catenin expression in colorectal cancers indicates tumor progression driven by the tumor environment. *Proc Natl Acad Sci U S A,* 98**,** 10356-61.

BRACCI, P. M. 2012. Obesity and pancreatic cancer: overview of epidemiologic evidence and biologic mechanisms. *Mol Carcinog,* 51**,** 53-63.

BRISCOE, J. & THEROND, P. P. 2013. The mechanisms of Hedgehog signalling and its roles in development and disease. *Nat Rev Mol Cell Biol,* 14**,** 416-29.

BURKHART, D. L. & SAGE, J. 2008. Cellular mechanisms of tumour suppression by the retinoblastoma gene. *Nat Rev Cancer,* 8**,** 671-82.

BURRIS, H. A., MOORE, M. J., ANDERSEN, J., GREEN, M. R., ROTHENBERG, M. L., MODIANO, M. R., CRIPPS, M. C., PORTENOY, R. K., STORNIOLO, A. M., TARASSOFF, P., NELSON, R., DORR, F. A., STEPHENS, C. D. & HOFF, D. D. V. 1997. Improvements in survival and clinical benefit with gemcitabine as first-line therapy for patients with advanced pancreas cancer: a randomized trial. *Journal of Clinical Oncology,* 15**,** 2403-2413.

CAI, J., ZHANG, N., ZHENG, Y., DE WILDE, R. F., MAITRA, A. & PAN, D. 2010. The Hippo signaling pathway restricts the oncogenic potential of an intestinal regeneration program. *Genes Dev,* 24**,** 2383-8.

CAJANEK, L., ADLERZ, L., BRYJA, V. & ARENAS, E. 2010. WNT unrelated activities in commercially available preparations of recombinant WNT3a. *J Cell Biochem,* 111**,** 1077-9.

CANTU, A. V. & LAIRD, D. J. 2013. Wnt and Bmp fit germ cells to a T. *Dev Cell,* 27**,** 485-7.

CARR, R. M. & FERNANDEZ-ZAPICO, M. E. 2016. Pancreatic cancer microenvironment, to target or not to target? *EMBO Mol Med,* 8**,** 80-2.

CASSIDY, J. W., CALDAS, C. & BRUNA, A. 2015. Maintaining Tumor Heterogeneity in Patient-Derived Tumor Xenografts. *Cancer Res,* 75**,** 2963-8.

CERQUEIRA, N. M., FERNANDES, P. A. & RAMOS, M. J. 2007. Understanding ribonucleotide reductase inactivation by gemcitabine. *Chemistry,* 13**,** 8507-15.

CHARI, S. T., KELLY, K., HOLLINGSWORTH, M. A., THAYER, S. P., AHLQUIST, D. A., ANDERSEN, D. K., BATRA, S. K., BRENTNALL, T. A., CANTO, M., CLEETER, D. F., FIRPO, M. A., GAMBHIR, S. S., GO, V. L., HINES, O. J., KENNER, B. J., KLIMSTRA, D. S., LERCH, M. M., LEVY, M. J., MAITRA, A., MULVIHILL, S. J., PETERSEN, G. M., RHIM, A. D., SIMEONE, D. M., SRIVASTAVA, S., TANAKA, M., VINIK, A. I. & WONG, D. 2015. Early detection of sporadic pancreatic cancer: summative review. *Pancreas,* 44**,** 693-712.

CHARI, S. T., LEIBSON, C. L., RABE, K. G., TIMMONS, L. J., RANSOM, J., DE ANDRADE, M. & PETERSEN, G. M. 2008. Pancreatic cancer-associated diabetes mellitus: prevalence and temporal association with diagnosis of cancer. *Gastroenterology,* 134**,** 95-101.

CHEN, H., ZUO, Q., WANG, Y., AHMED, M. F., JIN, K., SONG, J., ZHANG, Y. & LI, B. 2016. Regulation of Hedgehog Signaling in Chicken Embryonic Stem Cells Differentiation Into Male Germ Cells (Gallus). *J Cell Biochem*.

CHEN, M. H., LI, Y. J., KAWAKAMI, T., XU, S. M. & CHUANG, P. T. 2004. Palmitoylation is required for the production of a soluble multimeric Hedgehog protein complex and long-range signaling in vertebrates. *Genes Dev,* 18**,** 641-59.

CHEN, W. H., HOROSZEWICZ, J. S., LEONG, S. S., SHIMANO, T., PENETRANTE, R., SANDERS, W. H., BERJIAN, R., DOUGLASS, H. O., MARTIN, E. W. & CHU, T. M. 1982. Human pancreatic adenocarcinoma: in vitro and in vivo morphology of a new tumor line established from ascites. *In Vitro,* 18**,** 24-34.

CHIFENTI, B., MORELLI, M., ZAVAGLIA, M., COVIELLO, D. A., GUERNERI, S., SANTUCCI, A., PAFFETTI, A., MASETTI, M., LOCCI, M. T., BERTACCA, G., CAPODANNO, A., COLLECCHI, P., CAMPANI, D., MOSCA, F., BEVILACQUA, G. & CAVAZZANA, A. O. 2009. Establishment and characterization of 4 new human pancreatic cancer cell lines: evidences of different tumor phenotypes. *Pancreas,* 38**,** 184-96.

CHIURILLO, M. A. 2015. Role of the Wnt/beta-catenin pathway in gastric cancer: An in-depth literature review. *World J Exp Med,* 5**,** 84-102.

CHOE, J. Y., YUN, J. Y., JEON, Y. K., KIM, S. H., CHOUNG, H. K., OH, S., PARK, M. & KIM, J. E. 2015. Sonic hedgehog signalling proteins are

frequently expressed in retinoblastoma and are associated with aggressive clinicopathological features. *J Clin Pathol,* 68**,** 6-11.
CHOI, Y. S., ZHANG, Y., XU, M., YANG, Y., ITO, M., PENG, T., CUI, Z., NAGY, A., HADJANTONAKIS, A. K., LANG, R. A., COTSARELIS, G., ANDL, T., MORRISEY, E. E. & MILLAR, S. E. 2013. Distinct functions for Wnt/beta-catenin in hair follicle stem cell proliferation and survival and interfollicular epidermal homeostasis. *Cell Stem Cell,* 13**,** 720-33.
CHOUDHRY, Z., RIKANI, A. A., CHOUDHRY, A. M., TARIQ, S., ZAKARIA, F., ASGHAR, M. W., SARFRAZ, M. K., HAIDER, K., SHAFIQ, A. A. & MOBASSARAH, N. J. 2014. Sonic hedgehog signalling pathway: a complex network. *Ann Neurosci,* 21**,** 28-31.
CHUONG, C. M., PATEL, N., LIN, J., JUNG, H. S. & WIDELITZ, R. B. 2000. Sonic hedgehog signaling pathway in vertebrate epithelial appendage morphogenesis: perspectives in development and evolution. *Cell Mol Life Sci,* 57**,** 1672-81.
CICENAS, J., KVEDERAVICIUTE, K., MESKINYTE, I., MESKINYTE-KAUSILIENE, E., SKEBERDYTE, A. & CICENAS, J. 2017. KRAS, TP53, CDKN2A, SMAD4, BRCA1, and BRCA2 Mutations in Pancreatic Cancer. *Cancers (Basel),* 9.
CID-ARREGUI, A. & JUAREZ, V. 2015. Perspectives in the treatment of pancreatic adenocarcinoma. *World J Gastroenterol,* 21**,** 9297-316.
CLARK, C. E., HINGORANI, S. R., MICK, R., COMBS, C., TUVESON, D. A. & VONDERHEIDE, R. H. 2007. Dynamics of the immune reaction to pancreatic cancer from inception to invasion. *Cancer Res,* 67**,** 9518-27.
CLEVERS, H. 2006. Wnt/beta-catenin signaling in development and disease. *Cell,* 127**,** 469-80.
COHEN, M., KICHEVA, A., RIBEIRO, A., BLASSBERG, R., PAGE, K. M., BARNES, C. P. & BRISCOE, J. 2015. Ptch1 and Gli regulate Shh signalling dynamics via multiple mechanisms. *Nat Commun,* 6**,** 6709.
CONG, F. & VARMUS, H. 2004. Nuclear-cytoplasmic shuttling of Axin regulates subcellular localization of beta-catenin. *Proc Natl Acad Sci U S A,* 101**,** 2882-7.
COOK, N., FRESE, K. K., BAPIRO, T. E., JACOBETZ, M. A., GOPINATHAN, A., MILLER, J. L., RAO, S. S., DEMUTH, T., HOWAT, W. J., JODRELL, D. I. & TUVESON, D. A. 2012. Gamma secretase inhibition promotes hypoxic necrosis in mouse pancreatic ductal adenocarcinoma. *J Exp Med,* 209**,** 437-44.
CORDENONSI, M., ZANCONATO, F., AZZOLIN, L., FORCATO, M., ROSATO, A., FRASSON, C., INUI, M., MONTAGNER, M., PARENTI, A. R., POLETTI, A., DAIDONE, M. G., DUPONT, S., BASSO, G., BICCIATO, S. & PICCOLO, S. 2011. The Hippo transducer TAZ confers cancer stem cell-related traits on breast cancer cells. *Cell,* 147**,** 759-72.
CRUK. 2016. *Cancer Research UK* [Online]. Available: http://www.cancerresearchuk.org/health-professional/cancer-statistics/worldwide-cancer#heading-Two [Accessed 09/10/2016 2016].
CURTO, M., COLE, B. K., LALLEMAND, D., LIU, C. H. & MCCLATCHEY, A. I. 2007. Contact-dependent inhibition of EGFR signaling by Nf2/Merlin. *J Cell Biol,* 177**,** 893-903.
DALLA POZZA, E., DANDO, I., BIONDANI, G., BRANDI, J., COSTANZO, C., ZORATTI, E., FASSAN, M., BOSCHI, F., MELISI, D., CECCONI, D.,

SCUPOLI, M. T., SCARPA, A. & PALMIERI, M. 2015. Pancreatic ductal adenocarcinoma cell lines display a plastic ability to bidirectionally convert into cancer stem cells. *Int J Oncol,* 46**,** 1099-108.
DAMARAJU, V. L., DAMARAJU, S., YOUNG, J. D., BALDWIN, S. A., MACKEY, J., SAWYER, M. B. & CASS, C. E. 2003. Nucleoside anticancer drugs: the role of nucleoside transporters in resistance to cancer chemotherapy. *Oncogene,* 22**,** 7524-36.
DAMHOFER, H., EBBING, E. A., STEINS, A., WELLING, L., TOL, J. A., KRISHNADATH, K. K., VAN LEUSDEN, T., VAN DE VIJVER, M. J., BESSELINK, M. G., BUSCH, O. R., VAN BERGE HENEGOUWEN, M. I., VAN DELDEN, O., MEIJER, S. L., DIJK, F., MEDEMA, J. P., VAN LAARHOVEN, H. W. & BIJLSMA, M. F. 2015. Establishment of patient-derived xenograft models and cell lines for malignancies of the upper gastrointestinal tract. *J Transl Med,* 13**,** 115.
DANGLES-MARIE, V., POCARD, M., RICHON, S., WEISWALD, L. B., ASSAYAG, F., SAULNIER, P., JUDDE, J. G., JANNEAU, J. L., AUGER, N., VALIDIRE, P., DUTRILLAUX, B., PRAZ, F., BELLET, D. & POUPON, M. F. 2007. Establishment of human colon cancer cell lines from fresh tumors versus xenografts: comparison of success rate and cell line features. *Cancer Res,* 67**,** 398-407.
DAUER, P., NOMURA, A., SALUJA, A. & BANERJEE, S. 2017. Microenvironment in determining chemo-resistance in pancreatic cancer: Neighborhood matters. *Pancreatology,* 17**,** 7-12.
DAULAT, A. M. & BORG, J.-P. 2017. Wnt/Planar Cell Polarity Signaling: New Opportunities for Cancer Treatment. *Trends in Cancer,* 3**,** 113-125.
DE, A. 2011. Wnt/Ca2+ signaling pathway: a brief overview. *Acta Biochim Biophys Sin (Shanghai),* 43**,** 745-56.
DE LANGHE, S. P. & REYNOLDS, S. D. 2008. Wnt signaling in lung organogenesis. *Organogenesis,* 4**,** 100-8.
DE SOUSA, E. M. F. & VERMEULEN, L. 2016. Wnt Signaling in Cancer Stem Cell Biology. *Cancers (Basel),* 8.
DEER, E. L., GONZALEZ-HERNANDEZ, J., COURSEN, J. D., SHEA, J. E., NGATIA, J., SCAIFE, C. L., FIRPO, M. A. & MULVIHILL, S. J. 2010. Phenotype and genotype of pancreatic cancer cell lines. *Pancreas,* 39**,** 425-35.
DERAZ, E. M., KUDO, Y., YOSHIDA, M., OBAYASHI, M., TSUNEMATSU, T., TANI, H., SIRIWARDENA, S. B., KEIKHAEE, M. R., QI, G., IIZUKA, S., OGAWA, I., CAMPISI, G., LO MUZIO, L., ABIKO, Y., KIKUCHI, A. & TAKATA, T. 2011. MMP-10/stromelysin-2 promotes invasion of head and neck cancer. *PLoS One,* 6**,** e25438.
DEROSE, Y. S., WANG, G., LIN, Y. C., BERNARD, P. S., BUYS, S. S., EBBERT, M. T., FACTOR, R., MATSEN, C., MILASH, B. A., NELSON, E., NEUMAYER, L., RANDALL, R. L., STIJLEMAN, I. J., WELM, B. E. & WELM, A. L. 2011. Tumor grafts derived from women with breast cancer authentically reflect tumor pathology, growth, metastasis and disease outcomes. *Nat Med,* 17**,** 1514-20.
DICKSON, M. & GAGNON, J. P. 2004. Key factors in the rising cost of new drug discovery and development. *Nat Rev Drug Discov,* 3**,** 417-29.
DIJKSTERHUIS, J. P., PETERSEN, J. & SCHULTE, G. 2014. WNT/Frizzled signalling: receptor-ligand selectivity with focus on FZD-G protein signalling

and its physiological relevance: IUPHAR Review 3. *Br J Pharmacol,* 171**,** 1195-209.
DYER, M. A., FARRINGTON, S. M., MOHN, D., MUNDAY, J. R. & BARON, M. H. 2001. Indian hedgehog activates hematopoiesis and vasculogenesis and can respecify prospective neurectodermal cell fate in the mouse embryo. *Development,* 128**,** 1717-30.
EATON, S. 2008. Multiple roles for lipids in the Hedgehog signalling pathway. *Nat Rev Mol Cell Biol,* 9**,** 437-45.
ECHELARD, Y., EPSTEIN, D. J., ST-JACQUES, B., SHEN, L., MOHLER, J., MCMAHON, J. A. & MCMAHON, A. P. 1993. Sonic hedgehog, a member of a family of putative signaling molecules, is implicated in the regulation of CNS polarity. *Cell,* 75**,** 1417-1430.
EGEBLAD, M., RASCH, M. G. & WEAVER, V. M. 2010. Dynamic interplay between the collagen scaffold and tumor evolution. *Curr Opin Cell Biol,* 22**,** 697-706.
EGGENSCHWILER, J. T., BULGAKOV, O. V., QIN, J., LI, T. & ANDERSON, K. V. 2006. Mouse Rab23 regulates hedgehog signaling from smoothened to Gli proteins. *Dev Biol,* 290**,** 1-12.
EGGENSCHWILER, J. T., ESPINOZA, E. & ANDERSON, K. V. 2001. Rab23 is an essential negative regulator of the mouse Sonic hedgehog signalling pathway. *Nature,* 412**,** 194-8.
ENGVALL, E. & PERLMANN, P. 1971. Enzyme-linked immunosorbent assay (ELISA). Quantitative assay of immunoglobulin G. *Immunochemistry,* 8**,** 871-4.
ERKAN, M., ADLER, G., APTE, M. V., BACHEM, M. G., BUCHHOLZ, M., DETLEFSEN, S., ESPOSITO, I., FRIESS, H., GRESS, T. M., HABISCH, H. J., HWANG, R. F., JASTER, R., KLEEFF, J., KLOPPEL, G., KORDES, C., LOGSDON, C. D., MASAMUNE, A., MICHALSKI, C. W., OH, J., PHILLIPS, P. A., PINZANI, M., REISER-ERKAN, C., TSUKAMOTO, H. & WILSON, J. 2012a. StellaTUM: current consensus and discussion on pancreatic stellate cell research. *Gut,* 61**,** 172-8.
ERKAN, M., HAUSMANN, S., MICHALSKI, C. W., FINGERLE, A. A., DOBRITZ, M., KLEEFF, J. & FRIESS, H. 2012b. The role of stroma in pancreatic cancer: diagnostic and therapeutic implications. *Nat Rev Gastroenterol Hepatol,* 9**,** 454-67.
ERKAN, M., MICHALSKI, C. W., RIEDER, S., REISER-ERKAN, C., ABIATARI, I., KOLB, A., GIESE, N. A., ESPOSITO, I., FRIESS, H. & KLEEFF, J. 2008. The activated stroma index is a novel and independent prognostic marker in pancreatic ductal adenocarcinoma. *Clin Gastroenterol Hepatol,* 6**,** 1155-61.
ERKAN, M., REISER-ERKAN, C., MICHALSKI, C. W., DEUCKER, S., SAULIUNAITE, D., STREIT, S., ESPOSITO, I., FRIESS, H. & KLEEFF, J. 2009. Cancer-stellate cell interactions perpetuate the hypoxia-fibrosis cycle in pancreatic ductal adenocarcinoma. *Neoplasia,* 11**,** 497-508.
ESER, S., SCHNIEKE, A., SCHNEIDER, G. & SAUR, D. 2014. Oncogenic KRAS signalling in pancreatic cancer. *Br J Cancer,* 111**,** 817-22.
ESTEVE, P., SANDONIS, A., IBANEZ, C., SHIMONO, A., GUERRERO, I. & BOVOLENTA, P. 2011. Secreted frizzled-related proteins are required for Wnt/beta-catenin signalling activation in the vertebrate optic cup. *Development,* 138**,** 4179-84.

ESTRADA, M. F., REBELO, S. P., DAVIES, E. J., PINTO, M. T., PEREIRA, H., SANTO, V. E., SMALLEY, M. J., BARRY, S. T., GUALDA, E. J., ALVES, P. M., ANDERSON, E. & BRITO, C. 2016. Modelling the tumour microenvironment in long-term microencapsulated 3D co-cultures recapitulates phenotypic features of disease progression. *Biomaterials,* 78**,** 50-61.

FAGOTTO, F., GLUCK, U. & GUMBINER, B. M. 1998. Nuclear localization signal-independent and importin/karyopherin-independent nuclear import of beta-catenin. *Curr Biol,* 8**,** 181-90.

FANG, Y. & EGLEN, R. M. 2017. Three-Dimensional Cell Cultures in Drug Discovery and Development. *SLAS Discov,* 22**,** 456-472.

FARROW, B., ALBO, D. & BERGER, D. H. 2008. The role of the tumor microenvironment in the progression of pancreatic cancer. *J Surg Res,* 149**,** 319-28.

FECHER, L. A. & SHARFMAN, W. H. 2015. Advanced basal cell carcinoma, the hedgehog pathway, and treatment options - role of smoothened inhibitors. *Biologics,* 9**,** 129-40.

FEIG, C., GOPINATHAN, A., NEESSE, A., CHAN, D. S., COOK, N. & TUVESON, D. A. 2012. The pancreas cancer microenvironment. *Clin Cancer Res,* 18**,** 4266-76.

FELDMANN, G., DHARA, S., FENDRICH, V., BEDJA, D., BEATY, R., MULLENDORE, M., KARIKARI, C., ALVAREZ, H., IACOBUZIO-DONAHUE, C., JIMENO, A., GABRIELSON, K. L., MATSUI, W. & MAITRA, A. 2007. Blockade of hedgehog signaling inhibits pancreatic cancer invasion and metastases: a new paradigm for combination therapy in solid cancers. *Cancer Res,* 67**,** 2187-96.

FELIX RÜCKERT, C. P. A. R. G. 2012. *Establishment of Primary Cell Lines in Pancreatic Cancer, Pancreatic Cancer - Molecular Mechanism and Targets,* Available from: http://www.intechopen.com/books/pancreatic-cancermolecular-mechanism-and-targets/establishment-of-primary-cell-lines-in-pancreatic-cancer, *InTech*.

FENDRICH, V., ESNI, F., GARAY, M. V., FELDMANN, G., HABBE, N., JENSEN, J. N., DOR, Y., STOFFERS, D., JENSEN, J., LEACH, S. D. & MAITRA, A. 2008. Hedgehog signaling is required for effective regeneration of exocrine pancreas. *Gastroenterology,* 135**,** 621-31.

FERLAY, J., SOERJOMATARAM, I., DIKSHIT, R., ESER, S., MATHERS, C., REBELO, M., PARKIN, D. M., FORMAN, D. & BRAY, F. 2015. Cancer incidence and mortality worldwide: sources, methods and major patterns in GLOBOCAN 2012. *Int J Cancer,* 136**,** E359-86.

FERRARA, N. 2010. Pathways mediating VEGF-independent tumor angiogenesis. *Cytokine Growth Factor Rev,* 21**,** 21-6.

FILALI, M., CHENG, N., ABBOTT, D., LEONTIEV, V. & ENGELHARDT, J. F. 2002. Wnt-3A/beta-catenin signaling induces transcription from the LEF-1 promoter. *J Biol Chem,* 277**,** 33398-410.

FISCHER, A. H., JACOBSON, K. A., ROSE, J. & ZELLER, R. 2008. Hematoxylin and eosin staining of tissue and cell sections. *CSH Protoc,* 2008**,** pdb prot4986.

FOGLI, S., DANESI, R., GENNARI, A., DONATI, S., CONTE, P. F. & DEL TACCA, M. 2002. Gemcitabine, epirubicin and paclitaxel: pharmacokinetic

and pharmacodynamic interactions in advanced breast cancer. *Ann Oncol,* 13**,** 919-27.
FORD, C. E., JARY, E., MA, S. S., NIXDORF, S., HEINZELMANN-SCHWARZ, V. A. & WARD, R. L. 2013. The Wnt gatekeeper SFRP4 modulates EMT, cell migration and downstream Wnt signalling in serous ovarian cancer cells. *PLoS One,* 8**,** e54362.
FRESE, K. K., NEESSE, A., COOK, N., BAPIRO, T. E., LOLKEMA, M. P., JODRELL, D. I. & TUVESON, D. A. 2012. nab-Paclitaxel potentiates gemcitabine activity by reducing cytidine deaminase levels in a mouse model of pancreatic cancer. *Cancer Discov,* 2**,** 260-269.
FRESHNEY, R. I. & FRESHNEY, R. I. 2005. Culture of Specific Cell Types. *Culture of Animal Cells.* John Wiley & Sons, Inc.
FROELING, F. E., FEIG, C., CHELALA, C., DOBSON, R., MEIN, C. E., TUVESON, D. A., CLEVERS, H., HART, I. R. & KOCHER, H. M. 2011. Retinoic acid-induced pancreatic stellate cell quiescence reduces paracrine Wnt-beta-catenin signaling to slow tumor progression. *Gastroenterology,* 141**,** 1486-97, 1497 e1-14.
FUERER, C., HABIB, S. J. & NUSSE, R. 2010. A study on the interactions between heparan sulfate proteoglycans and Wnt proteins. *Dev Dyn,* 239**,** 184-90.
FUJITA, H., OHUCHIDA, K., MIZUMOTO, K., ITABA, S., ITO, T., NAKATA, K., YU, J., KAYASHIMA, T., SOUZAKI, R., TAJIRI, T., MANABE, T., OHTSUKA, T. & TANAKA, M. 2010. Gene expression levels as predictive markers of outcome in pancreatic cancer after gemcitabine-based adjuvant chemotherapy. *Neoplasia,* 12**,** 807-17.
GARRIDO-LAGUNA, I. & HIDALGO, M. 2015. Pancreatic cancer: from state-of-the-art treatments to promising novel therapies. *Nat Rev Clin Oncol,* 12**,** 319-34.
GHANEH, P., COSTELLO, E. & NEOPTOLEMOS, J. P. 2007. Biology and management of pancreatic cancer. *Gut,* 56**,** 1134-52.
GHORPADE, D. S., SINHA, A. Y., HOLLA, S., SINGH, V. & BALAJI, K. N. 2013. NOD2-nitric oxide-responsive microRNA-146a activates Sonic hedgehog signaling to orchestrate inflammatory responses in murine model of inflammatory bowel disease. *J Biol Chem,* 288**,** 33037-48.
GIOVANNETTI, E., DEL TACCA, M., MEY, V., FUNEL, N., NANNIZZI, S., RICCI, S., ORLANDINI, C., BOGGI, U., CAMPANI, D., DEL CHIARO, M., IANNOPOLLO, M., BEVILACQUA, G., MOSCA, F. & DANESI, R. 2006. Transcription analysis of human equilibrative nucleoside transporter-1 predicts survival in pancreas cancer patients treated with gemcitabine. *Cancer Res,* 66**,** 3928-35.
GOETZ, S. C., OCBINA, P. J. & ANDERSON, K. V. 2009. The primary cilium as a Hedgehog signal transduction machine. *Methods Cell Biol,* 94**,** 199-222.
GOMEZ-ORTE, E., SAENZ-NARCISO, B., MORENO, S. & CABELLO, J. 2013. Multiple functions of the noncanonical Wnt pathway. *Trends Genet,* 29**,** 545-53.
GORE, J. & KORC, M. 2014. Pancreatic cancer stroma: friend or foe? *Cancer Cell,* 25**,** 711-2.
GRADIZ, R., SILVA, H. C., CARVALHO, L., BOTELHO, M. F. & MOTA-PINTO, A. 2016. MIA PaCa-2 and PANC-1 – pancreas ductal adenocarcinoma cell lines with neuroendocrine differentiation and somatostatin receptors. 6**,** 21648.

GREEN, N. M. 1975. Avidin. *Adv Protein Chem,* 29**,** 85-133.
GRIESMANN, H., RIPKA, S., PRALLE, M., ELLENRIEDER, V., BAUMGART, S., BUCHHOLZ, M., PILARSKY, C., AUST, D., GRESS, T. M. & MICHL, P. 2013. WNT5A-NFAT signaling mediates resistance to apoptosis in pancreatic cancer. *Neoplasia,* 15**,** 11-22.
GU, D., SCHLOTMAN, K. E. & XIE, J. 2016. Deciphering the role of hedgehog signaling in pancreatic cancer. *J Biomed Res,* 30**,** 353-360.
GUNGOR, C., ZANDER, H., EFFENBERGER, K. E., VASHIST, Y. K., KALININA, T., IZBICKI, J. R., YEKEBAS, E. & BOCKHORN, M. 2011. Notch signaling activated by replication stress-induced expression of midkine drives epithelial-mesenchymal transition and chemoresistance in pancreatic cancer. *Cancer Res,* 71**,** 5009-19.
HABER, P. S., KEOGH, G. W., APTE, M. V., MORAN, C. S., STEWART, N. L., CRAWFORD, D. H., PIROLA, R. C., MCCAUGHAN, G. W., RAMM, G. A. & WILSON, J. S. 1999. Activation of pancreatic stellate cells in human and experimental pancreatic fibrosis. *Am J Pathol,* 155**,** 1087-95.
HAEGEBARTH, A. & CLEVERS, H. 2009. Wnt signaling, lgr5, and stem cells in the intestine and skin. *Am J Pathol,* 174**,** 715-21.
HAN, M. E., LEE, Y. S., BAEK, S. Y., KIM, B. S., KIM, J. B. & OH, S. O. 2009. Hedgehog signaling regulates the survival of gastric cancer cells by regulating the expression of Bcl-2. *Int J Mol Sci,* 10**,** 3033-43.
HANAHAN, D. & WEINBERG, R. A. 2000. The hallmarks of cancer. *Cell,* 100**,** 57-70.
HANAHAN, D. & WEINBERG, R. A. 2011. Hallmarks of cancer: the next generation. *Cell,* 144**,** 646-74.
HANNA, A. & SHEVDE, L. A. 2016. Hedgehog signaling: modulation of cancer properies and tumor mircroenvironment. *Mol Cancer,* 15**,** 24.
HAO, K., TIAN, X. D., QIN, C. F., XIE, X. H. & YANG, Y. M. 2013. Hedgehog signaling pathway regulates human pancreatic cancer cell proliferation and metastasis. *Oncol Rep,* 29**,** 1124-32.
HAQQ, J., HOWELLS, L. M., GARCEA, G., METCALFE, M. S., STEWARD, W. P. & DENNISON, A. R. 2014. Pancreatic stellate cells and pancreas cancer: current perspectives and future strategies. *Eur J Cancer,* 50**,** 2570-82.
HARADA, T., YAMAMOTO, H., KISHIDA, S., KISHIDA, M., AWADA, C., TAKAO, T. & KIKUCHI, A. 2017. Wnt5b-associated exosomes promote cancer cell migration and proliferation. *Cancer Sci,* 108**,** 42-52.
HARRIS, L. G., PANNELL, L. K., SINGH, S., SAMANT, R. S. & SHEVDE, L. A. 2012. Increased vascularity and spontaneous metastasis of breast cancer by hedgehog signaling mediated upregulation of cyr61. *Oncogene,* 31**,** 3370-80.
HASSAN, M. M., BONDY, M. L., WOLFF, R. A., ABBRUZZESE, J. L., VAUTHEY, J. N., PISTERS, P. W., EVANS, D. B., KHAN, R., CHOU, T. H., LENZI, R., JIAO, L. & LI, D. 2007. Risk factors for pancreatic cancer: case-control study. *Am J Gastroenterol,* 102**,** 2696-707.
HAYASHI, H., KURATA, T. & NAKAGAWA, K. 2011. Gemcitabine: efficacy in the treatment of advanced stage nonsquamous non-small cell lung cancer. *Clin Med Insights Oncol,* 5**,** 177-84.
HEBROK, M. 2003. Hedgehog signaling in pancreas development. *Mech Dev,* 120**,** 45-57.

HEESTAND, G. M., MURPHY, J. D. & LOWY, A. M. 2015. Approach to patients with pancreatic cancer without detectable metastases. *J Clin Oncol,* 33**,** 1770-8.
HELLERSTROM, C. 1984. The life story of the pancreatic B cell. *Diabetologia,* 26**,** 393-400.
HERNANDEZ, A. R., KLEIN, A. M. & KIRSCHNER, M. W. 2012. Kinetic responses of beta-catenin specify the sites of Wnt control. *Science,* 338**,** 1337-40.
HERREROS-VILLANUEVA, M., HIJONA, E., COSME, A. & BUJANDA, L. 2012. Mouse models of pancreatic cancer. *World J Gastroenterol,* 18**,** 1286-94.
HESSMANN, E., PATZAK, M. S., KLEIN, L., CHEN, N., KARI, V., RAMU, I., BAPIRO, T. E., FRESE, K. K., GOPINATHAN, A., RICHARDS, F. M., JODRELL, D. I., VERBEKE, C., LI, X., HEUCHEL, R., LOHR, J. M., JOHNSEN, S. A., GRESS, T. M., ELLENRIEDER, V. & NEESSE, A. 2017. Fibroblast drug scavenging increases intratumoural gemcitabine accumulation in murine pancreas cancer. *Gut*.
HIDALGO, M. 2010. Pancreatic cancer. *N Engl J Med,* 362**,** 1605-17.
HIGUCHI, R., FOCKLER, C., DOLLINGER, G. & WATSON, R. 1993. Kinetic PCR analysis: real-time monitoring of DNA amplification reactions. *Biotechnology (N Y),* 11**,** 1026-30.
HIKASA, H. & SOKOL, S. Y. 2013. Wnt signaling in vertebrate axis specification. *Cold Spring Harb Perspect Biol,* 5**,** a007955.
HINDRIKSEN, S. & BIJLSMA, M. F. 2012. Cancer Stem Cells, EMT, and Developmental Pathway Activation in Pancreatic Tumors. *Cancers (Basel),* 4**,** 989-1035.
HINGORANI, S. R., WANG, L., MULTANI, A. S., COMBS, C., DERAMAUDT, T. B., HRUBAN, R. H., RUSTGI, A. K., CHANG, S. & TUVESON, D. A. 2005. Trp53R172H and KrasG12D cooperate to promote chromosomal instability and widely metastatic pancreatic ductal adenocarcinoma in mice. *Cancer Cell,* 7**,** 469-83.
HINZ, B., PHAN, S. H., THANNICKAL, V. J., GALLI, A., BOCHATON-PIALLAT, M. L. & GABBIANI, G. 2007. The myofibroblast: one function, multiple origins. *Am J Pathol,* 170**,** 1807-16.
HOLLAND, P. M., ABRAMSON, R. D., WATSON, R. & GELFAND, D. H. 1991. Detection of specific polymerase chain reaction product by utilizing the 5'----3' exonuclease activity of Thermus aquaticus DNA polymerase. *Proc Natl Acad Sci U S A,* 88**,** 7276-80.
HOLSTEIN, T. W. 2012. The evolution of the Wnt pathway. *Cold Spring Harb Perspect Biol,* 4**,** a007922.
HONG, K. D., LEE, Y., KIM, B. H., LEE, S. I. & MOON, H. Y. 2013. Expression of GLI1 correlates with expression of lymphangiogenesis proteins, vascular endothelial growth factor C and vascular endothelial growth factor receptor 3, in colorectal cancer. *Am Surg,* 79**,** 198-204.
HORVATH, P., AULNER, N., BICKLE, M., DAVIES, A. M., NERY, E. D., EBNER, D., MONTOYA, M. C., OSTLING, P., PIETIAINEN, V., PRICE, L. S., SHORTE, S. L., TURCATTI, G., VON SCHANTZ, C. & CARRAGHER, N. O. 2016. Screening out irrelevant cell-based models of disease. *Nat Rev Drug Discov,* 15**,** 751-769.

HORWITZ, S. B. 1994. Taxol (paclitaxel): mechanisms of action. *Ann Oncol,* 5 Suppl 6**,** S3-6.
HRUBAN, R. H. & FUKUSHIMA, N. 2007. Pancreatic adenocarcinoma: update on the surgical pathology of carcinomas of ductal origin and PanINs. *Modern Pathology,* 20**,** S61.
HSIEH, J. C., RATTNER, A., SMALLWOOD, P. M. & NATHANS, J. 1999. Biochemical characterization of Wnt-frizzled interactions using a soluble, biologically active vertebrate Wnt protein. *Proc Natl Acad Sci U S A,* 96**,** 3546-51.
HUANG, P., CHUBB, S., HERTEL, L. W., GRINDEY, G. B. & PLUNKETT, W. 1991. Action of 2',2'-difluorodeoxycytidine on DNA synthesis. *Cancer Res,* 51**,** 6110-7.
HUANG, S., HE, J., ZHANG, X., BIAN, Y., YANG, L., XIE, G., ZHANG, K., TANG, W., STELTER, A. A., WANG, Q., ZHANG, H. & XIE, J. 2006. Activation of the hedgehog pathway in human hepatocellular carcinomas. *Carcinogenesis,* 27**,** 1334-40.
HUGHES, J. P., REES, S., KALINDJIAN, S. B. & PHILPOTT, K. L. 2011. Principles of early drug discovery. *Br J Pharmacol,* 162**,** 1239-49.
HUXLEY, R., ANSARY-MOGHADDAM, A., BERRINGTON DE GONZALEZ, A., BARZI, F. & WOODWARD, M. 2005. Type-II diabetes and pancreatic cancer: a meta-analysis of 36 studies. *Br J Cancer,* 92**,** 2076-83.
HWANG, R. F., MOORE, T. T., HATTERSLEY, M. M., SCARPITTI, M., YANG, B., DEVEREAUX, E., RAMACHANDRAN, V., ARUMUGAM, T., JI, B., LOGSDON, C. D., BROWN, J. L. & GODIN, R. 2012. Inhibition of the hedgehog pathway targets the tumor-associated stroma in pancreatic cancer. *Mol Cancer Res,* 10**,** 1147-57.
IODICE, S., GANDINI, S., MAISONNEUVE, P. & LOWENFELS, A. B. 2008. Tobacco and the risk of pancreatic cancer: a review and meta-analysis. *Langenbecks Arch Surg,* 393**,** 535-45.
IWAMURA, T., KATSUKI, T. & IDE, K. 1987. Establishment and characterization of a human pancreatic cancer cell line (SUIT-2) producing carcinoembryonic antigen and carbohydrate antigen 19-9. *Jpn J Cancer Res,* 78**,** 54-62.
IWANO, M., PLIETH, D., DANOFF, T. M., XUE, C., OKADA, H. & NEILSON, E. G. 2002. Evidence that fibroblasts derive from epithelium during tissue fibrosis. *J Clin Invest,* 110**,** 341-50.
JESSELL, T. M. 2000. Neuronal specification in the spinal cord: inductive signals and transcriptional codes. *Nat Rev Genet,* 1**,** 20-9.
JHO, E. H., ZHANG, T., DOMON, C., JOO, C. K., FREUND, J. N. & COSTANTINI, F. 2002. Wnt/beta-catenin/Tcf signaling induces the transcription of Axin2, a negative regulator of the signaling pathway. *Mol Cell Biol,* 22**,** 1172-83.
JIA, Y. & XIE, J. 2015. Promising molecular mechanisms responsible for gemcitabine resistance in cancer. *Genes & Diseases,* 2**,** 299-306.
JIANG, X., HAO, H. X., GROWNEY, J. D., WOOLFENDEN, S., BOTTIGLIO, C., NG, N., LU, B., HSIEH, M. H., BAGDASARIAN, L., MEYER, R., SMITH, T. R., AVELLO, M., CHARLAT, O., XIE, Y., PORTER, J. A., PAN, S., LIU, J., MCLAUGHLIN, M. E. & CONG, F. 2013. Inactivating mutations of RNF43 confer Wnt dependency in pancreatic ductal adenocarcinoma. *Proc Natl Acad Sci U S A,* 110**,** 12649-54.

JOHNSON, R. L., LAUFER, E., RIDDLE, R. D. & TABIN, C. 1994. Ectopic expression of Sonic hedgehog alters dorsal-ventral patterning of somites. *Cell,* 79**,** 1165-73.
KALININA, T., GUNGOR, C., THIELTGES, S., MOLLER-KRULL, M., PENAS, E. M., WICKLEIN, D., STREICHERT, T., SCHUMACHER, U., KALININ, V., SIMON, R., OTTO, B., DIERLAMM, J., SCHWARZENBACH, H., EFFENBERGER, K. E., BOCKHORN, M., IZBICKI, J. R. & YEKEBAS, E. F. 2010. Establishment and characterization of a new human pancreatic adenocarcinoma cell line with high metastatic potential to the lung. *BMC Cancer,* 10**,** 295.
KALLURI, R. & ZEISBERG, M. 2006. Fibroblasts in cancer. *Nat Rev Cancer,* 6**,** 392-401.
KANDA, M., MATTHAEI, H., WU, J., HONG, S. M., YU, J., BORGES, M., HRUBAN, R. H., MAITRA, A., KINZLER, K., VOGELSTEIN, B. & GOGGINS, M. 2012. Presence of somatic mutations in most early-stage pancreatic intraepithelial neoplasia. *Gastroenterology,* 142**,** 730-733 e9.
KASPERCZYK, H., BAUMANN, B., DEBATIN, K. M. & FULDA, S. 2009. Characterization of sonic hedgehog as a novel NF-kappaB target gene that promotes NF-kappaB-mediated apoptosis resistance and tumor growth in vivo. *FASEB J,* 23**,** 21-33.
KATOH, M. & KATOH, M. 2007. STAT3-induced WNT5A signaling loop in embryonic stem cells, adult normal tissues, chronic persistent inflammation, rheumatoid arthritis and cancer (Review). *Int J Mol Med,* 19**,** 273-8.
KAUFHOLD, S. & BONAVIDA, B. 2014. Central role of Snail1 in the regulation of EMT and resistance in cancer: a target for therapeutic intervention. *J Exp Clin Cancer Res,* 33**,** 62.
KAUR, S., BAINE, M. J., JAIN, M., SASSON, A. R. & BATRA, S. K. 2012. Early diagnosis of pancreatic cancer: challenges and new developments. *Biomark Med,* 6**,** 597-612.
KAWANO, Y. & KYPTA, R. 2003. Secreted antagonists of the Wnt signalling pathway. *J Cell Sci,* 116**,** 2627-34.
KENDALL, R. T. & FEGHALI-BOSTWICK, C. A. 2014. Fibroblasts in fibrosis: novel roles and mediators. *Front Pharmacol,* 5**,** 123.
KENNY, P. A., LEE, G. Y., MYERS, C. A., NEVE, R. M., SEMEIKS, J. R., SPELLMAN, P. T., LORENZ, K., LEE, E. H., BARCELLOS-HOFF, M. H., PETERSEN, O. W., GRAY, J. W. & BISSELL, M. J. 2007. The morphologies of breast cancer cell lines in three-dimensional assays correlate with their profiles of gene expression. *Mol Oncol,* 1**,** 84-96.
KHAN, S., JAGGI, M. & CHAUHAN, S. C. 2015. Revisiting stroma in pancreatic cancer. *Oncoscience,* 2**,** 819-20.
KIKUCHI, A., YAMAMOTO, H. & SATO, A. 2009. Selective activation mechanisms of Wnt signaling pathways. *Trends Cell Biol,* 19**,** 119-29.
KIMELMAN, D. & XU, W. 2006. beta-catenin destruction complex: insights and questions from a structural perspective. *Oncogene,* 25**,** 7482-91.
KISSELBACH, L., MERGES, M., BOSSIE, A. & BOYD, A. 2009. CD90 Expression on human primary cells and elimination of contaminating fibroblasts from cell cultures. *Cytotechnology,* 59**,** 31-44.
KLEMM, F., BLECKMANN, A., SIAM, L., CHUANG, H. N., RIETKOTTER, E., BEHME, D., SCHULZ, M., SCHAFFRINSKI, M., SCHINDLER, S., TRUMPER, L., KRAMER, F., BEISSBARTH, T., STADELMANN, C.,

BINDER, C. & PUKROP, T. 2011. beta-catenin-independent WNT signaling in basal-like breast cancer and brain metastasis. *Carcinogenesis,* 32**,** 434-42.
KOENIG, A., MUELLER, C., HASEL, C., ADLER, G. & MENKE, A. 2006. Collagen type I induces disruption of E-cadherin-mediated cell-cell contacts and promotes proliferation of pancreatic carcinoma cells. *Cancer Res,* 66**,** 4662-71.
KOLEVA, M. V., ROTHERY, S., SPITALER, M., NEIL, M. A. & MAGEE, A. I. 2015. Sonic hedgehog multimerization: a self-organizing event driven by post-translational modifications? *Mol Membr Biol,* 32**,** 65-74.
KOMIYA, Y. & HABAS, R. 2008. Wnt signal transduction pathways. *Organogenesis,* 4**,** 68-75.
KOONG, A. C., MEHTA, V. K., LE, Q. T., FISHER, G. A., TERRIS, D. J., BROWN, J. M., BASTIDAS, A. J. & VIERRA, M. 2000. Pancreatic tumors show high levels of hypoxia. *Int J Radiat Oncol Biol Phys,* 48**,** 919-22.
KROEP, J. R., LOVES, W. J., VAN DER WILT, C. L., ALVAREZ, E., TALIANIDIS, I., BOVEN, E., BRAAKHUIS, B. J., VAN GROENINGEN, C. J., PINEDO, H. M. & PETERS, G. J. 2002. Pretreatment deoxycytidine kinase levels predict in vivo gemcitabine sensitivity. *Mol Cancer Ther,* 1**,** 371-6.
LANGLEY, R. R. & FIDLER, I. J. 2011. The seed and soil hypothesis revisited--the role of tumor-stroma interactions in metastasis to different organs. *Int J Cancer,* 128**,** 2527-35.
LAUTH, M., BERGSTROM, A., SHIMOKAWA, T. & TOFTGARD, R. 2007. Inhibition of GLI-mediated transcription and tumor cell growth by small-molecule antagonists. *Proc Natl Acad Sci U S A,* 104**,** 8455-60.
LAVERGNE, E., HENDAOUI, I., COULOUARN, C., RIBAULT, C., LESEUR, J., ELIAT, P. A., MEBARKI, S., CORLU, A., CLEMENT, B. & MUSSO, O. 2011. Blocking Wnt signaling by SFRP-like molecules inhibits in vivo cell proliferation and tumor growth in cells carrying active beta-catenin. *Oncogene,* 30**,** 423-33.
LEDFORD, H. 2011. Translational research: 4 ways to fix the clinical trial. *Nature,* 477**,** 526-8.
LEE, J. J., HUANG, J., ENGLAND, C. G., MCNALLY, L. R. & FRIEBOES, H. B. 2013a. Predictive modeling of in vivo response to gemcitabine in pancreatic cancer. *PLoS Comput Biol,* 9**,** e1003231.
LEE, J. J., PERERA, R. M., WANG, H., WU, D. C., LIU, X. S., HAN, S., FITAMANT, J., JONES, P. D., GHANTA, K. S., KAWANO, S., NAGLE, J. M., DESHPANDE, V., BOUCHER, Y., KATO, T., CHEN, J. K., WILLMANN, J. K., BARDEESY, N. & BEACHY, P. A. 2014. Stromal response to Hedgehog signaling restrains pancreatic cancer progression. *Proc Natl Acad Sci U S A,* 111**,** E3091-100.
LEE, J. J., VON KESSLER, D. P., PARKS, S. & BEACHY, P. A. 1992. Secretion and localized transcription suggest a role in positional signaling for products of the segmentation gene hedgehog. *Cell,* 71**,** 33-50.
LEE, J. W., KOMAR, C. A., BENGSCH, F., GRAHAM, K. & BEATTY, G. L. 2016. Genetically Engineered Mouse Models of Pancreatic Cancer: The KPC Model (LSL-Kras(G12D/+) ;LSL-Trp53(R172H/+) ;Pdx-1-Cre), Its Variants, and Their Application in Immuno-oncology Drug Discovery. *Curr Protoc Pharmacol,* 73**,** 14 39 1-14 39 20.

LEE, S. J., LINDSEY, S., GRAVES, B., YOO, S., OLSON, J. M. & LANGHANS, S. A. 2013b. Sonic hedgehog-induced histone deacetylase activation is required for cerebellar granule precursor hyperplasia in medulloblastoma. *PLoS One,* 8**,** e71455.

LI, R., CAI, L., DING, J., HU, C. M., WU, T. N. & HU, X. Y. 2015. Inhibition of hedgehog signal pathway by cyclopamine attenuates inflammation and articular cartilage damage in rats with adjuvant-induced arthritis. *J Pharm Pharmacol,* 67**,** 963-71.

LI, X., WANG, Z., MA, Q., XU, Q., LIU, H., DUAN, W., LEI, J., MA, J., WANG, X., LV, S., HAN, L., LI, W., GUO, J., GUO, K., ZHANG, D., WU, E. & XIE, K. 2014. Sonic hedgehog paracrine signaling activates stromal cells to promote perineural invasion in pancreatic cancer. *Clin Cancer Res,* 20**,** 4326-38.

LI, X. Q., YANG, X. L., ZHANG, G., WU, S. P., DENG, X. B., XIAO, S. J., LIU, Q. Z., YAO, K. T. & XIAO, G. H. 2013. Nuclear beta-catenin accumulation is associated with increased expression of Nanog protein and predicts poor prognosis of non-small cell lung cancer. *J Transl Med,* 11**,** 114.

LI, Y. J. & JI, X. R. 2003. Relationship between expression of E-cadherin-catenin complex and clinicopathologic characteristics of pancreatic cancer. *World J Gastroenterol,* 9**,** 368-72.

LIAU, S. S., JAZAG, A. & WHANG, E. E. 2006. HMGA1 is a determinant of cellular invasiveness and in vivo metastatic potential in pancreatic adenocarcinoma. *Cancer Res,* 66**,** 11613-22.

LIAU, S. S. & WHANG, E. 2008. HMGA1 is a molecular determinant of chemoresistance to gemcitabine in pancreatic adenocarcinoma. *Clin Cancer Res,* 14**,** 1470-7.

LIEBER, M., MAZZETTA, J., NELSON-REES, W., KAPLAN, M. & TODARO, G. 1975. Establishment of a continuous tumor-cell line (panc-1) from a human carcinoma of the exocrine pancreas. *Int J Cancer,* 15**,** 741-7.

LIEBMANN, J. E., COOK, J. A., LIPSCHULTZ, C., TEAGUE, D., FISHER, J. & MITCHELL, J. B. 1993. Cytotoxic studies of paclitaxel (Taxol) in human tumour cell lines. *Br J Cancer,* 68**,** 1104-9.

LING, J., KANG, Y., ZHAO, R., XIA, Q., LEE, D. F., CHANG, Z., LI, J., PENG, B., FLEMING, J. B., WANG, H., LIU, J., LEMISCHKA, I. R., HUNG, M. C. & CHIAO, P. J. 2012. KrasG12D-induced IKK2/beta/NF-kappaB activation by IL-1alpha and p62 feedforward loops is required for development of pancreatic ductal adenocarcinoma. *Cancer Cell,* 21**,** 105-20.

LIU, J., PAN, S., HSIEH, M. H., NG, N., SUN, F., WANG, T., KASIBHATLA, S., SCHULLER, A. G., LI, A. G., CHENG, D., LI, J., TOMPKINS, C., PFERDEKAMPER, A., STEFFY, A., CHENG, J., KOWAL, C., PHUNG, V., GUO, G., WANG, Y., GRAHAM, M. P., FLYNN, S., BRENNER, J. C., LI, C., VILLARROEL, M. C., SCHULTZ, P. G., WU, X., MCNAMARA, P., SELLERS, W. R., PETRUZZELLI, L., BORAL, A. L., SEIDEL, H. M., MCLAUGHLIN, M. E., CHE, J., CAREY, T. E., VANASSE, G. & HARRIS, J. L. 2013. Targeting Wnt-driven cancer through the inhibition of Porcupine by LGK974. *Proc Natl Acad Sci U S A,* 110**,** 20224-9.

LIU, Y. & KULESZ-MARTIN, M. 2000. P53 regulation and function in normal cells and tumors. *Medicina (B Aires),* 60 Suppl 2**,** 9-11.

LONGATI, P., JIA, X., EIMER, J., WAGMAN, A., WITT, M. R., REHNMARK, S., VERBEKE, C., TOFTGARD, R., LOHR, M. & HEUCHEL, R. L. 2013.

3D pancreatic carcinoma spheroids induce a matrix-rich, chemoresistant phenotype offering a better model for drug testing. *BMC Cancer,* 13**,** 95.
LOVITT, C. J., SHELPER, T. B. & AVERY, V. M. 2014. Advanced cell culture techniques for cancer drug discovery. *Biology (Basel),* 3**,** 345-67.
LOWENFELS, A. B., MAISONNEUVE, P., CAVALLINI, G., AMMANN, R. W., LANKISCH, P. G., ANDERSEN, J. R., DIMAGNO, E. P., ANDREN-SANDBERG, A. & DOMELLOF, L. 1993. Pancreatitis and the risk of pancreatic cancer. International Pancreatitis Study Group. *N Engl J Med,* 328**,** 1433-7.
LOWENFELS, A. B., MAISONNEUVE, P., DIMAGNO, E. P., ELITSUR, Y., GATES, L. K., JR., PERRAULT, J. & WHITCOMB, D. C. 1997. Hereditary pancreatitis and the risk of pancreatic cancer. International Hereditary Pancreatitis Study Group. *J Natl Cancer Inst,* 89**,** 442-6.
MACDONALD, B. T., TAMAI, K. & HE, X. 2009. Wnt/beta-catenin signaling: components, mechanisms, and diseases. *Dev Cell,* 17**,** 9-26.
MADAR, S., GOLDSTEIN, I. & ROTTER, V. 2013. 'Cancer associated fibroblasts'--more than meets the eye. *Trends Mol Med,* 19**,** 447-53.
MAHADEVAN, D. & VON HOFF, D. D. 2007. Tumor-stroma interactions in pancreatic ductal adenocarcinoma. *Mol Cancer Ther,* 6**,** 1186-97.
MAK, I. W., EVANIEW, N. & GHERT, M. 2014. Lost in translation: animal models and clinical trials in cancer treatment. *Am J Transl Res,* 6**,** 114-8.
MALAFA, M. P. 2015. Defining borderline resectable pancreatic cancer: emerging consensus for an old challenge. *J Natl Compr Canc Netw,* 13**,** 501-4.
MALANCHI, I., SANTAMARIA-MARTINEZ, A., SUSANTO, E., PENG, H., LEHR, H. A., DELALOYE, J. F. & HUELSKEN, J. 2011. Interactions between cancer stem cells and their niche govern metastatic colonization. *Nature,* 481**,** 85-9.
MAO, B., WU, W., DAVIDSON, G., MARHOLD, J., LI, M., MECHLER, B. M., DELIUS, H., HOPPE, D., STANNEK, P., WALTER, C., GLINKA, A. & NIEHRS, C. 2002. Kremen proteins are Dickkopf receptors that regulate Wnt/beta-catenin signalling. *Nature,* 417**,** 664-7.
MAO, J., WANG, J., LIU, B., PAN, W., FARR, G. H., 3RD, FLYNN, C., YUAN, H., TAKADA, S., KIMELMAN, D., LI, L. & WU, D. 2001. Low-density lipoprotein receptor-related protein-5 binds to Axin and regulates the canonical Wnt signaling pathway. *Mol Cell,* 7**,** 801-9.
MARCHESI, F., PIEMONTI, L., FEDELE, G., DESTRO, A., RONCALLI, M., ALBARELLO, L., DOGLIONI, C., ANSELMO, A., DONI, A., BIANCHI, P., LAGHI, L., MALESCI, A., CERVO, L., MALOSIO, M., RENI, M., ZERBI, A., DI CARLO, V., MANTOVANI, A. & ALLAVENA, P. 2008. The chemokine receptor CX3CR1 is involved in the neural tropism and malignant behavior of pancreatic ductal adenocarcinoma. *Cancer Res,* 68**,** 9060-9.
MARIGO, V., ROBERTS, D. J., LEE, S. M., TSUKUROV, O., LEVI, T., GASTIER, J. M., EPSTEIN, D. J., GILBERT, D. J., COPELAND, N. G., SEIDMAN, C. E. & ET AL. 1995. Cloning, expression, and chromosomal location of SHH and IHH: two human homologues of the Drosophila segment polarity gene hedgehog. *Genomics,* 28**,** 44-51.
MARTI, E. & BOVOLENTA, P. 2002. Sonic hedgehog in CNS development: one signal, multiple outputs. *Trends Neurosci,* 25**,** 89-96.

MASCKAUCHAN, T. N., AGALLIU, D., VORONTCHIKHINA, M., AHN, A., PARMALEE, N. L., LI, C. M., KHOO, A., TYCKO, B., BROWN, A. M. & KITAJEWSKI, J. 2006. Wnt5a signaling induces proliferation and survival of endothelial cells in vitro and expression of MMP-1 and Tie-2. *Mol Biol Cell,* 17**,** 5163-72.

MASON, J. O., KITAJEWSKI, J. & VARMUS, H. E. 1992. Mutational analysis of mouse Wnt-1 identifies two temperature-sensitive alleles and attributes of Wnt-1 protein essential for transformation of a mammary cell line. *Mol Biol Cell,* 3**,** 521-33.

MATSUMOTO, K., SHIMO, T., KURIO, N., OKUI, T., OBATA, K., MASUI, M., PANG, P., HORIKIRI, Y. & SASAKI, A. 2016. Expression and Role of Sonic Hedgehog in the Process of Fracture Healing with Aging. *In Vivo,* 30**,** 99-105.

MAZUMDAR, T., SANDHU, R., QADAN, M., DEVECCHIO, J., MAGLOIRE, V., AGYEMAN, A., LI, B. & HOUGHTON, J. A. 2013. Hedgehog signaling regulates telomerase reverse transcriptase in human cancer cells. *PLoS One,* 8**,** e75253.

MCCARROLL, J. A., NAIM, S., SHARBEEN, G., RUSSIA, N., LEE, J., KAVALLARIS, M., GOLDSTEIN, D. & PHILLIPS, P. A. 2014. Role of pancreatic stellate cells in chemoresistance in pancreatic cancer. *Front Physiol,* 5**,** 141.

MCCONKEY, D. J., CHOI, W., FOURNIER, K., MARQUIS, L., RAMACHANDRAN, V. & ARUMUGAM, T. 2010. Molecular Characterization of Pancreatic Cancer Cell Lines. *Pancreatic Cancer.* New York, NY: Springer New York.

MCCONNELL, J. C., O'CONNELL, O. V., BRENNAN, K., WEIPING, L., HOWE, M., JOSEPH, L., KNIGHT, D., O'CUALAIN, R., LIM, Y., LEEK, A., WADDINGTON, R., ROGAN, J., ASTLEY, S. M., GANDHI, A., KIRWAN, C. C., SHERRATT, M. J. & STREULI, C. H. 2016. Increased peri-ductal collagen micro-organization may contribute to raised mammographic density. *Breast Cancer Res,* 18**,** 5.

MCGUIRE, S. 2016. World Cancer Report 2014. Geneva, Switzerland: World Health Organization, International Agency for Research on Cancer, WHO Press, 2015. *Adv Nutr,* 7**,** 418-9.

MCWILLIAMS, R. R., WIEBEN, E. D., RABE, K. G., PEDERSEN, K. S., WU, Y., SICOTTE, H. & PETERSEN, G. M. 2011. Prevalence of CDKN2A mutations in pancreatic cancer patients: implications for genetic counseling. *Eur J Hum Genet,* 19**,** 472-8.

MEHTA, G., HSIAO, A. Y., INGRAM, M., LUKER, G. D. & TAKAYAMA, S. 2012. Opportunities and challenges for use of tumor spheroids as models to test drug delivery and efficacy. *J Control Release,* 164**,** 192-204.

MEMARIAN, A., HOJJAT-FARSANGI, M., ASGARIAN-OMRAN, H., YOUNESI, V., JEDDI-TEHRANI, M., SHARIFIAN, R. A., KHOSHNOODI, J., RAZAVI, S. M., RABBANI, H. & SHOKRI, F. 2009. Variation in WNT genes expression in different subtypes of chronic lymphocytic leukemia. *Leuk Lymphoma,* 50**,** 2061-70.

MERCHANT, A. A. & MATSUI, W. 2010. Targeting Hedgehog--a cancer stem cell pathway. *Clin Cancer Res,* 16**,** 3130-40.

MICHEL, M., KUPINSKI, A. P., RAABE, I. & BOKEL, C. 2012. Hh signalling is essential for somatic stem cell maintenance in the Drosophila testis niche. *Development,* 139**,** 2663-9.
MII, Y. & TAIRA, M. 2009. Secreted Frizzled-related proteins enhance the diffusion of Wnt ligands and expand their signalling range. *Development,* 136**,** 4083-8.
MIKELS, A. J. & NUSSE, R. 2006. Wnts as ligands: processing, secretion and reception. *Oncogene,* 25**,** 7461-8.
MILLE, F., TAMAYO-ORREGO, L., LEVESQUE, M., REMKE, M., KORSHUNOV, A., CARDIN, J., BOUCHARD, N., IZZI, L., KOOL, M., NORTHCOTT, P. A., TAYLOR, M. D., PFISTER, S. M. & CHARRON, F. 2014. The Shh receptor Boc promotes progression of early medulloblastoma to advanced tumors. *Dev Cell,* 31**,** 34-47.
MOHAMMED, M. K., SHAO, C., WANG, J., WEI, Q., WANG, X., COLLIER, Z., TANG, S., LIU, H., ZHANG, F., HUANG, J., GUO, D., LU, M., LIU, F., LIU, J., MA, C., SHI, L. L., ATHIVIRAHAM, A., HE, T. C. & LEE, M. J. 2016. Wnt/beta-catenin signaling plays an ever-expanding role in stem cell self-renewal, tumorigenesis and cancer chemoresistance. *Genes Dis,* 3**,** 11-40.
MOHLER, J. & VANI, K. 1992. Molecular organization and embryonic expression of the hedgehog gene involved in cell-cell communication in segmental patterning of Drosophila. *Development,* 115**,** 957-71.
MORRIS, J. P. T., WANG, S. C. & HEBROK, M. 2010. KRAS, Hedgehog, Wnt and the twisted developmental biology of pancreatic ductal adenocarcinoma. *Nat Rev Cancer,* 10**,** 683-95.
MORVARIDI, S., DHALL, D., GREENE, M. I., PANDOL, S. J. & WANG, Q. 2015. Role of YAP and TAZ in pancreatic ductal adenocarcinoma and in stellate cells associated with cancer and chronic pancreatitis. *Sci Rep,* 5**,** 16759.
MUELLER-KLIESER, W. 1987. Multicellular spheroids. A review on cellular aggregates in cancer research. *J Cancer Res Clin Oncol,* 113**,** 101-22.
MULLIS, K., FALOONA, F., SCHARF, S., SAIKI, R., HORN, G. & ERLICH, H. 1986. Specific enzymatic amplification of DNA in vitro: the polymerase chain reaction. *Cold Spring Harb Symp Quant Biol,* 51 Pt 1**,** 263-73.
NAKASHIMA, H., NAKAMURA, M., YAMAGUCHI, H., YAMANAKA, N., AKIYOSHI, T., KOGA, K., YAMAGUCHI, K., TSUNEYOSHI, M., TANAKA, M. & KATANO, M. 2006. Nuclear factor-kappaB contributes to hedgehog signaling pathway activation through sonic hedgehog induction in pancreatic cancer. *Cancer Res,* 66**,** 7041-9.
NAKATSURA, T., HASEBE, T., TSUBONO, Y., RYU, M., KINOSHITA, T., KAWANO, N., KONISHI, M., KOSUGE, T., KANAI, Y. & MUKAI, K. 1997. Histological prognostic parameters for adenocarcinoma of the pancreatic head. Proposal for a scoring system for prediction of outcome. *Journal of Hepato-Biliary-Pancreatic Surgery,* 4**,** 441-448.
NAMBA, T., KODAMA, R., MORITOMO, S., HOSHINO, T. & MIZUSHIMA, T. 2015. Zidovudine, an anti-viral drug, resensitizes gemcitabine-resistant pancreatic cancer cells to gemcitabine by inhibition of the Akt-GSK3beta-Snail pathway. *Cell Death Dis,* 6**,** e1795.
NELSON, C. M. & BISSELL, M. J. 2005. Modeling dynamic reciprocity: engineering three-dimensional culture models of breast architecture, function, and neoplastic transformation. *Semin Cancer Biol,* 15**,** 342-52.

NEOPTOLEMOS, J. P., CUNNINGHAM, D., FRIESS, H., BASSI, C., STOCKEN, D. D., TAIT, D. M., DUNN, J. A., DERVENIS, C., LACAINE, F., HICKEY, H., RARATY, M. G., GHANEH, P. & BUCHLER, M. W. 2003. Adjuvant therapy in pancreatic cancer: historical and current perspectives. *Ann Oncol,* 14**,** 675-92.

NIIDA, A., HIROKO, T., KASAI, M., FURUKAWA, Y., NAKAMURA, Y., SUZUKI, Y., SUGANO, S. & AKIYAMA, T. 2004. DKK1, a negative regulator of Wnt signaling, is a target of the beta-catenin/TCF pathway. *Oncogene,* 23**,** 8520-6.

NOLAN-STEVAUX, O., LAU, J., TRUITT, M. L., CHU, G. C., HEBROK, M., FERNANDEZ-ZAPICO, M. E. & HANAHAN, D. 2009. GLI1 is regulated through Smoothened-independent mechanisms in neoplastic pancreatic ducts and mediates PDAC cell survival and transformation. *Genes Dev,* 23**,** 24-36.

NOVELLASDEMUNT, L., ANTAS, P. & LI, V. S. 2015. Targeting Wnt signaling in colorectal cancer. A Review in the Theme: Cell Signaling: Proteins, Pathways and Mechanisms. *Am J Physiol Cell Physiol,* 309**,** C511-21.

NUSSE, R. 2008. Wnt signaling and stem cell control. *Cell Res,* 18**,** 523-7.

NUSSLEIN-VOLHARD, C. & WIESCHAUS, E. 1980. Mutations affecting segment number and polarity in Drosophila. *Nature,* 287**,** 795-801.

NYGA, A., CHEEMA, U. & LOIZIDOU, M. 2011. 3D tumour models: novel in vitro approaches to cancer studies. *J Cell Commun Signal,* 5**,** 239-48.

O'TOOLE, S. A., MACHALEK, D. A., SHEARER, R. F., MILLAR, E. K. A., NAIR, R., SCHOFIELD, P., MCLEOD, D., COOPER, C. L., MCNEIL, C. M., MCFARLAND, A., NGUYEN, A., ORMANDY, C. J., QIU, M. R., RABINOVICH, B., MARTELOTTO, L. G., VU, D., HANNIGAN, G. E., MUSGROVE, E. A., CHRIST, D., SUTHERLAND, R. L., WATKINS, D. N. & SWARBRICK, A. 2011. Hedgehog Overexpression Is Associated with Stromal Interactions and Predicts for Poor Outcome in Breast Cancer. *Cancer Research,* 71**,** 4002-4014.

OBERSTEIN, P. E. & OLIVE, K. P. 2013. Pancreatic cancer: why is it so hard to treat? *Therap Adv Gastroenterol,* 6**,** 321-37.

OETTLE, H., POST, S., NEUHAUS, P., GELLERT, K., LANGREHR, J., RIDWELSKI, K., SCHRAMM, H., FAHLKE, J., ZUELKE, C., BURKART, C., GUTBERLET, K., KETTNER, E., SCHMALENBERG, H., WEIGANG-KOEHLER, K., BECHSTEIN, W. O., NIEDERGETHMANN, M., SCHMIDT-WOLF, I., ROLL, L., DOERKEN, B. & RIESS, H. 2007. Adjuvant chemotherapy with gemcitabine vs observation in patients undergoing curative-intent resection of pancreatic cancer: a randomized controlled trial. *JAMA,* 297**,** 267-77.

OLIVE, K. P., JACOBETZ, M. A., DAVIDSON, C. J., GOPINATHAN, A., MCINTYRE, D., HONESS, D., MADHU, B., GOLDGRABEN, M. A., CALDWELL, M. E., ALLARD, D., FRESE, K. K., DENICOLA, G., FEIG, C., COMBS, C., WINTER, S. P., IRELAND-ZECCHINI, H., REICHELT, S., HOWAT, W. J., CHANG, A., DHARA, M., WANG, L., RUCKERT, F., GRUTZMANN, R., PILARSKY, C., IZERADJENE, K., HINGORANI, S. R., HUANG, P., DAVIES, S. E., PLUNKETT, W., EGORIN, M., HRUBAN, R. H., WHITEBREAD, N., MCGOVERN, K., ADAMS, J., IACOBUZIO-DONAHUE, C., GRIFFITHS, J. & TUVESON, D. A. 2009. Inhibition of Hedgehog signaling enhances delivery of chemotherapy in a mouse model of pancreatic cancer. *Science,* 324**,** 1457-61.

OMARY, M. B., LUGEA, A., LOWE, A. W. & PANDOL, S. J. 2007. The pancreatic stellate cell: a star on the rise in pancreatic diseases. *J Clin Invest,* 117**,** 50-9.

ONISHI, H., KAI, M., ODATE, S., IWASAKI, H., MORIFUJI, Y., OGINO, T., MORISAKI, T., NAKASHIMA, Y. & KATANO, M. 2011. Hypoxia activates the hedgehog signaling pathway in a ligand-independent manner by upregulation of Smo transcription in pancreatic cancer. *Cancer Sci,* 102**,** 1144-50.

OWENS, R. B., SMITH, H. S., NELSON-REES, W. A. & SPRINGER, E. L. 1976. Epithelial cell cultures from normal and cancerous human tissues. *J Natl Cancer Inst,* 56**,** 843-9.

OZDEMIR, B. C., PENTCHEVA-HOANG, T., CARSTENS, J. L., ZHENG, X., WU, C. C., SIMPSON, T. R., LAKLAI, H., SUGIMOTO, H., KAHLERT, C., NOVITSKIY, S. V., DE JESUS-ACOSTA, A., SHARMA, P., HEIDARI, P., MAHMOOD, U., CHIN, L., MOSES, H. L., WEAVER, V. M., MAITRA, A., ALLISON, J. P., LEBLEU, V. S. & KALLURI, R. 2015. Depletion of Carcinoma-Associated Fibroblasts and Fibrosis Induces Immunosuppression and Accelerates Pancreas Cancer with Reduced Survival. *Cancer Cell,* 28**,** 831-833.

PACE, E., MELIS, M., SIENA, L., BUCCHIERI, F., VIGNOLA, A. M., PROFITA, M., GJOMARKAJ, M. & BONSIGNORE, G. 2000. Effects of gemcitabine on cell proliferation and apoptosis in non-small-cell lung cancer (NSCLC) cell lines. *Cancer Chemother Pharmacol,* 46**,** 467-76.

PAGAN-WESTPHAL, S. M. & TABIN, C. J. 1998. The transfer of left-right positional information during chick embryogenesis. *Cell,* 93**,** 25-35.

PAGET, S. 1889. The distribution of secondary growths in cancer of the breast. 1889. *Lancet***,** 571-3.

PANDOLFI, S. & STECCA, B. 2015. Cooperative integration between HEDGEHOG-GLI signalling and other oncogenic pathways: implications for cancer therapy. *Expert Rev Mol Med,* 17**,** e5.

PAPASPYROPOULOS, A., BRADLEY, L., THAPA, A., LEUNG, C. Y., TOSKAS, K., KOENNIG, D., PEFANI, D. E., RASO, C., GROU, C., HAMILTON, G., VLAHOV, N., GRAWENDA, A., HAIDER, S., CHAUHAN, J., BUTI, L., KANAPIN, A., LU, X., BUFFA, F., DIANOV, G., VON KRIEGSHEIM, A., MATALLANAS, D., SAMSONOVA, A., ZERNICKA-GOETZ, M. & O'NEILL, E. 2018. RASSF1A uncouples Wnt from Hippo signalling and promotes YAP mediated differentiation via p73. *Nat Commun,* 9**,** 424.

PASCA DI MAGLIANO, M., BIANKIN, A. V., HEISER, P. W., CANO, D. A., GUTIERREZ, P. J., DERAMAUDT, T., SEGARA, D., DAWSON, A. C., KENCH, J. G., HENSHALL, S. M., SUTHERLAND, R. L., DLUGOSZ, A., RUSTGI, A. K. & HEBROK, M. 2007. Common activation of canonical Wnt signaling in pancreatic adenocarcinoma. *PLoS One,* 2**,** e1155.

PATE, K. T., STRINGARI, C., SPROWL-TANIO, S., WANG, K., TESLAA, T., HOVERTER, N. P., MCQUADE, M. M., GARNER, C., DIGMAN, M. A., TEITELL, M. A., EDWARDS, R. A., GRATTON, E. & WATERMAN, M. L. 2014. Wnt signaling directs a metabolic program of glycolysis and angiogenesis in colon cancer. *EMBO J,* 33**,** 1454-73.

PATEL, A. V., RODRIGUEZ, C., BERNSTEIN, L., CHAO, A., THUN, M. J. & CALLE, E. E. 2005. Obesity, recreational physical activity, and risk of

pancreatic cancer in a large U.S. Cohort. *Cancer Epidemiol Biomarkers Prev,* 14**,** 459-66.
PATTEN, I. & PLACZEK, M. 2000. The role of Sonic hedgehog in neural tube patterning. *Cell Mol Life Sci,* 57**,** 1695-708.
PEREZ-MANCERA, P. A., GUERRA, C., BARBACID, M. & TUVESON, D. A. 2012. What we have learned about pancreatic cancer from mouse models. *Gastroenterology,* 142**,** 1079-92.
PETROVA, R. & JOYNER, A. L. 2014. Roles for Hedgehog signaling in adult organ homeostasis and repair. *Development,* 141**,** 3445-57.
PHAM, K., DELITTO, D., KNOWLTON, A. E., HARTLAGE, E. R., MADHAVAN, R., GONZALO, D. H., THOMAS, R. M., BEHRNS, K. E., GEORGE, T. J., JR., HUGHES, S. J., WALLET, S. M., LIU, C. & TREVINO, J. G. 2016. Isolation of Pancreatic Cancer Cells from a Patient-Derived Xenograft Model Allows for Practical Expansion and Preserved Heterogeneity in Culture. *Am J Pathol,* 186**,** 1537-46.
PILARSKY, C., AMMERPOHL, O., SIPOS, B., DAHL, E., HARTMANN, A., WELLMANN, A., BRAUNSCHWEIG, T., LOHR, M., JESENOFSKY, R., FRIESS, H., WENTE, M. N., KRISTIANSEN, G., JAHNKE, B., DENZ, A., RUCKERT, F., SCHACKERT, H. K., KLOPPEL, G., KALTHOFF, H., SAEGER, H. D. & GRUTZMANN, R. 2008. Activation of Wnt signalling in stroma from pancreatic cancer identified by gene expression profiling. *J Cell Mol Med,* 12**,** 2823-35.
PINTER, M., SIEGHART, W., SCHMID, M., DAUSER, B., PRAGER, G., DIENES, H. P., TRAUNER, M. & PECK-RADOSAVLJEVIC, M. 2013. Hedgehog inhibition reduces angiogenesis by downregulation of tumoral VEGF-A expression in hepatocellular carcinoma. *United European Gastroenterol J,* 1**,** 265-75.
PLAKS, V., KONG, N. & WERB, Z. 2015. The cancer stem cell niche: how essential is the niche in regulating stemness of tumor cells? *Cell Stem Cell,* 16**,** 225-38.
PLANUTIENE, M., PLANUTIS, K. & HOLCOMBE, R. F. 2011. Lymphoid enhancer-binding factor 1, a representative of vertebrate-specific Lef1/Tcf1 sub-family, is a Wnt-beta-catenin pathway target gene in human endothelial cells which regulates matrix metalloproteinase-2 expression and promotes endothelial cell invasion. *Vasc Cell,* 3**,** 28.
PORTER, J. A., YOUNG, K. E. & BEACHY, P. A. 1996. Cholesterol modification of hedgehog signaling proteins in animal development. *Science,* 274**,** 255-9.
PROVENZANO, P. P. & HINGORANI, S. R. 2013. Hyaluronan, fluid pressure, and stromal resistance in pancreas cancer. *Br J Cancer,* 108**,** 1-8.
PROVENZANO, P. P., INMAN, D. R., ELICEIRI, K. W., KNITTEL, J. G., YAN, L., RUEDEN, C. T., WHITE, J. G. & KEELY, P. J. 2008. Collagen density promotes mammary tumor initiation and progression. *BMC Med,* 6**,** 11.
QUESADA, I., TUDURI, E., RIPOLL, C. & NADAL, A. 2008. Physiology of the pancreatic alpha-cell and glucagon secretion: role in glucose homeostasis and diabetes. *J Endocrinol,* 199**,** 5-19.
RAHIB, L., SMITH, B. D., AIZENBERG, R., ROSENZWEIG, A. B., FLESHMAN, J. M. & MATRISIAN, L. M. 2014. Projecting cancer incidence and deaths to 2030: the unexpected burden of thyroid, liver, and pancreas cancers in the United States. *Cancer Res,* 74**,** 2913-21.

RAIMONDI, S., MAISONNEUVE, P. & LOWENFELS, A. B. 2009. Epidemiology of pancreatic cancer: an overview. *Nat Rev Gastroenterol Hepatol,* 6**,** 699-708.

RAMAKRISHNAN, A. B. & CADIGAN, K. M. 2017. Wnt target genes and where to find them. *F1000Res,* 6**,** 746.

RASHEED, Z. A., MATSUI, W. & MAITRA, A. 2012. Pathology of pancreatic stroma in PDAC. *In:* GRIPPO, P. J. & MUNSHI, H. G. (eds.) *Pancreatic Cancer and Tumor Microenvironment.* Trivandrum (India).

RATHOS, M. J., JOSHI, K., KHANWALKAR, H., MANOHAR, S. M. & JOSHI, K. S. 2012. Molecular evidence for increased antitumor activity of gemcitabine in combination with a cyclin-dependent kinase inhibitor, P276-00 in pancreatic cancers. *J Transl Med,* 10**,** 161.

RAYNAUD, C. M., HERNANDEZ, J., LLORCA, F. P., NUCIFORO, P., MATHIEU, M. C., COMMO, F., DELALOGE, S., SABATIER, L., ANDRE, F. & SORIA, J. C. 2010. DNA damage repair and telomere length in normal breast, preneoplastic lesions, and invasive cancer. *Am J Clin Oncol,* 33**,** 341-5.

RÉCAMIER, J. C. A. 1829. Recherches sur le traitement du cancer par la compression méthodique simple ou combinée, et sur l'histoire général de la même maladie. Paris: Gabon.

REEVES, G. K., PIRIE, K., BERAL, V., GREEN, J., SPENCER, E., BULL, D. & MILLION WOMEN STUDY, C. 2007. Cancer incidence and mortality in relation to body mass index in the Million Women Study: cohort study. *BMJ,* 335**,** 1134.

REICHSMAN, F., SMITH, L. & CUMBERLEDGE, S. 1996. Glycosaminoglycans can modulate extracellular localization of the wingless protein and promote signal transduction. *J Cell Biol,* 135**,** 819-27.

RHIM, A. D., MIREK, E. T., AIELLO, N. M., MAITRA, A., BAILEY, J. M., MCALLISTER, F., REICHERT, M., BEATTY, G. L., RUSTGI, A. K., VONDERHEIDE, R. H., LEACH, S. D. & STANGER, B. Z. 2012. EMT and dissemination precede pancreatic tumor formation. *Cell,* 148**,** 349-61.

RHIM, A. D., OBERSTEIN, P. E., THOMAS, D. H., MIREK, E. T., PALERMO, C. F., SASTRA, S. A., DEKLEVA, E. N., SAUNDERS, T., BECERRA, C. P., TATTERSALL, I. W., WESTPHALEN, C. B., KITAJEWSKI, J., FERNANDEZ-BARRENA, M. G., FERNANDEZ-ZAPICO, M. E., IACOBUZIO-DONAHUE, C., OLIVE, K. P. & STANGER, B. Z. 2014. Stromal elements act to restrain, rather than support, pancreatic ductal adenocarcinoma. *Cancer Cell,* 25**,** 735-47.

RICHARDS, K. E., ZELENIAK, A. E., FISHEL, M. L., WU, J., LITTLEPAGE, L. E. & HILL, R. 2017. Cancer-associated fibroblast exosomes regulate survival and proliferation of pancreatic cancer cells. *Oncogene,* 36**,** 1770-1778.

RICHING, K. M., COX, B. L., SALICK, M. R., PEHLKE, C., RICHING, A. S., PONIK, S. M., BASS, B. R., CRONE, W. C., JIANG, Y., WEAVER, A. M., ELICEIRI, K. W. & KEELY, P. J. 2014. 3D collagen alignment limits protrusions to enhance breast cancer cell persistence. *Biophys J,* 107**,** 2546-58.

RIDDLE, R. D., JOHNSON, R. L., LAUFER, E. & TABIN, C. 1993. Sonic hedgehog mediates the polarizing activity of the ZPA. *Cell,* 75**,** 1401-16.

RIMKUS, T. K., CARPENTER, R. L., QASEM, S., CHAN, M. & LO, H. W. 2016. Targeting the Sonic Hedgehog Signaling Pathway: Review of Smoothened and GLI Inhibitors. *Cancers (Basel),* 8.

RIOBO, N. A. & MANNING, D. R. 2007. Pathways of signal transduction employed by vertebrate Hedgehogs. *Biochem J,* 403**,** 369-79.

RIPKA, S., KONIG, A., BUCHHOLZ, M., WAGNER, M., SIPOS, B., KLOPPEL, G., DOWNWARD, J., GRESS, T. & MICHL, P. 2007. WNT5A--target of CUTL1 and potent modulator of tumor cell migration and invasion in pancreatic cancer. *Carcinogenesis,* 28**,** 1178-87.

RUCKERT, F., AUST, D., BOHME, I., WERNER, K., BRANDT, A., DIAMANDIS, E. P., KRAUTZ, C., HERING, S., SAEGER, H. D., GRUTZMANN, R. & PILARSKY, C. 2012. Five primary human pancreatic adenocarcinoma cell lines established by the outgrowth method. *J Surg Res,* 172**,** 29-39.

RUCKI, A. A., FOLEY, K., ZHANG, P., XIAO, Q., KLEPONIS, J., WU, A. A., SHARMA, R., MO, G., LIU, A., VAN EYK, J., JAFFEE, E. M. & ZHENG, L. 2017. Heterogeneous Stromal Signaling within the Tumor Microenvironment Controls the Metastasis of Pancreatic Cancer. *Cancer Res,* 77**,** 41-52.

RUCKI, A. A. & ZHENG, L. 2014. Pancreatic cancer stroma: understanding biology leads to new therapeutic strategies. *World J Gastroenterol,* 20**,** 2237-46.

RYSCHICH, E., KHAMIDJANOV, A., KERKADZE, V., BUCHLER, M. W., ZOLLER, M. & SCHMIDT, J. 2009. Promotion of tumor cell migration by extracellular matrix proteins in human pancreatic cancer. *Pancreas,* 38**,** 804-10.

SAITOH, T. & KATOH, M. 2002. Expression and regulation of WNT5A and WNT5B in human cancer: up-regulation of WNT5A by TNFalpha in MKN45 cells and up-regulation of WNT5B by beta-estradiol in MCF-7 cells. *Int J Mol Med,* 10**,** 345-9.

SAMOKHVALOV, A. V., REHM, J. & ROERECKE, M. 2015. Alcohol Consumption as a Risk Factor for Acute and Chronic Pancreatitis: A Systematic Review and a Series of Meta-analyses. *EBioMedicine,* 2**,** 1996-2002.

SAMPATH, K., CHENG, A. M., FRISCH, A. & WRIGHT, C. V. 1997. Functional differences among Xenopus nodal-related genes in left-right axis determination. *Development,* 124**,** 3293-302.

SANO, M., DRISCOLL, D. R., DEJESUS-MONGE, W. E., QUATTROCHI, B., APPLEMAN, V. A., OU, J., ZHU, L. J., YOSHIDA, N., YAMAZAKI, S., TAKAYAMA, T., SUGITANI, M., NEMOTO, N., KLIMSTRA, D. S. & LEWIS, B. C. 2016. Activation of WNT/beta-Catenin Signaling Enhances Pancreatic Cancer Development and the Malignant Potential Via Up-regulation of Cyr61. *Neoplasia,* 18**,** 785-794.

SANTO, V. E., REBELO, S. P., ESTRADA, M. F., ALVES, P. M., BOGHAERT, E. & BRITO, C. 2017. Drug screening in 3D in vitro tumor models: overcoming current pitfalls of efficacy read-outs. *Biotechnol J,* 12.

SAVANI, M., GUO, Y., CARBONE, D. P. & CSIKI, I. 2012. Sonic hedgehog pathway expression in non-small cell lung cancer. *Ther Adv Med Oncol,* 4**,** 225-33.

SCHATOFF, E. M., LEACH, B. I. & DOW, L. E. 2017. Wnt Signaling and Colorectal Cancer. *Curr Colorectal Cancer Rep,* 13**,** 101-110.

SCHILLING, T. F., CONCORDET, J. P. & INGHAM, P. W. 1999. Regulation of left-right asymmetries in the zebrafish by Shh and BMP4. *Dev Biol,* 210**,** 277-87.
SCHMIDT-OTT, K. M. & BARASCH, J. 2008. WNT/beta-catenin signaling in nephron progenitors and their epithelial progeny. *Kidney Int,* 74**,** 1004-8.
SCHOBER, M., JAVED, M. A., BEYER, G., LE, N., VINCI, A., SUND, M., NEESSE, A. & KRUG, S. 2015. New Advances in the Treatment of Metastatic Pancreatic Cancer. *Digestion,* 92**,** 175-84.
SEDGWICK, A. E. & D'SOUZA-SCHOREY, C. 2016. Wnt Signaling in Cell Motility and Invasion: Drawing Parallels between Development and Cancer. *Cancers (Basel),* 8.
SERRALBO, O. & MARCELLE, C. 2014. Migrating cells mediate long-range WNT signaling. *Development,* 141**,** 2057-63.
SHAHI, M. H., AFZAL, M., SINHA, S., EBERHART, C. G., REY, J. A., FAN, X. & CASTRESANA, J. S. 2010. Regulation of sonic hedgehog-GLI1 downstream target genes PTCH1, Cyclin D2, Plakoglobin, PAX6 and NKX2.2 and their epigenetic status in medulloblastoma and astrocytoma. *BMC Cancer,* 10**,** 614.
SHEN, X.-H. 2010. Perineural invasion in pancreatic cancer: Advanced research in the neuro-cancer interactions. *Clinical Oncology and Cancer Research,* 7**,** 337-341.
SHENG, T., LI, C., ZHANG, X., CHI, S., HE, N., CHEN, K., MCCORMICK, F., GATALICA, Z. & XIE, J. 2004. Activation of the hedgehog pathway in advanced prostate cancer. *Mol Cancer,* 3**,** 29.
SHERMAN, M. H., YU, R. T., TSENG, T. W., SOUSA, C. M., LIU, S., TRUITT, M. L., HE, N., DING, N., LIDDLE, C., ATKINS, A. R., LEBLANC, M., COLLISSON, E. A., ASARA, J. M., KIMMELMAN, A. C., DOWNES, M. & EVANS, R. M. 2017. Stromal cues regulate the pancreatic cancer epigenome and metabolome. *Proc Natl Acad Sci U S A,* 114**,** 1129-1134.
SHIELD, K., ACKLAND, M. L., AHMED, N. & RICE, G. E. 2009. Multicellular spheroids in ovarian cancer metastases: Biology and pathology. *Gynecol Oncol,* 113**,** 143-8.
SHIN, K., LIM, A., ZHAO, C., SAHOO, D., PAN, Y., SPIEKERKOETTER, E., LIAO, J. C. & BEACHY, P. A. 2014. Hedgehog signaling restrains bladder cancer progression by eliciting stromal production of urothelial differentiation factors. *Cancer Cell,* 26**,** 521-33.
SHIPLEY, G. L. 2006. Real-Time Quantitative PCR: Theory and Practice. *Reviews in Cell Biology and Molecular Medicine.* Wiley-VCH Verlag GmbH & Co. KGaA.
SIEGEL, P. M. & MASSAGUE, J. 2003. Cytostatic and apoptotic actions of TGF-beta in homeostasis and cancer. *Nat Rev Cancer,* 3**,** 807-21.
SIEGEL, R. L., MILLER, K. D. & JEMAL, A. 2015. Cancer statistics, 2015. *CA Cancer J Clin,* 65**,** 5-29.
SIPOS, B., MOSER, S., KALTHOFF, H., TOROK, V., LOHR, M. & KLOPPEL, G. 2003. A comprehensive characterization of pancreatic ductal carcinoma cell lines: towards the establishment of an in vitro research platform. *Virchows Arch,* 442**,** 444-52.
SMITH, M. 1982. Mutagenesis at Specific Sites: A Summary and Perspective. *In:* LEMONTT, J. F. & GENEROSO, W. M. (eds.) *Molecular and Cellular Mechanisms of Mutagenesis.* Boston, MA: Springer US.

STEWART, D. J. 2014. Wnt signaling pathway in non-small cell lung cancer. *J Natl Cancer Inst,* 106**,** djt356.
SUTHERLAND, R. M., INCH, W. R., MCCREDIE, J. A. & KRUUV, J. 1970. A multi-component radiation survival curve using an in vitro tumour model. *Int J Radiat Biol Relat Stud Phys Chem Med,* 18**,** 491-5.
SZKANDERA, J., KIESSLICH, T., HAYBAECK, J., GERGER, A. & PICHLER, M. 2013. Hedgehog signaling pathway in ovarian cancer. *Int J Mol Sci,* 14**,** 1179-96.
TABATA, T., EATON, S. & KORNBERG, T. B. 1992. The Drosophila hedgehog gene is expressed specifically in posterior compartment cells and is a target of engrailed regulation. *Genes Dev,* 6**,** 2635-45.
TAKADA, R., SATOMI, Y., KURATA, T., UENO, N., NORIOKA, S., KONDOH, H., TAKAO, T. & TAKADA, S. 2006. Monounsaturated fatty acid modification of Wnt protein: its role in Wnt secretion. *Dev Cell,* 11**,** 791-801.
TAKAHASHI, N., FUKUSHIMA, T., YORITA, K., TANAKA, H., CHIJIIWA, K. & KATAOKA, H. 2010. Dickkopf-1 is overexpressed in human pancreatic ductal adenocarcinoma cells and is involved in invasive growth. *Int J Cancer,* 126**,** 1611-20.
TALMADGE, J. E. & FIDLER, I. J. 2010. AACR centennial series: the biology of cancer metastasis: historical perspective. *Cancer Res,* 70**,** 5649-69.
TAN, M. H., NOWAK, N. J., LOOR, R., OCHI, H., SANDBERG, A. A., LOPEZ, C., PICKREN, J. W., BERJIAN, R., DOUGLASS, H. O., JR. & CHU, T. M. 1986. Characterization of a new primary human pancreatic tumor line. *Cancer Invest,* 4**,** 15-23.
TANAKA, K., KITAGAWA, Y. & KADOWAKI, T. 2002. Drosophila segment polarity gene product porcupine stimulates the posttranslational N-glycosylation of wingless in the endoplasmic reticulum. *J Biol Chem,* 277**,** 12816-23.
THAYER, S. P., DI MAGLIANO, M. P., HEISER, P. W., NIELSEN, C. M., ROBERTS, D. J., LAUWERS, G. Y., QI, Y. P., GYSIN, S., FERNANDEZ-DEL CASTILLO, C., YAJNIK, V., ANTONIU, B., MCMAHON, M., WARSHAW, A. L. & HEBROK, M. 2003. Hedgehog is an early and late mediator of pancreatic cancer tumorigenesis. *Nature,* 425**,** 851-6.
THOMAS, M. K., RASTALSKY, N., LEE, J. H. & HABENER, J. F. 2000. Hedgehog signaling regulation of insulin production by pancreatic beta-cells. *Diabetes,* 49**,** 2039-47.
TIAN, H., CALLAHAN, C. A., DUPREE, K. J., DARBONNE, W. C., AHN, C. P., SCALES, S. J. & DE SAUVAGE, F. J. 2009. Hedgehog signaling is restricted to the stromal compartment during pancreatic carcinogenesis. *Proc Natl Acad Sci U S A,* 106**,** 4254-9.
TOMASEK, J. J., GABBIANI, G., HINZ, B., CHAPONNIER, C. & BROWN, R. A. 2002. Myofibroblasts and mechano-regulation of connective tissue remodelling. *Nat Rev Mol Cell Biol,* 3**,** 349-63.
UNGER, C., KRAMER, N., WALZL, A., SCHERZER, M., HENGSTSCHLAGER, M. & DOLZNIG, H. 2014. Modeling human carcinomas: physiologically relevant 3D models to improve anti-cancer drug development. *Adv Drug Deliv Rev,* 79-80**,** 50-67.
VAINIO, S., HEIKKILA, M., KISPERT, A., CHIN, N. & MCMAHON, A. P. 1999. Female development in mammals is regulated by Wnt-4 signalling. *Nature,* 397**,** 405-9.

VAN AMERONGEN, R. 2012. Alternative Wnt pathways and receptors. *Cold Spring Harb Perspect Biol,* 4.
VAN DEN BRINK, G. R. 2007. Hedgehog signaling in development and homeostasis of the gastrointestinal tract. *Physiol Rev,* 87**,** 1343-75.
VELCHETI, V. & GOVINDAN, R. 2007. Hedgehog signaling pathway and lung cancer. *J Thorac Oncol,* 2**,** 7-10.
VERZI, M. P. & SHIVDASANI, R. A. 2008. Wnt signaling in gut organogenesis. *Organogenesis,* 4**,** 87-91.
VINCENT, J. P. & DUBOIS, L. 2002. Morphogen transport along epithelia, an integrated trafficking problem. *Dev Cell,* 3**,** 615-23.
VIRCHOW, R. 1989. Cellular pathology. As based upon physiological and pathological histology. Lecture XVI--Atheromatous affection of arteries. 1858. *Nutr Rev,* 47**,** 23-5.
VOGELSTEIN, B. & KINZLER, K. W. 2004. Cancer genes and the pathways they control. *Nat Med,* 10**,** 789-99.
VOLOSHANENKO, O., ERDMANN, G., DUBASH, T. D., AUGUSTIN, I., METZIG, M., MOFFA, G., HUNDSRUCKER, C., KERR, G., SANDMANN, T., ANCHANG, B., DEMIR, K., BOEHM, C., LEIBLE, S., BALL, C. R., GLIMM, H., SPANG, R. & BOUTROS, M. 2013. Wnt secretion is required to maintain high levels of Wnt activity in colon cancer cells. *Nat Commun,* 4**,** 2610.
VON AHRENS, D., BHAGAT, T. D., NAGRATH, D., MAITRA, A. & VERMA, A. 2017. The role of stromal cancer-associated fibroblasts in pancreatic cancer. *J Hematol Oncol,* 10**,** 76.
VON HOFF, D. D., ERVIN, T., ARENA, F. P., CHIOREAN, E. G., INFANTE, J., MOORE, M., SEAY, T., TJULANDIN, S. A., MA, W. W., SALEH, M. N., HARRIS, M., RENI, M., DOWDEN, S., LAHERU, D., BAHARY, N., RAMANATHAN, R. K., TABERNERO, J., HIDALGO, M., GOLDSTEIN, D., VAN CUTSEM, E., WEI, X., IGLESIAS, J. & RENSCHLER, M. F. 2013. Increased survival in pancreatic cancer with nab-paclitaxel plus gemcitabine. *N Engl J Med,* 369**,** 1691-703.
VORTKAMP, A., LEE, K., LANSKE, B., SEGRE, G. V., KRONENBERG, H. M. & TABIN, C. J. 1996. Regulation of rate of cartilage differentiation by Indian hedgehog and PTH-related protein. *Science,* 273**,** 613-22.
WADDELL, N., PAJIC, M., PATCH, A. M., CHANG, D. K., KASSAHN, K. S., BAILEY, P., JOHNS, A. L., MILLER, D., NONES, K., QUEK, K., QUINN, M. C., ROBERTSON, A. J., FADLULLAH, M. Z., BRUXNER, T. J., CHRIST, A. N., HARLIWONG, I., IDRISOGLU, S., MANNING, S., NOURSE, C., NOURBAKHSH, E., WANI, S., WILSON, P. J., MARKHAM, E., CLOONAN, N., ANDERSON, M. J., FINK, J. L., HOLMES, O., KAZAKOFF, S. H., LEONARD, C., NEWELL, F., POUDEL, B., SONG, S., TAYLOR, D., WADDELL, N., WOOD, S., XU, Q., WU, J., PINESE, M., COWLEY, M. J., LEE, H. C., JONES, M. D., NAGRIAL, A. M., HUMPHRIS, J., CHANTRILL, L. A., CHIN, V., STEINMANN, A. M., MAWSON, A., HUMPHREY, E. S., COLVIN, E. K., CHOU, A., SCARLETT, C. J., PINHO, A. V., GIRY-LATERRIERE, M., ROOMAN, I., SAMRA, J. S., KENCH, J. G., PETTITT, J. A., MERRETT, N. D., TOON, C., EPARI, K., NGUYEN, N. Q., BARBOUR, A., ZEPS, N., JAMIESON, N. B., GRAHAM, J. S., NICLOU, S. P., BJERKVIG, R., GRUTZMANN, R., AUST, D., HRUBAN, R. H., MAITRA, A.,

IACOBUZIO-DONAHUE, C. A., WOLFGANG, C. L., MORGAN, R. A., LAWLOR, R. T., CORBO, V., BASSI, C., FALCONI, M., ZAMBONI, G., TORTORA, G., TEMPERO, M. A., AUSTRALIAN PANCREATIC CANCER GENOME, I., GILL, A. J., ESHLEMAN, J. R., PILARSKY, C., SCARPA, A., MUSGROVE, E. A., PEARSON, J. V., BIANKIN, A. V. & GRIMMOND, S. M. 2015. Whole genomes redefine the mutational landscape of pancreatic cancer. *Nature,* 518**,** 495-501.

WAGHRAY, M., YALAMANCHILI, M., DI MAGLIANO, M. P. & SIMEONE, D. M. 2013. Deciphering the role of stroma in pancreatic cancer. *Curr Opin Gastroenterol,* 29**,** 537-43.

WALCK-SHANNON, E. & HARDIN, J. 2014. Cell intercalation from top to bottom. *Nat Rev Mol Cell Biol,* 15**,** 34-48.

WANG, L. M., SILVA, M. A., D'COSTA, Z., BOCKELMANN, R., SOONAWALLA, Z., LIU, S., O'NEILL, E., MUKHERJEE, S., MCKENNA, W. G., MUSCHEL, R. & FOKAS, E. 2016a. The prognostic role of desmoplastic stroma in pancreatic ductal adenocarcinoma. *Oncotarget,* 7**,** 4183-94.

WANG, L. R., LIU, J., HUANG, M. Z. & XU, N. 2007. Comparison of pharmacokinetics, efficacy and toxicity profile of gemcitabine using two different administration regimens in Chinese patients with non-small-cell lung cancer. *J Zhejiang Univ Sci B,* 8**,** 307-13.

WANG, Y. T., GOU, Y. W., JIN, W. W., XIAO, M. & FANG, H. Y. 2016b. Association between alcohol intake and the risk of pancreatic cancer: a dose-response meta-analysis of cohort studies. *BMC Cancer,* 16**,** 212.

WANG, Z. C., GAO, J., ZI, S. M., YANG, M., DU, P. & CUI, L. 2013. Aberrant expression of sonic hedgehog pathway in colon cancer and melanosis coli. *J Dig Dis,* 14**,** 417-24.

WARBURG 1931. The metabolism of tumours. Investigations from the Kaiser-Wilhelm Institute for Biology, Berlin-Dahlem. Edited by Otto Warburg, Kaiser-Wilhelm Institute for Biology, Berlin-Dahlem. Translated from the German edition, with accounts of additional recent researches, by Frank Dickens, M.A., Ph.D., whole-time worker for the Medical Research Council, Courtauld Institute of Biochemistry, Middlesex Hospital, London. Demy 8vo. Pp. 327 + xxix. Illustrated. 1930. London: Constable & Co. Ltd. 40s. net. *British Journal of Surgery,* 19**,** 168-168.

WARBURG, O. 1956. On the origin of cancer cells. *Science,* 123**,** 309-14.

WARE, M. J., COLBERT, K., KESHISHIAN, V., HO, J., CORR, S. J., CURLEY, S. A. & GODIN, B. 2016a. Generation of Homogenous Three-Dimensional Pancreatic Cancer Cell Spheroids Using an Improved Hanging Drop Technique. *Tissue Eng Part C Methods,* 22**,** 312-21.

WARE, M. J., KESHISHIAN, V., LAW, J. J., HO, J. C., FAVELA, C. A., REES, P., SMITH, B., MOHAMMAD, S., HWANG, R. F., RAJAPAKSHE, K., COARFA, C., HUANG, S., EDWARDS, D. P., CORR, S. J., GODIN, B. & CURLEY, S. A. 2016b. Generation of an in vitro 3D PDAC stroma rich spheroid model. *Biomaterials,* 108**,** 129-42.

WATANABE, I., HASEBE, T., SASAKI, S., KONISHI, M., INOUE, K., NAKAGOHRI, T., ODA, T., MUKAI, K. & KINOSHITA, T. 2003. Advanced pancreatic ductal cancer: fibrotic focus and beta-catenin expression correlate with outcome. *Pancreas,* 26**,** 326-33.

WATANABE, Y. & NAKAMURA, H. 2000. Control of chick tectum territory along dorsoventral axis by Sonic hedgehog. *Development,* 127**,** 1131-40.
WATARI, N., HOTTA, Y. & MABUCHI, Y. 1982. Morphological studies on a vitamin A-storing cell and its complex with macrophage observed in mouse pancreatic tissues following excess vitamin A administration. *Okajimas Folia Anat Jpn,* 58**,** 837-58.
WEAVER, B. A. 2014. How Taxol/paclitaxel kills cancer cells. *Mol Biol Cell,* 25**,** 2677-81.
WEEKES, C. D. & WINN, R. A. 2011. The many faces of wnt and pancreatic ductal adenocarcinoma oncogenesis. *Cancers (Basel),* 3**,** 3676-86.
WEHR, A. Y., FURTH, E. E., SANGAR, V., BLAIR, I. A. & YU, K. H. 2011. Analysis of the human pancreatic stellate cell secreted proteome. *Pancreas,* 40**,** 557-66.
WELLS, J. M., ESNI, F., BOIVIN, G. P., ARONOW, B. J., STUART, W., COMBS, C., SKLENKA, A., LEACH, S. D. & LOWY, A. M. 2007. Wnt/beta-catenin signaling is required for development of the exocrine pancreas. *BMC Dev Biol,* 7**,** 4.
WHITE, B. D., CHIEN, A. J. & DAWSON, D. W. 2012. Dysregulation of Wnt/beta-catenin signaling in gastrointestinal cancers. *Gastroenterology,* 142**,** 219-32.
WIJGERDE, M., OOMS, M., HOOGERBRUGGE, J. W. & GROOTEGOED, J. A. 2005. Hedgehog signaling in mouse ovary: Indian hedgehog and desert hedgehog from granulosa cells induce target gene expression in developing theca cells. *Endocrinology,* 146**,** 3558-66.
WILENTZ, R. E., IACOBUZIO-DONAHUE, C. A., ARGANI, P., MCCARTHY, D. M., PARSONS, J. L., YEO, C. J., KERN, S. E. & HRUBAN, R. H. 2000. Loss of expression of Dpc4 in pancreatic intraepithelial neoplasia: evidence that DPC4 inactivation occurs late in neoplastic progression. *Cancer Res,* 60**,** 2002-6.
WILLERT, K., BROWN, J. D., DANENBERG, E., DUNCAN, A. W., WEISSMAN, I. L., REYA, T., YATES, J. R., 3RD & NUSSE, R. 2003. Wnt proteins are lipid-modified and can act as stem cell growth factors. *Nature,* 423**,** 448-52.
WILLERT, K. & JONES, K. A. 2006. Wnt signaling: is the party in the nucleus? *Genes Dev,* 20**,** 1394-404.
WILSON, J. S., PIROLA, R. C. & APTE, M. V. 2014. Stars and stripes in pancreatic cancer: role of stellate cells and stroma in cancer progression. *Front Physiol,* 5**,** 52.
WITKIEWICZ, A. K., MCMILLAN, E. A., BALAJI, U., BAEK, G., LIN, W. C., MANSOUR, J., MOLLAEE, M., WAGNER, K. U., KODURU, P., YOPP, A., CHOTI, M. A., YEO, C. J., MCCUE, P., WHITE, M. A. & KNUDSEN, E. S. 2015. Whole-exome sequencing of pancreatic cancer defines genetic diversity and therapeutic targets. *Nat Commun,* 6**,** 6744.
WU, C. H. & NUSSE, R. 2002. Ligand receptor interactions in the Wnt signaling pathway in Drosophila. *J Biol Chem,* 277**,** 41762-9.
WU, M. & SWARTZ, M. A. 2014. Modeling tumor microenvironments in vitro. *J Biomech Eng,* 136**,** 021011.
XIE, D. & XIE, K. 2015. Pancreatic cancer stromal biology and therapy. *Genes Dis,* 2**,** 133-143.

XU, M., LI, L., LIU, Z., JIAO, Z., XU, P., KONG, X., HUANG, H. & ZHANG, Y. 2013. ABCB2 (TAP1) as the downstream target of SHH signaling enhances pancreatic ductal adenocarcinoma drug resistance. *Cancer Lett,* 333**,** 152-8.

YACHIDA, S., JONES, S., BOZIC, I., ANTAL, T., LEARY, R., FU, B., KAMIYAMA, M., HRUBAN, R. H., ESHLEMAN, J. R., NOWAK, M. A., VELCULESCU, V. E., KINZLER, K. W., VOGELSTEIN, B. & IACOBUZIO-DONAHUE, C. A. 2010. Distant metastasis occurs late during the genetic evolution of pancreatic cancer. *Nature,* 467**,** 1114-7.

YALOW, R. S. & BERSON, S. A. 1960. Immunoassay of endogenous plasma insulin in man. *J Clin Invest,* 39**,** 1157-75.

YAMAZAKI, M., NAKAMURA, K., MIZUKAMI, Y., II, M., SASAJIMA, J., SUGIYAMA, Y., NISHIKAWA, T., NAKANO, Y., YANAGAWA, N., SATO, K., MAEMOTO, A., TANNO, S., OKUMURA, T., KARASAKI, H., KONO, T., FUJIYA, M., ASHIDA, T., CHUNG, D. C. & KOHGO, Y. 2008. Sonic hedgehog derived from human pancreatic cancer cells augments angiogenic function of endothelial progenitor cells. *Cancer Sci,* 99**,** 1131-8.

YANG, Y. & MLODZIK, M. 2015. Wnt-Frizzled/planar cell polarity signaling: cellular orientation by facing the wind (Wnt). *Annu Rev Cell Dev Biol,* 31**,** 623-46.

YAUCH, R. L., GOULD, S. E., SCALES, S. J., TANG, T., TIAN, H., AHN, C. P., MARSHALL, D., FU, L., JANUARIO, T., KALLOP, D., NANNINI-PEPE, M., KOTKOW, K., MARSTERS, J. C., RUBIN, L. L. & DE SAUVAGE, F. J. 2008. A paracrine requirement for hedgehog signalling in cancer. *Nature,* 455**,** 406-10.

YOKOTA, J. 2000. Tumor progression and metastasis. *Carcinogenesis,* 21**,** 497-503.

YUNIS, A. A., ARIMURA, G. K. & RUSSIN, D. J. 1977. Human pancreatic carcinoma (MIA PaCa-2) in continuous culture: sensitivity to asparaginase. *Int J Cancer,* 19**,** 128-35.

ZENG, G., GERMINARO, M., MICSENYI, A., MONGA, N. K., BELL, A., SOOD, A., MALHOTRA, V., SOOD, N., MIDDA, V., MONGA, D. K., KOKKINAKIS, D. M. & MONGA, S. P. 2006. Aberrant Wnt/beta-catenin signaling in pancreatic adenocarcinoma. *Neoplasia,* 8**,** 279-89.

ZHAN, T., RINDTORFF, N. & BOUTROS, M. 2017. Wnt signaling in cancer. *Oncogene,* 36**,** 1461-1473.

ZHANG, J., GILL, A. J., ISSACS, J. D., ATMORE, B., JOHNS, A., DELBRIDGE, L. W., LAI, R. & MCMULLEN, T. P. 2012. The Wnt/beta-catenin pathway drives increased cyclin D1 levels in lymph node metastasis in papillary thyroid cancer. *Hum Pathol,* 43**,** 1044-50.

ZHANG, Y., MORRIS, J. P. T., YAN, W., SCHOFIELD, H. K., GURNEY, A., SIMEONE, D. M., MILLAR, S. E., HOEY, T., HEBROK, M. & PASCA DI MAGLIANO, M. 2013. Canonical wnt signaling is required for pancreatic carcinogenesis. *Cancer Res,* 73**,** 4909-22.

ZHU, A. J. & SCOTT, M. P. 2004. Incredible journey: how do developmental signals travel through tissue? *Genes Dev,* 18**,** 2985-97.

ZOLI, W., RICOTTI, L., DAL SUSINO, M., BARZANTI, F., FRASSINETI, G. L., FOLLI, S., TESEI, A., BACCI, F. & AMADORI, D. 1999. Docetaxel and gemcitabine activity in NSCLC cell lines and in primary cultures from human lung cancer. *Br J Cancer,* 81**,** 609-15.